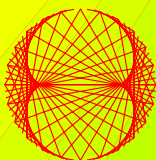


**ISSUE 2005**

# **PROGRESS IN PHYSICS**

**VOLUME 3**



**ISSN 1555-5534**

# PROGRESS IN PHYSICS

A quarterly issue scientific journal, registered with the Library of Congress (DC).  
This journal is peer reviewed and included in the abstracting and indexing coverage of:  
Mathematical Reviews and MathSciNet (AMS, USA), DOAJ of Lund University (Sweden),  
Referativnyi Zhurnal VINITI (Russia), etc.

ISSN: 1555-5534 (print)  
ISSN: 1555-5615 (online)  
4 issues per annum

Electronic version of this journal:  
[http://www.geocities.com/ptep\\_online](http://www.geocities.com/ptep_online)

To order printed issues of this journal, contact the Editor in Chief.

#### Chief Editor

Dmitri Rabounski  
rabounski@yahoo.com

#### Associate Editors

Prof. Florentin Smarandache  
smarand@unm.edu

Dr. Larissa Borissova  
lborissova@yahoo.com

Stephen J. Crothers  
thenarmis@yahoo.com

Department of Mathematics, University of  
New Mexico, 200 College Road, Gallup,  
NM 87301, USA

Copyright © *Progress in Physics*, 2005

All rights reserved. Any part of *Progress in Physics* howsoever used in other publications must include an appropriate citation of this journal.

Authors of articles published in *Progress in Physics* retain their rights to use their own articles in any other publications and in any way they see fit.

This journal is powered by BaKoMa-TeX

A variety of books can be downloaded free from the E-library of Science:  
<http://www.gallup.unm.edu/~smarandache>

ISSN: 1555-5534 (print)  
ISSN: 1555-5615 (online)

Standard Address Number: 297-5092  
Printed in the United States of America

OCTOBER 2005

VOLUME 3

## CONTENTS

<b>H. Arp</b> Observational Cosmology: From High Redshift Galaxies to the Blue Pacific.....	3
<b>S. J. Crothers</b> On the General Solution to Einstein's Vacuum Field for the Point-Mass when $\lambda \neq 0$ and Its Consequences for Relativistic Cosmology.....	7
<b>H. Ratcliffe</b> The First Crisis in Cosmology Conference. Monção, Portugal, June 23–25, 2005.....	19
<b>R. T. Cahill</b> The Michelson and Morley 1887 Experiment and the Discovery of Absolute Motion.....	25
<b>R. T. Cahill</b> Gravity Probe B Frame-Dragging Effect.....	30
<b>R. Oros di Bartini</b> Relations Between Physical Constants.....	34
<b>S. J. Crothers</b> Introducing Distance and Measurement in General Relativity: Changes for the Standard Tests and the Cosmological Large-Scale.....	41
<b>J. Dunning-Davies</b> A Re-Examination of Maxwell's Electromagnetic Equations.....	48
<b>R. T. Cahill</b> Black Holes in Elliptical and Spiral Galaxies and in Globular Clusters.....	51
<b>E. Gaastra</b> Is the Biggest Paradigm Shift in the History of Science at Hand?..	57
<b>N. Kozyrev</b> Sources of Stellar Energy and the Theory of the Internal Constitution of Stars.....	61

## **Information for Authors and Subscribers**

*Progress in Physics* has been created for publications on advanced studies in theoretical and experimental physics, including related themes from mathematics. All submitted papers should be professional, in good English, containing a brief review of a problem and obtained results.

All submissions should be designed in  $\text{\LaTeX}$  format using *Progress in Physics* template. This template can be downloaded from *Progress in Physics* home page [http://www.geocities.com/ptep\\_online](http://www.geocities.com/ptep_online). Abstract and the necessary information about author(s) should be included into the papers. To submit a paper, mail the file(s) to Chief Editor.

All submitted papers should be as brief as possible. Beginning from 2006 we accept only short papers, no longer than 8 journal pages. Short articles are preferable.

All that has been accepted for the online issue of *Progress in Physics* is printed in the paper version of the journal. To order printed issues, contact Chief Editor.

This journal is non-commercial, academic edition. It is printed from private donations.

---

# Observational Cosmology: From High Redshift Galaxies to the Blue Pacific

Halton Arp

*Max-Planck-Institut für Astrophysik, Karl Schwarzschild-Str.1,  
Postfach 1317, D-85741 Garching, Germany*

E-mail: arp@mpa-garching.mpg.de

## 1 Birth of galaxies

**Observed:** *Ejection of high redshift, low luminosity quasars from active galaxy nuclei.*

Shown by radio and X-ray pairs, alignments and luminous connecting filaments. Emergent velocities are much less than intrinsic redshift. Stripping of radio plasmas. Probabilities of accidental association negligible. See Arp, 2003 [4] for customarily suppressed details.

**Observed:** *Evolution of quasars into normal companion galaxies.*

The large number of ejected objects enables a view of empirical evolution from high surface brightness quasars through compact galaxies. From gaseous plasmoids to formation of atoms and stars. From high redshift to low.

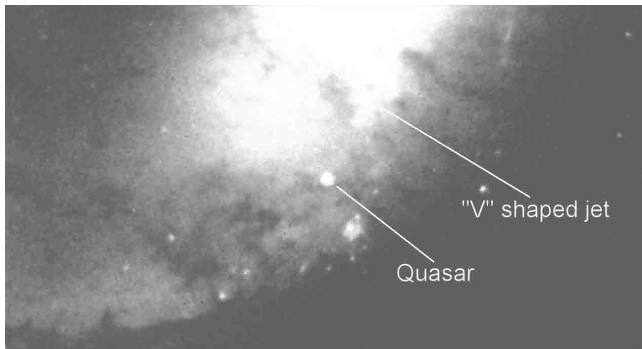


Fig. 1: Enhanced Hubble Space Telescope image showing ejection wake from the center of NGC 7319 (redshift  $z = 0.022$ ) to within about 3.4 arcsec of the quasar (redshift  $z = 2.11$ )

**Observed:** *Younger objects have higher intrinsic redshifts.*

In groups, star forming galaxies have systematically higher redshifts, e. g. spiral galaxies. Even companions in evolved groups like our own Andromeda Group or the nearby M81 group still have small, residual redshift excesses relative to their parent.

**Observed:** *X-ray and radio emission generally indicate early evolutionary stages and intrinsic redshift.*

Plasmoids ejected from an active nucleus can fragment or ablate during passage through galactic and intergalactic medium which results in the forming of groups and clusters of proto galaxies. The most difficult result for astronomers to accept is galaxy clusters which have intrinsic redshifts. Yet the association of clusters with lower redshift parents is

demonstrated in Arp and Russell, 2001 [1]. Individual cases of strong X-ray clusters are exemplified by elongations and connections as shown in the ejecting galaxy Arp 220, in Abell 3667 and from NGC 720 (again, summarized in Arp, 2003 [4]). Motion is confirmed by bow shocks and elongation is interpreted as ablation trails. In short — if a quasar evolves into a galaxy, a broken up quasar evolves into a group of galaxies.

## 2 Redshift is the key

**Observed:** *The whole quasar or galaxy is intrinsically redshifted.*

Objects with the same path length to the observer have much different redshifts and all parts of the object are shifted closely the same amount. Tired light is ruled out and also gravitational redshifting.

**The fundamental assumption:** *Are particle masses constant?*

The photon emitted in an orbital transition of an electron in an atom can only be redshifted if its mass is initially small. As time goes on the electron communicates with more and more matter within a sphere whose limit is expanding at velocity  $c$ . If the masses of electrons increase, emitted photons change from an initially high redshift to a lower redshift with time (see Narlikar and Arp, 1993 [6])

**Predicted consequences:** *Quasars are born with high redshift and evolve into galaxies of lower redshift.*

Near zero mass particles evolve from energy conditions in an active nucleus. (If particle masses have to be created sometime, it seems easier to grow things from a low mass state rather than producing them instantaneously in a finished state.)

**DARK MATTER:** *The establishment gets it right, sort of.*

In the Big Bang, gas blobs in the initial, hot universe have to condense into things we now see like quasars and galaxies. But we know hot gas blobs just go poof! Lots of dark matter (cold) had to be hypothesized to condense the gas cloud. They are still looking for it.

But low mass particles must slow their velocities in order to conserve momentum as their mass grows. Temperature is internal velocity. Thus the plasmoid cools and condenses its increasing mass into a compact quasar. So maybe we

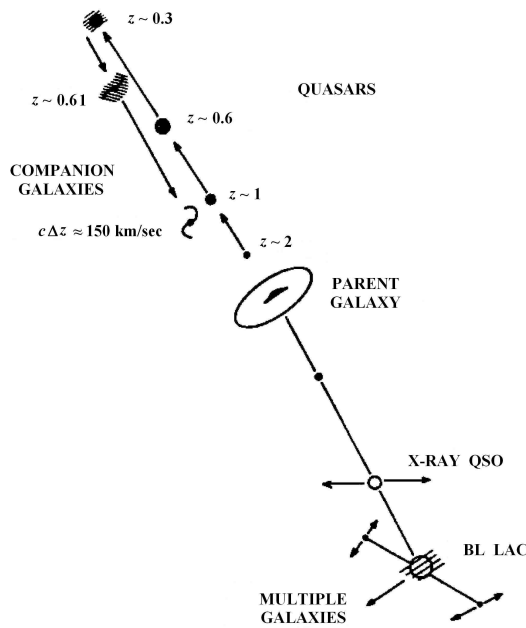


Fig. 2: Schematic representation of quasars and companion galaxies found associated with central galaxies from 1966 to present. The progression of characteristics is empirical but is also required by the variable mass theory of Narlikar and Arp, 1993 [6]

have been observing dark matter ever since the discovery of quasars! After all, what's in a name?

**Observed:** *Ambarzumian sees new galaxies.*

In the late 1950's when the prestigious Armenian astronomer, Viktor Ambarzumian was president of the International Astronomical Union he said that just looking at pictures convinced him that new galaxies were ejected out of old. Even now astronomers refuse to discuss it, saying that big galaxies cannot come out of other big galaxies. But we have just seen that the changing redshift is the key that unlocks the growth of new galaxies with time. They are small when they come from the small nucleus. Ambarzumian's superfluid just needed the nature of changing redshift. But Oort and conventional astronomers preferred to condense hot gas out of a hot expanding universe.

**Observed:** *The Hubble Relation.*

An article of faith in current cosmology is that the relation between faintness of galaxies and their redshift, the Hubble Relation, means that the more distant a galaxy is the faster it is receding from us. With our galaxy redshifts a function of age, however, the look back time to a distant galaxy shows it to us when it was younger and more intrinsically redshifted. No Doppler recession needed!

The latter non-expanding universe is even quantitative in that Narlikar's general solution of the General Relativistic equations ( $m = t^2$ ) gives a Hubble constant directly in term of the age of our own galaxy. ( $H_0 = 51 \text{ km/sec} \times \text{Mpc}$  for age of our galaxy = 13 billion years). The Hubble constant

observed from the most reliable Cepheid distances is  $H_0 = 55$  (Arp, 2002 [3]). What are the chances of obtaining the correct Hubble constant from an incorrect theory with no adjustable parameters? If this is correct there is negligible room for expansion of the universe.

**Observed:** *The current Hubble constant is too large.*

A large amount of observing time on the Hubble Space Telescope was devoted to observing Cepheid variables whose distances divided into their redshifts gave a definitive value of  $H_0 = 72$ . That required the reintroduction of Einstein's cosmological constant to adjust to the observations. But  $H_0 = 72$  was wrong because the higher redshift galaxies in the sample included younger (ScI) galaxies which had appreciable intrinsic redshifts.

Independent distances to these galaxies by means of rotational luminosity distances (Tully-Fisher distances) also showed this class of galaxies had intrinsic redshifts which gave too high a Hubble constant (Russell, 2002 [8]) In fact well known clusters of galaxies gives  $H_0$ 's in the 90's (Russell, private communication) which clearly shows that neither do we have a correct distance scale or understanding of the nature of galaxy clusters.

**DARK ENERGY:** *Expansion now claimed to be acceleration.*

As distance measures were extended to greater distances by using Supernovae as standard candles it was found that the distant Supernovae were somewhat too faint. This led to a smaller  $H_0$  and hence an acceleration compared to the supposed present day  $H_0 = 72$ . Of course the younger Supernovae could be intrinsically fainter and also we have seen the accepted present day  $H_0$  is too large. Nevertheless astronomers have again added a huge amount of undetected substance to the universe to make it agree with properties of a disproved set of assumptions. This is called the accordance model but we could easily imagine another name for it.

### 3 Physics – local and universal

Instead of extrapolating our local phenomena out to the universe one might more profitably consider our local region as a part of the physics of the universe.

**Note:** *Flat space, no curves, no expansion.*

The general solution of energy/momentum conservation (relativistic field equations) which Narlikar made with  $m = t^2$  gives a Euclidean, three dimensional, uncurved space. The usual assumption that particle masses are constant in time only projects our local, snapshot view onto the rest of the universe.

In any case it is not correct to solve the equations in a non-general case. In that case the usual procedure of assigning curvature and expansion properties to the mathematical term space (which has no physical attributes!) is only useful for

excusing the violations with the observations caused by the inappropriate assumption of constant elementary masses.

**Consequences:** *Relativity theory can furnish no gravity.*

Space (nothing) can not be a “rubber sheet”. Even if there could be a dimple — nothing would roll into it unless there was a previously existing pull of gravity. We need to find a plausible cause for gravity other than invisible bands pulling things together.

**Required:** *Very small wave/particles pushing against bodies.*

In 1747 the Genevoise philosopher-physicist George-Louis Le Sage postulated that pressure from the medium which filled space would push bodies together in accordance with the Newtonian Force  $= 1/r^2$  law. Well before the continuing fruitless effort to unify Relativistic gravity and quantum gravity, Le Sage had solved the problem by doing away with the need to warp space in order to account for gravity.

**Advantages:** *The Earth does not spiral into the Sun.*

Relativistic gravity is assigned an instantaneous component as well as a component that travels with the speed of light,  $c$ . If gravity were limited to  $c$ , the Earth would be rotating around the Sun where it was about 8 minutes ago. By calculating under the condition that no detectable reduction in the size of the Earth’s orbit has been observed, Tom Van Flandern arrives at the minimum speed of gravity of  $2 \times 10^{10} c$ . We could call these extremely fast, extremely penetrating particles gravitons.

*A null observation saves causality.*

The above reasoning essentially means that gravity can act as fast as it pleases, but not instantaneously because that would violate causality. This is reassuring since causality seems to be an accepted property of our universe (except for some early forms of quantum theory).

*Black holes into white holes.*

In its usual perverse way all the talk has been about black holes and all the observations have been about white holes. Forget for a moment that from the observer’s viewpoint it would take an infinity of time to form a black hole. The observations show abundant material being ejected from stars, nebulae, galaxies, quasars. What collimates these out of a region in which everything is supposed to fall into? (Even ephemeral photons of light.) After 30 years of saying nothing comes out of black holes, Stephen Hawking now approaches the observations saying maybe a little leaks out.

**Question:** *What happens when gravitons encounter a black hole?*

If the density inside the concentration of matter is very high the steady flux of gravitons absorbed will eventually heat the core and eventually this energy must escape. After all it is only a local concentration of matter against the continuous push of the whole of intergalactic space. Is it reasonable to say it will escape through the path of least resistance, for example through the flattened pole of a spinn-

ing sphere which is usual picture of the nucleus? Hence the directional nature of the observed plasmoid ejections.

#### 4 Planets and people

In our own solar system we know the gas giant planets increase in size as we go in toward the Sun through Neptune, Uranus, Saturn and Jupiter. On the Earth’s side of Jupiter, however, we find the asteroid belt. It does not take an advanced degree to come to the idea that the asteroids are the remains of a broken up planet. But how? Did something crash into it? What does it mean about our solar system?

**Mars:** *The Exploding Planet Hypothesis.*

We turn to a real expert on planets, Tom Van Flandern. For years he has argued in convincing detail that Mars, originally bigger than Earth, had exploded visibly scarring the surface of its moon, the object we now call Mars. One detail should be especially convincing, namely that the present Mars, unable to hold an atmosphere, had long been considered devoid of water, a completely arid desert. But recent up-close looks have revealed evidence for “water dumps”, lots of water in the past which rapidly went away. Where else could this water have come from except the original, close-by Mars as it exploded?

For me the most convincing progression is the increasing masses of the planets from the edge of the planetary system toward Jupiter and then the decreasing masses from Jupiter through Mercury. Except for the present Mars! But that continuity would be preserved with an original Mars larger than Earth and its moon larger than the Earth’s moon.

As for life on Mars, the Viking lander reported bacteria but the scientist said no. Then there was controversy about organic forms in meteorites from Mars. But the most straight forward statement that can be made is that features have now been observed that look “artificial” to some. Obviously no one is certain at this point but most scientists are trained to stop short of articulating the obvious.

**Gravitons:** *Are planets part of the universe?*

If a universal sea of very small, very high speed gravitons are responsible for gravity in galaxies and stars would not these same gravitons be passing through the solar system and the planets in it? What would be the effect if a small percentage were, over time, absorbed in the cores of planets?

**Speculation:** *What would we expect?*

Heating the core of a gas giant would cause the liquid/gaseous planet to expand in size. But if the core of a rocky planet would be too rigid to expand it would eventually explode. Was the asteroid planet the first to go? Then the original Mars? And next the Earth?

**Geology:** *Let’s argue about the details.*

Originally it was thought the Earth was flat. Then spherical but with the continents anchored in rock. When Alfred Wegener noted that continents fitted together like jigsaw

puzzle and therefore had been pulled apart, it was violently rejected because geologists said they were anchored in basaltic rock. Finally it was found that the Atlantic trench between the Americas and Africa/Europe was opening up at a rate of just about right for the Earth's estimated age (Kokus, 2002 [5]). So main stream geologists invented plate tectonics where the continents skated blythly around on top of this anchoring rock!

In 1958 the noted Geologist S. Warren Carey and in 1965 K. M. Creer (in the old, usefully scientific *Nature Magazine*) were among those who articulated the obvious, namely that the Earth is expanding. The controversy between plate tectonics and expanding Earth has been acrid ever since. (One recent conference proceedings by the latter adherents is "Why Expanding Earth?" (Scalera and Jacob, 2003 [7]).

*Let's look around us.*

The Earth is an obviously active place. volcanos, Earth quakes, island building. People seem to agree the Atlantic is widening and the continents separating. But the Pacific is violently contested with some satellite positioning claiming no expansion. I remember hearing S. Warren Carey painstakingly interpreting maps of the supposed subduction zone where the Pacific plate was supposed to be diving under the Andean land mass of Chile. He argued that there was no debris scraped off the supposedly diving Pacific Plate. But in any case, where was the energy coming from to drive a huge Pacific plate under the massive Andean plate?

My own suggestion about this is that the (plate) is stuck, not sliding under. Is it possible that the pressure from the Pacific Basin has been transmitted into the coastal ranges of the Americas where it is translated into mountain building? (Mountain building is a particularly contentious disagreement between static and expanding Earth proponents.)

It is an impressive, almost thought provoking sight, to see hot lava welling up from under the southwest edge of the Big Island of Hawaii forming new land mass in front of our eyes. All through the Pacific there are underground vents, volcanos, mountain and island building. Is it possible this upwelling of mass in the central regions of the Pacific is putting pressure on the edge? Does it represent the emergence of material comparable to that along the Mid Atlantic ridge on the other side of the globe?

**The future:** *Life as an escape from danger.*

The galaxy is an evolving, intermittently violent environment. The organic colonies that inhabit certain regions within it may or may not survive depending on how fast they recognize danger and how well they adapt, modify it or escape from it. Looking out over the beautiful blue Pacific one sees tropical paradises. On one mountain top, standing on barely cool lava, is the Earth's biggest telescope. Looking out in the universe for answers. Can humankind collectively understand these answers? Can they collectively ensure their continued appreciation of the beauty of existence.

## References

1. Arp H. and Russell D.G. A possible relationship between quasars and clusters of galaxies. *Astrophysical Journal*, 2001, v. 549, 802–819
2. Arp H. *Pushing Gravity*, ed. by M. R. Edwards, 2002, 1.
3. Arp H. Arguments for a Hubble constant near  $H_0 = 55$ . *Astrophysical Journal*, 2002, 571, 615–618.
4. Arp H. Catalog of discordant redshift associations. Apeiron, Montreal, 2003.
5. Kokus M. *Pushing Gravity*, ed. by M. R. Edwards, 2002, 285.
6. Narlikar J. and Arp H. Flat spacetime cosmology — a unified framework for extragalactic redshifts. *Astrophysical Journal*, 1993, 405, 51-56.
7. Scalera G. and Jacob K.-H. (editors). Why expanding Earth? Nazionale di Geofisica e Vulcanologia, Technisch Univ. Berlin, publ. INGV Roma, Italy, 2003.
8. Russell D.G. Morphological type dependence in the Tully-Fisher relationship. *Astrophysical Journal*, 2004, v.607, 241-246.
9. Van Flandern T. Dark matter, missing planets and new comets. 2nd ed., North Atlantic Books, Berkely, 1999.
10. Van Flandern T. *Pushing Gravity*, ed. by M. R. Edwards, 2002, 93.

# On the General Solution to Einstein's Vacuum Field for the Point-Mass when $\lambda \neq 0$ and Its Consequences for Relativistic Cosmology

Stephen J. Crothers

Sydney, Australia

E-mail: thenarmis@yahoo.com

It is generally alleged that Einstein's theory leads to a finite but unbounded universe. This allegation stems from an incorrect analysis of the metric for the point-mass when  $\lambda \neq 0$ . The standard analysis has incorrectly assumed that the variable  $r$  denotes a radius in the gravitational field. Since  $r$  is in fact nothing more than a real-valued parameter for the actual radial quantities in the gravitational field, the standard interpretation is erroneous. Moreover, the true radial quantities lead inescapably to  $\lambda = 0$  so that, cosmologically, Einstein's theory predicts an infinite, static, empty universe.

## 1 Introduction

It has been shown [1, 2, 3] that the variable  $r$  which appears in the metric for the gravitational field is neither a radius nor a coordinate in the gravitational field, and further [3], that it is merely a real-valued parameter in the pseudo-Euclidean spacetime  $(M_s, g_s)$  of Special Relativity, by which the Euclidean distance  $D = |r - r_0| \in (M_s, g_s)$  is mapped into the non-Euclidean distance  $R_p \in (M_g, g_g)$ , where  $(M_g, g_g)$  denotes the pseudo-Riemannian spacetime of General Relativity. Owing to their invalid assumptions about the variable  $r$ , the relativists claim that  $r = \sqrt{\frac{3}{\lambda}}$  defines a "horizon" for the universe (e.g. [4]), by which the universe is supposed to have a finite volume. Thus, they have claimed a finite but unbounded universe. This claim is demonstrably false.

The standard metric for the simple point-mass when  $\lambda \neq 0$  is,

$$ds^2 = \left(1 - \frac{2m}{r} - \frac{\lambda}{3} r^2\right) dt^2 - \left(1 - \frac{2m}{r} - \frac{\lambda}{3} r^2\right)^{-1} dr^2 - r^2 (d\theta^2 + \sin^2 \theta d\varphi^2). \quad (1)$$

The relativists simply look at (1) and make the following assumptions.

- The variable  $r$  is a radial coordinate in the gravitational field;
- $r$  can go down to 0;
- A singularity in the gravitational field can occur only where the Riemann tensor scalar curvature invariant (or Kretschmann scalar)  $f = R_{\alpha\beta\gamma\delta} R^{\alpha\beta\gamma\delta}$  is unbounded.

The standard analysis has never proved these assumptions, but nonetheless simply takes them as given. I have demonstrated elsewhere [3] that when  $\lambda = 0$ , these assumptions are false. I shall demonstrate herein that when  $\lambda \neq 0$

these assumptions are still false, and further, that  $\lambda$  can only take the value of zero in Einstein's theory.

## 2 Definitions

As is well-known, the basic spacetime of the General Theory of Relativity is a metric space of the Riemannian geometry family, namely — the four-dimensional pseudo-Riemannian space with Minkowski signature. Such a space, like any Riemannian metric space, is strictly negative non-degenerate, i. e. the fundamental metric tensor  $g_{\alpha\beta}$  of such a space has a determinant which is strictly negative:  $g = \det \|g_{\alpha\beta}\| < 0$ .

Space metrics obtained from Einstein's equations can be very different. This splits General Relativity's spaces into numerous families. The two main families are derived from the fact that the energy-momentum tensor of matter  $T_{\alpha\beta}$ , contained in the Einstein equations, can (1) be linearly proportional to the fundamental metric tensor  $g_{\alpha\beta}$  or (2) have a more compound functional dependence. The first case is much more attractive to scientists, because in this case one can use  $g_{\alpha\beta}$ , taken with a constant numerical coefficient, instead of the usual  $T_{\alpha\beta}$ , in the Einstein equations. Spaces of the first family are known as *Einstein spaces*.

From the purely geometrical perspective, an Einstein space [5] is described by any metric obtained from

$$R_{\alpha\beta} - \frac{1}{2} g_{\alpha\beta} R = \kappa T_{\alpha\beta} - \lambda g_{\alpha\beta},$$

where  $\kappa$  is a constant and  $T_{\alpha\beta} \propto g_{\alpha\beta}$ , and therefore includes all partially degenerate metrics. Accordingly, such spaces become non-Einstein only when the determinant  $g$  of the metric becomes

$$g = \det \|g_{\alpha\beta}\| = 0.$$

In terms of the required physical meaning of General Relativity I shall call a spacetime associated with a non-



degenerate metric, an Einstein universe, and the associated metric an Einstein metric.

Cosmological models involving either  $\lambda \neq 0$  or  $\lambda = 0$ , which do not result in a degenerate metric, I shall call relativistic cosmological models, which are necessarily Einstein universes, with associated Einstein metrics.

Thus, any ‘‘partially’’ degenerate metric where  $g \neq 0$  is not an Einstein metric, and the associated space is not an Einstein universe. Any cosmological model resulting in a ‘‘partially’’ degenerate metric where  $g \neq 0$  is neither a relativistic cosmological model nor an Einstein universe.

### 3 The general solution when $\lambda \neq 0$

The general solution for the simple point-mass [3] is,

$$ds^2 = \left( \frac{\sqrt{C_n} - \alpha}{\sqrt{C_n}} \right) dt^2 - \left( \frac{\sqrt{C_n}}{\sqrt{C_n} - \alpha} \right) \frac{C_n'^2}{4C_n} dr^2 - C_n (d\theta^2 + \sin^2 \theta d\varphi^2), \quad (2)$$

$$C_n(r) = [|r - r_0|^n + \alpha^n]^{\frac{2}{n}}, \quad n \in \mathfrak{R}^+, \\ \alpha = 2m, \quad r_0 \in \mathfrak{R},$$

where  $n$  and  $r_0$  are arbitrary and  $r$  is a real-valued parameter in  $(M_s, g_s)$ .

The most general static metric for the gravitational field [3] is,

$$ds^2 = A(D)dt^2 - B(D)dr^2 - C(D)(d\theta^2 + \sin^2 \theta d\varphi^2), \quad (3)$$

$$D = |r - r_0|, \quad r_0 \in \mathfrak{R},$$

where analytic  $A, B, C > 0 \forall r \neq r_0$ .

In relation to (3) I identify the coordinate radius  $D$ , the  $r$ -parameter, the radius of curvature  $R_c$ , and the proper radius (proper distance)  $R_p$ .

1. The coordinate radius is  $D = |r - r_0|$ .
2. The  $r$ -parameter is the variable  $r$ .
3. The radius of curvature is  $R_c = \sqrt{C(D(r))}$ .
4. The proper radius is  $R_p = \int \sqrt{B(D(r))} dr$ .

I remark that  $R_p(D(r))$  gives the mapping of the Euclidean distance  $D = |r - r_0| \in (M_s, g_s)$  into the non-Euclidean distance  $R_p \in (M_g, g_g)$  [3]. Furthermore, the geometrical relations between the components of the metric tensor are inviolable and therefore hold for all metrics with the form of (3).

Thus, on the metric (2),

$$R_c = \sqrt{C_n(D(r))}, \\ R_p = \int \sqrt{\frac{\sqrt{C_n}}{\sqrt{C_n} - \alpha} \frac{C_n'}{2\sqrt{C_n}}} dr.$$

Transform (3) by setting,

$$r^* = \sqrt{C(D(r))}, \quad (4)$$

to carry (3) into,

$$ds^2 = A^*(r^*)dt^2 - B^*(r^*)dr^{*2} - r^{*2}(d\theta^2 + \sin^2 \theta d\varphi^2). \quad (5)$$

For  $\lambda \neq 0$ , one finds in the usual way that the solution to (5) is,

$$ds^2 = \left( 1 - \frac{\alpha}{r^*} - \frac{\lambda}{3} r^{*2} \right) dt^2 - \left( 1 - \frac{\alpha}{r^*} - \frac{\lambda}{3} r^{*2} \right)^{-1} dr^{*2} - r^{*2}(d\theta^2 + \sin^2 \theta d\varphi^2). \quad (6)$$

$$\alpha = \text{const.}$$

Then by (4),

$$ds^2 = \left( 1 - \frac{\alpha}{\sqrt{C}} - \frac{\lambda}{3} C \right) dt^2 - \left( 1 - \frac{\alpha}{\sqrt{C}} - \frac{\lambda}{3} C \right)^{-1} \frac{C'^2}{4C} dr^2 - C(d\theta^2 + \sin^2 \theta d\varphi^2), \quad (7)$$

$$C = C(D(r)), \quad D = D(r) = |r - r_0|, \quad r_0 \in \mathfrak{R},$$

$$\alpha = \text{const.}$$

where  $r \in (M_s, g_s)$  is a real-valued parameter and also  $r_0 \in (M_s, g_s)$  is an arbitrary constant which specifies the position of the point-mass in parameter space.

When  $\alpha = 0$ , (7) reduces to the empty de Sitter metric, which I write generally, in view of (7), as

$$ds^2 = \left( 1 - \frac{\lambda}{3} F \right) dt^2 - \left( 1 - \frac{\lambda}{3} F \right)^{-1} d\sqrt{F}^2 - F(d\theta^2 + \sin^2 \theta d\varphi^2), \quad (8)$$

$$F = F(D(r)), \quad D = D(r) = |r - r_0|, \quad r_0 \in \mathfrak{R}.$$

If  $F(D(r)) = r^2$ ,  $r_0 = 0$ , and  $r \geq r_0$ , then the usual form of (8) is obtained,

$$ds^2 = \left( 1 - \frac{\lambda}{3} r^2 \right) dt^2 - \left( 1 - \frac{\lambda}{3} r^2 \right)^{-1} dr^2 - r^2(d\theta^2 + \sin^2 \theta d\varphi^2). \quad (9)$$

The admissible forms for  $C(D(r))$  and  $F(D(r))$  must now be generally ascertained.

If  $C' \equiv 0$ , then  $B(D(r)) = 0 \forall r$ , in violation of (3). Therefore  $C' \neq 0 \forall r \neq r_0$ .

Now  $C(D(r))$  must be such that when  $r \rightarrow \pm \infty$ , equation (7) must reduce to (8) asymptotically. So,

$$\text{as } r \rightarrow \pm \infty, \frac{C(D(r))}{F(D(r))} \rightarrow 1.$$

I have previously shown [3] that the condition for singularity on a metric describing the gravitational field of the point-mass is,

$$g_{00}(r_0) = 0. \tag{10}$$

Thus, by (7), it is required that,

$$1 - \frac{\alpha}{\sqrt{C(D(r_0))}} - \frac{\lambda}{3} C(D(r_0)) = 1 - \frac{\alpha}{\beta} - \frac{\lambda}{3} \beta^2 = 0, \tag{11}$$

having set  $\sqrt{C(D(r_0))} = \beta$ . Thus,  $\beta$  is a scalar invariant for (7) that must contain the independent factors contributing to the gravitational field, i.e.  $\beta = \beta(\alpha, \lambda)$ . Consequently it is required that when  $\lambda = 0$ ,  $\beta = \alpha = 2m$  to recover (2), when  $\alpha = 0$ ,  $\beta = \sqrt{\frac{3}{\lambda}}$  to recover (8), and when  $\alpha = \lambda = 0$ , and  $\beta = 0$ ,  $C(D(r)) = |r - r_0|^2$  to recover the flat spacetime of Special Relativity. Also, when  $\alpha = 0$ ,  $C(D(r))$  must reduce to  $F(D(r))$ . The value of  $\beta = \beta(\lambda) = \sqrt{F(D(r_0))}$  in (8) is also obtained from,

$$g_{00}(r_0) = 0 = 1 - \frac{\lambda}{3} F(D(r_0)) = 1 - \frac{\lambda}{3} \beta^2.$$

Therefore,

$$\beta = \sqrt{\frac{3}{\lambda}}. \tag{12}$$

Thus, to render a solution to (7),  $C(D(r))$  must at least satisfy the following conditions.

1.  $C'(D(r)) \neq 0 \forall r \neq r_0$ .
2. As  $r \rightarrow \pm \infty$ ,  $\frac{C(D(r))}{F(D(r))} \rightarrow 1$ .
3.  $C(D(r_0)) = \beta^2$ ,  $\beta = \beta(\alpha, \lambda)$ .
4.  $\lambda = 0 \Rightarrow \beta = \alpha = 2m$  and  $C = (|r - r_0|^n + \alpha^n)^{\frac{2}{n}}$ .
5.  $\alpha = 0 \Rightarrow \beta = \sqrt{\frac{3}{\lambda}}$  and  $C(D(r)) = F(D(r))$ .
6.  $\alpha = \lambda = 0 \Rightarrow \beta = 0$  and  $C(D(r)) = |r - r_0|^2$ .

Both  $\alpha$  and  $\beta(\alpha, \lambda)$  must also be determined.

Since (11) is a cubic, it cannot be solved exactly for  $\beta$ . However, I note that the two positive roots of (11) are approximately  $\alpha$  and  $\sqrt{\frac{3}{\lambda}}$ . Let  $P(\beta) = 1 - \frac{\alpha}{\beta} - \frac{\lambda}{3} \beta^2$ . Then according to Newton's method,

$$\beta_{m+1} = \beta_m - \frac{P(\beta_m)}{P'(\beta_m)} = \beta_m - \frac{\left(1 - \frac{\alpha}{\beta_m} - \frac{\lambda}{3} \beta_m^2\right)}{\left(\frac{\alpha}{\beta_m^2} - \frac{2\lambda}{3} \beta_m\right)}. \tag{13}$$

Taking  $\beta_1 = \alpha$  into (13) gives,

$$\beta \approx \beta_2 = \frac{3\alpha - \lambda\alpha^3}{3 - 2\lambda\alpha^2}, \tag{14a}$$

and

$$\beta \approx \beta_3 = \frac{3\alpha - \lambda\alpha^3}{3 - 2\lambda\alpha^2} - \left[ \frac{1 - \frac{\alpha(3-2\lambda\alpha^2)}{(3\alpha-\lambda\alpha^3)} - \frac{\lambda}{3} \left(\frac{3\alpha-\lambda\alpha^3}{3-2\lambda\alpha^2}\right)^2}{\alpha \left(\frac{3-2\lambda\alpha^2}{3\alpha-\lambda\alpha^3}\right)^2 - \frac{2\lambda}{3} \left(\frac{3\alpha-\lambda\alpha^3}{3-2\lambda\alpha^2}\right)} \right], \tag{14b}$$

etc., which satisfy the requirement that  $\beta = \beta(\alpha, \lambda)$ .

Taking  $\beta_1 = \sqrt{\frac{3}{\lambda}}$  into (13) gives,

$$\beta \approx \beta_2 = \sqrt{\frac{3}{\lambda}} + \frac{\alpha}{\alpha\sqrt{\frac{\lambda}{3}} - 2}, \tag{15a}$$

and

$$\beta \approx \beta_3 = \sqrt{\frac{3}{\lambda}} + \frac{\alpha}{\alpha\sqrt{\frac{\lambda}{3}} - 2} - \left[ \frac{1 - \frac{\alpha}{\left(\sqrt{\frac{3}{\lambda}} + \frac{\alpha}{\alpha\sqrt{\frac{\lambda}{3}} - 2}\right)} - \frac{\lambda}{3} \left(\sqrt{\frac{3}{\lambda}} + \frac{\alpha}{\alpha\sqrt{\frac{\lambda}{3}} - 2}\right)^2}{\frac{\alpha}{\left(\sqrt{\frac{3}{\lambda}} + \frac{\alpha}{\alpha\sqrt{\frac{\lambda}{3}} - 2}\right)^2} - \frac{2\lambda}{3} \left(\sqrt{\frac{3}{\lambda}} + \frac{\alpha}{\alpha\sqrt{\frac{\lambda}{3}} - 2}\right)} \right], \tag{15b}$$

etc., which satisfy the requirement that  $\beta = \beta(\alpha, \lambda)$ .

However, according to (14a) and (14b), when  $\lambda = 0$ ,  $\beta = \alpha = 2m$ , and when  $\alpha = 0$ ,  $\beta \neq \sqrt{\frac{3}{\lambda}}$ . According to (15a), (15b), when  $\lambda = 0$ ,  $\beta \neq \alpha = 2m$ , and when  $\alpha = 0$ ,  $\beta = \sqrt{\frac{3}{\lambda}}$ . The required form for  $\beta$ , and therefore the required form for  $C(D(r))$ , cannot be constructed, i.e. it does not exist. There is no way  $C(D(r))$  can be constructed to satisfy all the required conditions to render an admissible solution to (7) in the form of (3). Therefore, the assumption that  $\lambda \neq 0$  is incorrect, and so  $\lambda = 0$ . This can be confirmed in the following way.

The proper radius  $R_p(r)$  of (8) is given by,

$$R_p(r) = \int \frac{d\sqrt{F}}{\sqrt{1 - \frac{\lambda}{3}F}} = \sqrt{\frac{3}{\lambda}} \arcsin \sqrt{\frac{\lambda}{3}F(r)} + K,$$

where  $K$  is a constant. Now, the following condition must be satisfied,

$$\text{as } r \rightarrow r_0^\pm, R_p \rightarrow 0^\pm,$$

and therefore,

$$R_p(r_0) = 0 = \sqrt{\frac{3}{\lambda}} \arcsin \sqrt{\frac{\lambda}{3}F(r_0)} + K,$$

and so,

$$R_p(r) = \sqrt{\frac{3}{\lambda}} \left[ \arcsin \sqrt{\frac{\lambda}{3} F(r)} - \arcsin \sqrt{\frac{\lambda}{3} F(r_0)} \right]. \quad (16)$$

According to (8),

$$g_{00}(r_0) = 0 \Rightarrow F(r_0) = \frac{3}{\lambda}.$$

But then, by (16),

$$\begin{aligned} \sqrt{\frac{\lambda}{3} F(r)} &\equiv 1, \\ R_p(r) &\equiv 0. \end{aligned}$$

Indeed, by (16),

$$\sqrt{\frac{\lambda}{3} F(r_0)} \leq \sqrt{\frac{\lambda}{3} F(r)} \leq 1,$$

or

$$\sqrt{\frac{3}{\lambda}} \leq \sqrt{F(r)} \leq \sqrt{\frac{3}{\lambda}},$$

and so

$$F(r) \equiv \frac{3}{\lambda}, \quad (17)$$

and

$$R_p(r) \equiv 0. \quad (18)$$

Then  $F'(D(r)) \equiv 0$ , and so there exists no function  $F(r)$  which renders a solution to (8) in the form of (3) when  $\lambda \neq 0$  and therefore there exists no function  $C(D(r))$  which renders a solution to (7) in the form of (3) when  $\lambda \neq 0$ . Consequently,  $\lambda = 0$ .

Owing to their erroneous assumptions about the  $r$ -parameter, the relativists have disregarded the requirement that  $A, B, C > 0$  in (3) must be met. If the required form (3) is relaxed, in which case the resulting metric is *non-Einstein*, and cannot therefore describe an Einstein universe, (8) can be written as,

$$ds^2 = -\frac{3}{\lambda} (d\theta^2 + \sin^2 \theta d\varphi^2). \quad (8b)$$

This means that metric (8)  $\equiv$  (8b) maps the whole of  $(M_s, g_s)$  into the point  $R_p(D(r)) \equiv 0$  of the de Sitter “space”  $(M_{ds}, g_{ds})$ .

Einstein, de Sitter, Eddington, Friedmann, and the modern relativists all, have incorrectly *assumed* that  $r$  is a radial coordinate in (8), and consequently think of the “space” associated with (8) as extended in the sense of having a volume greater than zero. This is incorrect.

The radius of curvature of the point  $R_p(D(r)) \equiv 0$  is,

$$R_c(D(r)) \equiv \sqrt{\frac{3}{\lambda}}.$$

The “surface area” of the point is,

$$A = \frac{12\pi}{\lambda}.$$

De Sitter’s empty spherical universe has zero volume. Indeed, by (8) and (8b),

$$V = \lim_{r \rightarrow \pm\infty} \frac{3}{\lambda} \int_{r_0}^r 0 \, dr \int_0^\pi \sin \theta \, d\theta \int_0^{2\pi} d\varphi = 0,$$

consequently, de Sitter’s empty spherical universe is indeed “empty”; and meaningless. It is *not* an Einstein universe.

On (8) and (8b) the ratio,

$$\frac{2\pi \sqrt{F(r)}}{R_p(r)} = \infty \quad \forall r.$$

Therefore, the lone point which constitutes the empty de Sitter “universe”  $(M_{ds}, g_{ds})$  is a quasiregular singularity and consequently cannot be extended.

It is the unproven and invalid assumptions about the variable  $r$  which have lead the relativists astray. They have carried this error through all their work and consequently have completely lost sight of legitimate scientific theory, producing all manner of nonsense along the way. Eddington [4], for instance, writes in relation to (1),  $\gamma = 1 - \frac{2m}{r} - \frac{\alpha r^2}{3}$  for his equation (45.3), and said,

*At a place where  $\gamma$  vanishes there is an impassable barrier; since any change  $dr$  corresponds to an infinite distance *ids* surveyed by measuring rods. The two positive roots of the cubic (45.3) are approximately*

$$r = 2m \quad \text{and} \quad r = \sqrt{\left(\frac{3}{\alpha}\right)}.$$

*The first root would represent the boundary of the particle – if a genuine particle could exist – and give it the appearance of impenetrability. The second barrier is at a very great distance and may be described as the horizon of the world.*

Note that Eddington, despite these erroneous claims, did not admit the sacred black hole. His arguments however, clearly betray his assumption that  $r$  is a radius on (1). I also note that he has set the constant numerator of the middle term of his  $\gamma$  to  $2m$ , as is usual, however, like all the modern relativists, he did not indicate how this identity is to be achieved. This is just another assumption. As Abrams [6] has pointed out in regard to (1), one cannot appeal to far-field Keplerian orbits to fix the constant to  $2m$  – but the issue is moot, since  $\lambda = 0$ .

There is no black hole associated with (1). The Lake-Roeder black hole is inconsistent with Einstein’s theory.

#### 4 The homogeneous static models

It is routinely alleged by the relativists that the static homogeneous cosmological models are exhausted by the line-elements of Einstein's cylindrical model, de Sitter's spherical model, and that of Special Relativity. This is not correct, as I shall now demonstrate that the only homogeneous universe admitted by Einstein's theory is that of his Special Theory of Relativity, which is a static, infinite, pseudo-Euclidean, empty world.

The cosmological models of Einstein and de Sitter are composed of a single world line and a single point respectively, neither of which can be extended. Their line-elements therefore *cannot* describe any Einstein universe.

If the Universe is considered as a continuous distribution of matter of proper macroscopic density  $\rho_{00}$  and pressure  $P_0$ , the stress-energy tensor is,

$$T_1^1 = T_2^2 = T_3^3 = -P_0, \quad T_4^4 = \rho_{00},$$

$$T_\nu^\mu = 0, \quad \mu \neq \nu.$$

Rewrite (5) by setting,

$$A^*(r^*) = e^\nu, \quad \nu = \nu(r^*),$$

$$B^*(r^*) = e^\sigma, \quad \sigma = \sigma(r^*). \quad (19)$$

Then (5) becomes,

$$ds^2 = e^\nu dt^2 - e^\sigma dr^{*2} - r^{*2} (d\theta^2 + \sin^2 \theta d\varphi^2). \quad (20)$$

It then follows in the usual way that,

$$8\pi P_0 = e^{-\sigma} \left( \frac{\bar{\nu}}{r^*} + \frac{1}{r^{*2}} \right) - \frac{1}{r^{*2}} + \lambda, \quad (21)$$

$$8\pi \rho_{00} = e^{-\sigma} \left( \frac{\bar{\sigma}}{r^*} - \frac{1}{r^{*2}} \right) + \frac{1}{r^{*2}} - \lambda, \quad (22)$$

$$\frac{dP_0}{dr^*} = -\frac{\rho_{00} + P_0}{2} \bar{\nu}, \quad (23)$$

where

$$\bar{\nu} = \frac{d\nu}{dr^*}, \quad \bar{\sigma} = \frac{d\sigma}{dr^*}.$$

Since  $P_0$  is to be the same everywhere, (23) becomes,

$$\frac{\rho_{00} + P_0}{2} \bar{\nu} = 0.$$

Therefore, the following three possibilities arise,

1.  $\frac{d\nu}{dr^*} = 0$ ;
2.  $\rho_{00} + P_0 = 0$ ;
3.  $\frac{d\nu}{dr^*} = 0$  and  $\rho_{00} + P_0 = 0$ .

The 1st possibility yields Einstein's so-called cylindrical model, the 2nd yields de Sitter's so-called spherical model, and the 3rd yields Special Relativity.

#### 5 Einstein's cylindrical cosmological model

In this case, to reduce to Special Relativity,

$$\nu = \text{const} = 0.$$

Therefore, by (21),

$$8\pi P_0 = \frac{e^{-\sigma}}{r^{*2}} - \frac{1}{r^{*2}} + \lambda,$$

and by (19),

$$8\pi P_0 = \frac{1}{B^*(r^*)r^{*2}} - \frac{1}{r^{*2}} + \lambda,$$

and by (4),

$$8\pi P_0 = \frac{1}{BC} - \frac{1}{C} + \lambda,$$

so

$$\frac{1}{B} = 1 - (\lambda - 8\pi P_0) C,$$

$$C = C(D(r)), \quad D(r) = |r - r_0|, \quad B = B(D(r)),$$

$$r_0 \in \mathfrak{R}.$$

Consequently, Einstein's line-element can be written as,

$$ds^2 = dt^2 - [1 - (\lambda - 8\pi P_0) C]^{-1} d\sqrt{C}^2 - C (d\theta^2 + \sin^2 \theta d\varphi^2) = dt^2 - [1 - (\lambda - 8\pi P_0) C]^{-1} \frac{C'^2}{4C} dr^2 - C (d\theta^2 + \sin^2 \theta d\varphi^2), \quad (24)$$

$$C = C(D(r)), \quad D(r) = |r - r_0|, \quad r_0 \in \mathfrak{R},$$

where  $r_0$  is arbitrary.

It is now required to determine the admissible form of  $C(D(r))$ .

Clearly, if  $C' \equiv 0$ , then  $B = 0 \forall r$ , in violation of (3). Therefore,  $C' \neq 0 \forall r \neq r_0$ .

When  $P_0 = \lambda = 0$ , (24) must reduce to Special Relativity, in which case,

$$P_0 = \lambda = 0 \Rightarrow C(D(r)) = |r - r_0|^2.$$

The metric (24) is singular when  $g_{11}^{-1}(r_0) = 0$ , i.e. when,

$$1 - (\lambda - 8\pi P_0) C(r_0) = 0,$$

$$\Rightarrow C(r_0) = \frac{1}{\lambda - 8\pi P_0}. \quad (25)$$

Therefore, for  $C(D(r))$  to render an admissible solution to (24) in the form of (3), it must at least satisfy the following conditions:

1.  $C' \neq 0 \forall r \neq r_0$ ;
2.  $P_0 = \lambda = 0 \Rightarrow C(D(r)) = |r - r_0|^2$ ;
3.  $C(r_0) = \frac{1}{\lambda - 8\pi P_0}$ .

Now the proper radius on (24) is,

$$R_p(r) = \int \frac{d\sqrt{C}}{\sqrt{1 - (\lambda - 8\pi P_0)C}} = \frac{1}{\sqrt{\lambda - 8\pi P_0}} \arcsin \sqrt{(\lambda - 8\pi P_0)C(r)} + K, \\ K = \text{const.},$$

which must satisfy the condition,

$$\text{as } r \rightarrow r_0^\pm, R_p \rightarrow 0^+.$$

Therefore,

$$R_p(r_0) = 0 = \frac{1}{\sqrt{\lambda - 8\pi P_0}} \times \arcsin \sqrt{(\lambda - 8\pi P_0)C(r_0)} + K,$$

so

$$R_p(r) = \frac{1}{\sqrt{\lambda - 8\pi P_0}} \left[ \arcsin \sqrt{(\lambda - 8\pi P_0)C(r)} - \arcsin \sqrt{(\lambda - 8\pi P_0)C(r_0)} \right]. \tag{26}$$

Now it follows from (26) that,

$$\sqrt{(\lambda - 8\pi P_0)C(r_0)} \leq \sqrt{(\lambda - 8\pi P_0)C(r)} \leq 1,$$

so

$$C(r_0) \leq C(r) \leq \frac{1}{(\lambda - 8\pi P_0)},$$

and therefore by (25),

$$\frac{1}{(\lambda - 8\pi P_0)} \leq C(r) \leq \frac{1}{(\lambda - 8\pi P_0)}.$$

Thus,

$$C(r) \equiv \frac{1}{(\lambda - 8\pi P_0)},$$

and so  $C'(r) \equiv 0 \Rightarrow B(r) \equiv 0$ , in violation of (3). Therefore there exists no  $C(D(r))$  to satisfy (24) in the form of (3) when  $\lambda \neq 0, P_0 \neq 0$ . Consequently,  $\lambda = P_0 = 0$ , and (24) reduces to,

$$ds^2 = dt^2 - \frac{C'^2}{4C} dr^2 - C (d\theta^2 + \sin^2 \theta d\varphi^2). \tag{27}$$

The form of  $C(D(r))$  must still be determined.

Clearly, if  $C' \equiv 0, B(D(r)) = 0 \forall r$ , in violation of (3). Therefore,  $C' \neq 0 \forall r \neq r_0$ .

Since there is no matter present, it is required that,

$$C(r_0) = 0 \quad \text{and} \quad \frac{C(D(r))}{|r - r_0|^2} = 1.$$

This requires trivially that,

$$C(D(r)) = |r - r_0|^2.$$

Therefore (27) becomes,

$$ds^2 = dt^2 - \frac{(r - r_0)^2}{|r - r_0|^2} dr^2 - |r - r_0|^2 (d\theta^2 + \sin^2 \theta d\varphi^2) = dt^2 - dr^2 - |r - r_0|^2 (d\theta^2 + \sin^2 \theta d\varphi^2),$$

which is precisely the metric of Special Relativity, according to the natural reduction on (2).

If the required form (3) is relaxed, in which case the resulting metric is *not* an Einstein metric, Einstein's cylindrical line-element is,

$$ds^2 = dt^2 - \frac{1}{(\lambda - 8\pi P_0)} (d\theta^2 + \sin^2 \theta d\varphi^2). \tag{28}$$

This is a line-element which cannot describe an Einstein universe. The Einstein space described by (28) consists of only one "world line", through the point,

$$R_p(r) \equiv 0.$$

The spatial extent of (28) is a single point. The radius of curvature of this point space is,

$$R_c(r) \equiv \frac{1}{\sqrt{\lambda - 8\pi P_0}}.$$

For all  $r$ , the ratio  $\frac{2\pi R_c}{R_p}$  is,

$$\frac{2\pi}{\sqrt{\lambda - 8\pi P_0} R_p(r)} = \infty.$$

Therefore  $R_p(r) \equiv 0$  is a quasiregular singular point and consequently cannot be extended.

The "surface area" of this point space is,

$$A = \frac{4\pi}{\lambda - 8\pi P_0}.$$

The volume of the point space is,

$$V = \lim_{r \rightarrow \pm\infty} \frac{1}{(\lambda - 8\pi P_0)} \int_0^r dr \int_0^\pi \sin \theta d\theta \int_0^{2\pi} d\varphi = 0.$$

Equation (28) maps the whole of  $(M_s, g_s)$  into a quasiregular singular "world line".

Einstein's so-called "cylindrical universe" is meaningless. It does not contain a black hole.

### 6 De Sitter's spherical cosmological model

In this case,

$$\rho_{00} + P_0 = 0.$$

Adding (21) to (22) and setting to zero gives,

$$8\pi(\rho_{00} + P_0) = e^{-\sigma} \left( \frac{\bar{\sigma}}{r^*} + \frac{\bar{\nu}}{r^*} \right) = 0,$$

or

$$\bar{\nu} = -\bar{\sigma}.$$

Therefore,

$$\nu(r^*) = -\sigma(r^*) + \ln K_1, \quad (29)$$

$$K_1 = \text{const.}$$

Since  $\rho_{00}$  is required to be a constant independent of position, equation (22) can be immediately integrated to give,

$$e^{-\sigma} = 1 - \frac{\lambda + 8\pi\rho_{00}}{3} r^{*2} + \frac{K_2}{r^*}, \quad (30)$$

$$K_2 = \text{const.}$$

According to (30),

$$-\sigma = \ln \left( 1 - \frac{\lambda + 8\pi\rho_{00}}{3} r^{*2} + \frac{K_2}{r^*} \right),$$

and therefore, by (29),

$$\nu = \ln \left[ \left( 1 - \frac{\lambda + 8\pi\rho_{00}}{3} r^{*2} + \frac{K_2}{r^*} \right) K_1 \right].$$

Substituting into (20) gives,

$$ds^2 = \left[ \left( 1 - \frac{\lambda + 8\pi\rho_{00}}{3} r^{*2} + \frac{K_2}{r^*} \right) K_1 \right] dt^2 - \left( 1 - \frac{\lambda + 8\pi\rho_{00}}{3} r^{*2} + \frac{K_2}{r^*} \right)^{-1} dr^{*2} - r^{*2} (d\theta^2 + \sin^2 \theta d\varphi^2),$$

which is, by (4),

$$ds^2 = \left[ \left( 1 - \frac{\lambda + 8\pi\rho_{00}}{3} C + \frac{K_2}{\sqrt{C}} \right) K_1 \right] dt^2 - \left( 1 - \frac{\lambda + 8\pi\rho_{00}}{3} C + \frac{K_2}{\sqrt{C}} \right)^{-1} \frac{C'^2}{4C} dr^2 - C (d\theta^2 + \sin^2 \theta d\varphi^2). \quad (31)$$

Now, when  $\lambda = \rho_{00} = 0$ , equation (31) must reduce to the metric for Special Relativity. Therefore,

$$K_1 = 1, \quad K_2 = 0,$$

and so de Sitter's line-element is,

$$ds^2 = \left( 1 - \frac{\lambda + 8\pi\rho_{00}}{3} C \right) dt^2 - \left( 1 - \frac{\lambda + 8\pi\rho_{00}}{3} C \right)^{-1} \frac{C'^2}{4C} dr^2 - C (d\theta^2 + \sin^2 \theta d\varphi^2), \quad (32)$$

$$C = C(D(r)), \quad D(r) = |r - r_0|, \quad r_0 \in \mathfrak{R},$$

where  $r_0$  is arbitrary.

It remains now to determine the admissible form of  $C(D(r))$  to render a solution to equation (32) in the form of equation (3).

If  $C' \equiv 0$ , then  $B(D(r)) = 0 \forall r$ , in violation of (3). Therefore  $C' \neq 0 \forall r \neq r_0$ .

When  $\lambda = \rho_{00} = 0$ , (32) must reduce to that for Special Relativity. Therefore,

$$\lambda = \rho_{00} = 0 \Rightarrow C(D(r)) = |r - r_0|^2.$$

Metric (32) is singular when  $g_{00}(r_0) = 0$ , i.e. when

$$1 - \frac{\lambda + 8\pi\rho_{00}}{3} C(r_0) = 0, \Rightarrow C(r_0) = \frac{3}{\lambda + 8\pi\rho_{00}}. \quad (33)$$

Therefore, to render a solution to (32) in the form of (3),  $C(D(r))$  must at least satisfy the following conditions:

1.  $C' \neq 0 \forall r \neq r_0$ ;
2.  $\lambda = \rho_{00} = 0 \Rightarrow C(D(r)) = |r - r_0|^2$ ;
3.  $C(r_0) = \frac{3}{\lambda + 8\pi\rho_{00}}$ .

The proper radius on (32) is,

$$R_p(r) = \int \frac{d\sqrt{C}}{\sqrt{1 - \left( \frac{\lambda + 8\pi\rho_{00}}{3} \right) C}} = \sqrt{\frac{3}{\lambda + 8\pi\rho_{00}}} \arcsin \sqrt{\left( \frac{\lambda + 8\pi\rho_{00}}{3} \right) C(r) + K}, \quad (34)$$

$$K = \text{const},$$

which must satisfy the condition,

$$\text{as } r \rightarrow r_0^\pm, R_p(r) \rightarrow 0^+.$$

Therefore,

$$R_p(r_0) = 0 = \sqrt{\frac{3}{\lambda + 8\pi\rho_{00}}} \arcsin \sqrt{\left( \frac{\lambda + 8\pi\rho_{00}}{3} \right) C(r_0) + K},$$

so (34) becomes,

$$R_p(r) = \sqrt{\frac{3}{\lambda + 8\pi\rho_{00}}} \left[ \arcsin \sqrt{\left(\frac{\lambda + 8\pi\rho_{00}}{3}\right) C(r)} - \arcsin \sqrt{\left(\frac{\lambda + 8\pi\rho_{00}}{3}\right) C(r_0)} \right]. \tag{35}$$

It then follows from (35) that,

$$\sqrt{\left(\frac{\lambda + 8\pi\rho_{00}}{3}\right) C(r_0)} \leq \sqrt{\left(\frac{\lambda + 8\pi\rho_{00}}{3}\right) C(r)} \leq 1,$$

or

$$C(r_0) \leq C(r) \leq \frac{3}{\lambda + 8\pi\rho_{00}}.$$

Then, by (33),

$$\frac{3}{\lambda + 8\pi\rho_{00}} \leq C(r) \leq \frac{3}{\lambda + 8\pi\rho_{00}}.$$

Therefore,  $C(r)$  is a constant function for all  $r$ ,

$$C(r) \equiv \frac{3}{\lambda + 8\pi\rho_{00}}, \tag{36}$$

and so,

$$C'(r) \equiv 0,$$

which implies that  $B(D(r)) \equiv 0$ , in violation of (3). Consequently, there exists no function  $C(D(r))$  to render a solution to (32) in the form of (3). Therefore,  $\lambda = \rho_{00} = 0$ , and (32) reduces to the metric of Special Relativity in the same way as does (24).

If the required form (3) is relaxed, in which case the resulting metric is *not* an Einstein metric, de Sitter's line-element is,

$$ds^2 = -\frac{3}{\lambda + 8\pi\rho_{00}} (d\theta^2 + \sin^2 \theta d\varphi^2). \tag{37}$$

This line-element cannot describe an Einstein universe. The Einstein space described by (37) consists of only one point:

$$R_p(r) \equiv 0.$$

The radius of curvature of this point is,

$$R_c(r) \equiv \sqrt{\frac{3}{\lambda + 8\pi\rho_{00}}},$$

and the "surface area" of the point is,

$$A = \frac{12\pi}{\lambda + 8\pi\rho_{00}}.$$

The volume of de Sitter's "spherical universe" is,

$$V = \left(\frac{3}{\lambda + 8\pi\rho_{00}}\right) \lim_{r \rightarrow \pm\infty} \int_{r_0}^r dr \int_0^\pi \sin \theta d\theta \int_0^{2\pi} d\varphi = 0.$$

For all values of  $r$ , the ratio,

$$\frac{2\pi \sqrt{\frac{3}{\lambda + 8\pi\rho_{00}}}}{R_p(r)} = \infty.$$

Therefore,  $R_p(r) \equiv 0$  is a quasiregular singular point and consequently cannot be extended.

According to (32), metric (37) maps the whole of  $(M_s, g_s)$  into a quasiregular singular point.

Thus, de Sitter's spherical universe is meaningless. It does not contain a black hole.

When  $\rho_{00} = 0$  and  $\lambda \neq 0$ , de Sitter's empty universe is obtained from (37). I have already dealt with this case in section 3.

### 7 The infinite static homogeneous universe of special relativity

In this case, by possibility 3 in section 4,

$$\bar{\nu} = \frac{d\nu}{dr^*} = 0, \quad \text{and} \quad \rho_{00} + P_0 = 0.$$

Therefore,

$$\nu = \text{const} = 0 \quad \text{by section 5}$$

and

$$\bar{\sigma} = -\bar{\nu} \quad \text{by section 6.}$$

Hence, also by section 6,

$$\sigma = -\nu = 0.$$

Therefore, (20) becomes,

$$ds^2 = dt^2 - dr^{*2} - r^{*2} (d\theta^2 + \sin^2 \theta d\varphi^2),$$

which becomes, by using (4),

$$ds^2 = dt^2 - \frac{C'^2}{4C} dr^2 - C (d\theta^2 + \sin^2 \theta d\varphi^2),$$

$$C = C(D(r)), \quad D(r) = |r - r_0|, \quad r_0 \in \mathfrak{R},$$

which, by the analyses in sections 5 and 6, becomes,

$$ds^2 = dt^2 - \frac{(r - r_0)^2}{|r - r_0|^2} dr^2 - |r - r_0|^2 (d\theta^2 + \sin^2 \theta d\varphi^2), \tag{38}$$

$$r_0 \in \mathfrak{R},$$

which is the flat, empty, and infinite spacetime of Special Relativity, obtained from (2) by natural reduction.

When  $r_0 = 0$  and  $r \geq r_0$ , (38) reduces to the usual form used by the relativists,

$$ds^2 = dt^2 - dr^2 - r^2 (d\theta^2 + \sin^2 \theta d\varphi^2) .$$

The radius of curvature of (38) is,

$$D(r) = |r - r_0| .$$

The proper radius of (38) is,

$$R_p(r) = \int_0^{|r-r_0|} d|r - r_0| = \int_{r_0}^r \frac{(r - r_0)}{|r - r_0|} dr = |r - r_0| \equiv D .$$

The ratio,

$$\frac{2\pi D(r)}{R_p(r)} = \frac{2\pi|r - r_0|}{|r - r_0|} = 2\pi \forall r .$$

Thus, only (38) can represent a static homogeneous universe in Einstein's theory, contrary to the claims of the modern relativists. However, since (38) contains no matter it cannot model the universe other than locally.

### 8 Cosmological models of expansion

In view of the foregoing it is now evident that the models proposed by the relativists purporting an expanding universe are also untenable in the framework of Einstein's theory. The line-element obtained by the Abbé Lemaître and by Robertson, for instance, is inadmissible. Under the false assumption that  $r$  is a radius in de Sitter's spherical universe, they proposed the following transformation of coordinates on the metric (32) (with  $\rho_{00} \neq 0$  in the misleading form given in formula 9),

$$\bar{r} = \frac{r}{\sqrt{1 - \frac{r^2}{W^2}}} e^{-\frac{t}{W}}, \quad \bar{t} = t + \frac{1}{2} W \ln \left( 1 - \frac{r^2}{W^2} \right) , \quad (39)$$

$$W^2 = \frac{\lambda + 8\pi\rho_{00}}{3} ,$$

to get

$$ds^2 = d\bar{t}^2 - e^{\frac{2\bar{t}}{W}} (d\bar{r}^2 + \bar{r}^2 d\theta^2 + \bar{r}^2 \sin^2 \theta d\varphi^2) ,$$

or, by dropping the bar and setting  $k = \frac{1}{W}$ ,

$$ds^2 = dt^2 - e^{2kt} (dr^2 + r^2 d\theta^2 + r^2 \sin^2 \theta d\varphi^2) . \quad (40)$$

Now, as I have shown, (32) has no solution in  $C(D(r))$  in the form (3), so transformations (39) and metric (40) are meaningless concoctions of mathematical symbols. Owing to

their false assumptions about the parameter  $r$ , the relativists mistakenly think that  $C(D(r)) \equiv r^2$  in (32). Furthermore, if the required form (3) is relaxed, thereby producing *non-Einstein metrics*, de Sitter's "spherical universe" is given by (37), and so, by (35), (36), and (40),

$$C(D(r)) = r^2 \equiv \frac{\lambda + 8\pi\rho_{00}}{3} ,$$

and the transformations (39) and metric (40) are again utter nonsense. The Lemaître-Robertson line-element is inevitably, unmitigated claptrap. This can be proved generally as follows.

The most general non-static line-element is

$$ds^2 = A(D, t) dt^2 - B(D, t) dD^2 - C(D, t) (d\theta^2 + \sin^2 \theta d\varphi^2) , \quad (41)$$

$$D = |r - r_0|, \quad r_0 \in \mathfrak{R}$$

where analytic  $A, B, C > 0 \forall r \neq r_0$  and  $\forall t$ .

Rewrite (41) by setting,

$$\begin{aligned} A(D, t) &= e^\nu, \quad \nu = \nu(G(D), t), \\ B(D, t) &= e^\sigma, \quad \sigma = \sigma(G(D), t), \\ C(D, t) &= e^\mu G^2(D), \quad \mu = \mu(G(D), t), \end{aligned}$$

to get

$$ds^2 = e^\nu dt^2 - e^\sigma dG^2 - e^\mu G^2(D) (d\theta^2 + \sin^2 \theta d\varphi^2) . \quad (42)$$

Now set,

$$r^* = G(D(r)) , \quad (43)$$

to get

$$ds^2 = e^\nu dt^2 - e^\sigma dr^{*2} - e^\mu r^{*2} (d\theta^2 + \sin^2 \theta d\varphi^2) , \quad (44)$$

$$\nu = \nu(r^*, t), \quad \sigma = \sigma(r^*, t), \quad \mu = \mu(r^*, t) .$$

One then finds in the usual way that the solution to (44) is,

$$ds^2 = dt^2 - \frac{e^{g(t)}}{\left(1 + \frac{k}{4} r^{*2}\right)^2} \times [dr^{*2} + r^{*2} (d\theta^2 + \sin^2 \theta d\varphi^2)] , \quad (45)$$

where  $k$  is a constant.

Then by (43) this becomes,

$$ds^2 = dt^2 - \frac{e^{g(t)}}{\left(1 + \frac{k}{4} G^2\right)^2} [dG^2 + G^2 (d\theta^2 + \sin^2 \theta d\varphi^2)] ,$$

or,

$$ds^2 = dt^2 - \frac{e^{g(t)}}{\left(1 + \frac{k}{4} G^2\right)^2} \times [G'^2 dr^2 + G^2 (d\theta^2 + \sin^2 \theta d\varphi^2)] , \quad (46)$$



$$G' = \frac{dG}{dr},$$

$$G = G(D(r)), \quad D(r) = |r - r_0|, \quad r_0 \in \mathfrak{R}.$$

The admissible form of  $G(D(r))$  must now be determined.

If  $G' \equiv 0$ , then  $B(D, t) = 0 \forall r$  and  $\forall t$ , in violation of (41). Therefore  $G' \neq 0 \forall r \neq r_0$ .

Metric (46) is singular when,

$$1 + \frac{k}{4}G^2(r_0) = 0, \\ \Rightarrow G(r_0) = \frac{2}{\sqrt{-k}} \Rightarrow k < 0. \quad (47)$$

The proper radius on (46) is,

$$R_p(r, t) = e^{\frac{1}{2}g(t)} \int \frac{dG}{1 + \frac{k}{4}G^2} = \\ = e^{\frac{1}{2}g(t)} \left( \frac{2}{\sqrt{k}} \arctan \frac{\sqrt{k}}{2}G(r) + K \right), \\ K = \text{const},$$

which must satisfy the condition,

$$\text{as } r \rightarrow r_0^\pm, \quad R_p \rightarrow 0^+.$$

Therefore,

$$R_p(r_0, t) = e^{\frac{1}{2}g(t)} \left( \frac{2}{\sqrt{k}} \arctan \frac{\sqrt{k}}{2}G(r_0) + K \right) = 0,$$

and so

$$R_p(r, t) = e^{\frac{1}{2}g(t)} \frac{2}{\sqrt{k}} \left[ \arctan \frac{\sqrt{k}}{2}G(r) - \arctan \frac{\sqrt{k}}{2}G(r_0) \right]. \quad (48)$$

Then by (47),

$$R_p(r, t) = e^{\frac{1}{2}g(t)} \frac{2}{\sqrt{k}} \left[ \arctan \frac{\sqrt{k}}{2}G(r) - \arctan \sqrt{-1} \right], \quad (49) \\ k < 0.$$

Therefore, there exists no function  $G(D(r))$  rendering a solution to (46) in the required form of (41).

The relativists however, owing to their invalid assumptions about the parameter  $r$ , write equation (46) as,

$$ds^2 = dt^2 - \frac{e^{g(t)}}{\left(1 + \frac{k}{4}r^2\right)^2} \left[ dr^2 + r^2 (d\theta^2 + \sin^2 \theta d\varphi^2) \right], \quad (50)$$

having assumed that  $G(D(r)) \equiv r$ , and erroneously take  $r$  as a radius on the metric (50), valid down to 0. Metric (50) is a meaningless concoction of mathematical symbols. Nevertheless, the relativists transform this meaningless expression with a meaningless change of ‘‘coordinates’’ to obtain the Robertson-Walker line-element, as follows.

Transform (46) by setting,

$$\bar{G}(\bar{r}) = \frac{G(r)}{1 + \frac{k}{4}G^2}.$$

This carries (46) into,

$$ds^2 = dt^2 - e^{g(t)} \left[ \frac{d\bar{G}^2}{(1 - \kappa \bar{G}^2)} + \bar{G}^2 (d\theta^2 + \sin^2 \theta d\varphi^2) \right]. \quad (51)$$

This is easily seen to be the familiar Robertson-Walker line-element if, following the relativists, one incorrectly assumes  $\bar{G} \equiv \bar{r}$ , disregarding the fact that the admissible form of  $\bar{G}$  must be ascertained. In any event (51) is meaningless, owing to the meaninglessness of (50), which I confirm as follows.

$\bar{G}' \equiv 0 \Rightarrow \bar{B} = 0 \forall \bar{r}$ , in violation of (41). Therefore  $\bar{G}' \neq 0 \forall \bar{r} \neq \bar{r}_0$ .

Equation (51) is singular when,

$$1 - k\bar{G}^2(\bar{r}_0) = 0 \Rightarrow \bar{G}(\bar{r}_0) = \frac{1}{\sqrt{k}} \Rightarrow k > 0. \quad (52)$$

The proper radius on (51) is,

$$\bar{R}_p = e^{\frac{1}{2}g(t)} \int \frac{d\bar{G}}{\sqrt{1 - k\bar{G}^2}} \\ = e^{\frac{1}{2}g(t)} \left( \frac{1}{\sqrt{k}} \arcsin \sqrt{k}\bar{G}(\bar{r}) + K \right), \\ K = \text{const},$$

which must satisfy the condition,

$$\text{as } \bar{r} \rightarrow \bar{r}_0^\pm, \quad \bar{R}_p \rightarrow 0^+,$$

so

$$\bar{R}_p(\bar{r}_0, t) = 0 = e^{\frac{1}{2}g(t)} \left( \frac{1}{\sqrt{k}} \arcsin \sqrt{k}\bar{G}(\bar{r}_0) + K \right).$$

Therefore,

$$\bar{R}_p(\bar{r}, t) = e^{\frac{1}{2}g(t)} \frac{1}{\sqrt{k}} \times \\ \times \left[ \arcsin \sqrt{k}\bar{G}(\bar{r}) - \arcsin \sqrt{k}\bar{G}(\bar{r}_0) \right]. \quad (53)$$

Then

$$\sqrt{k}\bar{G}(\bar{r}_0) \leq \sqrt{k}\bar{G}(\bar{r}) \leq 1,$$

or

$$\bar{G}(\bar{r}_0) \leq \bar{G}(\bar{r}) \leq \frac{1}{\sqrt{k}}.$$

Then by (52),

$$\frac{1}{\sqrt{k}} \leq \bar{G}(\bar{r}) \leq \frac{1}{\sqrt{k}},$$

so

$$\bar{G}(\bar{r}) \equiv \frac{1}{\sqrt{k}}.$$

Consequently,  $\bar{G}'(\bar{r}) = 0 \forall \bar{r}$  and  $\forall t$ , in violation of (41). Therefore, there exists no function  $\bar{G}(\bar{D}(\bar{r}))$  to render a solution to (51) in the required form of (41).

If the conditions on (41) are relaxed in the fashion of the relativists, non-Einstein metrics with expanding radii of curvature are obtained. Nonetheless the associated spaces have zero volume. Indeed, equation (40) becomes,

$$ds^2 = dt^2 - e^{2kt} \frac{(\lambda + 8\pi\rho_{00})}{3} (d\theta^2 + \sin^2\theta d\varphi^2). \quad (54)$$

This is not an Einstein universe. The radius of curvature of (54) is,

$$R_c(r, t) = e^{kt} \sqrt{\frac{\lambda + 8\pi\rho_{00}}{3}},$$

which expands or contracts with the sign of the constant  $k$ . Even so, the proper radius of the “space” of (54) is,

$$R_p(r, t) = \lim_{r \rightarrow \pm\infty} \int_{r_0}^r 0 \, dr \equiv 0.$$

The volume of this point-space is,

$$V = \lim_{r \rightarrow \pm\infty} e^{2kt} \frac{(\lambda + 8\pi\rho_{00})}{3} \int_{r_0}^r 0 \, dr \int_0^\pi \sin\theta \, d\theta \int_0^{2\pi} \equiv 0.$$

Metric (54) consists of a single “world line” through the point  $R_p(r, t) \equiv 0$ . Furthermore,  $R_p(r, t) \equiv 0$  is a quasi-regular singular point-space since the ratio,

$$\frac{2\pi e^{kt} \sqrt{\lambda + 8\pi\rho_{00}}}{\sqrt{3}R_p(r, t)} \equiv \infty.$$

Therefore,  $R_p(r, t) \equiv 0$  cannot be extended.

Similarly, equation (51) becomes,

$$ds^2 = dt^2 - \frac{e^{g(t)}}{k} (d\theta^2 + \sin^2\theta d\varphi^2), \quad (55)$$

which is not an Einstein metric. The radius of curvature of (55) is,

$$R_c(r, t) = \frac{e^{\frac{1}{2}g(t)}}{\sqrt{k}},$$

which changes with time. The proper radius is,

$$R_p(r, t) = \lim_{r \rightarrow \pm\infty} \int_{r_0}^r 0 \, dr \equiv 0,$$

and the volume of the point-space is

$$V = \lim_{r \rightarrow \pm\infty} \frac{e^{g(t)}}{k} \int_{r_0}^r 0 \, dr \int_0^\pi \sin\theta \, d\theta \int_0^{2\pi} \equiv 0.$$

Metric (55) consists of a single “world line” through the point  $R_p(r, t) \equiv 0$ . Furthermore,  $R_p(r, t) \equiv 0$  is a quasi-regular singular point-space since the ratio,

$$\frac{2\pi e^{\frac{1}{2}g(t)}}{\sqrt{k}R_p(r, t)} \equiv \infty.$$

Therefore,  $R_p(r, t) \equiv 0$  cannot be extended.

It immediately follows that the Friedmann models are all invalid, because the so-called Friedmann equation, with its associated equation of continuity,  $T_{;\mu}^{\mu\nu} = 0$ , is based upon metric (51), which, as I have proven, has *no solution* in  $\bar{G}(\bar{r})$  in the required form of (41). Furthermore, metric (55) cannot represent an Einstein universe and therefore has no cosmological meaning. Consequently, the Friedmann equation is also nothing more than a meaningless concoction of mathematical symbols, destitute of any physical significance whatsoever. Friedmann incorrectly assumed, just as the relativists have done all along, that the parameter  $r$  is a radius in the gravitational field. Owing to this erroneous assumption, his treatment of the metric for the gravitational field violates the inherent geometry of the metric and therefore violates the geometrical form of the pseudo-Riemannian spacetime manifold. The same can be said of Einstein himself, who did not understand the geometry of his own creation, and by making the same mistakes, failed to understand the implications of his theory.

Thus, the Friedmann models are all invalid, as is the Einstein-de Sitter model, and all other general relativistic cosmological models purporting an expansion of the universe. Furthermore, there is no general relativistic substantiation of the Big Bang hypothesis. Since the Big Bang hypothesis rests solely upon an invalid interpretation of General Relativity, it is abject nonsense. The standard interpretations of the Hubble-Humason relation and the cosmic microwave background are not consistent with Einstein’s theory. Einstein’s theory cannot form the basis of a cosmology.

### 9 Singular points in Einstein’s universe

It has been pointed out before [7, 8, 3] that singular points in Einstein’s universe are quasiregular. No curvature type

singularities arise in Einstein's universe. The oddity of a point being associated with a non-zero radius of curvature is an inevitable consequence of Einstein's geometry. There is *nothing* more pointlike in Einstein's universe, and nothing more pointlike in the de Sitter point world or the Einstein cylindrical world line. A point as it is usually conceived of in Minkowski space *does not exist* in Einstein's universe. The modern relativists have not understood this inescapable fact.

### Acknowledgements

I would like to extend my thanks to Dr. D. Rabounski and Dr. L. Borissova for their kind advice as to the clarification of my definitions and my terminology, manifest as section 2 herein.

### Dedication

I dedicate this paper to the memory of Dr. Leonard S. Abrams: (27 Nov. 1924 – 28 Dec. 2001).

### References

1. Stavroulakis N. On a paper by J. Smoller and B. Temple. *Annales de la Fondation Louis de Broglie*, 2002, v. 27, 3 (see also in [www.geocities.com/theometria/Stavroulakis-1.pdf](http://www.geocities.com/theometria/Stavroulakis-1.pdf)).
2. Stavroulakis N. On the principles of general relativity and the  $S\Theta(4)$ -invariant metrics. *Proc. 3rd Panhellenic Congr. Geometry*, Athens, 1997, 169 (see also in [www.geocities.com/theometria/Stavroulakis-2.pdf](http://www.geocities.com/theometria/Stavroulakis-2.pdf)).
3. Crothers S. J. On the geometry of the general solution for the vacuum field of the point-mass. *Progress in Physics*, 2005, v. 2, 3–14.
4. Eddington A. S. *The mathematical theory of relativity*. Cambridge University Press, Cambridge, 2nd edition, 1960.
5. Petrov A. Z. *Einstein spaces*. Pergamon Press, London, 1969.
6. Abrams L. S. The total space-time of a point-mass when  $\Lambda \neq 0$ , and its consequences for the Lake-Roeder black hole. *Physica A*, v. 227, 1996, 131–140 (see also in arXiv: gr-qc/0102053).
7. Brillouin M. The singular points of Einstein's Universe. *Journ. Phys. Radium*, 1923, v. 23, 43 (see also in arXiv: physics/0002009).
8. Abrams L. S. Black holes: the legacy of Hilbert's error. *Can. J. Phys.*, 1989, v. 67, 919 (see also in arXiv: gr-qc/0102055).

## The First Crisis in Cosmology Conference

Monção, Portugal, June 23–25 2005

Hilton Ratcliffe

*Astronomical Society of Southern Africa*

E-mail: ratcliff@iafrica.com

The author attended the first Crisis in Cosmology Conference of the recently associated Alternative Cosmology Group, and makes an informal report on the proceedings with some detail on selected presentations.

In May 2004, a group of about 30 concerned scientists published an open letter to the global scientific community in *New Scientist* in which they protested the stranglehold of Big Bang theory on cosmological research and funding. The letter was placed on the Internet\* and rapidly attracted wide attention. It currently has about 300 signatories representing scientists and researchers of disparate backgrounds, and has led to a loose association now known as the Alternative Cosmology Group†. This writer was one of the early signatories to the letter, and holding the view that the Big Bang explanation of the Universe is scientifically untenable, patently illogical, and without any solid observational support whatsoever, became involved in the organisation of an international forum where we could share ideas and plan our way forward. That idea became a reality with the staging of the *First Crisis in Cosmology Conference (CCC-1)* in the lovely, medieval walled village of Monção, far northern Portugal, over 3 days in June of this year.

It was sponsored in part by the University of Minho in Braga, Portugal, and the Institute for Advanced Studies at Austin, Texas. Professor José Almeida of the Department of Physics at the University of Minho was instrumental in the organisation and ultimate success of an event that is now to be held annually. The conference was arranged in 3 sessions. On the first day, papers were presented on observations that challenge the present model, the second day dealt with conceptual difficulties in the standard model, and we concluded with alternative cosmological world-views. Since it is not practicable here to review all the papers presented (some 34 in total, plus 6 posters), I'll selectively confine my comments to those that interested me particularly. The American Institute of Physics will publish the proceedings of the conference in their entirety in due course for those interested in the detail.

First up was professional astronomer Dr. Riccardo Scarpa of the European Southern Observatory, Santiago, Chile. His job involves working with the magnificent Very Large Telescope array at Paranal, and I guess that makes him the envy of just about every astronomer with blood in his veins!

His paper was on Modified Newtonian Dynamics (MOND), which I had eagerly anticipated and thoroughly appreciated. MOND is a very exciting development in observational astronomy used to make Dark Matter redundant in the explanation of cosmic gravitational effects like the anomalous rotational speeds of galaxies. Mordehai Milgrom of the Weizmann Institute in Israel first noticed that mass discrepancies in stellar systems are detected only when the internal acceleration of gravity falls below the well-established value  $a_0 = 1.2 \times 10^{-8} \text{ cm} \times \text{s}^{-2}$ . The standard Newtonian gravitational values fit perfectly above this threshold, and below  $a_0$  MOND posits a breakdown of Newton's law. The dependence then becomes linear with an asymptotic value of acceleration  $a = (a_0 g)^{1/2}$ , where  $g$  is the Newtonian value. Scarpa has called this the *weak gravitational regime*, and he and colleagues Marconi and Gilmozzi have applied it extensively to globular clusters with 100% success. What impressed me most was that the clear empirical basis of MOND has been thoroughly tested, and is now in daily use by professional astronomers at what is arguably the most sophisticated and advanced optical-infrared observatory in the world. In practice, there is no need to invoke Dark Matter. Quote from Riccardo: "*Dark Matter is the craziest idea we've ever had in astronomy. It can appear when you need it, it can do what you like, be distributed in any way you like. It is the fairy tale of astronomy*".

Big Bang theory depends critically on three first principles: that the Universe is holistically and systematically expanding as per the Friedmann model; that General Relativity correctly describes gravitation; and that Milne's Cosmological Principle, which declares that the Universe at some arbitrary "large scale" is isotropic and homogeneous, is true. The falsification of any one of these principles would lead to the catastrophic failure of the theory. We saw at the conference that all three can be successfully challenged on the basis of empirical science. Retired electrical engineer Tom Andrews presented a novel approach to the validation (or rather, invalidation) of the expanding Universe model. It is well known that type 1A supernovae (SNe) show measurable anomalous dimming (with distance or remoteness in time) in a flat expanding Universe model. Andrews used

\*<http://www.cosmologystatement.org/>

†<http://www.cosmology.info/>

observational data from two independent sets of measurements of brightest cluster galaxies (defined as the brightest galaxy in a cluster). It was expected, since the light from the SNe and the bright galaxies traverses the same space to get to us, that the latter should also be anomalously dimmed. They clearly are not. The orthodox explanation for SNe dimming — that it is the result of the progressive expansion of space — is thereby refuted. He puts a further nail in the coffin by citing Goldhaber's study of SNe light curves, which did not reveal the second predicted light-broadening effect due to time dilation. Says Andrews: "*The Hubble redshift of Fourier harmonic frequencies [for SNe] is shown to broaden the light curve at the observer by  $(1+z)$ . Since this broadening spreads the total luminosity over a longer time period, the apparent luminosity at the observer is decreased by the same factor. This accounts quantitatively for the dimming of SNe. On the other hand, no anomalous dimming occurs for galaxies since the luminosity remains constant over time periods much longer than the light travel time to the observer. This effect is consistent with the non-expanding Universe model. The expanding model is logically falsified*".

Professor Mike Disney of the School of Physics and Astronomy at Cardiff University calls a spade a spade. He has created an interesting benchmark for the evaluation of scientific models — he compares the number of free parameters in a theory with the number of independent measurements, and sets an arbitrary minimum of +3 for the excess of measurements over free parameters to indicate that the theory is empirically viable. He ran through the exercise for the Big Bang model, and arrived at a figure of -3 (17 free parameters against 14 measured). He therefore argued that there is little statistical significance in the good fits claimed by Big Bang cosmologists since the surfeit of free parameters can easily mould new data to fit a desired conclusion. Quote: "*The study of some 60 cultures, going back 12,000 years, shows that, like it or not, we will always have a cosmology, and there have always been more free parameters than independent measurements. The best model is a compromise between parsimony (Occam's razor) and goodness-of-fit*".

Disney has a case there, and it is amply illustrated when it comes to Big Bang Nucleosynthesis (which depends initially on an arbitrarily set baryon/photon ratio), and the abundances of chemical elements. Dr. Tom van Flandern is another straight talking, no frills man of science. He opened his abstract with the words "*The Big Bang has never achieved a true prediction success where the theory was placed at risk of falsification before the results were known*". Ten years ago, Tom's web site listed the Top Ten Problems with the Big Bang, and today he has limited it to the Top Fifty. He pointed out the following contradictions in predicted light element abundances: observed deuterium abundances don't tie up with observed abundances of  $^4\text{He}$  and  $^7\text{Li}$ , and attempts to explain this inconsistency have failed. The ratio

of deuterium to hydrogen near the centre of the Milky Way is 5 orders of magnitude higher than the Standard Model predicts, and measuring either for quasars produces deviation from predictions. Also problematic for BBN are barium and beryllium, produced assumedly as secondary products of supernovae by the process of spallation. However, observations of metal-poor stars show greater abundance of Be than possible by spallation. Van Flandern: "*It should be evident to objective minds that nothing about the Universe interpreted with the Big Bang theory is necessarily right, not even the most basic idea in it that the Universe is expanding*".

Problems in describing the geometry of the Universe were dealt with by several speakers, and we must here of course drill down a bit to where the notion came from (in the context of Big Bang theory). The theory originated in Father Georges Lemaitre's extensions to Friedmann's solution of the Einstein General Relativity (GR) field equations, which showed that the Universe described in GR could not be static as Einstein believed. From this starting point emerged some irksome dilemmas regarding the fundamental nature of space and the distribution of matter within it. It was here more than anywhere that the rich diversity of opinion and approach within the Alternative Cosmology Group was demonstrated. Professor Yuriy Baryshev of the Institute of Astronomy at St. Petersburg State University quietly presented his argument against the Cosmological Principle: large-scale structure is not possible in the Friedmann model, yet observation shows it for as far as we can see. I had recently read Yuriy's book *The Discovery of Cosmic Fractals*, and knew that he had studied the geometric fractals of Yale's famous Professor Benoit Mandelbrot, which in turn led to his extrapolation of a fractal (inhomogeneous, anisotropic) non-expanding large-scale universe. Baryshev discussed gravitation from the standpoint that the physics of gravity should be the focus of cosmological research. General Relativity and the Feynman field are different at all scales, although to date, all relativistic tests cannot distinguish between them. He pointed out that if one reversed the flow and shrunk the radius, eventually the point would be reached where the energy density of the Universe would exceed the rest mass, and that is logically impossible. He left us with this gem: Feynman to his wife (upon returning from a conference) "*Remind me not to attend any more gravity conferences!*"

Conference co-ordinator Professor José Almeida presented a well-argued case for an interesting and unusual worldview: a hyperspherical Universe of 4-D Euclidean space (called 4-Dimensional Optics or 4DO) rather than the standard non-Euclidean Minkowski space. Dr. Franco Selleri of the Università di Bari in Italy provided an equally interesting alternative — the certainty that the Universe in which we live and breathe is a construction in simple 3-D Euclidean space precludes the possibility of the Big Bang model. He says: "*No structure in three dimensional space, born from an explosion that occurred 10 to 20 billion years ago, could*

*resemble the Universe we observe*". The key to Selleri's theory is absolute simultaneity, obtained by using a term  $e_1$  (the coefficient of  $x$  in the transformation of time) in the Lorentz transformations, so that  $e_1 = 0$ . Setting  $e_1 = 0$  separates time and space, and a conception of reality is introduced in which no room is left for a fourth dimension. Both Big Bang and its progenitor General Relativity depend critically on 4-D Minkowski space, so the argument regressed even further to the viability of Relativity itself. And here is where the big guns come in!

World-renowned mathematical physicist Professor Huseyin Yilmaz, formerly of the Institute for Advanced Studies at Princeton University, and his hands-on experimentalist colleague Professor Carrol Alley of the University of Maryland, introduced us to the Yilmaz cosmology. Altogether 4 papers were presented at CCC-1 on various aspects of Yilmaz theory, and a fifth, by Dr. Hal Puthoff of the Institute for Advanced Studies at Austin, was brought to the conference but not presented. It is no longer controversial to suggest that GR has flaws, although I still feel awkward saying it out loud! Professor Yilmaz focussed on the fact that GR excludes gravitational stress-energy as a source of curvature. Consequently, stress-energy is merely a coordinate artefact in GR, whereas in the Yilmaz modification it is a true tensor. Hal Puthoff described the GR term to me as a "*pseudo-tensor, which can appear or disappear depending on how you treat mass*". The crucial implication of this, in the words of Professor Alley, is that since "*interactions are carried by the field stress energy, there are no interactive n-body solutions to the field equations of General Relativity*". In plain language, GR is a single-body description of gravity! The Yilmaz equations contain the correct terms, and they have been applied with success to various vexing problems, for example the precession of Mercury's perihelion, lunar laser ranging measurements, the flying of atomic clocks in aircraft, the relativistic behaviour of clocks in the GPS, and the predicted *Sagnac effect* in the one-way speed of light on a rotating table. Anecdote from Professor Alley: at a lecture by Einstein in the 1920's, Professor Sagnac was in the audience. He questioned Einstein on the *gedanken* experiment regarding contra-radiating light on a rotating plate. Einstein thought for a while and said, "That has got nothing to do with relativity". Sagnac loudly replied, "In that case, Dr. Einstein, relativity has got nothing to do with reality!"

The great observational "proof" of Big Bang theory is undoubtedly the grandly titled Cosmic Microwave Background Radiation, stumbled upon by radio engineers Penzias and Wilson in 1965, hijacked by Princeton cosmologist Jim Peebles, and demurely described by UC's COBE data analyst Dr. George Smoot as "*like looking at the fingerprint of God*". Well, it's come back to haunt them! I was delighted that despite some difficulties Glenn Starkman of Case Western Reserve University was able to get his paper presented

at the conference as I had been keenly following his work on the Wilkinson Microwave Anisotropy Probe (WMAP) data. Dr. Starkman has discovered some unexpected (for Big Bangers) characteristics (he describes them as "bizarre") in the data that have serious consequences for the Standard Model. Far from having the smooth, Gaussian distribution predicted by Big Bang, the microwave picture has distinct anisotropies, and what's more says Starkman, they are clearly aligned with local astrophysical structures, particularly the ecliptic of the Solar System. Once the dipole harmonic is stripped to remove the effect of the motion of the Solar System, the other harmonics, quadrupole, octopole, and so on reveal a distinct alignment with local objects, and show also a preferred direction towards the Virgo supercluster. Conference chair, plasma physicist Eric Lerner concurred in his paper. He suggested that the microwave background is nothing more than a radio fog produced by plasma filaments, which has reached a natural isotropic thermal equilibrium of just under 3K. The radiation is simply starlight that has been absorbed and re-radiated, and echoes the anisotropies of the world around us. These findings correlate with the results of a number of other independent studies, including that of Larson and Wandelt at the University of Illinois, and also of former Cambridge *enfant terrible* and current Imperial College theoretical physics prodigy, Professor João Magueijo. Quote from Starkman: "*This suggests that the reported microwave background fluctuations on large angular scales are not in fact cosmic, with important consequences*". Phew!

The final day saw us discussing viable alternative cosmologies, and here one inevitably leans towards personal preferences. My own bias is unashamedly towards scientists who adopt the classical empirical method, and there is no better example of this than Swedish plasma physics pioneer and Nobel laureate Hannes Alfvén. Consequently, I favoured the paper on Plasma Cosmology presented by Eric Lerner, and as a direct result of that inclination find it very difficult here to be brief! Lerner summarised the basic premises: most of the Universe is plasma, so the effect of electromagnetic force on a cosmic scale is at least comparable to gravitation. Plasma cosmology assumes no origin in time for the Universe, and can therefore accommodate the conservation of energy/matter. Since we see evidence of evolution all around us, we can assume evolution in the Universe, though not at the pace or on the scale of the Big Bang. Lastly, plasma cosmology tries to explain as much of the Universe as possible using known physics, and does not invoke assistance from supernatural elements. Plasmas are scale invariant, so we can safely infer large-scale plasma activity from what we see terrestrially. Gravity acts on filaments, which condense into "blobs" and disks form. As the body contracts, it gets rid of angular momentum which is conducted away by plasma. Lerner's colleague Anthony Peratt of Los Alamos Laboratory modelled plasma interaction on a computer and has arrived

**The First Crisis in Cosmology Conference, Monção, Portugal, June 23–25 2005**  
**Schedule of Presentations**

Name	Location	Paper Title
Antonio Alfonso-Faus aalfonsofaus@yahoo.es	Madrid Polytech. Univ., Spain	Mass boom vs Big Bang
Carrol Alley coalley@physics.umd.edu	Univ. of Maryland, USA	Going “beyond Einstein” with Yilmaz theory
José Almeida bda@fisica.uminho.pt	Universidade do Minho	Geometric drive of Universal expansion
Thomas Andrews tba@xoba.com	USA	Falsification of the expanding Universe model
Yurij Baryshev yuba@astro.spbu.ru	St. Petersburg Univ., Russia	Conceptual problems of the standard cosmological model
Yurij Baryshev yuba@astro.spbu.ru	St. Petersburg Univ., Russia	Physics of gravitational interaction
Alain Blanchard alain.blanchard@ast.obs-mip.fr	Lab. d’Astrophys. Toulouse, France	The Big Bang picture: a wonderful success of modern science
M. de Campos campos@dfis.ufrr.br	Univ. Federal de Roraima, Brazil	The Dyer-Roeder relation
George Chapline chapline1@llnl.gov	Lawrence Livermore National Lab., USA	Tommy Gold revisited
Mike Disney mike.disney@astro.cf.ac.uk	Univ. of Cardiff, Great Britain	The insignificance of current cosmology
Anne M. Hofmeister and R. E. Criss   hofmeister@wustl.edu	Washington Univ., USA	Implications of thermodynamics on cosmologic models
Michael Ibison ibison@earthtech.org	Inst. for Adv. Studies, Austin, USA	The Yilmaz cosmology
Michael Ibison ibison@earthtech.org	Inst. for Adv. Studies, Austin, USA	The steady-state cosmology
Michael Ivanov ivanovma@gw.bsuir.unibel.by	Belarus State Univ., Belarus	Low-energy quantum gravity
Moncy John moncyjohn@yahoo.co.uk	St. Thomas College, India	Decelerating past for the Universe?
Christian Joos and Josef Lutz jooss@ump.gwdg.de; josef.lutz@etit.tu-chemnitz.de	Univ. of Göttingen; Chemnitz Univ., Germany	Quantum redshift
Christian Joos and Josef Lutz jooss@ump.gwdg.de; josef.lutz@etit.tu-chemnitz.de	Univ. of Göttingen; Chemnitz Univ., Germany	Evolution of Universe in high-energy physics
S. P. Leaning		High redshift Supernovae data show no time dilation
Eric Lerner elermer@igc.org	Lawrenceville Plasma Physics, USA	Is the Universe expanding? Some tests of physical geometry

**The First Crisis in Cosmology Conference, Monção, Portugal, June 23–25 2005**  
**Schedule of Presentations (*continúe*)**

Eric Lerner elerner@igc.org	Lawrenceville Plasma Physics, USA	Overview of plasma cosmology
Sergey Levshakov lev@astro.ioffe.rssi.ru	Ioffe Phys. Tech. Inst., St. Petersburg, Russia	The cosmological variability of the fine-structure constant
Martin López-Corredoira martinlc@iac.es	Inst. de Astrofísica de Canarias, Spain	Research on non-cosmological redshifts
Oliver Manuel om@umr.edu	University of Missouri, USA	Isotopes tell Sun's origin and operation
Jaques Moret-Bailly Jacques.Moret-Bailly@u-bourgogne.fr	France	Parametric light-matter interactions
Frank Potter and Howard Preston drpotter@lycos.com	Univ. of California; Preston Research, USA	Large-scale gravitational quantisation states
Eugene Savov eugen savov@mail.orbitel.bg	Bulgarian Acad. of Sciences	Unique firework Universe and 3-D spiral code
Riccardo Scarpa rscarpa@eso.org	European Southern Observatory, Chile	Modified Newtonian Dynamics: alternative to non-baryonic dark matter
Riccardo Scarpa, Gianni Marconi, and Roberto Gilmozzi rscarpa@eso.org; gmarconi@eso.org; rgilmozz@eso.org	European Southern Observatory, Chile	Using globular clusters to test gravity
Donald Scott dascott2@cox.net	USA	Real properties of magnetism and plasma
Franco Selleri Franco.Selleri@ba.infn.it	Università di Bari, Italy	Absolute simultaneity forbids Big Bang
Glenn Starkman starkman@balin.cwru.edu	Case Western Reserve Univ., USA	Is the low-lambda microwave background cosmic?
Glenn Starkman starkman@balin.cwru.edu	Case Western Reserve Univ., USA	Differentiating between modified gravity and dark energy
Tuomo Suntola tuomo.suntola@sci.fi	Finland	Spherically closed dynamic space
Francesco Sylos Labini	E. Fermi Centre, Italy	Non-linear structures in gravitation and cosmology
Y. P. Varshni ypvsj@uottawa.ca	Univ. of Ottawa, Canada	Common absorption lines in two quasars
Y. P. Varshni, J. Talbot and Z. Ma ypvsj@uottawa.ca	Univ. of Ottawa; Chin. Acad. of Sci. (China)	Peaks in emission lines in the spectra of quasars
Thomas van Flandern tomvf@metaresearch.org	Meta Research, USA	Top problems with Big Bang: the light elements
Mogens Wegener mwegener@aarhusmail.dk	University of Aarhus, Denmark	Kinematic cosmology
Huseyin Yilmaz	Princeton Univ., USA	Beyond Einstein



at a compelling simulation of the morphogenesis of galaxies. Since plasma cosmology has no time constraints, the development of large-scale structures — so problematic for Big Bang — is accommodated. Lerner admits that there's still a lot of work to be done, but with the prospect of more research funding coming our way, he foresees the tidying up of the theory into a workable cosmological model.

Dr. Alain Blanchard of the Laboratoire d'Astrophysique in Toulouse had come to CCC-1 explicitly to defend Big Bang, and he did so admirably. My fears that the inclusion of a single speaker against the motion might amount to mere tokenism were entirely unfounded. Despite the fact that many of us disagreed with much of what he said, he acquitted himself most competently and I would say ended up making a number of good friends at the conference. Two quotes from Dr. Blanchard: "*We are all scientists, and we all want to progress. Where we differ is in our own prejudice.*" "*When you do an experiment, you can get a 'yes' or 'no' answer from your equipment. When you work with astrophysical data, you are dealing with an altogether more complex situation, infused with unknowns.*"

No account of CCC-1 would be near complete without a summary of a paper that caught all of us by complete surprise. Professor Oliver Manuel is not an astronomer. Nor indeed is he a physicist. He is a nuclear chemist, chairman of the Department of Chemistry at the University of Missouri, and held in high enough esteem to be one of a handful of scientists entrusted with the job of analysing Moon rock brought back by the Apollo missions. His "telescope" is a mass spectrometer, and he uses it to identify and track isotopes in the terrestrial neighbourhood. His conclusions are astonishing, yet I can find no fault with his arguments. The hard facts that emerge from Professor Manuel's study indicate that the chemical composition of the Sun beneath the photosphere is predominantly iron! Manuel's thesis has passed peer review in several mainstream journals, including *Nature*, *Science*, and the *Journal of Nuclear Fusion*. He derives a completely revolutionary Solar Model, one which spells big trouble for BBN. Subsequent investigation has shown that it is likely to represent a major paradigm shift in solar physics, and has implications also for the field of nuclear chemistry. He makes the following claims:

1. The chemical composition of the Sun is predominantly iron.
2. The energy of the Sun is *not* derived from nuclear fusion, but rather from neutron repulsion.
3. The Sun has a solid, electrically conducting ferrite surface beneath the photosphere, and rotates uniformly at all latitudes.
4. The solar system originated from a supernova about 5 billion years ago, and the Sun formed from the neutron star that remained.

Manuel's study contains much more than the sample points

mentioned above. Data freely available from NASA's SOHO and TRACE satellites graphically and unambiguously support Manuel's contentions (to the extent of images illustrating fixed surface formations revolving with a period of 27.3 days), and suggest that the standard Solar Model is grossly inaccurate. The implications, if Manuel's ideas are validated, are exciting indeed. His words: "*The question is, are neutron stars 'dead' nuclear matter, with tightly bound neutrons at minus 93 MeV relative to the free neutron, as widely believed? Or are neutron stars the greatest known source of nuclear energy, with neutrons at plus 10 to 22 MeV relative to free neutrons, as we conclude from the properties of the 2,850 known isotopes?*"

The conference concluded with a stirring concert by a 3-piece baroque chamber music ensemble, and it gave me cause to reflect that it appeared that only in our appreciation of music did we find undiluted harmony. That the Big Bang theory will pass into history as an artefact of man's obsession with dogma is a certainty; it will do so on its own merits, however, because it stands on feet of clay. For a viable replacement theory to emerge solely from the efforts of the Alternative Cosmology Group is unlikely unless the group can soon find cohesive direction, and put into practice the undertaking that we become completely interdisciplinary in our approach. Nonetheless, that there is a crisis in the world of science is now confirmed. Papers presented at the conference by some of the world's leading scientists showed beyond doubt that the weight of scientific evidence clearly indicates that the dominant theory on the origin and destiny of the Universe is deeply flawed. The implications of this damning consensus are serious indeed, and will in time fundamentally affect not only the direction of many scientific disciplines, but also threaten to change the very way that we do science.

# The Michelson and Morley 1887 Experiment and the Discovery of Absolute Motion

Reginald T. Cahill

*School of Chemistry, Physics and Earth Sciences, Flinders University, Adelaide 5001, Australia*

E-mail: Reg.Cahill@flinders.edu.au

Physics textbooks assert that in the famous interferometer 1887 experiment to detect absolute motion Michelson and Morley saw no rotation-induced fringe shifts – the signature of absolute motion; it was a null experiment. However this is incorrect. Their published data revealed to them the expected fringe shifts, but that data gave a speed of some 8 km/s using a Newtonian theory for the calibration of the interferometer, and so was rejected by them solely because it was less than the 30 km/s orbital speed of the Earth. A 2002 post relativistic-effects analysis for the operation of the device however gives a different calibration leading to a speed  $> 300$  km/s. So this experiment detected both absolute motion and the breakdown of Newtonian physics. So far another six experiments have confirmed this first detection of absolute motion in 1887.

## 1 Introduction

The first detection of absolute motion, that is motion relative to space itself, was actually by Michelson and Morley in 1887 [1]. However they totally bungled the reporting of their own data, an achievement that Michelson managed again and again throughout his life-long search for experimental evidence of absolute motion.

The Michelson interferometer was a brilliantly conceived instrument for the detection of absolute motion, but only in 2002 [2] was its principle of operation finally understood and used to analyse, for the first time ever, the data from the 1887 experiment, despite the enormous impact of that experiment on the foundations of physics, particularly as they were laid down by Einstein. So great was Einstein's influence that the 1887 data was never re-analysed post-1905 using a proper relativistic-effects based theory for the interferometer. For that reason modern-day vacuum Michelson interferometer experiments, as for example in [3], are badly conceived, and their null results continue to cause much confusion: only a Michelson interferometer in gas-mode can detect absolute motion, as we now see. So as better and better vacuum interferometers were developed over the last 70 years the rotation-induced fringe shift signature of absolute motion became smaller and smaller. But what went unnoticed until 2002 was that the gas in the interferometer was a key component of this instrument when used as an "absolute motion detector", and over time the experimental physicists were using instruments with less and less sensitivity; and in recent years they had finally perfected a totally dud instrument. Reports from such experiments claim that absolute motion is not observable, as Einstein had postulated, despite the fact that the apparatus is totally insensitive to absolute motion. It must be emphasised that absolute motion is not inconsistent with the various well-established relativistic ef-

fects; indeed the evidence is that absolute motion is the cause of these relativistic effects, a proposal that goes back to Lorentz in the 19th century. Then of course one must use a relativistic theory for the operation of the Michelson interferometer. What also follows from these experiments is that the Einstein-Minkowski spacetime ontology is invalidated, and in particular that Einstein's postulates regarding the invariant speed of light have always been in disagreement with experiment from the beginning. This does not imply that the use of a mathematical spacetime is not permitted; in quantum field theory the mathematical spacetime encodes absolute motion effects. An ongoing confusion in physics is that absolute motion is incompatible with Lorentz symmetry, when the evidence is that it is the cause of that dynamical symmetry.

## 2 Michelson interferometer

The Michelson interferometer compares the change in the difference between travel times, when the device is rotated, for two coherent beams of light that travel in orthogonal directions between mirrors; the changing time difference being indicated by the shift of the interference fringes during the rotation. This effect is caused by the absolute motion of the device through 3-space with speed  $v$ , and that the speed of light is relative to that 3-space, and not relative to the apparatus/observer. However to detect the speed of the apparatus through that 3-space gas must be present in the light paths for purely technical reasons. A theory is required to calibrate this device, and it turns out that the calibration of gas-mode Michelson interferometers was only worked out in 2002. The post relativistic-effects theory for this device is remarkably simple. The Fitzgerald-Lorentz contraction effect causes the arm AB parallel to the absolute velocity to be physically contracted to length

$$L_{||} = L\sqrt{1 - \frac{v^2}{c^2}}. \quad (1)$$

The time  $t_{AB}$  to travel  $AB$  is set by  $Vt_{AB} = L_{||} + vt_{AB}$ , while for  $BA$  by  $Vt_{BA} = L_{||} - vt_{BA}$ , where  $V = c/n$  is the speed of light, with  $n$  the refractive index of the gas present (we ignore here the Fresnel drag effect for simplicity – an effect caused by the gas also being in absolute motion). For the total  $ABA$  travel time we then obtain

$$t_{ABA} = t_{AB} + t_{BA} = \frac{2LV}{V^2 - v^2} \sqrt{1 - \frac{v^2}{c^2}}. \quad (2)$$

For travel in the  $AC$  direction we have, from the Pythagoras theorem for the right-angled triangle in Fig. 1 that  $(Vt_{AC})^2 = L^2 + (vt_{AC})^2$  and that  $t_{CA} = t_{AC}$ . Then for the total  $ACA$  travel time

$$t_{ACA} = t_{AC} + t_{CA} = \frac{2L}{\sqrt{V^2 - v^2}}. \quad (3)$$

Then the difference in travel time is

$$\Delta t = \frac{(n^2 - 1)L}{c} \frac{v^2}{c^2} + O\left(\frac{v^4}{c^4}\right). \quad (4)$$

after expanding in powers of  $v/c$  (here the sign  $O$  means for “order”). This clearly shows that the interferometer can only operate as a detector of absolute motion when not in vacuum ( $n = 1$ ), namely when the light passes through a gas, as in the early experiments (in transparent solids a more complex phenomenon occurs and rotation-induced fringe shifts from absolute motion do not occur). A more general analysis [2, 9, 10], including Fresnel drag, gives

$$\Delta t = k^2 \frac{L v_P^2}{c^3} \cos [2(\theta - \psi)], \quad (5)$$

where  $k^2 \approx n(n^2 - 1)$ , while neglect of the Fitzgerald-Lorentz contraction effect gives  $k^2 \approx n^3 \approx 1$  for gases, which is essentially the Newtonian calibration that Michelson used. All the rotation-induced fringe shift data from the 1887 Michelson-Morley experiment, as tabulated in [1], is shown in Fig. 2. The existence of this data continues to be denied by the world of physics.

The interferometers are operated with the arms horizontal, as shown by Miller’s interferometer in Fig. 3. Then in (5)  $\theta$  is the azimuth of one arm (relative to the local meridian), while  $\psi$  is the azimuth of the absolute motion velocity projected onto the plane of the interferometer, with projected component  $v_P$ . Here the Fitzgerald-Lorentz contraction is a real dynamical effect of absolute motion, unlike the Einstein spacetime view that it is merely a spacetime perspective artefact, and whose magnitude depends on the choice of observer. The instrument is operated by rotating at a rate of one rotation over several minutes, and observing the shift in the fringe pattern through a telescope during the rotation.

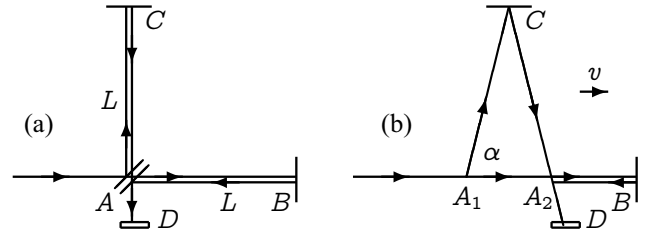


Fig. 1: Schematic diagrams of the Michelson Interferometer, with beamsplitter/mirror at  $A$  and mirrors at  $B$  and  $C$  on arms from  $A$ , with the arms of equal length  $L$  when at rest.  $D$  is the detector screen. In (a) the interferometer is at rest in space. In (b) the interferometer is moving with speed  $v$  relative to space in the direction indicated. Interference fringes are observed at  $D$ . If the interferometer is rotated in the plane through  $90^\circ$ , the roles of arms  $AC$  and  $AB$  are interchanged, and during the rotation shifts of the fringes are seen in the case of absolute motion, but only if the apparatus operates in a gas. By measuring fringe shifts the speed  $v$  may be determined.

Then fringe shifts from six (Michelson and Morley) or twenty (Miller) successive rotations are averaged, and the average sidereal time noted, giving in the case of Michelson and Morley the data in Fig. 2, or the Miller data like that in Fig. 4. The form in (5) is then fitted to such data, by varying the parameters  $v_P$  and  $\psi$ . However Michelson and Morley implicitly assumed the Newtonian value  $k = 1$ , while Miller used an indirect method to estimate the value of  $k$ , as he understood that the Newtonian theory was invalid, but had no other theory for the interferometer. Of course the Einstein postulates have that absolute motion has no meaning, and so effectively demands that  $k = 0$ . Using  $k = 1$  gives only a nominal value for  $v_P$ , being some 8 km/s for the Michelson and Morley experiment, and some 10 km/s from Miller; the difference arising from the different latitude of Cleveland and Mt. Wilson. The relativistic theory for the calibration of gas-mode interferometers was first used in 2002 [2].

### 3 Michelson-Morley data

Fig.2 shows all the Michelson and Morley air-mode interferometer fringe shift data, based upon a total of only 36 rotations in July 1887, revealing the nominal speed of some 8 km/s when analysed using the prevailing but incorrect Newtonian theory which has  $k = 1$  in (5); and this value was known to Michelson and Morley. Including the Fitzgerald-Lorentz dynamical contraction effect as well as the effect of the gas present as in (5) we find that  $n_{air} = 1.00029$  gives  $k^2 = 0.00058$  for air, which explains why the observed fringe shifts were so small. We then obtain the speeds shown in Fig. 2. In some cases the data does not have the expected form in (5); because the device was being operated at almost the limit of sensitivity. The remaining fits give a speed in excess of 300 km/s. The often-repeated statement that Michelson and Morley did not see any rotation-induced fringe shifts

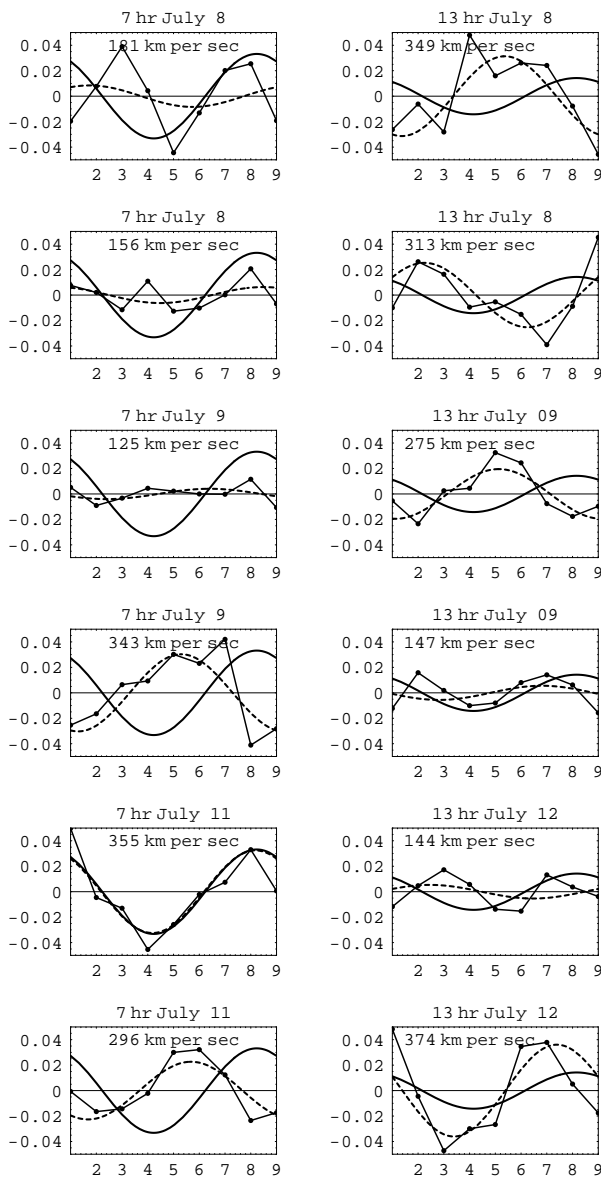


Fig. 2: Shows all the Michelson-Morley 1887 data after removal of the temperature induced linear fringe drifts. The data for each 360° full turn (the average of 6 individual turns) is divided into the 1st and 2nd 180° parts and plotted one above the other. The dotted curve shows a best fit to the data using (5), while the full curves show the expected forms using the Miller direction for  $\mathbf{v}$  and the location and times of the Michelson-Morley observations in Cleveland, Ohio in July, 1887. While the amplitudes are in agreement in general with the Miller based predictions, the phase varies somewhat. Miller also saw a similar effect. This may be related to the Hick's effect [4] when, necessarily, the mirrors are not orthogonal, or may correspond to a genuine fluctuation in the direction of  $\mathbf{v}$  associated with wave effects. We see that this data corresponds to a speed in excess of 300 km/s, and not the 8 km/s reported in [1], which was based on using Newtonian physics to calibrate the interferometer.

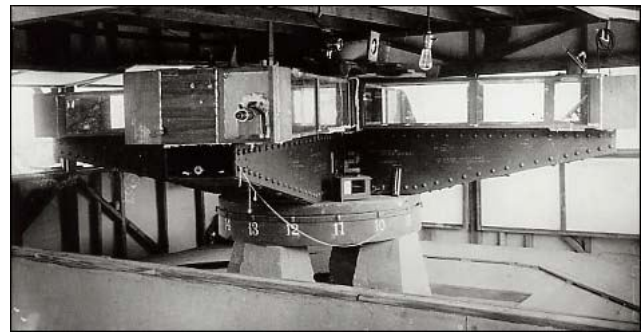


Fig. 3: Miller's interferometer with an effective arm length of  $L = 32$  m achieved by multiple reflections. Used by Miller on Mt. Wilson to perform the 1925–1926 observations of absolute motion. The steel arms weighed 1200 kilograms and floated in a tank of 275 kilograms of Mercury. From Case Western Reserve University Archives.

is completely wrong; all physicists should read their paper [1] for a re-education, and indeed their paper has a table of the observed fringe shifts. To get the Michelson-Morley Newtonian based value of some 8 km/s we must multiply the above speeds by  $k = \sqrt{0.00058} = 0.0241$ . They rejected their own data on the sole but spurious ground that the value of 8 km/s was smaller than the speed of the Earth about the Sun of 30 km/s. What their result really showed was that (i) absolute motion had been detected because fringe shifts of the correct form, as in (5), had been detected, and (ii) that the theory giving  $k^2 = 1$  was wrong, that Newtonian physics had failed. Michelson and Morley in 1887 should have announced that the speed of light did depend of the direction of travel, that the speed was relative to an actual physical 3-space. However contrary to their own data they concluded that absolute motion had not been detected. This bungle has had enormous implications for fundamental theories of space and time over the last 100 years, and the resulting confusion is only now being finally corrected.

#### 4 Miller interferometer

It was Miller [4] who saw the flaw in the 1887 paper and realised that the theory for the Michelson interferometer must be wrong. To avoid using that theory Miller introduced the scaling factor  $k$ , even though he had no theory for its value. He then used the effect of the changing vector addition of the Earth's orbital velocity and the absolute galactic velocity of the solar system to determine the numerical value of  $k$ , because the orbital motion modulated the data, as shown in Fig. 5. By making some 12,000 rotations of the interferometer at Mt. Wilson in 1925/26 Miller determined the first estimate for  $k$  and for the absolute linear velocity of the solar system. Fig. 4 shows typical data from averaging the fringe shifts from 20 rotations of the Miller interferometer, performed over a short period of time, and clearly shows the expected

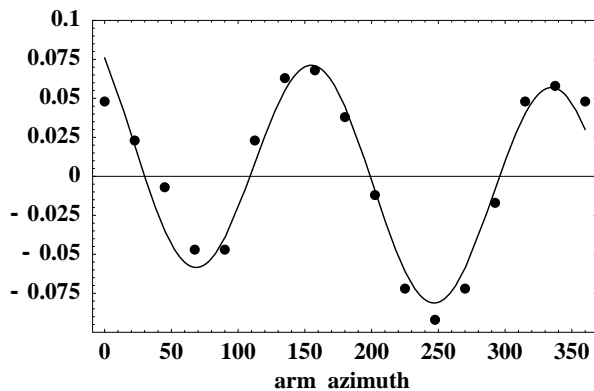


Fig. 4: Typical Miller rotation-induced fringe shifts from average of 20 rotations, measured every  $22.5^\circ$ , in fractions of a wavelength  $\Delta\lambda/\lambda$ , vs azimuth  $\theta$  (deg), measured clockwise from North, from Cleveland Sept. 29, 1929 16:24 UT; 11:29 average sidereal time. This shows the quality of the fringe data that Miller obtained, and is considerably better than the comparable data by Michelson and Morley in Fig. 2. The curve is the best fit using the form in (5) but including a Hick's [4]  $\cos(\theta - \beta)$  component that is required when the mirrors are not orthogonal, and gives  $\psi = 158^\circ$ , or  $22^\circ$  measured from South, and a projected speed of  $v_P = 351$  km/s. This value for  $v$  is different from that in Fig. 2 because of the difference in latitude of Cleveland and Mt. Wilson. This process was repeated some 12,000 times over days and months throughout 1925/1926 giving, in part, the data in Fig. 5.

form in (5) (only a linear drift caused by temperature effects on the arm lengths has been removed — an effect also removed by Michelson and Morley and also by Miller). In Fig. 4 the fringe shifts during rotation are given as fractions of a wavelength,  $\Delta\lambda/\lambda = \Delta t/T$ , where  $\Delta t$  is given by (5) and  $T$  is the period of the light. Such rotation-induced fringe shifts clearly show that the speed of light is different in different directions. The claim that Michelson interferometers, operating in gas-mode, do not produce fringe shifts under rotation is clearly incorrect. But it is that claim that lead to the continuing belief, within physics, that absolute motion had never been detected, and that the speed of light is invariant. The value of  $\psi$  from such rotations together lead to plots like those in Fig. 5, which show  $\psi$  from the 1925/1926 Miller [4] interferometer data for four different months of the year, from which the RA = 5.2 hr is readily apparent. While the orbital motion of the Earth about the Sun slightly affects the RA in each month, and Miller used this effect to determine the value of  $k$ , the new theory of gravity required a reanalysis of the data [9, 11], revealing that the solar system has a large observed galactic velocity of some  $420 \pm 30$  km/s in the direction (RA = 5.2 hr, Dec =  $-67^\circ$ ). This is different from the speed of 369 km/s in the direction (RA = 11.20 hr, Dec =  $-7.22^\circ$ ) extracted from the Cosmic Microwave Background (CMB) anisotropy, and which describes a motion relative to the distant universe, but not relative to the local 3-space. The Miller velocity is explained

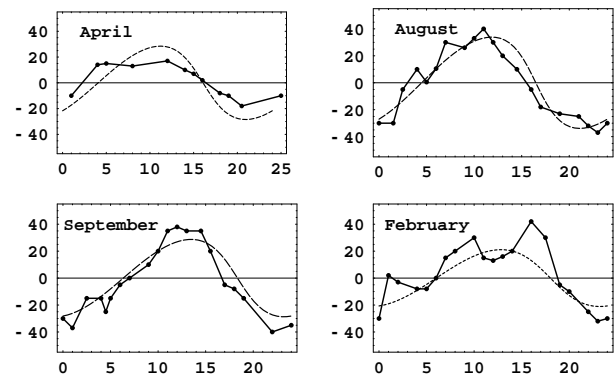


Fig. 5: Miller azimuths  $\psi$ , measured from south and plotted against sidereal time in hrs, showing both data and best fit of theory giving  $v = 433$  km/s in the direction ( $\alpha = 5.2^{\text{hr}}$ ,  $\delta = -67^\circ$ ), using  $n = 1.000226$  appropriate for the altitude of Mt. Wilson. The variation from month to month arises from the orbital motion of the Earth about the Sun: in different months the vector sum of the galactic velocity of the solar system with the orbital velocity and sun in-flow velocity is different. As shown in Fig. 6 DeWitte using a completely different experiment detected the same direction and speed.

by galactic gravitational in-flows\*.

Two other interferometer experiments, by Illingworth [5] and Joos [6], used helium, enabling the refractive index effect to be recently confirmed, because for helium, with  $n = 1.000036$ , we find that  $k^2 = 0.00007$ . Until the refractive index effect was taken into account the data from the helium-mode experiments appeared to be inconsistent with the data from the air-mode experiments; now they are seen to be consistent. Ironically helium was introduced in place of air to reduce any possible unwanted effects of a gas, but we now understand the essential role of the gas. The data from an interferometer experiment by Jaseja *et al* [7], using two orthogonal masers with a He-Ne gas mixture, also indicates that they detected absolute motion, but were not aware of that as they used the incorrect Newtonian theory and so considered the fringe shifts to be too small to be real, reminiscent of the same mistake by Michelson and Morley. The Michelson interferometer is a 2nd order device, as the effect of absolute motion is proportional to  $(v/c)^2$ , as in (5).

## 5 1st order experiments

However much more sensitive 1st order experiments are also possible. Ideally they simply measure the change in the one-way EM travel-time as the direction of propagation is changed. Fig. 6 shows the North-South orientated coaxial cable Radio Frequency (RF) travel time variations measured by DeWitte in Brussels in 1991 [9, 10, 11], which gives the same RA of absolute motion as found by Miller. That ex-

\*See online papers [http://www.mountainman.com.au/process\\_physics/](http://www.mountainman.com.au/process_physics/) [http://www.scieng.flinders.edu.au/cpes/people/cahill\\_r/processphysics.html](http://www.scieng.flinders.edu.au/cpes/people/cahill_r/processphysics.html)

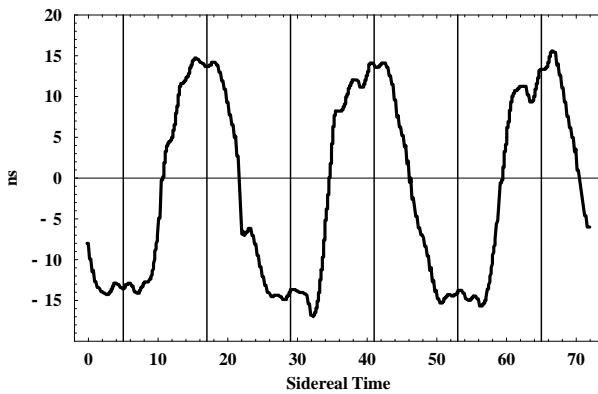


Fig. 6: Variations in twice the one-way travel time, in ns, for an RF signal to travel 1.5 km through a coaxial cable between Rue du Marais and Rue de la Paille, Brussels. An offset has been used such that the average is zero. The cable has a North-South orientation, and the data is the difference of the travel times for NS and SN propagation. The sidereal time for maximum effect of  $\sim 5$  hr and  $\sim 17$  hr (indicated by vertical lines) agrees with the direction found by Miller. Plot shows data over 3 sidereal days and is plotted against sidereal time. DeWitte recorded such data from 178 days, and confirmed that the effect tracked sidereal time, and not solar time. Miller also confirmed this sidereal time tracking. The fluctuations are evidence of turbulence in the flow.

periment showed that RF waves travel at speeds determined by the orientation of the cable relative to the Miller direction. That these very different experiments show the same speed and RA of absolute motion is one of the most startling discoveries of the twentieth century. Torr and Kolen [8] using an East-West orientated nitrogen gas-filled coaxial cable also detected absolute motion. It should be noted that analogous optical fibre experiments give null results for the same reason, apparently, that transparent solids in a Michelson interferometer also give null results, and so behave differently to coaxial cables.

Modern resonant-cavity interferometer experiments, for which the analysis leading to (5) is applicable, use vacuum with  $n = 1$ , and then  $k = 0$ , predicting no rotation-induced fringe shifts. In analysing the data from these experiments the consequent null effect is misinterpreted, as in [3], to imply the absence of absolute motion. But it is absolute motion which causes the dynamical effects of length contractions, time dilations and other relativistic effects, in accord with Lorentzian interpretation of relativistic effects. The detection of absolute motion is not incompatible with Lorentz symmetry; the contrary belief was postulated by Einstein, and has persisted for over 100 years, since 1905. So far the experimental evidence is that absolute motion and Lorentz symmetry are real and valid phenomena; absolute motion is motion presumably relative to some substructure to space, whereas Lorentz symmetry parameterises dynamical effects caused by the motion of systems through that substructure. There are novel wave phenomena that could also be studied;

see footnote on page 28. In order to check Lorentz symmetry we can use vacuum-mode resonant-cavity interferometers, but using gas within the resonant-cavities would enable these devices to detect absolute motion with great precision.

## 6 Conclusions

So absolute motion was first detected in 1887, and again in at least another six experiments over the last 100 years. Had Michelson and Morley been as astute as their younger colleague Miller, and had been more careful in reporting their *non-null* data, the history of physics over the last 100 years would have totally different, and the spacetime ontology would never have been introduced. That ontology was only mandated by the mistaken belief that absolute motion had not been detected. By the time Miller had sorted out that bungle, the world of physics had adopted the spacetime ontology as a model of reality because that model appeared to be confirmed by many relativistic phenomena, mainly from particle physics, although these phenomena could equally well have been understood using the Lorentzian interpretation which involved no spacetime. We should now understand that in quantum field theory a mathematical spacetime encodes absolute motion effects upon the elementary particle systems, but that there exists a physically observable foliation of that spacetime into a geometrical model of time and a separate geometrical model of 3-space.

## References

1. Michelson A. A. and Morley A. A. *Philos. Mag.*, S. 5, 1887, v. 24, No. 151, 449–463.
2. Cahill R. T. and Kitto K. Michelson-Morley experiments revisited and the cosmic background radiation preferred frame. *Apeiron*, 2003, v. 10, No. 2, 104–117.
3. Müller H. *et al.* Modern Michelson-Morley experiment using cryogenic optical resonators. *Phys. Rev. Lett.*, 2003, v. 91(2), 020401-1.
4. Miller D. C. *Rev. Mod. Phys.*, 1933, v. 5, 203–242.
5. Illingworth K. K. *Phys. Rev.*, 1927, v. 3, 692–696.
6. Joos G. *Annalen der Physik*, 1930, Bd. 7, 385.
7. Jaseja T. S. *et al.* *Phys. Rev. A*, 1964, v. 133, 1221.
8. Torr D. G. and Kolen P. *Precision Measurements and Fundamental Constants*, ed. by Taylor B. N. and Phillips W. D. Nat. Bur. Stand. (U.S.), Spec. Pub., 1984, v. 617, 675.
9. Cahill R. T. *Relativity, Gravitation, Cosmology*, Nova Science Pub., NY, 2004, 168–226.
10. Cahill R. T. Absolute motion and gravitational effects. *Apeiron*, 2004, v. 11, No. 1, 53–111.
11. Cahill R. T. *Process Physics: from information theory to quantum space and matter*. Nova Science Pub., NY, 2005.

# Novel Gravity Probe B Frame-Dragging Effect

Reginald T. Cahill

*School of Chemistry, Physics and Earth Sciences, Flinders University, Adelaide 5001, Australia*

E-mail: Reg.Cahill@flinders.edu.au

The Gravity Probe B (GP-B) satellite experiment will measure the precession of on-board gyroscopes to extraordinary accuracy. Such precessions are predicted by General Relativity (GR), and one component of this precession is the “frame-dragging” or Lense-Thirring effect, which is caused by the rotation of the Earth. A new theory of gravity, which passes the same extant tests of GR, predicts, however, a second and much larger “frame-dragging” precession. The magnitude and signature of this larger effect is given for comparison with the GP-B data.

## 1 Introduction

The Gravity Probe B (GP-B) satellite experiment was launched in April 2004. It has the capacity to measure the precession of four on-board gyroscopes to unprecedented accuracy [1, 2, 3, 4]. Such a precession is predicted by the Einstein theory of gravity, General Relativity (GR), with two components (i) a geodetic precession, and (ii) a “frame-dragging” precession known as the Lense-Thirring effect. The latter is particularly interesting effect induced by the rotation of the Earth, and described in GR in terms of a “gravitomagnetic” field. According to GR this smaller effect will give a precession of 0.042 arcsec per year for the GP-B gyroscopes. However a recently developed theory gives a different account of gravity. While agreeing with GR for all the standard tests of GR this theory gives a dynamical account of the so-called “dark matter” effect in spiral galaxies. It also successfully predicts the masses of the black holes found in the globular clusters M15 and G1. Here we show that GR and the new theory make very different predictions for the “frame-dragging” effect, and so the GP-B experiment will be able to decisively test both theories. While predicting the same earth-rotation induced precession, the new theory has an additional much larger “frame-dragging” effect caused by the observed translational motion of the Earth. As well the new theory explains the “frame-dragging” effect in terms of vorticity in a “substratum flow”. Herein the magnitude and signature of this new component of the gyroscope precession is predicted for comparison with data from GP-B when it becomes available.

## 2 Theories of gravity

The Newtonian “inverse square law” for gravity,

$$F = \frac{Gm_1m_2}{r^2}, \quad (1)$$

was based on Kepler’s laws for the motion of the planets. Newton formulated gravity in terms of the gravitational ac-

celeration vector field  $\mathbf{g}(\mathbf{r}, t)$ , and in differential form

$$\nabla \cdot \mathbf{g} = -4\pi G\rho, \quad (2)$$

where  $\rho(\mathbf{r}, t)$  is the matter density. However there is an alternative formulation [5] in terms of a vector “flow” field  $\mathbf{v}(\mathbf{r}, t)$  determined by

$$\frac{\partial}{\partial t}(\nabla \cdot \mathbf{v}) + \nabla \cdot [(\mathbf{v} \cdot \nabla) \mathbf{v}] = -4\pi G\rho, \quad (3)$$

with  $\mathbf{g}$  now given by the Euler “fluid” acceleration

$$\mathbf{g} = \frac{\partial \mathbf{v}}{\partial t} + (\mathbf{v} \cdot \nabla) \mathbf{v} = \frac{d\mathbf{v}}{dt}. \quad (4)$$

Trivially this  $\mathbf{g}$  also satisfies (2). External to a spherical mass  $M$  of radius  $R$  a velocity field solution of (2) is

$$\mathbf{v}(\mathbf{r}) = -\sqrt{\frac{2GM}{r}} \hat{\mathbf{r}}, \quad r > R, \quad (5)$$

which gives from (4) the usual inverse square law  $\mathbf{g}$  field

$$\mathbf{g}(\mathbf{r}) = -\frac{GM}{r^2} \hat{\mathbf{r}}, \quad r > R. \quad (6)$$

However the flow equation (2) is not uniquely determined by Kepler’s laws because

$$\frac{\partial}{\partial t}(\nabla \cdot \mathbf{v}) + \nabla \cdot [(\mathbf{v} \cdot \nabla) \mathbf{v}] + C(\mathbf{v}) = -4\pi G\rho, \quad (7)$$

where

$$C(\mathbf{v}) = \frac{\alpha}{8} [(\text{tr} D)^2 - \text{tr}(D^2)], \quad (8)$$

and

$$D_{ij} = \frac{1}{2} \left( \frac{\partial v_i}{\partial x_j} + \frac{\partial v_j}{\partial x_i} \right), \quad (9)$$

also has the same external solution (5), because  $C(\mathbf{v})=0$  for the flow in (5). So the presence of the  $C(\mathbf{v})$  would not have manifested in the special case of planets in orbit about the massive central sun. Here  $\alpha$  is a dimensionless

constant – a new gravitational constant, in addition to usual the Newtonian gravitational constant  $G$ . However inside a spherical mass we find [5] that  $C(\mathbf{v}) \neq 0$ , and using the Greenland borehole  $g$  anomaly data [4] we find that  $\alpha^{-1} = 139 \pm 5$ , which gives the fine structure constant  $\alpha = e^2 \hbar / c \approx 1/137$  to within experimental error. From (4) we can write

$$\nabla \cdot \mathbf{g} = -4\pi G\rho - 4\pi G\rho_{DM}, \quad (10)$$

where

$$\rho_{DM}(\mathbf{r}) = \frac{\alpha}{32\pi G} [(\text{tr}D)^2 - \text{tr}(D^2)], \quad (11)$$

which introduces an effective “matter density” representing the flow dynamics associated with the  $C(\mathbf{v})$  term. In [5] this dynamical effect is shown to be the “dark matter” effect. The interpretation of the vector flow field  $\mathbf{v}$  is that it is a manifestation, at the classical level, of a quantum substratum to space; the flow is a rearrangement of that substratum, and not a flow *through* space. However (7) needs to be further generalised [5] to include vorticity, and also the effect of the motion of matter through this substratum via

$$\mathbf{v}_R \{ \mathbf{r}_0(t), t \} = \mathbf{v}_0(t) - \mathbf{v} \{ \mathbf{r}_0(t), t \}, \quad (12)$$

where  $\mathbf{v}_0(t)$  is the velocity of an object, at  $\mathbf{r}_0(t)$ , relative to the same frame of reference that defines the flow field; then  $\mathbf{v}_R$  is the velocity of that matter relative to the substratum. The flow equation (7) is then generalised to, with  $d/dt = \partial/\partial t + \mathbf{v} \cdot \nabla$  the Euler fluid or total derivative,

$$\begin{aligned} & \frac{dD_{ij}}{dt} + \frac{\delta_{ij}}{3} \text{tr}(D^2) + \frac{\text{tr}D}{2} \left( D_{ij} - \frac{\delta_{ij}}{3} \text{tr}D \right) + \\ & + \frac{\delta_{ij}}{3} \frac{\alpha}{8} [(\text{tr}D)^2 - \text{tr}(D^2)] + (\Omega D - D\Omega)_{ij} = \end{aligned} \quad (13)$$

$$= -4\pi G\rho \left( \frac{\delta_{ij}}{3} + \frac{v_R^i v_R^j}{2c^2} + \dots \right), \quad i, j = 1, 2, 3,$$

$$\nabla \times (\nabla \times \mathbf{v}) = \frac{8\pi G\rho}{c^2} \mathbf{v}_R, \quad (14)$$

$$\Omega_{ij} = \frac{1}{2} \left( \frac{\partial v_i}{\partial x_j} - \frac{\partial v_j}{\partial x_i} \right) = \quad (15)$$

$$= -\frac{1}{2} \epsilon_{ijk} \omega_k = -\frac{1}{2} \epsilon_{ijk} (\nabla \times \mathbf{v})_k,$$

and the vorticity vector field is  $\vec{\omega} = \nabla \times \mathbf{v}$ . For zero vorticity and  $v_R \ll c$  (13) reduces to (7). We obtain from (14) the Biot-Savart form for the vorticity

$$\vec{\omega}(\mathbf{r}, t) = \frac{2G}{c^2} \int d^3r' \frac{\rho(\mathbf{r}', t)}{|\mathbf{r} - \mathbf{r}'|^3} \mathbf{v}_R(\mathbf{r}', t) \times (\mathbf{r} - \mathbf{r}'). \quad (16)$$

The path  $\mathbf{r}_0(t)$  of an object through this flow is obtained by extremising the relativistic proper time

$$\tau[\mathbf{r}_0] = \int dt \left( 1 - \frac{v_R^2}{c^2} \right)^{1/2} \quad (17)$$

giving, as a generalisation of (4), the acceleration

$$\begin{aligned} \frac{d\mathbf{v}_0}{dt} = & \left[ \frac{\partial \mathbf{v}}{\partial t} + (\mathbf{v} \cdot \nabla) \mathbf{v} \right] + (\nabla \times \mathbf{v}) \times \mathbf{v}_R - \\ & - \frac{\mathbf{v}_R}{1 - \frac{v_R^2}{c^2}} \frac{1}{2} \frac{d}{dt} \left( \frac{v_R^2}{c^2} \right). \end{aligned} \quad (18)$$

Formulating gravity in terms of a flow is probably unfamiliar, but General Relativity (GR) permits an analogous result for metrics of the Panlevé-Gullstrand class [7],

$$d\tau^2 = g_{\mu\nu} dx^\mu dx^\nu = dt^2 - \frac{1}{c^2} [d\mathbf{r} - \mathbf{v}(\mathbf{r}, t) dt]^2. \quad (19)$$

The external-Schwarzschild metric belongs to this class [8], and when expressed in the form of (19) the  $\mathbf{v}$  field is identical to (5). Substituting (19) into the Einstein equations

$$G_{\mu\nu} \equiv R_{\mu\nu} - \frac{1}{2} R g_{\mu\nu} = \frac{8\pi G}{c^2} T_{\mu\nu}, \quad (20)$$

gives

$$\begin{aligned} G_{00} = & \sum_{i,j=1,2,3} v_i \mathcal{G}_{ij} v_j - c^2 \sum_{j=1,2,3} \mathcal{G}_{0j} v_j - \\ & - c^2 \sum_{i=1,2,3} v_i \mathcal{G}_{i0} + c^2 \mathcal{G}_{00}, \end{aligned} \quad (21)$$

$$G_{i0} = - \sum_{j=1,2,3} \mathcal{G}_{ij} v_j + c^2 \mathcal{G}_{i0},$$

$$G_{ij} = \mathcal{G}_{ij}, \quad i, j = 1, 2, 3,$$

where the  $\mathcal{G}_{\mu\nu}$  are given by

$$\mathcal{G}_{00} = \frac{1}{2} [(\text{tr}D)^2 - \text{tr}(D^2)],$$

$$\mathcal{G}_{i0} = \mathcal{G}_{0i} = -\frac{1}{2} [\nabla \times (\nabla \times \mathbf{v})]_i, \quad (22)$$

$$\begin{aligned} \mathcal{G}_{ij} = & \frac{d}{dt} \left( D_{ij} - \delta_{ij} \text{tr}D \right) + \left( D_{ij} - \frac{1}{2} \delta_{ij} \text{tr}D \right) \text{tr}D - \\ & - \frac{1}{2} \delta_{ij} \text{tr}(D^2) + (\Omega D - D\Omega)_{ij}, \quad i, j = 1, 2, 3 \end{aligned}$$

and so GR also uses the Euler “fluid” derivative, and we obtain a set of equations analogous but not identical to (13)–(14). In vacuum, with  $T_{\mu\nu} = 0$ , we find that (22) demands that

$$[(\text{tr}D)^2 - \text{tr}(D^2)] = 0. \quad (23)$$

This simply corresponds to the fact that GR does not permit the “dark matter” dynamical effect, namely that  $\rho_{DM} = 0$ , according to (10). This happens because GR was forced to agree with Newtonian gravity, in the appropriate limits, and that theory also has no such effect. The predictions from (13)–(14) and from (22) for the Gravity Probe B experiment are different, and provide an opportunity to test both gravity theories.



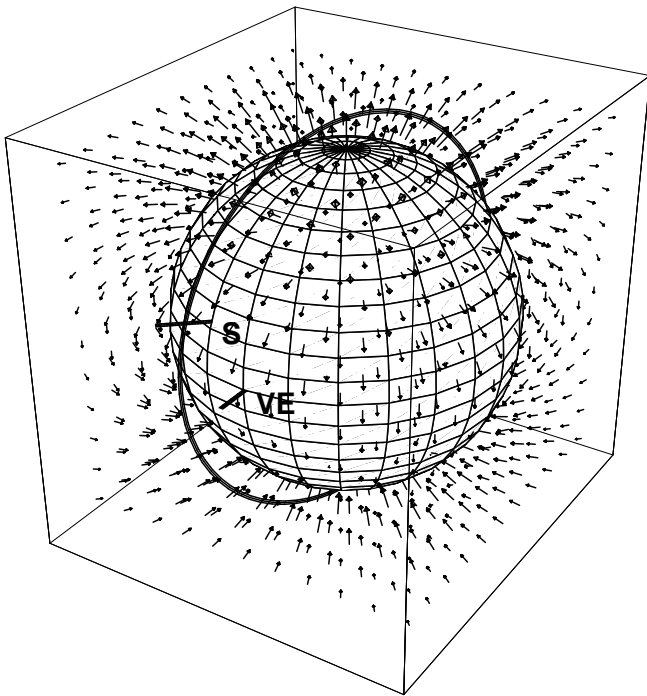


Fig. 1: Shows the Earth (N is up) and vorticity vector field component  $\vec{\omega}$  induced by the rotation of the Earth, as in (24). The polar orbit of the GP-B satellite is shown,  $\mathbf{S}$  is the gyroscope starting spin orientation, directed towards the guide star IM Pegasi,  $RA = 22^h 53' 2.26''$ ,  $Dec = 16^\circ 50' 28.2''$ , and  $\mathbf{VE}$  is the vernal equinox.

### 3 “Frame-dragging” as a vorticity effect

Here we consider one difference between the two theories, namely that associated with the vorticity part of (18), leading to the “frame-dragging” or Lense-Thirring effect. In GR the vorticity field is known as the “gravitomagnetic” field  $\mathbf{B} = -c \vec{\omega}$ . In both GR and the new theory the vorticity is given by (16) but with a key difference: in GR  $\mathbf{v}_R$  is *only* the rotational velocity of the matter in the Earth, whereas in (13)–(14)  $\mathbf{v}_R$  is the vector sum of the rotational velocity and the translational velocity of the Earth through the substratum. At least seven experiments have detected this translational velocity; some were gas-mode Michelson interferometers and others coaxial cable experiments [8, 9, 10], and the translational velocity is now known to be approximately 430 km/s in the direction  $RA = 5.2^h$ ,  $Dec = -67^\circ$ . This direction has been known since the Miller [11] gas-mode interferometer experiment, but the RA was more recently confirmed by the 1991 DeWitte coaxial cable experiment performed in the Brussels laboratories of Belgacom [9]. This flow is related to galactic gravity flow effects [8, 9, 10], and so is different to that of the velocity of the Earth with respect to the Cosmic Microwave Background (CMB), which is 369 km/s in the direction  $RA = 11.20^h$ ,  $Dec = -7.22^\circ$ .

First consider the common but much smaller rotation

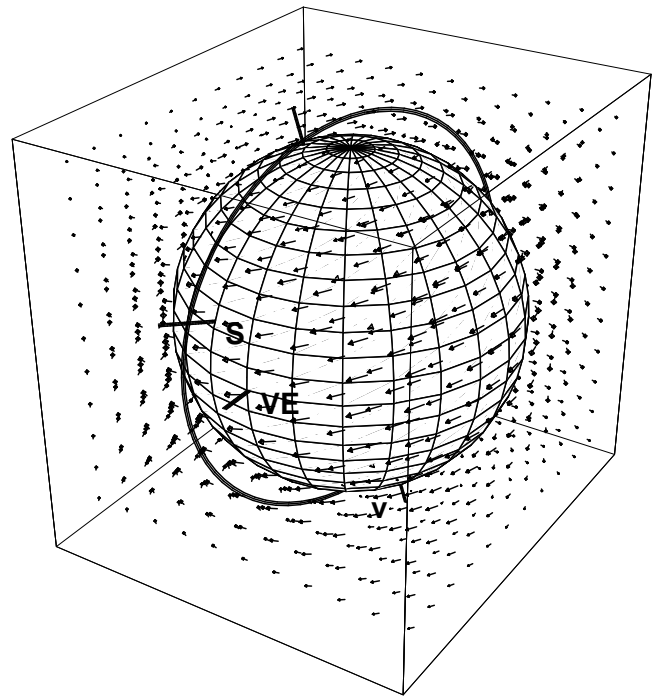


Fig. 2: Shows the Earth (N is up) and the much larger vorticity vector field component  $\vec{\omega}$  induced by the translation of the Earth, as in (27). The polar orbit of the GP-B satellite is shown, and  $\mathbf{S}$  is the gyroscope starting spin orientation, directed towards the guide star IM Pegasi,  $RA = 22^h 53' 2.26''$ ,  $Dec = 16^\circ 50' 28.2''$ ,  $\mathbf{VE}$  is the vernal equinox, and  $\mathbf{V}$  is the direction  $RA = 5.2^h$ ,  $Dec = -67^\circ$  of the translational velocity  $\mathbf{v}_c$ .

induced “frame-dragging” or vorticity effect. Then  $\mathbf{v}_R(\mathbf{r}) = \mathbf{w} \times \mathbf{r}$  in (16), where  $\mathbf{w}$  is the angular velocity of the Earth, giving

$$\vec{\omega}(\mathbf{r}) = 4 \frac{G}{c^2} \frac{3(\mathbf{r} \cdot \mathbf{L})\mathbf{r} - r^2 \mathbf{L}}{2r^5}, \quad (24)$$

where  $\mathbf{L}$  is the angular momentum of the Earth, and  $\mathbf{r}$  is the distance from the centre. This component of the vorticity field is shown in Fig. 1. Vorticity may be detected by observing the precession of the GP-B gyroscopes. The vorticity term in (18) leads to a torque on the angular momentum  $\mathbf{S}$  of the gyroscope,

$$\vec{\tau} = \int d^3r \rho(\mathbf{r}) \mathbf{r} \times [\vec{\omega}(\mathbf{r}) \times \mathbf{v}_R(\mathbf{r})], \quad (25)$$

where  $\rho$  is its density, and where  $\mathbf{v}_R$  is used here to describe the rotation of the gyroscope. Then  $d\mathbf{S} = \vec{\tau} dt$  is the change in  $\mathbf{S}$  over the time interval  $dt$ . In the above case  $\mathbf{v}_R(\mathbf{r}) = \mathbf{s} \times \mathbf{r}$ , where  $\mathbf{s}$  is the angular velocity of the gyroscope. This gives

$$\vec{\tau} = \frac{1}{2} \vec{\omega} \times \mathbf{S} \quad (26)$$

and so  $\vec{\omega}/2$  is the instantaneous angular velocity of precession of the gyroscope. This corresponds to the well known fluid

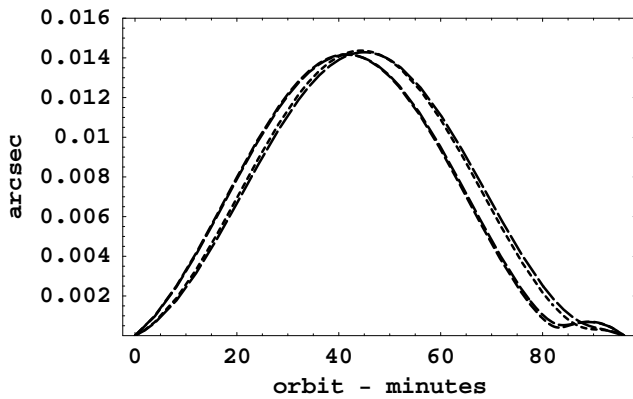


Fig. 3: Predicted variation of the precession angle  $\Delta\Theta = |\Delta\mathbf{S}(t)|/|\mathbf{S}(0)|$ , in arcsec, over one 97 minute GP-B orbit, from the vorticity induced by the translation of the Earth, as given by (28). The orbit time begins at location  $\mathbf{S}$ . Predictions are for the months of April, August, September and February, labeled by increasing dash length. The “glitches” near 80 minutes are caused by the angle effects in (28). These changes arise from the effects of the changing orbital velocity of the Earth about the Sun. The GP-B expected angle measurement accuracy is 0.0005 arcsec. Novel gravitational waves will affect these plots.

result that the vorticity vector is twice the angular velocity vector. For GP-B the direction of  $\mathbf{S}$  has been chosen so that this precession is cumulative and, on averaging over an orbit, corresponds to some  $7.7 \times 10^{-6}$  arcsec per orbit, or 0.042 arcsec per year. GP-B has been superbly engineered so that measurements to a precision of 0.0005 arcsec are possible.

However for the unique translation-induced precession if we use  $v_R \approx v_C = 430$  km/s in the direction  $RA = 5.2^{\text{hr}}$ ,  $Dec = -67^\circ$ , namely ignoring the effects of the orbital motion of the Earth, the observed flow past the Earth towards the Sun, and the flow into the Earth, and effects of the gravitational waves, then (16) gives

$$\vec{\omega}(\mathbf{r}) = \frac{2GM}{c^2} \frac{\mathbf{v}_C \times \mathbf{r}}{r^3}. \quad (27)$$

This much larger component of the vorticity field is shown in Fig. 2. The maximum magnitude of the speed of this precession component is  $\omega/2 = gv_C/c^2 = 8 \times 10^{-6}$  arcsec/s, where here  $g$  is the gravitational acceleration at the altitude of the satellite. This precession has a different signature: it is not cumulative, and is detectable by its variation over each single orbit, as its orbital average is zero, to first approximation. Fig. 3 shows  $\Delta\Theta = |\Delta\mathbf{S}(t)|/|\mathbf{S}(0)|$  over one orbit, where, as in general,

$$\begin{aligned} \Delta\mathbf{S}(t) &= \left[ \int_0^t dt' \frac{1}{2} \vec{\omega}(\mathbf{r}(t')) \right] \times \mathbf{S}(t') \approx \\ &\approx \left[ \int_0^t dt' \frac{1}{2} \vec{\omega}(\mathbf{r}(t')) \right] \times \mathbf{S}(0). \end{aligned} \quad (28)$$

Here  $\Delta\mathbf{S}(t)$  is the integrated change in spin, and where the approximation arises because the change in  $\mathbf{S}(t')$  on the RHS of (28) is negligible. The plot in Fig. 3 shows this effect to be some  $30 \times$  larger than the expected GP-B errors, and so easily detectable, if it exists as predicted herein. This precession is about the instantaneous direction of the vorticity  $\vec{\omega}(\mathbf{r}(t))$  at the location of the satellite, and so is neither in the plane, as for the geodetic precession, nor perpendicular to the plane of the orbit, as for the earth-rotation induced vorticity effect.

Because the yearly orbital rotation of the Earth about the Sun slightly effects  $\mathbf{v}_C$  [9] predictions for four months throughout the year are shown in Fig. 3. Such yearly effects were first seen in the Miller [11] experiment.

**References**

1. Schiff L. I. *Phys. Rev. Lett.*, 1960, v. 4, 215.
2. Van Patten R. A. and Everitt C. W. F. *Phys. Rev. Lett.*, 1976, v. 36, 629.
3. Everitt C. W. F. et al. *Near Zero: Festschrift for William M. Fairbank*, ed. by Everitt C. W. F., Freeman, S. Francisco, 1986.
4. Turneure J. P., Everitt C. W. F., Parkinson B. W. et al. The Gravity Probe B relativity gyroscope experiment. *Proc. of the Fourth Marcell Grossmann Meeting in General Relativity*, ed. by R. Ruffini, Elsevier, Amsterdam, 1986.
5. Cahill R. T. “Dark matter” as a quantum foam in-flow effect. *Trends In Dark Matter Research*, ed. by Blain J. Val, Nova Science Pub, NY, 2005; Cahill R. T. Gravitation, the “dark matter” effect and the fine structure constant. *Apeiron*, 2005, v. 12, No. 2, 144–177.
6. Ander M. E. et al. *Phys. Rev. Lett.*, 1989, v. 62, 985.
7. Panlevé P. *Com. Rend. Acad. Sci.*, 1921, v. 173, 677; Gullstrand A. *Ark. Mat. Astron. Fys.*, 1922, v. 16, 1.
8. Cahill R. T. Quantum foam, gravity and gravitational waves. *Relativity, Gravitation, Cosmology*, ed. by Dvoeglazov V. V. and Espinoza Garrido A. A. Nova Science Pub., NY, 2004, 168–226.
9. Cahill R. T. Absolute motion and gravitational effects. *Apeiron*, 2004, v. 11, No. 1, 53–111.
10. Cahill R. T. Process Physics: from information theory to quantum space and matter. Nova Science Pub., NY, 2005.
11. Miller D. C. *Rev. Mod. Phys.*, 1993, v. 5, 203–242.

## Relations Between Physical Constants

Roberto Oros di Bartini\*

This article discusses the main analytic relationship between physical constants, and applications thereof to cosmology. The mathematical bases herein are group theoretical methods and topological methods. From this it is argued that the Universe was born from an Inversion Explosion of the primordial particle (pre-particle) whose outer radius was that of the classical electron, and inner radius was that of the gravitational radius of the electron. All the mass was concentrated in the space between the radii, and was inverted outside the particle through the pre-particle's surface (the inversion classical radius). This inversion process continues today, determining evolutionary changes in the fundamental physical constants.

As is well known, group theoretical methods, and also topological methods, can be effectively employed in order to interpret physical problems. We know of studies setting up the discrete interior of space-time, and also relationships between atomic quantities and cosmological quantities.

However, no analytic relationship between fundamental physical quantities has been found. They are determined only by experimental means, because there is no theory that could give a theoretical determination of them.

In this brief article we give the results of our own study, which, employing group theoretical methods and topological methods, gives an analytic relationship between physical constants.

Let us consider a predicative unbounded and hence unique specimen  $A$ . Establishing an identity between this specimen  $A$  and itself

$$A \equiv A, \quad A \frac{1}{A} = 1,$$

\*Brief contents of this paper was presented by Prof. Bruno Pontecorvo to the Proceedings of the Academy of Sciences of the USSR (*Doklady Acad. Sci. USSR*), where it was published in 1965 [19]. Roberto di Bartini (1897–1974), the author, was an Italian mathematician and aircraft engineer who, from 1923, worked in the USSR where he headed an aircraft project bureau. Because di Bartini attached great importance to this article, he signed it with his full name, including his titular prefix and baronial name Oros — from Orosti, the patrimony near Fiume (now Rijeka, located in Croatian territory near the border), although he regularly signed papers as Roberto Bartini. The limited space in the Proceedings did not permit publication of the whole article. For this reason Pontecorvo acquainted di Bartini with Prof. Kyril Stanyukovich, who published this article in his bulletin, in Russian. Pontecorvo and Stanyukovich regarded di Bartini's paper highly. Decades later Stanyukovich suggested that it would be a good idea to publish di Bartini's article in English, because of the great importance of his idea of applying topological methods to cosmology and the results he obtained. (Translated by D. Rabounski and S. J. Crothers.) — Editor's remark.



Roberto di Bartini, 1920's  
(in Italian Air Force uniform)

is the mapping which transfers images of  $A$  in accordance with the pre-image of  $A$ .

The specimen  $A$ , by definition, can be associated only with itself. For this reason it's inner mapping can, according to Stoilow's theorem, be represented as the superposition of a topological mapping and subsequently by an analytic mapping.

The population of images of  $A$  is a point-containing system, whose elements are equivalent points; an  $n$ -dimensional affine spread, containing  $(n + 1)$ -elements of the system, transforms into itself in linear manner

$$x'_i = \sum_{k=1}^{n+1} a_{ik} x_k.$$

With all  $a_{ik}$  real numbers, the unitary transformation

$$\sum_k a_{ik}^* a_{lk} = \sum_k a_{ki}^* a_{kl}, \quad i, k = 1, 2, 3 \dots, n + 1,$$

is orthogonal, because  $\det a_{ik} = \pm 1$ . Hence, this transformation is rotational or, in other words, an inversion twist.

A projective space, containing a population of all images of the object  $A$ , can be metrizable. The metric spread  $R^n$  (coinciding completely with the projective spread) is closed, according to Hamel's theorem.

A coincidence group of points, drawing elements of the set of images of the object  $A$ , is a finite symmetric system, which can be considered as a topological spread mapped into the spherical space  $R^n$ . The surface of an  $(n + 1)$ -dimensional sphere, being equivalent to the volume of an  $n$ -dimensional torus, is completely and everywhere densely filled by the  $n$ -dimensional excellent, closed and finite point-containing system of images of the object  $A$ .

The dimension of the spread  $R^n$ , which consists only of the set of elements of the system, can be any integer  $n$  inside the interval  $(1 - N)$  to  $(N - 1)$  where  $N$  is the number of entities in the ensemble.

We are going to consider sequences of stochastic transitions between different dimension spreads as stochastic vector

quantities, i. e. as fields. Then, given a distribution function for frequencies of the stochastic transitions dependent on  $n$ , we can find the most probable number of the dimension of the ensemble in the following way.

Let the differential function of distribution of frequencies  $\nu$  in the spectra of the transitions be given by

$$\varphi(\nu) = \nu^n \exp[-\pi\nu^2].$$

If  $n \gg 1$ , the mathematical expectation for the frequency of a transition from a state  $n$  is equal to

$$m(\nu) = \frac{\int_0^\infty \nu^n \exp[-\pi\nu^2] d\nu}{2 \int_0^\infty \exp[-\pi\nu^2] d\nu} = \frac{\Gamma\left(\frac{n+1}{2}\right)}{2\pi^{\frac{n+1}{2}}}.$$

The statistical weight of the time duration for a given state is a quantity inversely proportional to the probability of this state to be changed. For this reason the most probable dimension of the ensemble is that number  $n$  under which the function  $m(\nu)$  has its minimum.

The inverse function of  $m(\nu)$ , is

$$\Phi_n = \frac{1}{m(\nu)} = S_{(n+1)} = {}_T V_n,$$

where the function  $\Phi_n$  is isomorphic to the function of the surface's value  $S_{(n+1)}$  of a unit radius hypersphere located in an  $(n+1)$ -dimensional space (this value is equal to the volume of an  $n$ -dimensional hypertorus). This isomorphism is adequate for the ergodic concept, according to which the spatial and time spreads are equivalent aspects of a manifold. So, this isomorphism shows that realization of the object  $A$  as a configuration (a form of its real existence) proceeds from the objective probability of the existence of this form.

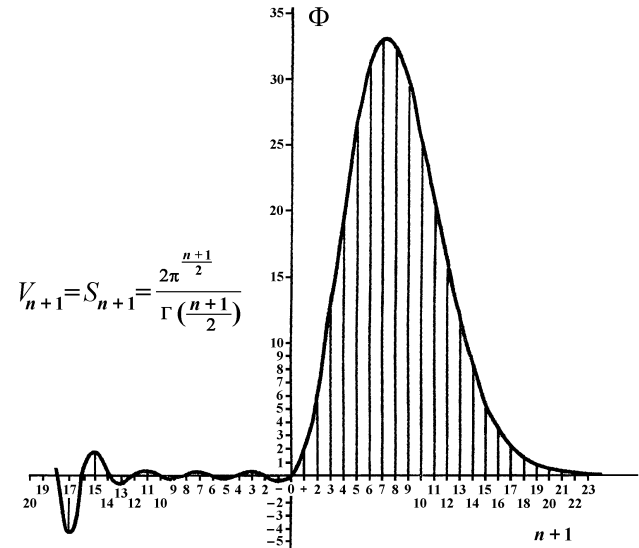
The positive branch of the function  $\Phi_n$  is unimodal; for negative values of  $(n+1)$  this function becomes sign-alternating (see the figure).

The formation takes its maximum length when  $n = \pm 6$ , hence the most probable and most unprobable extremal distributions of primary images of the object  $A$  are presented in the 6-dimensional closed configuration: the existence of the total specimen  $A$  we are considering is 6-dimensional.

Closure of this configuration is expressed by the finitude of the volume of the states, and also the symmetry of distribution inside the volume.

Any even-dimensional space can be considered as the product of two odd-dimensional spreads, which, having the same odd-dimension and the opposite directions, are embedded within each other. Any spherical formation of  $n$  dimensions is directed in spaces of  $(n+1)$  and higher dimensions. Any odd-dimensional projective space, if immersed in its own dimensions, becomes directed, while any even-dimensional projective space is one-sided. Thus the form

of the real existence of the object  $A$  we are considering is a  $(3+3)$ -dimensional complex formation, which is the product of the 3-dimensional spatial-like and 3-dimensional time-like spreads (each of them has its own direction in the  $(3+3)$ -dimensional complex formation).



One of the main concepts in dimension theory and combinatorial topology is nerve. Using this term, we come to the statement that any compact metric space of  $n$  dimensions can be mapped homeomorphically into a subset located in a Euclidean space of  $(2n+1)$  dimensions. And conversely, any compact metric space of  $(2n+1)$  dimensions can be mapped homeomorphically way into a subset of  $n$  dimensions. There is a unique correspondence between the mapping  $7 \rightarrow 3$  and the mapping  $3 \rightarrow 7$ , which consists of the geometrical realization of the abstract complex  $A$ .

The geometry of the aforementioned manifolds is determined by their own metrics, which, being set up inside them, determines the quadratic interval

$$\Delta s^2 = \Phi_n^2 \sum_{ik}^n g_{ik} \Delta x^i \Delta x^k, \quad i, k = 1, 2, \dots, n,$$

which depends not only on the function  $g_{ik}$  of coordinates  $i$  and  $k$ , but also on the function of the number of independent parameters  $\Phi_n$ .

The total length of a manifold is finite and constant, hence the sum of the lengths of all formations, realized in the manifold, is a quantity invariant with respect to orthogonal transformations. Invariance of the total length of the formation is expressed by the quadratic form

$$N_i r_i^2 = N_k r_k^2,$$

where  $N$  is the number of entities,  $r$  is the radial equivalent of the formation. From here we see, the ratio of the radii is

$$\frac{R\rho}{r^2} = 1,$$

where  $R$  is the largest radius;  $\rho$  is the smallest radius, realised in the area of the transformation;  $r$  is the radius of spherical inversion of the formation (this is the calibre of the area). The transformation areas are included in each other, the inversion twist inside them is cascaded

$$\sqrt{\frac{Rr}{2\pi}} = R_e, \quad \sqrt{R\rho} = r, \quad \sqrt{\frac{r\rho}{2\pi}} = \rho_e.$$

Negative-dimensional configurations are inversion images, corresponding to anti-states of the system. They have mirror symmetry if  $n = l(2m - 1)$  and direct symmetry if  $n = 2(2m)$ , where  $m = 1, 2, 3$ . Odd-dimensional configurations have no anti-states. The volume of the anti-states is

$$V_{(-n)} = 4 \frac{-1}{V_n}.$$

Equations of physics take a simple form if we use the  $LT$  kinematic system of units, whose units are two aspects  $l$  and  $t$  of the radius through which areas of the space  $R^n$  undergo inversion:  $l$  is the element of the spatial-like spread of the subspace  $L$ , and  $t$  is the element of time-like spread of the subspace  $T$ . Introducing homogeneous coordinates permits reduction of projective geometry theorems to algebraic equivalents, and geometrical relations to kinematic relations.

The kinematic equivalent of the formation corresponds the following model.

An elementary  $(3+3)$ -dimensional image of the object  $A$  can be considered as a wave or a rotating oscillator, which, in turn, becomes the sink and source, produced by the singularity of the transformation. There in the oscillator polarization of the background components occurs — the transformation  $L \rightarrow T$  or  $T \rightarrow L$ , depending on the direction of the oscillator, which makes branching  $L$  and  $T$  spreads. The transmutation  $L \leftrightarrow T$  corresponds the shift of the field vector at  $\pi/2$  in its parallel transfer along closed arcs of radii  $R$  and  $r$  in the affine coherence space  $R^n$ .

The effective abundance of the pole is

$$e = \frac{1}{2} \frac{1}{4\pi} \int_s E ds.$$

A charge is an elementary oscillator, making a field around itself and inside itself. There in the field a vector's length depends only on the distance  $r_i$  or  $1/r_i$  from the centre of the peculiarity. The inner field is the inversion map of the outer field; the mutual correspondence between the outer spatial-like and the inner time-like spreads leads to torsion of the field.

The product of the space of the spherical surface and the strength in the surface is independent of  $r_i$ ; this value depends only on properties of the charge  $q$

$$4\pi q = S\dot{V} = 4\pi r^2 \frac{d^2 l}{dt^2}.$$

Because the charge manifests in the spread  $R^n$  only as the strength of its field, and both parts of the equations are equivalent, we can use the right side of the equation instead of the left one.

The field vector takes its ultimate value

$$c = \frac{l}{t} = \sqrt{\frac{S\dot{V}}{4\pi r_i}} = 1$$

in the surface of the inversion sphere with the radius  $r$ . The ultimate value of the field strength  $lt^{-2}$  takes a place in the same surface;  $\nu = t^{-1}$  is the fundamental frequency of the oscillator. The effective (half) product of the sphere surface space and the oscillation acceleration equals the value of the pulsating charge, hence

$$4\pi q = \frac{1}{2} 4\pi \nu r_i^2 \frac{l}{t} = 2\pi r_i c^2.$$

In  $LT$  kinematic system of units the dimension of a charge (both gravitational and electric) is

$$\dim m = \dim e = L^3 T^{-2}.$$

In the kinematic system  $LT$ , exponents in structural formulae of dimensions of all physical quantities, including electromagnetic quantities, are integers.

Denoting the fundamental ratio  $l/t$  as  $C$ , in the kinematic system  $LT$  we obtain the generalized structural formula for physical quantities

$$D^{\Sigma n} = c^\gamma T^{n-\gamma},$$

where  $D^{\Sigma n}$  is the dimensional volume of a given physical quantity,  $\Sigma n$  is the sum of exponents in the formula of dimensions (see above),  $T$  is the radical of dimensions,  $n$  and  $\gamma$  are integers.

Thus we calculate dimensions of physical quantities in the kinematic  $LT$  system of units (see Table 1).

Physical constants are expressed by some relations in the geometry of the ensemble, reduced to kinematic structures. The kinematic structures are aspects of the probability and configuration realization of the abstract complex  $A$ . The most stable form of a kinematic state corresponds to the most probable form of the stochastic existence of the formation.

The value of any physical constant can be obtained in the following way.

The maximum value of the probability of the state we are considering is the same as the volume of a 6-dimensional torus,

$$V_6 = \frac{16\pi^3}{15} r^3 = 33.0733588 r^6.$$

The extreme numerical values — the maximum of the positive branch and the minimum of the negative branches of the function  $\Phi_n$  are collected in Table 2.

Table 1

Parameter	$\Sigma n$	Quantity $D^{\Sigma n}$ , taken under $\gamma$ equal to:							
		5	4	3	2	1	0	-1	-2
		$C^5 T^{n-5}$	$C^4 T^{n-4}$	$C^3 T^{n-3}$	$C^2 T^{n-2}$	$C^1 T^{n-1}$	$C^0 T^{n-0}$	$C^{-1} T^{n+1}$	$C^{-2} T^{n+2}$
Surface power	-2			$L^3 T^{-5}$					
Pressure					$L^2 T^{-4}$				
Current density						$L^1 T^{-3}$			
Mass density, angular acceleration							$L^0 T^{-2}$		
Volume charge density								$L^{-1} T^{-1}$	
Electromagnetic field strength	-1				$L^2 T^{-3}$				
Magnetic displacement, acceleration						$L^1 T^{-2}$			
Frequency							$L^0 T^{-1}$		
Power	0	$L^5 T^{-5}$							
Force			$L^4 T^{-4}$						
Current, loss mass				$L^3 T^{-3}$					
Potential difference					$L^2 T^{-2}$				
Velocity						$L^1 T^{-1}$			
Dimensionless constants							$L^0 T^0$		
Conductivity								$L^{-1} T^1$	
Magnetic permittivity									$L^{-2} T^2$
Force momentum, energy	+1	$L^5 T^{-4}$							
Motion quantity, impulse				$L^4 T^{-3}$					
Mass, quantity of magnetism or electricity					$L^3 T^{-2}$				
Two-dimensional abundance						$L^2 T^{-1}$			
Length, capacity, self-induction							$L^1 T^0$		
Period, duration								$L^0 T^1$	
Angular momentum, action	+2	$L^5 T^{-3}$							
Magnetic momentum				$L^4 T^{-2}$					
Loss volume					$L^3 T^{-1}$				
Surface						$L^2 T^0$			
							$L^1 T^1$		
							$L^0 T^2$		
Moment of inertia	+3	$L^5 T^{-2}$							
				$L^4 T^{-1}$					
Volume of space					$L^3 T^0$				
Volume of time								$L^0 T^3$	

Table 2

$n + 1$	+7.256946404	-4.99128410
$S_{n+1}$	+33.161194485	-0.1209542108

The ratio between the ultimate values of the function  $S_{n+1}$  is

$$\bar{E} = \frac{|+S_{(n+1)_{max}}|}{|-S_{(n+1)_{min}}|} = 274.163208 r^{12}.$$

On the other hand, a finite length of a spherical layer of  $R^n$ , homogeneously and everywhere densely filled by doublets of the elementary formations  $A$ , is equivalent to a vortical torus, concentric with the spherical layer. The mirror image of the layer is another concentric homogeneous double layer, which, in turn, is equivalent to a vortical torus coaxial with the first one. Such formations were studied by Lewis and Larmore for the  $(3+1)$ -dimensional case.

Conditions of stationary vortical motion are realized if

$$V \times \text{rot} V = \text{grad} \varphi, \quad 2v ds = d\Gamma,$$

where  $\varphi$  is the potential of the circulation,  $\Gamma$  is the main kinematic invariant of the field. A vortical motion is stable only if the current lines coincide with the trajectory of the vortex core. For a  $(3+1)$ -dimensional vortical torus we have

$$V_x = \frac{\Gamma}{2\pi D} \left[ \ln \frac{4D}{r} - \frac{1}{4} \right],$$

where  $r$  is the radius of the circulation,  $D$  is the torus diameter.

The velocity at the centre of the formation is

$$V_\circ = \frac{u\pi D}{2r}.$$

The condition  $V_x = V_\circ$ , in the case we are considering, is true if  $n = 7$

$$\begin{aligned} \ln \frac{4D}{r} &= (2\pi + 0.25014803) \frac{2n+1}{2n} = \\ &= 2\pi + 0.25014803 + \frac{n}{2n+1} = 7, \end{aligned}$$

$$\frac{D}{r} = \bar{E} = \frac{1}{4} e^7 = 274.15836.$$

In the field of a vortical torus, with Bohr radius of the charge,  $r = 0.9999028$ , the quantity  $\pi$  takes the numerical value  $\pi^* = 0.9999514\pi$ . So  $\bar{E} = \frac{1}{4} e^{6.9996968} = 274.074996$ . In the  $LT$  kinematic system of units, and introducing the relation  $B = V_6 \bar{E} / \pi = 2885.3453$ , we express values of all constants by prime relations between  $\bar{E}$  and  $B$

$$K = \delta \tilde{E}^\alpha \tilde{B}^\beta,$$

where  $\delta$  is equal to a quantized turn,  $\alpha$  and  $\beta$  are integers.

Table 3 gives numerical values of physical constants, obtained analytically and experimentally. The appendix gives experimental determinations in units of the CGS system (cm, gramme, sec), because they are conventional quantities, not physical constants.

The fact that the theoretically and experimentally obtained values of physical constants coincide permits us to suppose that all metric properties of the considered total and unique specimen  $A$  can be identified as properties of our observed World, so the World is identical to the unique "particle"  $A$ . In another paper it will be shown that a  $(3+3)$ -dimensional structure of space-time can be proven in an experimental way, and also that this 6-dimensional model is free of logical difficulties derived from the  $(3+1)$ -dimensional concept of the space-time background\*.

In the system of units we are using here the gravitational constant is

$$\kappa = \frac{1}{4\pi} \left[ \frac{l^0}{t^0} \right].$$

If we convert its dimensions back to the CGS system, so that  $G = \left[ \frac{l^3}{mt^2} \right]$ , appropriate numerical values of the physical quantities will be determined in another form (Column 5 in Table 3). Reduced physical quantities are given in Column 8. Column 9 gives evolutionary changes of the physical quantities with time according to the theory, developed by Stanyukovich [17]†.

The gravitational "constant", according to his theory, increases proportionally to the space radius (and also the world-time) and the number of elementary entities, according to Dirac [18], increases proportional to the square of the space radius (and the square of world-time as well). Therefore we obtain  $N = T_m^2 \simeq B^{24}$ , hence  $B \simeq T_m^{\frac{1}{12}}$ .

Because  $T_m = t_0 \omega_0 \simeq 10^{40}$ , where  $t_0 \simeq 10^{17}$  sec is the space age of our Universe and  $\omega_0 = \frac{c}{\rho} = 10^{23} \text{ sec}^{-1}$  is the frequency of elementary interactions, we obtain  $B \simeq 10^{\frac{10}{3}} = 10^{\frac{1}{3}} \times 1000$ .

In this case we obtain  $m \sim e^2 \sim \hbar \sim T_m^{-2} \sim B^{-24}$ , which is in good agreement with the evolution concept developed by Stanyukovich.

## Appendix

Here is a determination of the quantity 1 cm in the CGS system of units. The analytic value of Rydberg constant is

\*Roberto di Bartini died before he prepared the second paper. He died sitting at his desk, looking at papers with drawings of vortical tori and draft formulae. According to Professor Stanyukovich, Bartini was not in the habit of keeping many drafts, so unfortunately, we do not know anything about the experimental statement that he planned to provide as the proof to his concept of the  $(3+3)$ -dimensional space-time background. — D. R.

†Stanyukovich's theory is given in Part II of his book [17]. Here  $T_{0m}$  is the world-time moment when a particle (electron, nucleon, etc.) was born,  $T_m$  is the world-time moment when we observe the particle. — D. R.

Table 3

Parameter	Notation	Structural formula	$K = \delta E^\alpha B^\beta$	Analytically obtained numerical values		Observed numerical values in CGS-system	Structural formula in CGS	Dependence on time
				LT-system of units	CGS-system			
Sommerfeld constant	$1/\alpha$	$1/2E$	$2^{-1}\pi^0 E^0 B^0$	$1.370375 \times 10^2$	$1.370375 \times 10^2$	$1.370374 \times 10^2 \text{ cm}^0 \text{ gm}^0 \text{ sec}^0$	$\frac{1}{2}E$	const
Gravitational constant	$\kappa$	$1/4\pi F^*$	$2^{-2}\pi^{-1} E^0 B^0$	$7.986889 \times 10^{-2}$	$6.670024 \times 10^{-8}$	$6.670 \times 10^{-8} \text{ cm}^3 \text{ gm}^{-1} \text{ sec}^{-1}$	$\kappa$	$\frac{T_m}{T_{0m}}$
Fundamental velocity	$c$	$l/t$	$2^0\pi^0 E^0 B^0$	$1.000000 \times 10^0$	$2.997930 \times 10^{10}$	$2.997930 \times 10^{10} \text{ cm}^1 \text{ gm}^0 \text{ sec}^{-1}$	$C$	const
Mass basic ratio	$n/m$	$2B/\pi$	$2^1\pi^{-1} E^0 B^1$	$1.836867 \times 10^3$	$1.836867 \times 10^3$	$1.83630 \times 10^3 \text{ cm}^0 \text{ gm}^0 \text{ sec}^0$	$\frac{n}{m}$	$\frac{n}{m} \left( \frac{T_m}{T_{0m}} \right)^{1/2}$
Charge basic ratio	$e/m$	$B^6$	$2^0\pi^0 E^0 B^6$	$5.770146 \times 10^{20}$	$5.273048 \times 10^{17}$	$5.273058 \times 10^{17} \text{ cm}^2 \text{ gm}^{-2} \text{ sec}^{1/2}$	$\frac{e}{\sqrt{\kappa m}}$	$\frac{e}{\sqrt{\kappa m} \left( \frac{T_m}{T_{0m}} \right)^{1/2}}$
Gravitational radius of electron	$\rho$	$\tau/2\pi B^{12}$	$2^{-1}\pi^{-1} E^0 B^{-12}$	$4.7802045 \times 10^{-43}$	$1.346990 \times 10^{-55}$	$1.348 \times 10^{-55} \text{ cm}^1 \text{ gm}^0 \text{ sec}^0$	$S$	const
Electric radius of electron	$\rho_e$	$r/2\pi B^6$	$2^{-1}\pi^{-1} E^0 B^{-6}$	$2.753248 \times 10^{-21}$	$7.772329 \times 10^{-35}$	—	$S_e$	$S_e \left( \frac{T_{0m}}{T_m} \right)^{1/2}$
Classical radius of inversion	$\tau$	$\sqrt{R\rho}$	$2^0\pi^0 E^0 B^0$	$1.000000 \times 10^0$	$2.817850 \times 10^{-13}$	$2.817850 \times 10^{-13} \text{ cm}^1 \text{ gm}^0 \text{ sec}^0$	$\tau$	const
Space radius	$R$	$2\pi B^{12} r$	$2^1\pi^1 E^0 B^{12}$	$2.091961 \times 10^{42}$	$5.894831 \times 10^{29}$	$10^{29} > 10^{28} \text{ cm}^1 \text{ gm}^0 \text{ sec}^0$	$R$	$R \frac{T_m}{T_{0m}}$
Electron mass	$m$	$2\pi\rho c^2$	$2^0\pi^0 E^0 B^{-12}$	$3.003491 \times 10^{-42}$	$9.108300 \times 10^{-28}$	$9.1083 \times 10^{-28} \text{ cm}^0 \text{ gm}^1 \text{ sec}^0$	$\kappa m$	$\kappa m \frac{T_{0m}}{T_m}$
Nucleon mass	$n$	$2rc^2/\pi B^{11}$	$2^1\pi^{-1} E^0 B^{-11}$	$5.517016 \times 10^{-39}$	$1.673074 \times 10^{-24}$	$1.67239 \times 10^{-24} \text{ cm}^0 \text{ gm}^1 \text{ sec}^0$	$\kappa n$	$\kappa n \left( \frac{T_{0m}}{T_m} \right)^{1/2}$
Electron charge	$e$	$2\pi\rho_e c^2$	$2^0\pi^0 E^0 B^{-6}$	$1.733058 \times 10^{-21}$	$4.802850 \times 10^{-10}$	$4.80286 \times 10^{-10} \text{ cm}^2 \text{ gm}^{1/2} \text{ sec}^{-1}$	$\sqrt{\kappa e}$	$\sqrt{\kappa e} \left( \frac{T_{0m}}{T_m} \right)^{1/2}$
Space mass	$M$	$2\pi R c^2$	$2^2\pi^2 E^0 B^{12}$	$1.314417 \times 10^{43}$	$3.986064 \times 10^{57}$	$10^{57} > 10^{56} \text{ cm}^0 \text{ gm}^1 \text{ sec}^0$	$\kappa M$	$\kappa M \frac{T_{0m}}{T_m}$
Space period	$T$	$2\pi B^{12} t$	$2^1\pi^1 E^0 B^{12}$	$2.091961 \times 10^{42}$	$1.966300 \times 10^{19}$	$10^{19} > 10^{17} \text{ cm}^0 \text{ gm}^0 \text{ sec}^1$	$T$	$T \frac{T_{0m}}{T_m}$
Space density	$\gamma_k$	$M/2\pi^2 R^3$	$2^{-2}\pi^{-3} E^0 B^{-24}$	$7.273495 \times 10^{-86}$	$9.858261 \times 10^{-34}$	$\sim 10^{-31} \text{ cm}^{-3} \text{ gm}^3 \text{ sec}^0$	$\kappa\gamma_k$	$\kappa\gamma_k \left( \frac{T_{0m}}{T_m} \right)^2$
Space action	$H$	$Mc2\pi R$	$2^4\pi^4 E^0 B^{24}$	$1.727694 \times 10^{86}$	$4.426057 \times 10^{98}$	—	$H$	const
Number of actual entities	$N$	$R/\rho$	$2^2\pi^2 E^0 B^{24}$	$4.376299 \times 10^{84}$	$4.376299 \times 10^{84}$	$> 10^{82} \text{ cm}^0 \text{ gm}^0 \text{ sec}^0$	$N$	$N \frac{T_m^2}{T_{0m}^2}$
Number of primary interactions	$A$	$NT$	$2^3\pi^3 E^0 B^{36}$	$9.155046 \times 10^{126}$	$9.155046 \times 10^{126}$	—	$NT$	$NM \left( \frac{T_m}{T_{0m}} \right)^3$
Planck constant	$\hbar$	$mc\pi Er$	$2^0\pi^1 E^1 B^{-12}$	$2.586100 \times 10^{-39}$	$6.625152 \times 10^{-27}$	$6.62517 \times 10^{-27} \text{ cm}^2 \text{ gm}^1 \text{ sec}^{-1}$	$\kappa\hbar$	$\frac{T_{0m}}{\kappa\hbar} \frac{T_m}{T_m}$
Bohr magneton	$\mu_b$	$Er^2 c^2/4B^6$	$2^{-2}\pi^0 E^1 B^{-6}$	$1.187469 \times 10^{-19}$	$9.273128 \times 10^{-21}$	$9.2734 \times 10^{-21} \text{ cm}^{5/2} \text{ gm}^{1/2} \text{ sec}^{-1}$	$\sqrt{\kappa\mu}$	$\sqrt{\kappa\mu} \left( \frac{T_{0m}}{T_m} \right)^{1/2}$
Compton frequency	$\nu_c$	$c/2\pi Er$	$2^{-1}\pi^{-1} E^{-1} B^0$	$5.806987 \times 10^{-4}$	$6.178094 \times 10^{19}$	$6.1781 \times 10^{19} \text{ cm}^0 \text{ gm}^0 \text{ sec}^{-1}$	$\sqrt{c}$	const

\*  $F = E/(E - 1) = 1.003662$



$[R_\infty] = (1/4\pi E^3)l^{-1} = 3.0922328 \times 10^{-8}l^{-1}$ , the experimentally obtained value of the constant is  $(R_\infty) = 109737.311 \pm \pm 0.012 \text{cm}^{-1}$ . Hence 1 cm is determined in the CGS system as  $(R_\infty)/[R_\infty] = 3.5488041 \times 10^{12}l$ .

Here is a determination of the quantity 1 sec in the CGS system of units. The analytic value of the fundamental velocity is  $[c] = l/t = 1$ , the experimentally obtained value of the velocity of light in vacuum is  $(c) = 2.997930 \pm \pm 0.0000080 \times 10^{-10} \text{cm} \times \text{sec}^{-1}$ . Hence 1 sec is determined in the CGS system as  $(c)/l[c] = 1.0639066 \times 10^{23}t$ .

Here is a determination of the quantity 1 gramme in the CGS system of units. The analytic value of the ratio  $e/mc$  is  $[e/mc] = \tilde{B}^6 = 5.7701460 \times 10^{20}l^{-1}t$ . This quantity, measured in experiments, is  $(e/mc) = 1.758897 \pm 0.000032 \times 10^7 (\text{cm} \times \text{gm}^{-1})^{\frac{1}{2}}$ . Hence 1 gramme is determined in the CGS system as  $\frac{(e/mc)^2}{l[e/mc]^2} = 3.297532510 \times 10^{-15}l^3t^{-2}$ , so CGS' one gramme is  $1 \text{ gm (CGS)} = 8.351217 \times 10^{-7} \text{cm}^3 \text{sec}^{-2} \text{ (CS)}$ .

17. Stanyukovich K. P. Gravitational field and elementary particles. Nauka, Moscow, 1965.
18. Dirac P. A. M. *Nature*, 1957, v. 139, 323; *Proc. Roy. Soc. A*, 1938, v. 6, 199.
19. Oros di Bartini R. Some relations between physical constants. *Doklady Acad. Nauk USSR*, 1965, v. 163, No. 4, 861–864.

## References

1. Pauli W. Relativitätstheorie. *Encyclopädie der mathematischen Wissenschaften*, Band V, Heft IV, Art. 19, 1921 (Pauli W. Theory of Relativity. Pergamon Press, 1958).
2. Eddington A. S. The mathematical theory of relativity, Cambridge University Press, Cambridge, 2nd edition, 1960.
3. Hurewicz W. and Wallman H. Dimension theory. Foreign Literature, Moscow, 1948.
4. Zeivert H. and Threphall W. Topology. GONTI, Moscow, 1938.
5. Chzgen Schen-Schen (Chern S. S.) Complex manifolds. Foreign Literature, Moscow, 1961
6. Pontriagine L. Foundations of combinatory topology. OGIZ, Moscow, 1947.
7. Busemann G. and Kelley P. Projective geometry. Foreign Literature, Moscow, 1957.
8. Mors M. Topological methods in the theory of functions. Foreign Literature, Moscow, 1951.
9. Hilbert D. und Cohn-Vossen S. Anschauliche Geometrie. Springer Verlag, Berlin, 1932 (Hilbert D. and Kon-Fossen S. Obvious geometry. GTTI, Moscow, 1951).
10. Vigner E. The theory of groups. Foreign Literature, Moscow, 1961.
11. Lamb G. Hydrodynamics. GTTI, Moscow, 1947.
12. Madelunge E. The mathematical apparatus in physics. PhysMathGiz, Moscow, 1960.
13. Bartlett M. Introduction into probability processes theory. Foreign Literature, Moscow, 1958.
14. McVittie G. The General Theory of Relativity and cosmology. Foreign Literature, Moscow, 1961.
15. Wheeler D. Gravitation, neutrino, and the Universe. Foreign Literature, Moscow, 1962.
16. Dicke R. *Review of Modern Physics*, 1957, v. 29, No. 3.

# Introducing Distance and Measurement in General Relativity: Changes for the Standard Tests and the Cosmological Large-Scale

Stephen J. Crothers

*Sydney, Australia*

E-mail: thenarmis@yahoo.com

Relativistic motion in the gravitational field of a massive body is governed by the external metric of a spherically symmetric extended object. Consequently, any solution for the point-mass is inadequate for the treatment of such motions since it pertains to a fictitious object. I therefore develop herein the physics of the standard tests of General Relativity by means of the generalised solution for the field external to a sphere of incompressible homogeneous fluid.

## 1 Introduction

The orthodox treatment of physics in the vicinity of a massive body is based upon the Hilbert [1] solution for the point-mass, a solution which is neither correct nor due to Schwarzschild [2], as the latter is almost universally claimed.

In previous papers [3, 4] I derived the correct general solution for the point-mass and the point-charge in all their standard configurations, and demonstrated that the Hilbert solution is invalid. The general solution for the point-mass is however, inadequate for any real physical situation since the material point (and also the material point-charge) is a fictitious object, and so quite meaningless. Therefore, I avail myself of the general solution for the external field of a sphere of incompressible homogeneous fluid, obtained in a particular case by K. Schwarzschild [5] and generalised by myself [6] to,

$$ds^2 = \left[ \frac{(\sqrt{C_n} - \alpha)}{\sqrt{C_n}} \right] dt^2 - \left[ \frac{\sqrt{C_n}}{(\sqrt{C_n} - \alpha)} \right] \frac{C_n'^2}{4C_n} dr^2 - C_n (d\theta^2 + \sin^2 \theta d\varphi^2), \quad (1)$$

$$C_n(r) = \left( |r - r_0|^n + \epsilon^n \right)^{\frac{2}{n}},$$

$$\alpha = \sqrt{\frac{3}{\kappa\rho_0}} \sin^3 |\chi_a - \chi_0|,$$

$$R_{c_a} = \sqrt{\frac{3}{\kappa\rho_0}} \sin |\chi_a - \chi_0|,$$

$$\epsilon = \sqrt{\frac{3}{\kappa\rho_0}} \left\{ \frac{3}{2} \sin^3 |\chi_a - \chi_0| - \frac{9}{4} \cos |\chi_a - \chi_0| \left[ |\chi_a - \chi_0| - \frac{1}{2} \sin 2 |\chi_a - \chi_0| \right] \right\}^{\frac{1}{3}},$$

$$r_0 \in \mathfrak{R}, \quad r \in \mathfrak{R}, \quad n \in \mathfrak{R}^+, \quad \chi_0 \in \mathfrak{R}, \quad \chi_a \in \mathfrak{R},$$

$$\arccos \frac{1}{3} < |\chi_a - \chi_0| < \frac{\pi}{2},$$

$$|r_a - r_0| \leq |r - r_0| < \infty,$$

where  $\rho_0$  is the constant density of the fluid,  $k^2$  is Gauss' gravitational constant, the sign  $a$  denotes values at the surface of the sphere,  $|\chi - \chi_0|$  parameterizes the radius of curvature of the interior of the sphere centred arbitrarily at  $\chi_0$ ,  $|r - r_0|$  is the coordinate radius in the spacetime manifold of Special Relativity which is a parameter space for the gravitational field external to the sphere centred arbitrarily at  $r_0$ .

To eliminate the infinite number of coordinate systems admitted by (1), I rewrite the said metric in terms of the only measurable distance in the gravitational field, i.e. the circumference  $G$  of a great circle, thus

$$ds^2 = \left( 1 - \frac{2\pi\alpha}{G} \right) dt^2 - \left( 1 - \frac{2\pi\alpha}{G} \right)^{-1} \frac{dG^2}{4\pi^2} - \frac{G^2}{4\pi^2} (d\theta^2 + \sin^2 \theta d\varphi^2), \quad (2)$$

$$\alpha = \sqrt{\frac{3}{\kappa\rho_0}} \sin^3 |\chi_a - \chi_0|,$$

$$2\pi \sqrt{\frac{3}{\kappa\rho_0}} \sin |\chi_a - \chi_0| \leq G < \infty,$$

$$\arccos \frac{1}{3} < |\chi_a - \chi_0| < \frac{\pi}{2}.$$

## 2 Distance and time

According to (1), if  $t$  is constant, a three-dimensional manifold results, having the line-element,

$$ds^2 = \left[ \frac{\sqrt{C_n}}{(\sqrt{C_n} - \alpha)} \right] \frac{C_n'^2}{4C_n} dr^2 + C_n (d\theta^2 + \sin^2 \theta d\varphi^2). \quad (3)$$

If  $\alpha = 0$ , (1) reduces to the line-element of flat spacetime,

$$ds^2 = dt^2 - dr^2 - |r - r_0|^2(d\theta^2 + \sin^2 \theta d\varphi^2), \quad (4)$$

$$0 \leq |r - r_0| < \infty,$$

since then  $r_a \equiv r_0$ .

The introduction of matter makes  $r_a \neq r_0$ , owing to the extended nature of a real body, and introduces distortions from the Euclidean in time and distance. The value of  $\alpha$  is effectively a measure of this distortion and therefore fixes the spacetime.

When  $\alpha = 0$ , the distance  $D = |r - r_0|$  is the radius of a sphere centred at  $r_0$ . If  $r_0 = 0$  and  $r \geq 0$ , then  $D \equiv r$  and is then both a radius and a coordinate, as is clear from (4).

If  $r$  is constant in (3), then  $C_n(r) = R_c^2$  is constant, and so (3) becomes,

$$ds^2 = R_c^2(d\theta^2 + \sin^2 \theta d\varphi^2), \quad (5)$$

which describes a sphere of constant radius  $R_c$  embedded in Euclidean space. The infinitesimal tangential distances on (5) are simply,

$$ds = R_c \sqrt{d\theta^2 + \sin^2 \theta d\varphi^2}.$$

When  $\theta$  and  $\varphi$  are constant, (3) yields the proper radius,

$$R_p = \int \sqrt{\frac{\sqrt{C_n(r)}}{\sqrt{C_n(r)} - \alpha}} \frac{C'_n(r)}{2\sqrt{C_n(r)}} dr =$$

$$= \int \sqrt{\frac{\sqrt{C_n(r)}}{\sqrt{C_n(r)} - \alpha}} d\sqrt{C_n(r)}, \quad (6)$$

from which it clearly follows that the parameter  $r$  does not measure radial distances in the gravitational field.

Integrating (6) gives,

$$R_p(r) = \sqrt{\sqrt{C_n(r)}(\sqrt{C_n(r)} - \alpha)} + \alpha \ln \left| \frac{\sqrt{\sqrt{C_n(r)} + \sqrt{C_n(r) - \alpha}}}{\sqrt{\sqrt{C_n(r)} - \alpha}} \right| + K,$$

$$K = \text{const},$$

which must satisfy the condition,

$$r \rightarrow r_a^\pm \Rightarrow R_p \rightarrow R_{p_a}^\pm,$$

where  $r_a$  is the parameter value at the surface of the body and  $R_{p_a}$  the indeterminate proper radius of the sphere from outside the sphere. Therefore,

$$R_p(r) = R_{p_a} + \sqrt{\sqrt{C_n(r)}(\sqrt{C_n(r)} - \alpha)} -$$

$$- \sqrt{\sqrt{C_n(r_a)}(\sqrt{C_n(r_a)} - \alpha)} +$$

$$+ \alpha \ln \left| \frac{\sqrt{\sqrt{C_n(r)} + \sqrt{C_n(r) - \alpha}}}{\sqrt{\sqrt{C_n(r_a)} + \sqrt{C_n(r_a) - \alpha}}} \right|, \quad (7)$$

which, by the use of (1) and (2), becomes

$$R_p(r) = R_{p_a} + \sqrt{\frac{G}{2\pi} \left( \frac{G}{2\pi} - \alpha \right)} -$$

$$- \sqrt{\sqrt{\frac{3}{\kappa\rho_0}} \sin |\chi_a - \chi_0| \left( \sqrt{\frac{3}{\kappa\rho_0}} \sin |\chi_a - \chi_0| - \alpha \right)} +$$

$$+ \alpha \ln \left| \frac{\sqrt{\frac{G}{2\pi}} + \sqrt{\frac{G}{2\pi} - \alpha}}{\sqrt{\sqrt{\frac{3}{\kappa\rho_0}} \sin |\chi_a - \chi_0| + \sqrt{\sqrt{\frac{3}{\kappa\rho_0}} \sin |\chi_a - \chi_0| - \alpha}}} \right|, \quad (8)$$

$$\alpha = \sqrt{\frac{3}{\kappa\rho_0}} \sin^3 |\chi_a - \chi_0|.$$

According to (1), the proper time is related to the coordinate time by,

$$d\tau = \sqrt{g_{00}} dt = \sqrt{1 - \frac{\alpha}{\sqrt{C_n(r)}}} dt. \quad (9)$$

When  $\alpha = 0$ ,  $d\tau = dt$  so that proper time and coordinate time are one and the same in flat spacetime. With the introduction of matter, proper time and coordinate time are no longer the same. It is evident from (9) that both  $\tau$  and  $t$  are finite and non-zero, since according to (1),

$$\frac{1}{9} < 1 - \frac{\alpha}{\sqrt{C_n(r_a)}} \leq 1 - \frac{\alpha}{\sqrt{C_n(r)}},$$

i.e.

$$\frac{1}{9} < \cos^2 |\chi_a - \chi_0| \leq 1 - \frac{\alpha}{\sqrt{C_n(r)}},$$

or

$$\frac{1}{3} dt \leq d\tau \leq dt,$$

since in the far field, according to (9),

$$\sqrt{C_n(r)} \rightarrow \infty \Rightarrow d\tau \rightarrow dt,$$

recovering flat spacetime asymptotically.

Therefore, if a body falls from rest from a point distant from the gravitating mass, it will reach the surface of the mass in a finite coordinate time and a finite proper time. According to an external observer, time does not stop at the surface of the body, where  $dt = 3d\tau$ , contrary to the orthodox analysis based upon the fictitious point-mass.

### 3 Radar sounding

Consider an observer in the field of a massive body. Let the observer have coordinates,  $(r_1, \theta_0, \varphi_0)$ . Let the coordinates of a small body located between the observer and the massive

body along a radial line be  $(r_2, \theta_0, \varphi_0)$ . Let the observer emit a radar pulse towards the small body. Then by (1),

$$\begin{aligned} \left(1 - \frac{\alpha}{\sqrt{C_n(r)}}\right) dt^2 &= \left(1 - \frac{\alpha}{\sqrt{C_n(r)}}\right)^{-1} \frac{C_n'^2(r)}{4C_n(r)} dr^2 = \\ &= \left(1 - \frac{\alpha}{\sqrt{C_n(r)}}\right)^{-1} d\sqrt{C_n(r)}^2, \end{aligned}$$

so

$$\frac{d\sqrt{C_n(r)}}{dt} = \pm \left(1 - \frac{\alpha}{\sqrt{C_n(r)}}\right),$$

or

$$\frac{dr}{dt} = \pm \frac{2\sqrt{C_n(r)}}{C_n'(r)} \left(1 - \frac{\alpha}{\sqrt{C_n(r)}}\right).$$

The coordinate time for the pulse to travel to the small body and return to the observer is,

$$\begin{aligned} \Delta t &= - \int_{\sqrt{C_n(r_2)}}^{\sqrt{C_n(r_1)}} \frac{d\sqrt{C_n}}{1 - \frac{\alpha}{\sqrt{C_n}}} + \int_{\sqrt{C_n(r_2)}}^{\sqrt{C_n(r_1)}} \frac{d\sqrt{C_n}}{1 - \frac{\alpha}{\sqrt{C_n}}} = \\ &= 2 \int_{\sqrt{C_n(r_2)}}^{\sqrt{C_n(r_1)}} \frac{d\sqrt{C_n}}{1 - \frac{\alpha}{\sqrt{C_n}}}. \end{aligned}$$

The proper time lapse is, according to the observer, by formula (1),

$$\begin{aligned} \Delta \tau &= \sqrt{1 - \frac{\alpha}{\sqrt{C_n}}} dt = 2\sqrt{1 - \frac{\alpha}{\sqrt{C_n}}} \int_{\sqrt{C_n(r_2)}}^{\sqrt{C_n(r_1)}} \frac{d\sqrt{C_n}}{1 - \frac{\alpha}{\sqrt{C_n}}} = \\ &= 2\sqrt{1 - \frac{\alpha}{\sqrt{C_n}}} \left( \sqrt{C_n(r_1)} - \sqrt{C_n(r_2)} + \alpha \ln \left| \frac{\sqrt{C_n(r_1)} - \alpha}{\sqrt{C_n(r_2)} - \alpha} \right| \right). \end{aligned}$$

The proper distance between the observer and the small body is,

$$\begin{aligned} R_p &= \int_{\sqrt{C_n(r_2)}}^{\sqrt{C_n(r_1)}} \sqrt{\frac{\sqrt{C_n}}{\sqrt{C_n} - \alpha}} d\sqrt{C_n} \\ &= \sqrt{\sqrt{C_n(r_1)}(\sqrt{C_n(r_1)} - \alpha)} - \\ &\quad - \sqrt{\sqrt{C_n(r_2)}(\sqrt{C_n(r_2)} - \alpha)} + \\ &\quad + \alpha \ln \left| \frac{\sqrt{\sqrt{C_n(r_1)} + \sqrt{\sqrt{C_n(r_1)} - \alpha}}}{\sqrt{\sqrt{C_n(r_2)} + \sqrt{\sqrt{C_n(r_2)} - \alpha}}} \right|. \end{aligned}$$

Then according to classical theory, the round trip time is

$$\Delta \bar{\tau} = 2R_p,$$

so  $\Delta \tau \neq \Delta \bar{\tau}$ .

If  $\frac{\alpha}{\sqrt{C_n(r)}}$  is small for

$$\sqrt{C_n(r_2)} < \sqrt{C_n(r)} < \sqrt{C_n(r_1)},$$

then

$$\begin{aligned} \Delta \tau &\approx 2 \left[ \sqrt{C_n(r_1)} - \sqrt{C_n(r_2)} - \right. \\ &\quad \left. - \frac{\alpha(\sqrt{C_n(r_1)} - \sqrt{C_n(r_2)})}{2\sqrt{C_n(r_1)}} + \alpha \ln \sqrt{\frac{\sqrt{C_n(r_1)}}{\sqrt{C_n(r_2)}}} \right], \\ \Delta \bar{\tau} &\approx 2 \left[ \sqrt{C_n(r_1)} - \sqrt{C_n(r_2)} + \frac{\alpha}{2} \ln \sqrt{\frac{\sqrt{C_n(r_1)}}{\sqrt{C_n(r_2)}}} \right]. \end{aligned}$$

Therefore,

$$\begin{aligned} \Delta \tau - \Delta \bar{\tau} &\approx \alpha \left[ \ln \sqrt{\frac{\sqrt{C_n(r_1)}}{\sqrt{C_n(r_2)}}} - \right. \\ &\quad \left. - \frac{(\sqrt{C_n(r_1)} - \sqrt{C_n(r_2)})}{\sqrt{C_n(r_1)}} \right] = \\ &= \alpha \left( \ln \sqrt{\frac{G_1}{G_2}} - \frac{G_1 - G_2}{G_1} \right) = \end{aligned} \tag{10}$$

$$= \sqrt{\frac{3}{\kappa \rho_0}} \sin^3 |\chi_\alpha - \chi_0| \left( \ln \sqrt{\frac{G_1}{G_2}} - \frac{G_1 - G_2}{G_1} \right),$$

$$G = G(r) = 2\pi\sqrt{C_n(D(r))}.$$

Equation (10) gives the time delay for a radar signal in the gravitational field.

#### 4 Spectral shift

Let an emitter of light have coordinates  $(t_E, r_E, \theta_E, \varphi_E)$ . Let a receiver have coordinates  $(t_R, r_R, \theta_R, \varphi_R)$ . Let  $u$  be an affine parameter along a null geodesic with the values  $u_E$  and  $u_R$  at emitter and receiver respectively. Then,

$$\begin{aligned} \left(1 - \frac{\alpha}{\sqrt{C_n}}\right) \left(\frac{dt}{du}\right)^2 &= \left(1 - \frac{\alpha}{\sqrt{C_n}}\right)^{-1} \left(\frac{d\sqrt{C_n}}{du}\right)^2 + \\ &\quad + C_n \left(\frac{d\theta}{du}\right)^2 + C_n \sin^2 \theta \left(\frac{d\varphi}{du}\right)^2, \end{aligned}$$

so

$$\frac{dt}{du} = \left[ \left(1 - \frac{\alpha}{\sqrt{C_n}}\right)^{-1} \bar{g}_{ij} \frac{dx^i}{du} \frac{dx^j}{du} \right]^{\frac{1}{2}},$$

where  $\bar{g}_{ij} = -g_{ij}$ . Then,

$$t_R - t_E = \int_{u_E}^{u_R} \left[ \left( 1 - \frac{\alpha}{\sqrt{C_n}} \right)^{-1} \bar{g}_{ij} \frac{dx^i}{du} \frac{dx^j}{du} \right]^{\frac{1}{2}} du,$$

and so, for spatially fixed emitter and receiver,

$$t_R^{(1)} - t_E^{(1)} = t_R^{(2)} - t_E^{(2)},$$

and therefore,

$$\Delta t_R = t_R^{(2)} - t_R^{(1)} = t_E^{(2)} - t_E^{(1)} = \Delta t_E. \quad (11)$$

Now by (1), the proper time is,

$$\Delta \tau_E = \sqrt{1 - \frac{\alpha}{\sqrt{C_n(r_E)}}} \Delta t_E,$$

and

$$\Delta \tau_R = \sqrt{1 - \frac{\alpha}{\sqrt{C_n(r_R)}}} \Delta t_R.$$

Then by (11),

$$\frac{\Delta \tau_R}{\Delta \tau_E} = \left[ \frac{1 - \frac{\alpha}{\sqrt{C_n(r_R)}}}{1 - \frac{\alpha}{\sqrt{C_n(r_E)}}} \right]^{\frac{1}{2}}. \quad (12)$$

If  $z$  regular pulses of light are emitted, the emitted and received frequencies are,

$$\nu_E = \frac{z}{\Delta \tau_E}, \quad \nu_R = \frac{z}{\Delta \tau_R},$$

so by (12),

$$\begin{aligned} \frac{\Delta \nu_R}{\Delta \nu_E} &= \left[ \frac{1 - \frac{\alpha}{\sqrt{C_n(r_E)}}}{1 - \frac{\alpha}{\sqrt{C_n(r_R)}}} \right]^{\frac{1}{2}} \approx \\ &\approx 1 + \frac{\alpha}{2} \left( \frac{1}{\sqrt{C_n(r_R)}} - \frac{1}{\sqrt{C_n(r_E)}} \right), \end{aligned}$$

whence,

$$\begin{aligned} \frac{\Delta \nu}{\nu_E} &= \frac{\nu_R - \nu_E}{\nu_E} \approx \frac{\alpha}{2} \left( \frac{1}{\sqrt{C_n(r_R)}} - \frac{1}{\sqrt{C_n(r_E)}} \right) = \\ &= \pi \alpha \left( \frac{1}{G_R} - \frac{1}{G_E} \right) = \\ &= \pi \sqrt{\frac{3}{\kappa \rho_0}} \sin^3 |\chi_a - \chi_0| \left( \frac{1}{G_R} - \frac{1}{G_E} \right). \end{aligned}$$

## 5 Advance of the perihelia

Consider the Lagrangian,

$$\begin{aligned} L &= \frac{1}{2} \left[ \left( 1 - \frac{\alpha}{\sqrt{C_n}} \right) \left( \frac{dt}{d\tau} \right)^2 \right] - \\ &- \frac{1}{2} \left[ \left( 1 - \frac{\alpha}{\sqrt{C_n}} \right)^{-1} \left( \frac{d\sqrt{C_n}}{d\tau} \right)^2 \right] - \\ &- \frac{1}{2} \left[ C_n \left( \left( \frac{d\theta}{d\tau} \right)^2 + \sin^2 \theta \left( \frac{d\varphi}{d\tau} \right)^2 \right) \right], \end{aligned} \quad (13)$$

where  $\tau$  is the proper time. Restricting motion, without loss of generality, to the equatorial plane,  $\theta = \frac{\pi}{2}$ , the Euler-Lagrange equations for (13) are,

$$\left( 1 - \frac{\alpha}{\sqrt{C_n}} \right)^{-1} \frac{d^2 \sqrt{C_n}}{d\tau^2} + \frac{\alpha}{2C_n} \left( \frac{dt}{d\tau} \right)^2 - \quad (14)$$

$$- \left( 1 - \frac{\alpha}{\sqrt{C_n}} \right)^{-2} \frac{\alpha}{2C_n} \left( \frac{d\sqrt{C_n}}{d\tau} \right)^2 - \sqrt{C_n} \left( \frac{d\varphi}{d\tau} \right)^2 = 0,$$

$$\left( 1 - \frac{\alpha}{\sqrt{C_n}} \right) \frac{dt}{d\tau} = \text{const} = K, \quad (15)$$

$$C_n \frac{d\varphi}{d\tau} = \text{const} = h, \quad (16)$$

and  $ds^2 = g_{\mu\nu} dx^\mu dx^\nu$  becomes,

$$\left( 1 - \frac{\alpha}{\sqrt{C_n}} \right) \left( \frac{dt}{d\tau} \right)^2 - \quad (17)$$

$$- \left( 1 - \frac{\alpha}{\sqrt{C_n}} \right)^{-1} \left( \frac{d\sqrt{C_n}}{d\tau} \right)^2 - C_n \left( \frac{d\varphi}{d\tau} \right)^2 = 1.$$

Rearrange (17) for,

$$\left( 1 - \frac{\alpha}{\sqrt{C_n}} \right) \frac{t^2}{\dot{\varphi}^2} - \left( 1 - \frac{\alpha}{\sqrt{C_n}} \right) \left( \frac{d\sqrt{C_n}}{d\varphi} \right)^2 - C_n = \frac{1}{\dot{\varphi}^2}. \quad (18)$$

Substituting (15) and (16) into (18) gives,

$$\left( \frac{d\sqrt{C_n}}{d\varphi} \right)^2 + C_n \left( 1 + \frac{C_n}{h^2} \right) \left( 1 - \frac{\alpha}{\sqrt{C_n}} \right) - \frac{K^2}{h^2} C_n^2 = 0.$$

Setting  $u = \frac{1}{\sqrt{C_n}}$  reduces (18) to,

$$\left( \frac{du}{d\varphi} \right)^2 + u^2 = E + \frac{\alpha}{h^2} u + \alpha u^3, \quad (19)$$

where  $E = \frac{K^2 - 1}{h^2}$ . The term  $\alpha u^3$  represents the general-relativistic perturbation of the Newtonian orbit.

Aphelion and perihelion occur when  $\frac{du}{d\varphi} = 0$ , so by (19),

$$\alpha u^3 - u^2 + \frac{\alpha}{h^2} u + E = 0, \quad (20)$$

Let  $u = u_1$  at aphelion and  $u = u_2$  at perihelion, so  $u_1 \leq u \leq u_2$ . One then finds in the usual way that the angle  $\Delta\varphi$  between aphelion and subsequent perihelion is,

$$\Delta\varphi = \left[ 1 + \frac{3\alpha}{4} (u_1 + u_2) \right] \pi.$$

Therefore, the angular advance  $\psi$  between successive perihelia is,

$$\begin{aligned} \psi &= \frac{3\alpha\pi}{2} (u_1 + u_2) = \frac{3\alpha\pi}{2} \left( \frac{1}{\sqrt{C_n(r_1)}} + \frac{1}{\sqrt{C_n(r_2)}} \right) = \\ &= 3\alpha\pi^2 \left( \frac{1}{G_1} + \frac{1}{G_2} \right), \end{aligned} \quad (21)$$

where  $G_1$  and  $G_2$  are the measurable circumferences of great circles at aphelion and at perihelion. Thus, to correctly determine the value of  $\psi$ , the values of the said circumferences must be ascertained by direct measurement. Only the circumferences are measurable in the gravitational field. The radii of curvature and the proper radii must be calculated from the circumference values.

If the field is weak, as in the case of the Sun, one may take  $G \approx 2\pi r$ , for  $r$  as an approximately “measurable” distance from the gravitating sphere to a spacetime event. In such a situation equation (21) becomes,

$$\psi \approx \frac{3\alpha\pi}{2} \left( \frac{1}{r_1} + \frac{1}{r_2} \right). \quad (22)$$

In the case of the Sun,  $\alpha \approx 3000$  m, and for the planet Mercury, the usual value of  $\psi \approx 43$  arcseconds per century is obtained from (22). I emphasize however, that this value is a Euclidean approximation for a weak field. In a strong field equation (22) is entirely inappropriate and equation (21) must be used. Unfortunately, this means that accurate solutions cannot be obtained since there is no obvious way of obtaining the required circumferences in practise. This aspect of Einstein’s theory seriously limits its utility. Since the relativists have not detected this limitation the issue has not previously arisen in general.

## 6 Deflection of light

In the case of a photon, equation (17) becomes,

$$\begin{aligned} &\left( 1 - \frac{\alpha}{\sqrt{C_n}} \right) \left( \frac{dt}{d\tau} \right)^2 - \\ &- \left( 1 - \frac{\alpha}{\sqrt{C_n}} \right)^{-1} \left( \frac{d\sqrt{C_n}}{d\tau} \right)^2 - C_n \left( \frac{d\varphi}{d\tau} \right)^2 = 1, \end{aligned}$$

which leads to,

$$\left( \frac{du}{d\varphi} \right)^2 + u^2 = F + \alpha u^3. \quad (23)$$

Let the radius of curvature of a great circle at closest approach be  $\sqrt{C_n(r_c)}$ . Now when there is no mass present, (23) becomes

$$\left( \frac{du}{d\varphi} \right)^2 + u^2 = F,$$

and has solution,

$$u = u_c \sin \varphi \Rightarrow \sqrt{C_n(r_c)} = \sqrt{C_n(r)} \sin \varphi,$$

and

$$u_c^2 = \frac{1}{\sqrt{C_n(r_c)}} = F.$$

If

$$\sqrt{C_n(r)} \gg \alpha, \quad \sqrt{C_n(r)} > \sqrt{C_n(r_a)},$$

and  $u = u_c > u_a$  at closest approach, then

$$\frac{du}{d\varphi} = 0 \quad \text{at} \quad u = u_c,$$

so  $F = u_c^2 (1 - u_c \alpha)$ , and (23) becomes,

$$\left( \frac{du}{d\varphi} \right)^2 + u^2 = u_c^2 (1 - u_c \alpha) + \alpha u^3. \quad (24)$$

Equation (24) must have a solution close to flat spacetime, so let

$$u = u_c \sin \varphi + \alpha w(\varphi).$$

Putting this into (24) and working to first order in  $\alpha$ , gives

$$2 \left( \frac{dw}{d\varphi} \right) \cos \varphi + 2w \sin \varphi = u_c^2 (\sin^3 \varphi - 1),$$

or

$$\frac{d}{d\varphi} (w \sec \varphi) = \frac{1}{2} u_c^2 (\sec \varphi \tan \varphi - \sin \varphi - \sec^2 \varphi),$$

and so,

$$w = \frac{1}{2} u_c^2 (1 + \cos^2 \varphi - \sin \varphi) + A \cos \varphi,$$

where  $A$  is an integration constant. If the photon originates at infinity in the direction  $\varphi = 0$ , then  $w(0) = 0$ , so  $A = -u_c^2$ , and

$$u = u_c \left( 1 - \frac{1}{2} \alpha u_c \right) \sin \varphi + \frac{1}{2} \alpha u_c^2 (1 - \cos \varphi)^2, \quad (25)$$

to first order in  $\alpha$ . Putting  $u = 0$  and  $\varphi = \pi + \Delta\varphi$  into (25), then to first order in  $\Delta\varphi$ ,

$$0 = -u_c \Delta\varphi + 2\alpha u_c^2,$$

so the angle of deflection is,

$$\Delta\varphi = 2\alpha u_c = \frac{2\alpha}{\sqrt{C_n(r_c)}} = \frac{2\alpha}{\left( |r_c - r_0|^n + \epsilon^n \right)^{\frac{1}{n}}} = \frac{4\pi\alpha}{G_c},$$

$$G_c \geq G_a.$$

At a grazing trajectory to the surface of the body,

$$G_c = G_a = 2\pi\sqrt{C_n(r_a)},$$

$$\sqrt{C_n(r_a)} = \sqrt{\frac{3}{\kappa\rho_0}} \sin|\chi_a - \chi_0|,$$

so then

$$\Delta\varphi = \frac{2\sqrt{\frac{3}{\kappa\rho_0}} \sin^3|\chi_a - \chi_0|}{\sqrt{\frac{3}{\kappa\rho_0}} \sin|\chi_a - \chi_0|} = 2\sin^2|\chi_a - \chi_0|. \quad (26)$$

For the Sun [5],

$$\sin|\chi_a - \chi_0| \approx \frac{1}{500},$$

so the deflection of light grazing the limb of the Sun is,

$$\Delta\varphi \approx \frac{2}{500^2} \approx 1.65''.$$

Equation (26) is an interesting and quite surprising result, for  $\sin|\chi_a - \chi_0|$  gives the ratio of the “naturally measured” fall velocity of a free test particle falling from rest at infinity down to the surface of the spherical body, to the speed of light in vacuo. Thus,

*the deflection of light grazing the limb of a spherical gravitating body is twice the square of the ratio of the fall velocity of a free test particle falling from rest at infinity down to the surface, to the speed of light in vacuo, i.e.,*

$$\Delta\varphi = 2\sin^2|\chi_a - \chi_0| = 2\left(\frac{v_a}{c}\right)^2 = \frac{4GM_g}{c^2 R_{c_a}},$$

where  $R_{c_a}$  is the radius of curvature of the body,  $M_g$  the active mass, and  $G$  is the gravitational constant. The quantity  $v_a$  is the escape velocity,

$$v_a = \sqrt{\frac{2GM_g}{R_{c_a}}}.$$

## 7 Practical constraints and general comment

Owing to their invalid assumptions about the  $r$ -parameter [7], the relativists have not recognised the practical limitations associated with the application of General Relativity. It is now clear that the fundamental element of distance in the gravitational field is the circumference of a great circle, centred at the heart of an extended spherical body and passing through a spacetime event external thereto. Heretofore the orthodox theorists have incorrectly taken the  $r$ -parameter,

not just as a radius in the gravitational field, but also as a *measurable* radius in the field. This is not correct. The only measurable distance in the gravitational field is the aforesaid circumference of a great circle, from which the radius of curvature  $\sqrt{C_n(r)}$  and the proper radius  $R_p(r)$  must be calculated, thus,

$$\sqrt{C_n(r)} = \frac{G}{2\pi},$$

$$R_p(r) = \int \sqrt{-g_{11}} dr.$$

Only in the weak field, where the spacetime curvature is very small, can  $\sqrt{C_n(r)}$  be taken approximately as the Euclidean value  $r$ , thereby making  $R_p(r) \equiv \sqrt{C_n(r)} \equiv r$ , as in flat spacetime. In a strong field this *cannot* be done. Consequently, the problem arises as to how to accurately measure the required great circumference? The correct determination, for example, of the circumferences of great circles at aphelion and perihelion seem to be beyond practical determination. Any method adopted for determining the required circumference must be completely independent of any Euclidean quantity since, other than the great circumference itself, only non-Euclidean distances are valid in the gravitational field, being determined by it. Therefore, anything short of physically measuring the great circumference will fail. Consequently, General Relativity, whether right or wrong as theories go, suffers from a serious practical limitation.

The value of the  $r$ -parameter is coordinate dependent and is rightly determined from the coordinate independent value of the circumference of the great circle associated with a spacetime event. One cannot obtain a circumference for the great circle of a given spacetime event, and hence the related radius of curvature and associated proper radius, from the specification of a coordinate radius, because the latter is not unique, being conditioned by arbitrary constants. The coordinate radius is therefore superfluous. It is for this reason that I completely eliminated the coordinate radius from the metric for the gravitational field, to describe the metric in terms of the only quantity that is measurable in the gravitational field — the great circumference (see also [6]). The presence of the  $r$ -parameter has proved misleading to the relativists. Stavroulakis [8, 9, 10] has also completely eliminated the  $r$ -parameter from the equations, but does not make use of the great circumference. His approach is formally correct, but rather less illuminating, because his resulting line element is in terms of the a quantity which is not measurable in the gravitational field. One cannot obtain an explicit expression for the great circumference in terms of the proper radius.

As to the cosmological large-scale, I have proved elsewhere [11] that General Relativity adds nothing to Special Relativity. Einstein's field equations do not admit of solutions when the cosmological constant is not zero, and they do not admit of the expanding universe solutions alleged by

the relativists. The lambda “solutions” and the expanding universe “solutions” are the result of such a muddleheadedness that it is difficult to apprehend the kind of thoughtlessness that gave them birth. Since Special Relativity describes an empty world (no gravity) it cannot form a basis for any cosmology. This theoretical result is all the more interesting owing to its agreement with observation. Arp [12], for instance, has adduced considerable observational data which is consistent on the large-scale with a flat, infinite, non-expanding Universe in Heraclitian flux. Bearing in mind that both Special Relativity and General Relativity *cannot* yield a spacetime on the cosmological “large-scale”, there is currently no theoretical replacement for Newton’s cosmology, which accords with deep-space observations for a flat space, infinite in time and in extent. The all pervasive rôle given heretofore by the relativists to General Relativity, can be justified no longer. General Relativity is a theory of only *local* phenomea, as is Special Relativity.

Another serious shortcoming of General Relativity is its current inability to deal with the gravitational interaction of two comparable masses. It is not even known if Einstein’s theory admits of configurations involving two or more masses [13]. This shortcoming seems rather self evident, but apparently not so for the relativists, who routinely talk of black hole binary systems and colliding black holes (e.g. [14]), aside of the fact that no theory predicts the existence of black holes to begin with, but to the contrary, precludes them.

### Acknowledgement

I am indebted to Dr. Dmitri Rabounski for drawing my attention to a serious error in a preliminary draft of this paper, and for additional helpful suggestions.

### Dedication

I dedicate this paper to the memory of Dr. Leonard S. Abrams: (27 Nov. 1924 – 28 Dec. 2001).

### References

1. Hilbert D. *Nachr. Ges. Wiss. Gottingen, Math. Phys. Kl.*, 1917, 53 (arXiv: physics/0310104, [www.geocities.com/theometria/hilbert.pdf](http://www.geocities.com/theometria/hilbert.pdf)).
2. Schwarzschild K. On the gravitational field of a mass point according to Einstein’s theory. *Sitzungsber. Preuss. Akad. Wiss., Phys. Math. Kl.*, 1916, 189 (arXiv: physics/9905030, [www.geocities.com/theometria/schwarzschild.pdf](http://www.geocities.com/theometria/schwarzschild.pdf)).
3. Crothers S.J. On the general solution to Einstein’s vacuum field and it implications for relativistic degeneracy. *Progress in Physics*, 2005, v. 1, 68–73.
4. Crothers S.J. On the ramifications of the Schwarzschild spacetime metric. *Progress in Physics*, 2005, v. 1, 74–80.
5. Schwarzschild K. On the gravitational field of a sphere of incompressible fluid according to Einstein’s theory. *Sitzungsber. Preuss. Akad. Wiss., Phys. Math. Kl.*, 1916, 424 (arXiv: physics/9912033, [www.geocities.com/theometria/Schwarzschild2.pdf](http://www.geocities.com/theometria/Schwarzschild2.pdf)).
6. Crothers S.J. On the vacuum field of a sphere of incompressible fluid. *Progress in Physics*, 2005, v. 2, 43–47.
7. Crothers S.J. On the geometry of the general solution for the vacuum field of the point-mass. *Progress in Physics*, 2005, v. 2, 3–14.
8. Stavroulakis N. A statical smooth extension of Schwarzschild’s metric. *Lettere al Nuovo Cimento*, 1974, v.11, 8 ([www.geocities.com/theometria/Stavroulakis-3.pdf](http://www.geocities.com/theometria/Stavroulakis-3.pdf)).
9. Stavroulakis N. On the Principles of General Relativity and the  $S\Theta(4)$ -invariant metrics. *Proc. 3rd Panhellenic Congr. Geometry*, Athens, 1997, 169 ([www.geocities.com/theometria/Stavroulakis-2.pdf](http://www.geocities.com/theometria/Stavroulakis-2.pdf)).
10. Stavroulakis N. On a paper by J.Smoller and B.Temple. *Annales de la Fondation Louis de Broglie*, 2002, v.27, 3 ([www.geocities.com/theometria/Stavroulakis-1.pdf](http://www.geocities.com/theometria/Stavroulakis-1.pdf)).
11. Crothers S.J. On the general solution to Einstein’s vacuum field for the point-mass when  $\lambda \neq 0$  and its implications for relativistic cosmology, *Progress in Physics*, 2005, v. 3, 7–18.
12. Arp, H. Observational cosmology: from high redshift galaxies to the blue pacific, *Progress in Physics*, 2005, v. 3, 3–6.
13. McVittie G.C. Laplace’s alleged “black hole”. *The Observatory*, 1978, v. 98, 272 ([www.geocities.com/theometria/McVittie.pdf](http://www.geocities.com/theometria/McVittie.pdf)).
14. Misner C.W., Thorne K.S., Wheeler J.A. *Gravitation*. W.H. Freeman and Company, New York, 1973.



# A Re-Examination of Maxwell's Electromagnetic Equations

Jeremy Dunning-Davies

*Department of Physics, University of Hull, Hull, England*

E-mail: J.Dunning-Davies@hull.ac.uk

It is pointed out that the usual derivation of the well-known Maxwell electromagnetic equations holds only for a medium at rest. A way in which the equations may be modified for the case when the mean flow of the medium is steady and uniform is proposed. The implication of this for the problem of the origin of planetary magnetic fields is discussed.

## 1 Introduction

Maxwell's electromagnetic equations are surely among the best known and most widely used sets of equations in physics. However, possibly because of this and since they have been used so successfully in so many areas for so many years, they are, to some extent, taken for granted and used with little or no critical examination of their range of validity. This is particularly true of the two equations

$$\nabla \times \mathbf{E} = -\frac{1}{c} \frac{\partial \mathbf{B}}{\partial t}$$

and

$$\nabla \times \mathbf{H} = 4\pi \mathbf{j} + \frac{1}{c} \frac{\partial \mathbf{D}}{\partial t}.$$

Both these equations are used widely but, although the point is made quite clearly in most elementary, as well as more advanced, textbooks, it is often forgotten that these equations apply *only* when the medium involved is assumed to be at rest. This assumption is actually crucial in the derivation of these equations since it is because of it that it is allowable to take the operator  $d/dt$  inside the integral sign as a partial derivative and so finally derive each of the above equations. This leaves open the question of what happens if the medium is not at rest?

As is well known, for a non-conducting medium at rest, Maxwell's electromagnetic equations, when no charge is present, reduce to

$$\nabla \cdot \mathbf{E} = 0, \quad \nabla \times \mathbf{E} = -\frac{\mu}{c} \frac{\partial \mathbf{H}}{\partial t},$$

$$\nabla \cdot \mathbf{H} = 0, \quad \nabla \times \mathbf{H} = -\frac{\varepsilon}{c} \frac{\partial \mathbf{E}}{\partial t},$$

where  $\mathbf{D} = \varepsilon \mathbf{E}$ ,  $\mathbf{B} = \mu \mathbf{H}$  and  $\mu$ ,  $\varepsilon$  are assumed constant in time.

The first two equations are easily seen to lead to

$$\nabla^2 \mathbf{E} = \frac{\varepsilon \mu}{c^2} \frac{\partial^2 \mathbf{E}}{\partial t^2},$$

and the latter two to

$$\nabla^2 \mathbf{H} = \frac{\varepsilon \mu}{c^2} \frac{\partial^2 \mathbf{H}}{\partial t^2}.$$

Therefore, in this special case, *provided* the medium is at rest, both  $\mathbf{E}$  and  $\mathbf{H}$  satisfy the well-known wave equation. However, it has been shown [1] that, if the mean flow is steady and uniform, and, therefore, both homentropic and irrotational, the system of equations governing small-amplitude homentropic irrotational wave motion in such a flow reduces to the equation

$$\nabla^2 \varphi = \frac{1}{c^2} \frac{D^2 \varphi}{Dt^2},$$

which is sometimes referred to as the convected, or progressive, wave equation. The question which remains is, for the case of a medium not at rest, should Maxwell's electromagnetic equations be modified so as to reduce to this progressive wave equation in the case of a non-conducting medium with no charge present?

## 2 Generalisation of Maxwell's equations

In the derivation of

$$\nabla \times \mathbf{E} = -\frac{\mu}{c} \frac{\partial \mathbf{H}}{\partial t}$$

it proves necessary to consider the integral

$$-\frac{\mu}{c} \frac{d}{dt} \int \mathbf{B} \cdot d\mathbf{S}$$

and interchange the derivative and the integral. This operation may be carried out only for a medium at rest. However, if the medium is moving, then the surface  $\mathbf{S}$  in the integral will be moving also, and the mere change of  $\mathbf{S}$  in the field  $\mathbf{B}$  will cause changes in the flux. Hence, following Abraham and Becker [2], a new kind of differentiation with respect to time is defined by the symbol  $\dot{\mathbf{B}}$  as follows:

$$\frac{d}{dt} \int \mathbf{B} \cdot d\mathbf{S} = \int \dot{\mathbf{B}} \cdot d\mathbf{S}. \quad (\text{a})$$

Here,  $\dot{\mathbf{B}}$  is a vector, the flux of which across the moving surface equals the rate of increase with time of the flux of  $\mathbf{B}$  across the same surface. In order to find  $\dot{\mathbf{B}}$ , the exact details of the motion of the surface concerned must be known. Suppose this motion described by a vector  $\mathbf{u}$ , which is assumed given for each element  $d\mathbf{S}$  of the surface and is the velocity of the element.

Let  $S_1$  be the position of the surface  $S$  at time  $(t - dt)$  and  $S_2$  the position at some later time  $t$ .  $S_2$  may be obtained from  $S_1$  by giving each element of  $S_1$  a displacement  $\mathbf{u}dt$ . The surfaces  $S_1$  and  $S_2$ , together with the strip produced during the motion, bound a volume  $dt \int \mathbf{u} \cdot d\mathbf{S}$ .

The rate of change with time of the flux of  $\mathbf{B}$  across  $S$  may be found from the difference between the flux across  $S_2$  at time  $t$  and that across  $S_1$  at time  $(t - dt)$ ; that is

$$\frac{d}{dt} \int \mathbf{B} \cdot d\mathbf{S} = \frac{\int \mathbf{B}_t \cdot d\mathbf{S}_2 - \int \mathbf{B}_{t-dt} \cdot d\mathbf{S}_1}{dt},$$

where the subscript indicates the time at which the flux is measured.

The divergence theorem may be applied at time  $t$  to the volume bounded by  $S_1$ ,  $S_2$  and the strip connecting them. Here the required normal to  $S_2$  will be the outward pointing normal and that to  $S_1$  the inward pointing normal. Also, a surface element of the side face will be given by  $ds \times \mathbf{u}dt$ . Then, the divergence theorem gives

$$\int_{S_2} \mathbf{B}_t \cdot d\mathbf{S}_2 + dt \oint \mathbf{B} \cdot ds \times \mathbf{u} - \int_{S_1} \mathbf{B}_{t-dt} \cdot d\mathbf{S}_1 = dt \int (\nabla \cdot \mathbf{B}) \mathbf{u} \cdot d\mathbf{S}.$$

Also

$$\int \mathbf{B}_{t-dt} \cdot d\mathbf{S}_1 = \int \mathbf{B}_t \cdot d\mathbf{S}_1 - \int \frac{\partial \mathbf{B}}{\partial t} \cdot d\mathbf{S}_1 dt.$$

Hence,

$$\int \mathbf{B}_t \cdot d\mathbf{S}_2 - \int \mathbf{B}_{t-dt} \cdot d\mathbf{S}_1 = dt \left\{ \int \dot{\mathbf{B}} \cdot d\mathbf{S}_1 + \int (\nabla \cdot \mathbf{B}) \mathbf{u} \cdot d\mathbf{S}_1 - \oint \mathbf{B} \cdot ds \times \mathbf{u} \right\}.$$

Using Stokes' theorem, the final term on the right-hand side of this equation may be written

$$\oint \mathbf{B} \cdot ds \times \mathbf{u} = \oint \mathbf{u} \times \mathbf{B} \cdot ds = \int \left\{ \nabla \times (\mathbf{u} \times \mathbf{B}) \right\} \cdot d\mathbf{S},$$

and so finally

$$\frac{d}{dt} \int \mathbf{B} \cdot d\mathbf{S} = \int \left\{ \frac{\partial \mathbf{B}}{\partial t} + \mathbf{u} (\nabla \cdot \mathbf{B}) - \nabla \times (\mathbf{u} \times \mathbf{B}) \right\} \cdot d\mathbf{S}.$$

Therefore, the  $\dot{\mathbf{B}}$ , introduced in (a) above, is given by

$$\dot{\mathbf{B}} = \frac{\partial \mathbf{B}}{\partial t} + \mathbf{u} (\nabla \cdot \mathbf{B}) - \nabla \times (\mathbf{u} \times \mathbf{B})$$

or, noting that

$$\nabla \times (\mathbf{u} \times \mathbf{B}) = \mathbf{u} (\nabla \cdot \mathbf{B}) - \mathbf{B} (\nabla \cdot \mathbf{u}) + (\mathbf{B} \cdot \nabla) \mathbf{u} - (\mathbf{u} \cdot \nabla) \mathbf{B},$$

$$\dot{\mathbf{B}} = \frac{\partial \mathbf{B}}{\partial t} + (\mathbf{u} \cdot \nabla) \mathbf{B} + \mathbf{B} (\nabla \cdot \mathbf{u}) - (\mathbf{B} \cdot \nabla) \mathbf{u}.$$

However, if the mean flow is steady and uniform and, therefore, both homentropic and irrotational, the fluid velocity,  $\mathbf{u}$ , will be constant and this latter equation will reduce to

$$\dot{\mathbf{B}} = \frac{\partial \mathbf{B}}{\partial t} + (\mathbf{u} \cdot \nabla) \mathbf{B} = \frac{D\mathbf{B}}{Dt},$$

that is, for such flow,  $\dot{\mathbf{B}}$  becomes the well-known Euler derivative. It might be noted, though, that, for more general flows, the expression for  $\dot{\mathbf{B}}$  is somewhat more complicated.

It follows that, if the mean flow is steady and uniform, the Maxwell equation, mentioned above, becomes

$$\nabla \times \mathbf{E} = -\frac{\mu}{c} \frac{D\mathbf{H}}{Dt} = -\frac{\mu}{c} \left[ \frac{\partial \mathbf{H}}{\partial t} + (\mathbf{u} \cdot \nabla) \mathbf{H} \right].$$

Also, in this particular case, the remaining three Maxwell equations will be

$$\nabla \cdot \mathbf{E} = 0, \quad \nabla \cdot \mathbf{H} = 0,$$

$$\nabla \times \mathbf{H} = \frac{\varepsilon}{c} \frac{D\mathbf{E}}{Dt} = \frac{\varepsilon}{c} \left[ \frac{\partial \mathbf{E}}{\partial t} + (\mathbf{u} \cdot \nabla) \mathbf{E} \right],$$

with this form for the final equation following in a manner similar to that adopted above when noting that, for a steady, uniform mean flow,  $\partial/\partial t$  is replaced by  $D/Dt$  in the equation for  $\nabla \times \mathbf{E}$ .

These four modified Maxwell equations lead to both  $\mathbf{E}$  and  $\mathbf{H}$  satisfying the above mentioned progressive wave equation, as they surely must.

### 3 The origin of planetary magnetic fields

It is conceivable that use of these modified Maxwell electromagnetic equations could provide new insight into the problem of the origin of planetary magnetic fields. This is a problem which has existed, without a really satisfactory explanation, for many years. It would seem reasonable to expect all such fields to arise from the same physical mechanism, although the minute detail might vary from case to case. The mechanism generally favoured as providing the best explanation for the origin of these fields was the dynamo mechanism, although the main reason for its adoption was the failure of the alternatives to provide a consistent explanation. However, Cowling [3] showed that there is a limit to the degree of symmetry encountered in a steady dynamo mechanism; this result, based on the traditional electromagnetic equations of Maxwell, shows that the steady maintenance of a poloidal field is simply not possible — the result is in

reality an anti-dynamo theorem which raises difficulties in understanding the observed symmetry of the dipole field.

Following Alfvén [4], it might be noted that, in a stationary state, there is no electromagnetic field along a neutral line because that would imply a non-vanishing  $\nabla \times \mathbf{E}$ , and so a time varying  $\mathbf{B}$ . The induced electric field  $\mathbf{v} \times \mathbf{B}$  vanishes on the neutral line since  $\mathbf{B}$  does. Thus, there can be no electromotive force along the neutral line, and therefore the current density in the stationary state vanishes, the conductivity being infinite. On the other hand,  $\nabla \times \mathbf{B}$  does not vanish on the neutral line. By Maxwell's usual equations, the non-vanishing  $\nabla \times \mathbf{B}$  and the vanishing current density are in contradiction and so the existence of a rotationally symmetric steady-state dynamo is disproved. However, this conclusion may not be drawn if the modified Maxwell equations, alluded to earlier, are used, since, even in the steady state where the partial derivatives with respect to time will all be zero, the equation for  $\nabla \times \mathbf{B}$  will reduce to

$$\nabla \times \mathbf{B} = \frac{1}{\mu} \left[ \mathbf{j} + \varepsilon \frac{\partial \mathbf{E}}{\partial t} + \varepsilon \mathbf{v} \cdot \nabla \mathbf{E} \right] \rightarrow \frac{\varepsilon}{\mu} \mathbf{v} \cdot \nabla \mathbf{E}$$

and there is no reason why this extra term on the right-hand side should be identically equal to zero. Also, the non-vanishing of  $\nabla \times \mathbf{E}$  will not imply a time varying  $\mathbf{B}$  since, once again, there is an extra term  $-\mathbf{v} \cdot \nabla \mathbf{B}$  remaining to equate with the  $\nabla \times \mathbf{E}$ . It follows that an electromagnetic field may exist along the neutral line under these circumstances. Hence, no contradiction occurs; instead, a consistent system of differential equations remains to be solved.

## References

1. Thornhill C. K. *Proc. Roy. Soc. Lond.*, 1993, v. 442, 495.
2. Abraham M., Becker, R. *The Classical Theory of Electricity and Magnetism*. Blackie and Son Ltd., London, 1932.
3. Cowling T. G. *Monthly Notices of the Royal Astronomical Society*, 1934, v. 94, 39.
4. Alfvén H., Fälthammar C. G. *Cosmical Electrodynamics*. Oxford at the Clarendon Press, 1963.

# Black Holes in Elliptical and Spiral Galaxies and in Globular Clusters

Reginald T. Cahill

*School of Chemistry, Physics and Earth Sciences, Flinders University, Adelaide 5001, Australia*

E-mail: Reg.Cahill@flinders.edu.au

Supermassive black holes have been discovered at the centers of galaxies, and also in globular clusters. The data shows correlations between the black hole mass and the elliptical galaxy mass or globular cluster mass. It is shown that this correlation is accurately predicted by a theory of gravity which includes the new dynamics of self-interacting space. In spiral galaxies this dynamics is shown to explain the so-called “dark matter” rotation-curve anomaly, and also explains the Earth based bore-hole  $g$  anomaly data. Together these effects imply that the strength of the self-interaction dynamics is determined by the fine structure constant. This has major implications for fundamental physics and cosmology.

## 4 Introduction

Our understanding of gravity is based on Newton’s modelling of Kepler’s phenomenological laws for the motion of the planets within the solar system. In this model Newton took the gravitational acceleration field to be the fundamental dynamical degree of freedom, and which is determined by the matter distribution; essentially via the “universal inverse square law”. However the observed linear correlation between masses of black holes with the masses of the “host” elliptical galaxies or globular clusters suggests that either the formation of these systems involves common evolutionary dynamical processes or that perhaps some new aspect to gravity is being revealed. Here it is shown that if rather than an acceleration field a velocity field is assumed to be fundamental to gravity, then we immediately find that these black hole effects arise as a space self-interaction dynamical effect, and that the observed correlation is simply that  $M_{BH}/M = \alpha/2$  for spherical systems, where  $\alpha$  is the fine structure constant ( $\alpha = e^2/\hbar c = 1/137.036$ ), as shown in Fig. 1. This dynamics also manifests within the Earth, as revealed by the bore hole  $g$  anomaly data, as in Fig. 2. It also offers an explanation of the “dark matter” rotation-velocity effect, as illustrated in Fig. 3. This common explanation for a range of seemingly unrelated effects has deep implications for fundamental physics and cosmology.

## 5 Modelling gravity

Let us phenomenologically investigate the consequences of using a velocity field  $\mathbf{v}(\mathbf{r}, t)$  to be the fundamental dynamical degree of freedom to model gravity. The gravitational acceleration field is then defined by the Euler form

$$\mathbf{g}(\mathbf{r}, t) \equiv \lim_{\Delta t \rightarrow 0} \frac{\mathbf{v}(\mathbf{r} + \mathbf{v}(\mathbf{r}, t)\Delta t, t + \Delta t) - \mathbf{v}(\mathbf{r}, t)}{\Delta t} = \frac{\partial \mathbf{v}}{\partial t} + (\mathbf{v} \cdot \nabla) \mathbf{v}. \quad (1)$$

This form is mandated by Galilean covariance under change of observer. A minimalist non-relativistic modelling of the dynamics for this velocity field gives a direct account of the various phenomena noted above; basically the Newtonian formulation of gravity missed a key dynamical effect that did not manifest within the solar system.

In terms of the velocity field Newtonian gravity dynamics involves using  $\nabla \cdot$  to construct a rank-0 tensor that can be related to the matter density  $\rho$ . The coefficient turns out to be the Newtonian gravitational constant  $G$ .

$$\nabla \cdot \left( \frac{\partial \mathbf{v}}{\partial t} + (\mathbf{v} \cdot \nabla) \mathbf{v} \right) = -4\pi G \rho. \quad (2)$$

This is clearly equivalent to the differential form of Newtonian gravity,  $\nabla \cdot \mathbf{g} = -4\pi G \rho$ . Outside of a spherical mass  $M$  (2) has solution\*

$$\mathbf{v}(\mathbf{r}) = -\sqrt{\frac{2GM}{r}} \hat{\mathbf{r}}, \quad (3)$$

for which (1) gives the usual inverse square law

$$\mathbf{g}(\mathbf{r}) = -\frac{GM}{r^2} \hat{\mathbf{r}}. \quad (4)$$

The simplest non-Newtonian dynamics involves the two rank-0 tensors constructed at 2nd order from  $\partial v_i / \partial x_j$

$$\nabla \cdot \left( \frac{\partial \mathbf{v}}{\partial t} + (\mathbf{v} \cdot \nabla) \mathbf{v} \right) + \frac{\alpha}{8} (\text{tr} D)^2 + \frac{\beta}{8} \text{tr}(D^2) = -4\pi G \rho, \quad (5)$$

$$D_{ij} = \frac{1}{2} \left( \frac{\partial v_i}{\partial x_j} + \frac{\partial v_j}{\partial x_i} \right), \quad (6)$$

and involves two arbitrary dimensionless constants. The velocity in (3) is also a solution to (5) if  $\beta = -\alpha$ , and we then define

$$C(\mathbf{v}, t) = \frac{\alpha}{8} \left( (\text{tr} D)^2 - \text{tr}(D^2) \right). \quad (7)$$

\*We assume  $\nabla \times \mathbf{v} = \mathbf{0}$ , then  $(\mathbf{v} \cdot \nabla) \mathbf{v} = \frac{1}{2} \nabla(\mathbf{v}^2)$ .

Hence the modelling of gravity by (5) and (1) now involves two gravitational constants  $G$  and  $\alpha$ , with  $\alpha$  being the strength of the self-interaction dynamics, but which was not apparent in the solar system dynamics. We now show that all the various phenomena discussed herein imply that  $\alpha$  is the fine structure constant  $\approx 1/137$  up to experimental errors [1]. Hence non-relativistic gravity is a more complex phenomenon than currently understood. The new key feature is that (5) has a one-parameter  $\mu$  class of vacuum ( $\rho=0$ ) “black hole” solutions in which the velocity field self-consistently maintains the singular form

$$\mathbf{v}(\mathbf{r}) = -\mu r^{-\alpha/4} \hat{\mathbf{r}}. \quad (8)$$

This class of solutions will be seen to account for the “black holes” observed in galaxies and globular cluster. As well this velocity field, from (1), gives rise to a non-“inverse square law” acceleration

$$\mathbf{g}(\mathbf{r}) = -\frac{\alpha\mu}{4} r^{-(1+\alpha/4)} \hat{\mathbf{r}}. \quad (9)$$

This turns out to be the cause of the so-called “dark-matter” effect observed in spiral galaxies. For this reason we define

$$\rho_{DM}(\mathbf{r}) = \frac{\alpha}{32\pi G} \left( (\text{tr} D)^2 - \text{tr}(D^2) \right), \quad (10)$$

so that (5) and (1) can be written as

$$\nabla \cdot \mathbf{g} = -4\pi G \rho - 4\pi G \rho_{DM}, \quad (11)$$

which shows that we can think of the new self-interaction dynamics as generating an effective “dark matter” density.

## 6 Spherical systems

It is sufficient here to consider time-independent and spherically symmetric solutions of (5) for which  $v$  is radial. Then we have the integro-differential form for (5)

$$v^2(r) = 2G \int d^3s \frac{\rho(s) + \rho_{DM}(v(s))}{|\mathbf{r} - \mathbf{s}|}, \quad (12)$$

$$\rho_{DM}(v(r)) = \frac{\alpha}{8\pi G} \left( \frac{v^2}{2r^2} + \frac{vv'}{r} \right). \quad (13)$$

as  $\nabla^2 \frac{1}{|\mathbf{r}-\mathbf{s}|} = -4\pi\delta^4(\mathbf{r}-\mathbf{s})$ . This then gives

$$v^2(r) = \frac{8\pi G}{r} \int_0^r s^2 ds \left[ \rho(s) + \rho_{DM}(v(s)) \right] + 8\pi G \int_r^\infty s ds \left[ \rho(s) + \rho_{DM}(v(s)) \right] \quad (14)$$

on doing the angle integrations. We can also write (5) as a non-linear differential equation

$$2 \frac{vv'}{r} + (v')^2 + vv'' = -4\pi G \rho(r) - 4\pi G \rho_{DM}(v(r)). \quad (15)$$

## 7 Minimal black hole systems

There are two classes of solutions when matter is present. The simplest is when the black hole forms as a consequence of the velocity field generated by the matter, this generates what can be termed an induced minimal black hole. This is in the main applicable to systems such as planets, stars, globular clusters and elliptical galaxies. The second class of solutions correspond to non-minimal black hole systems; these arise when the matter congregates around a pre-existing “vacuum” black hole. The minimal black holes are simpler to deal with, particularly when the matter system is spherically symmetric. In this case the non-Newtonian gravitational effects are confined to within the system. A simple way to arrive at this property is to solve (14) perturbatively. When the matter density is confined to a sphere of radius  $R$  we find on iterating (14) that the “dark matter” density is confined to that sphere, and that consequently  $g(r)$  has an inverse square law behaviour outside of the sphere. Iterating (14) once we find inside radius  $R$  that

$$\rho_{DM}(r) = \frac{\alpha}{2r^2} \int_r^R s \rho(s) ds + O(\alpha^2). \quad (16)$$

and that the total “dark matter”

$$\begin{aligned} M_{DM} &\equiv 4\pi \int_0^R r^2 dr \rho_{DM}(r) = \\ &= \frac{4\pi\alpha}{2} \int_0^R r^2 dr \rho(r) + O(\alpha^2) = \frac{\alpha}{2} M + O(\alpha^2), \end{aligned} \quad (17)$$

where  $M$  is the total amount of (actual) matter. Hence, to  $O(\alpha)$ ,  $M_{DM}/M = \alpha/2$  independently of the matter density profile. This turns out to be a very useful property as knowledge of the density profile is then not required in order to analyse observational data. Fig. 1 shows the value of  $M_{BH}/M$  for, in particular, globular clusters  $M15$  and  $G1$  and highly spherical “elliptical” galaxies  $M32$ ,  $M87$  and  $NGC 4374$ , showing that this ratio lies close to the “ $\alpha/2$ -line”, where  $\alpha$  is the fine structure constant  $\approx 1/137$ . However for the spiral galaxies their  $M_{DM}/M$  values do not cluster close to the  $\alpha/2$ -line. Hence it is suggested that these spherical systems manifest the minimal black hole dynamics outlined above. However this dynamics is universal, so that any spherical system must induce such a minimal black hole mode, but for which outside of such a system only the Newtonian inverse square law would be apparent. So this mode must also apply to the Earth, which is certainly a surprising prediction. However just such an effect has manifested in measurements of  $g$  in mine shafts and bore holes since the 1980’s. It will now be shown that data from these geophysical measurements give us a very accurate determination of the value of  $\alpha$  in (5).

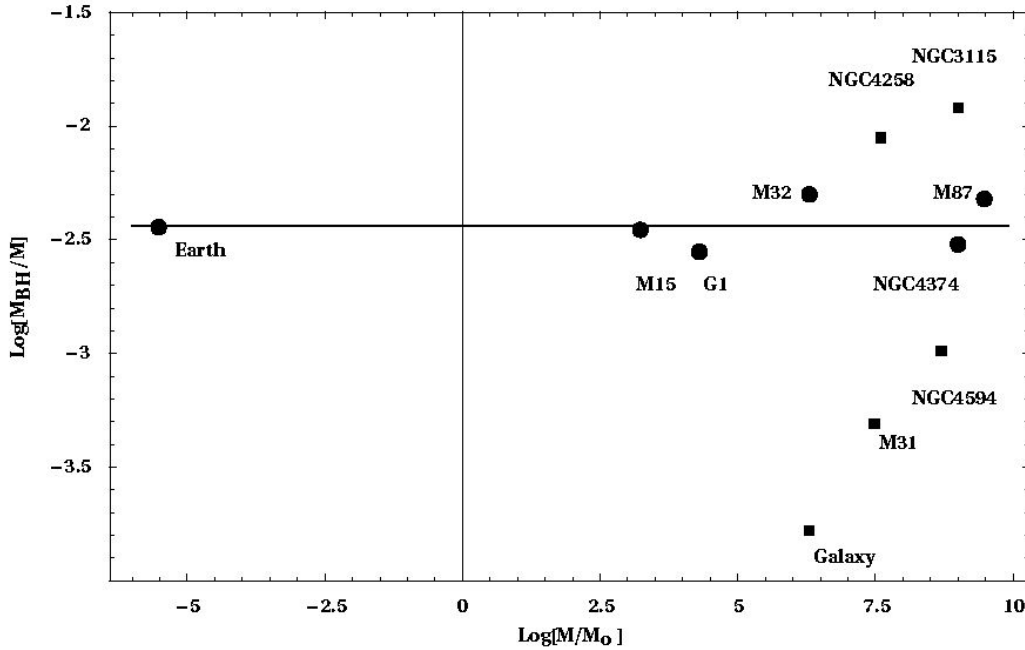


Fig. 1: The data shows  $\text{Log}_{10}[M_{BH}/M]$  for the “black hole” or “dark matter” masses  $M_{BH}$  for a variety of spherical matter systems with masses  $M$ , shown by solid circles, plotted against  $\text{Log}_{10}[M/M_0]$ , where  $M_0$  is the solar mass, showing agreement with the “ $\alpha/2$ -line” ( $\text{Log}_{10}[\alpha/2] = -2.44$ ) predicted by (17), and ranging over 15 orders of magnitude. The “black hole” effect is the same phenomenon as the “dark matter” effect. The data ranges from the Earth, as observed by the bore hole  $g$  anomaly, to globular cluster M15 [5, 6] and G1 [7], and then to spherical “elliptical” galaxies M32 (E2), NGC 4374 (E1) and M87 (E0). Best fit to the data from these star systems gives  $\alpha = 1/134$ , while for the Earth data in Fig. 2  $\alpha = 1/139$ . A best fit to all the spherical systems in the plot gives  $\alpha = 1/136$ . In these systems the “dark matter” or “black hole” spatial self-interaction effect is induced by the matter. For the spiral galaxies, shown by the filled boxes, where here  $M$  is the bulge mass, the black hole masses do not correlate with the “ $\alpha/2$ -line”. This is because these systems form by matter in-falling to a primordial black hole, and so these systems are more contingent. For spiral galaxies this dynamical effect manifests most clearly via the non-Keplerian rotation-velocity curve, which decrease asymptotically very slowly, as shown in Fig. 3, as determined by the small value of  $\alpha \approx 1/137$ . The galaxy data is from Table 1 of [8, updated].

### 8 Bore hole $g$ anomaly

To understand this bore hole anomaly we need to compute the expression for  $g(r)$  just beneath and just above the surface of the Earth. To lowest order in  $\alpha$  the “dark-matter” density in (16) is substituted into (14) finally gives via (1) the acceleration

$$g(r) = \begin{cases} \frac{(1 + \frac{\alpha}{2})GM}{r^2}, & r > R, \\ \frac{4\pi G}{r^2} \int_0^r s^2 ds \rho(s) + \\ + \frac{2\pi\alpha G}{r^2} \int_0^r \left( \int_s^R s' ds' \rho(s') \right) ds, & r < R. \end{cases} \quad (18)$$

This gives Newton’s “inverse square law” for  $r > R$ , but in which we see that the effective Newtonian gravitational constant is  $G_N = (1 + \frac{\alpha}{2})G$ , which is different to the fundamental gravitational constant  $G$  in (2). This caused by the

additional “dark matter mass” in (17). Inside the Earth we see that (18) gives a  $g(r)$  different from Newtonian gravity. This has actually been observed in mine/borehole measurements of  $g(r)$  [2, 3, 4], though of course there had been no explanation for the effect, and indeed the reality of the effect was eventually doubted. The effect is that  $g$  decreases more slowly with depth than predicted by Newtonian gravity. Here the corresponding Newtonian form for  $g(r)$  is

$$g(r)_{Newton} = \begin{cases} \frac{G_N M}{r^2}, & r > R, \\ \frac{4\pi G_N}{r^2} \int_0^r s^2 ds \rho(s), & r < R, \end{cases} \quad (19)$$

with  $G_N = (1 + \frac{\alpha}{2})G$ . The gravity residual is defined as the difference between the Newtonian  $g(r)$  and the measured  $g(r)$ , which we here identify with the  $g(r)$  from (18),

$$\Delta g(r) \equiv g(r)_{Newton} - g(r)_{observed}. \quad (20)$$

Then  $\Delta g(r)$  is found to be, to 1st order in  $R - r$ , i.e.

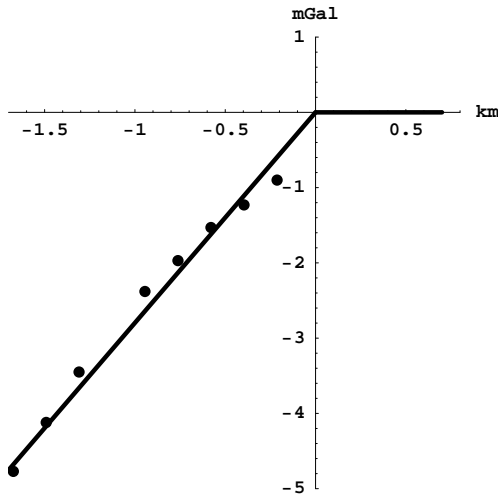


Fig. 2: The data shows the gravity residuals for the Greenland Ice Cap [4] measurements of the  $g(r)$  profile, defined as  $\Delta g(r) = g_{Newton} - g_{observed}$ , and measured in mGal ( $1 \text{ mGal} = 10^{-3} \text{ cm/sec}^2$ ), plotted against depth in km. Using (21) we obtain  $\alpha^{-1} = 139 \pm 5$  from fitting the slope of the data, as shown.

near the surface,

$$\Delta g(r) = \begin{cases} 0, & r > R, \\ -2\pi\alpha G_N \rho(R)(R-r), & r < R, \end{cases} \quad (21)$$

which is the form actually observed [4], as shown in Fig. 2.

Gravity residuals from a bore hole into the Greenland Ice Cap were determined down to a depth of 1.5km. The ice had a measured density of  $\rho = 930 \text{ kg/m}^3$ , and from (21), using  $G_N = 6.6742 \times 10^{-11} \text{ m}^3 \text{ s}^{-2} \text{ kg}^{-1}$ , we obtain from a linear fit to the slope of the data points in Fig. 2 that  $\alpha^{-1} = 139 \pm 5$ , which equals the value of the fine structure constant  $\alpha^{-1} = 137.036$  to within the errors, and for this reason we identify the constant  $\alpha$  in (5) as being the fine structure constant. Then we arrive at the conclusion that there is indeed “black hole” or “dark matter” dynamics within the Earth, and that from (17) we have again for the Earth that  $M_{BH}/M = \alpha/2$ , as is also shown in Fig. 1.

This “minimal black hole” effect must also occur within stars, although that could only be confirmed by indirect observations. This effect results in  $g(r)$  becoming large at the center, unlike Newtonian gravity, which would affect nuclear reaction rates. This effect may already have manifested in the solar neutrino count problem [9, 10]. To study this will require including the new gravity dynamics into solar models.

## 9 Spiral galaxies

We now consider the situation in which matter in-falls around an existing primordial black hole. Immediately we see some

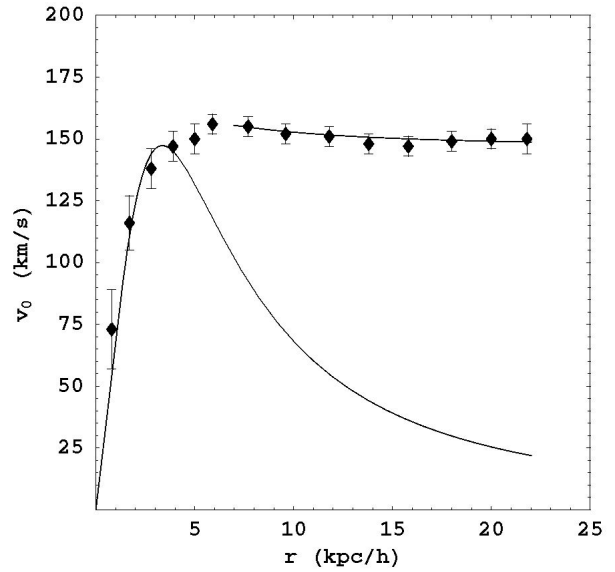


Fig. 3: Data shows the non-Keplerian rotation-speed curve  $v_0$  for the spiral galaxy NGC 3198 in km/s plotted against radius in kpc/h. Lower curve is the rotation curve from the Newtonian theory for an exponential disk, which decreases asymptotically like  $1/\sqrt{r}$ . The upper curve shows the asymptotic form from (24), with the decrease determined by the small value of  $\alpha$ . This asymptotic form is caused by the primordial black holes at the centres of spiral galaxies, and which play a critical role in their formation. The spiral structure is caused by the rapid in-fall towards these primordial black holes.

of the consequences of this time evolution: (i) because the acceleration field falls off much slower than the Newtonian inverse square law, as in (9), this in-fall would happen very rapidly, and (ii) the resultant in-flow would result in the matter rotating much more rapidly than would be predicted by Newtonian gravity, (iii) so forming a quasar which, after the in-fall of some of the matter into the black hole has ceased, would (iv) result in a spiral galaxy exhibiting non-Keplerian rotation of stars and gas clouds, *viz* the so-called “dark matter” effect. The study of this time evolution will be far from simple. Here we simply illustrate the effectiveness of the new theory of gravity in explaining this “dark matter” or non-Keplerian rotation-velocity effect.

We can determine the star orbital speeds for highly non-spherical galaxies in the asymptotic region by solving (15), for asymptotically where  $\rho \approx 0$  the velocity field will be approximately spherically symmetric and radial; nearer in we would match such a solution to numerically determined solutions of (5). Then (15) has an exact non-perturbative two-parameter ( $K$  and  $R_S$ ) analytic solution,

$$v(r) = K \left( \frac{1}{r} + \frac{1}{R_S} \left( \frac{R_S}{r} \right)^{\frac{\alpha}{2}} \right)^{1/2}; \quad (22)$$

this velocity field then gives using (1) the non-Newtonian

asymptotic acceleration

$$g(r) = \frac{K^2}{2} \left( \frac{1}{r^2} + \frac{\alpha}{2rR_S} \left( \frac{R_S}{r} \right)^{\frac{\alpha}{2}} \right), \quad (23)$$

applicable to the outer regions of spiral galaxies.

We then compute circular orbital speeds using  $v_o(r) = \sqrt{rg(r)}$  giving the predicted “universal rotation-speed curve”

$$v_o(r) = \frac{K}{2} \left( \frac{1}{r} + \frac{\alpha}{2R_S} \left( \frac{R_S}{r} \right)^{\frac{\alpha}{2}} \right)^{1/2}. \quad (24)$$

Because of the  $\alpha$  dependent part this rotation-speed curve falls off extremely slowly with  $r$ , as is indeed observed for spiral galaxies. This is illustrated in Fig. 3 for the spiral galaxy NGC 3198.

## 10 Interpretation and discussion

Section 2 outlines a model of space developed in [1, 11] in which space has a “substratum” structure which is in differential motion. This means that the substratum in one region may have movement relative to another region. The substratum is not embedded in a deeper space; the substratum itself defines space, and requiring that, at some level of description, it may be approximately described by a “classical” 3-vector velocity field  $\mathbf{v}(\mathbf{r}, t)$ . Then the dynamics of space involves specifying dynamical equations for this vector field. Here the coordinates  $\mathbf{r}$  is not space itself, but a means of labelling points in space. Of course in dealing with this dynamics we are required to define  $\mathbf{v}(\mathbf{r}, t)$  relative to some set of observers, and then the dynamical equations must be such that the vector field transforms covariantly with respect to changes of observers. As noted here Newtonian gravity itself may be written in terms of a vector field, as well as in terms of the usual acceleration field  $\mathbf{g}(\mathbf{r}, t)$ . General Relativity also has a special class of metric known as the Panlevé-Gullstrand metrics in which the metrics are specified by a velocity field. Most significantly the major tests of General Relativity involved the Schwarzschild metric, and this metric belongs to the Panlevé-Gullstrand class. So in both cases these putatively successful models of gravity involved, in fact, velocity fields, and so the spacetime metric description was not essential. As well there are in total some seven experiments that have detected this velocity field [12], so that it is more than a choice of dynamical degree of freedom: indeed it is more fundamental in the sense that from it the acceleration field or metric may be mathematically constructed.

Hence the evidence, both experimental and theoretical, is that space should be described by a velocity field. This implies that space is a complex dynamical system which is best thought of as some kind of “flow system”. However

the implicit question posed in this paper is that, given the physical existence of such a velocity field, are the Newtonian and/or General Relativity formalisms the appropriate descriptions of the velocity field dynamics? The experimental evidence herein implies that a different dynamics is required to be developed, because when we generalise the velocity field modelling to include a spatial self-interaction dynamics, the experimental evidence is that the strength of this dynamics is determined by the fine structure constant,  $\alpha$ . This is an extraordinary outcome, implying that gravity is determined by two fundamental constants,  $G$  and  $\alpha$ . As  $\alpha$  clearly is not in Newtonian gravity nor in General Relativity the various observational and experimental data herein is telling us that neither of these theories of gravity is complete. The modelling discussed here is non-relativistic, and essentially means that Newtonian gravity was incomplete from the very beginning. This happened because the self-interaction dynamics did not manifest in the solar system planetary orbit motions, and so neither Kepler nor later Newton were aware of the intrinsic complexity of the phenomenon of gravity. General Relativity was of course constructed to agree with Newtonian gravity in the non-relativistic limit, and so missed out on this key non-relativistic self-interaction effect.

Given both the experimental detection of the velocity field, including in particular the recent discovery [11] of an in-flow velocity component towards the Sun in the 1925/26 Miller interferometer data, and in agreement with the speed value from (3) for the Sun, together with the data from various observations herein, all showing the presence of the  $\alpha$  dependent effect, we should also discuss the physical interpretation of the vacuum “black hole” solutions. These are different in character from the so-called “black holes” of General Relativity: we use the same name only because these new “black holes” have an event horizon, but otherwise they are completely different. In particular the mathematical existence of such vacuum “black holes” in General Relativity is doubtful. In the new theory of gravity these black holes are exact mathematical solutions of the velocity equations and correspond to self-sustaining in-flow singularities, that is, where the in-flow speed becomes very large within the classical description. This singularity would then require a quantum description to resolve and explain what actually happens there. The in-flow does not involve any conserved measure, and there is no notion of this in-flow connecting to wormholes etc. The in-flow is merely a self-destruction of space, and in [11] it is suggested that space is in essence an “information” system, in which case the destruction process is easier to comprehend. As for the in-flow into the Earth, which is completely analogous to the observed in-flow towards the Sun, the in-flow singularities or “black holes” are located at the centre of the Earth, but it is unclear whether there is one such singularity or multiple singularities. The experimental existence of the Earth-centred in-flow singularity is indirect, as it is inferred solely by the anomalous var-



iation of  $g$  with depth, and that this variation is determined by the value of  $\alpha$ . In the case of the globular clusters and elliptical galaxies, the in-flow singularities are observed by means of the large accelerations of stars located near the centres of such systems and so are more apparent, and as shown here in all case the effective mass of the in-flow singularity is  $\alpha/2$  times the total mass of these systems. It is important to note here that even if we disregard the theoretical velocity field theory, we would still be left with the now well established  $\alpha/2$  observational effect. But then this velocity field theory gives a simple explanation for this data, although that in itself does not exclude other theories offering a different explanation. It is hard to imagine however how either Newtonian gravity or General Relativity could offer such a simple explanation, seeing that neither involves  $\alpha$ , and involve only  $G$ . As well we see that the new theory of gravity offers a very effective explanation for the rotation characteristics of spiral galaxies; the effect here being that the vacuum black hole(s) at the centres of such galaxies do not generate an acceleration field that falls off with distance according the inverse square law, but rather according to (23). Remarkably this is what the spiral galaxy data shows. This means that the so-called “dark matter” effect is not about a new and undetected form of matter. So the success of the new velocity field dynamics is that one theory explains a whole range of phenomena: this is the hallmark of any theory, namely economy of explanation.

## 11 Conclusion

The observational and experimental data confirm that the massive black holes in globular clusters and galaxies are necessary phenomena within a theory for gravity which uses a velocity field as the fundamental degree of freedom. This involves two constants  $G$  and  $\alpha$  and the data reveals that  $\alpha$  is the fine structure constant. This suggests that the spatial self-interaction dynamics, which is missing in the Newtonian theory of gravity, may be a manifestation at the classical level of the quantum behaviour of space. It also emerges that the “black hole” effect and the “dark matter” effect are one phenomenon, namely the non-Newtonian acceleration caused by singular solutions. This effect must manifest in planets and stars, and the bore hole  $g$  anomaly confirms that for planets. For stars it follows that the structure codes should be modified to include the new spatial self-interaction dynamics, and to determine the effect upon neutrino count rates. The data shows that spherical systems with masses varying over 15 orders of magnitude exhibit the  $\alpha$ -dependent dynamical effect. The non-Newtonian gravitational acceleration of primordial black holes will cause rapid formation of quasars and stars, explaining why recent observations have revealed that these formed very early in the history of the universe. In this way the new theory of gravity makes the big bang theory

compatible with these recent observations. These developments clearly have major implications for cosmology and fundamental physics. The various experiments that detected the velocity field are discussed in [11, 12].

This research is supported by an Australian Research Council Discovery Grant.

## References

1. Cahill R. T. *Trends in Dark Matter Research*, ed. by Blain J. Val, Nova Science Pub, NY, 2005; *Apeiron*, 2005, v. 12, No. 2, 155–177.
2. Stacey F. D. et al. *Phys. Rev. D*, 1981, v. 23, 2683.
3. Holding S. C., Stacey F. D. & Tuck G. J. *Phys. Rev. D*, 1986, v. 33, 3487.
4. Ander M. E. et al. *Phys. Rev. Lett.*, 1989, v. 62, 985.
5. Gerssen J., van der Marel R. P., Gebhardt K., Guhathakurta P., Peterson R. & Pryor C. *Astrophys. J.*, 2002, v. 124, 3270; Addendum 2003, v. 125, 376.
6. Murphy B. W., Cohn H. N., Lugger P. N., & Dull J. D. *Bull. of American Astron. Society*, 1994, v. 26, No. 4, 1487.
7. Gebhardt K., Rich R. M., & Ho L. C. *Astrophys. J.*, 2002, v. L41, 578.
8. Kormendy J. & Richstone D. *Astronomy and Astrophysics*, 1995, v. 33, 581.
9. Davies R. *Phys. Rev. Lett.*, 1964, v. 12, 300.
10. Bahcall J. *Phys. Rev. Lett.*, 1964, v. 12, 303.
11. Cahill R. T., *Process Physics: From Information Theory to Quantum Space and Matter*. Nova Science Pub., NY, 2005.
12. Cahill R. T. *Progress in Physics*, 2005, v. 3, 25–29.

# Is the Biggest Paradigm Shift in the History of Science at Hand?

Eit Gaastra

*Groningen, The Netherlands*

E-mail: eitgaastra@freeler.nl

According to a growing number of scientists cosmology is at the end of an era. This era started 100 years ago with the publication of Albert Einstein's special theory of relativity and came to its height in the 1920s when the theory of relativity was used to develop the big bang model. However, at this moment there is a crisis within cosmology. More and more scientists openly doubt the big bang. There are alternatives for the theory of relativity as well as for the big bang model, but so far most scientists are scared to pass over Einstein.

## 1 Introduction

The big bang model rests on three pillars [1]. This trinity is the cosmology of the twentieth century.

The first pillar is the Theory of General Relativity. In 1905 Einstein came with his Theory of Special Relativity which describes the behaviour of light and in 1916 he published a theory about gravity, the Theory of General Relativity. In publications in 1922 and 1924 the Russian mathematician Alexander Friedmann used the formulae of the General Theory of Relativity to prove that the universe was dynamic: either it expanded or it shrunk. In 1927 it was the Belgian priest and astronomer-cosmologist Georges Lemaître, using the cosmological equations of Friedmann, who suggested for the first time that the universe once could have sprung from a point of very high-density, the *primaeval atom*. Another link in the realization of the big bang model was the Dutch astronomer-cosmologist Willem de Sitter, who suggested in 1917, together with Einstein, the de-Sitter-universe, which was based on the formulae of the General Theory of Relativity. The de-Sitter-universe has no mass, but has the feature that mass particles that form in it will accelerate away from each other.

The second pillar on which the big bang model rests is the stretching of light in an expanding universe. In the 1920s Edwin Hubble discovered that certain dots in the night sky are not stars but galaxies instead. From 1924 on he measured the distances of the galaxies and in 1929 he announced that the wavelength of light of galaxies is shifted towards a longer wavelength. The further away the galaxy the more "stretched" the light. At the time this stretching of light was explained with the big bang model of Lemaître. The universe could have sprung from a point of very high-density mass and ever since the universe would expand as a balloon. Because of the expansion of the universe space in the universe would stretch and in that case light would stretch along with space. The stretching of light of faraway galaxies is still explained this way, although a lot of astronomers customarily to refer

to this stretching as if it is caused by the recessional velocity of galaxies in the big bang universe.

The third pillar was discovered in 1965. In 1948 a group of cosmologists calculated that in the case of a big bang certain radiation still had to be left over from a period shortly after the big bang. In 1965 such radiation was measured. This radiation (of 3 Kelvin) is now known as the cosmic background radiation and since 1965 it is seen as the big proof of the big bang model.

## 2 Alternatives for the theory of relativity

Einstein unfolded his special theory of relativity in an article in 1905, in which he states that the velocity of light is always constant relative to an observer. But the apparent constancy of the velocity of light can be explained differently.

Gravitons or other not yet detected particles may act as the medium that is needed by light to propagate itself. This is somewhat comparable to air molecules that are needed as a medium by sound to propagate itself. A theory that calls a medium into existence to explain the propagation of light is called an aether theory. Aether theories created a furore in the nineteenth century, but fell into oblivion after 1905, because of the rise of the theory of relativity. However, the last decennium the aether concept is making a come back and is getting more and more advocates, among whom is the Italian professor of physics Selleri [2]. (Also more advocates because despite the announcements by Michelson and Morley about the "null result", their famous interferometer 1887 experiment actually may have detected both absolute motion and the breakdown of Newtonian physics [3].)

Albert Einstein's theory of General Relativity of 1916 describes the movement of light and matter with the curvature of space-time more accurately than Isaac Newton's universal law of gravitation from the seventeenth century. There are alternatives, both for the Theory of General Relativity and Newtonian gravity. The physics professors Assis [4] and

Ghosh [5] look at inertia and gravity as forces that are caused by all the matter in the universe. This is called the extended Mach principle, after Ernst Mach who suggested in the nineteenth century that the inertia of any body is caused by its interaction with the rest of the universe.

There is also the so-called pushing gravity concept, a gravity model with gravitons going in and out of matter and by doing so pushing objects towards each other (on a macro-scale, for instance a teacup that falls to the ground or stars that are pushed towards each other; on a subatomic level things are different). Pushing gravity too is an alternative for both the Theory of General Relativity and Newtonian gravity. The pushing gravity concept was first suggested by Nicolas Fatio de Duillier in the seventeenth century [6].

An aether theory, the extended Mach principle as well as pushing gravity, takes the line that smaller particles (like gravitons) that we cannot yet detect do exist. The three theories can stand alone, but can be combined as well. The pushing gravity concept for instance, can be used as an explanation for the extended Mach principle.

In a bizarre way individual photons and individual atoms seem to interfere with themselves in the famous two-slit experiment in Quantum Mechanics. An aether theory can explain the baffling interference in a very simple way [7, 8]. That is why, with an aether theory, Quantum Mechanics may also be unsettled. Next to that the intriguing black holes, sprung from the mathematics of the theory of relativity, may vanish by embracing the pushing gravity concept. (Besides, black holes may not be predicted by General Relativity [9, 10].)

### 3 Alternatives for the big bang

Fritz Zwicky suggested in 1929 that photons may lose energy while travelling through space, but so far his idea has always been overshadowed by the big bang explanation with stretching space. Zwicky's explanation is known as the tired light concept and it is used by alternative thinking scientists as part of a model that looks at the universe as infinite in time and space. In a tired light theory photons lose energy by interaction with gravitons or other small particles. The tired light model can be combined with an aether theory, the extended Mach principle and pushing gravity.

Next to alternatives for the theory of relativity and the stretching of light, scientists have found alternatives for the third pillar of current conventional cosmology, the cosmic background radiation discovered in 1965. That a cosmic background radiation can originate as a result of the equilibrium temperature of the universe was already suggested by many scientists in the half century preceding 1948, the year in which cosmologists predicted the cosmic background radiation of the big bang universe [11]. In a space and time infinite universe many old cooled down remnants (amongst

which are dust and asteroids) of planets and stars may exist between the stars, between galaxies and between clusters of galaxies. Such remnants will eventually reach the very cold temperature (3 Kelvin) of the universe and send out radiation that corresponds with that temperature. Other examples of alternatives that can explain an equilibrium temperature are direct energy exchange between photons or indirect energy exchange between photons via gravitons or other small particles. A growing number of scientists looks at the cosmic background radiation as a result of the equilibrium temperature of a universe infinite in space and time.

In the sixteenth century Thomass Digges was the first scientist to advance a universe filled with an infinite number of stars. In the last decennium more and more scientists have taken the line of an infinite universe filled with an infinite number of galaxies. (Also because, despite all beliefs to the contrary, General Relativity may not predict an expanding universe; the Friedmann models and the Einstein-de Sitter model may be invalid [12].)

### 4 Clusters of galaxies at large distances?

If there was no big bang, and if we live in an infinite universe, then distances of faraway galaxies are much larger than presently thought. A few years back big bang cosmologists concluded that the big bang ought to have taken place 13.7 billion years ago. Therefore within the big bang model objects are always less than 13.7 years old. Big bang astronomers observe certain galaxies with enormous shifts of the wavelength of light and therefore think these objects sent out their light very long ago, for instance 13 billion years. With the tired light model in an infinite universe objects with such large shifts of the wavelength of light will be at distances of more than 70 billion light-years. The galaxies, which big bang astronomers now think they observe at these large distances, may therefore be clusters of galaxies in reality.

In the 1920s Edwin Hubble inaugurated a new era by finding that certain dots in the night sky are not stars, but galaxies instead. Only then did scientists realize that certain objects are at much larger distances than accepted at the time. Within the years to come new telescopes will deliver sharper images of faraway objects which are now addressed as galaxies. The big bang model already has difficulty explaining galaxies in the very early universe, because in the big bang formed, loose matter, needs time to aggregate into stars and galaxies. If it turns out that not only galaxies but also big clusters of galaxies exist in the very early universe the big bang model will probably go down. In that case there will be a lot of change within cosmology, and also the theory of relativity will then be highly questioned. With the festivities of 100 years of relativity we may have come close to the end of a scientific era.

## 5 Knowledge and power

If the big bang model goes down then of course the first question is: What will replace it? If the here named alternatives break through then also another question rises: Why did the alternatives need so much time to break through?

A good theory needing a lot of time to break through has happened before. In the third century BC the Greek philosopher and scientist Aristarchus published a book in which he proposed that the Earth rotates daily and revolves annually about the Sun. Eighteen hundred years later Copernicus was aware of the proposition by Aristarchus. Aristarchus and Copernicus were the heroes of the Copernican Revolution that followed after the publication of Copernicus' book *Revolutions of the Celestial Spheres* in 1543 [1]. The power of the Sun-centred model was its simplicity compared to the epicycles of the Earth-centred model.

It took a long time, after the publication of Copernicus' greatest work, before the Earth-centred model was left *en masse* for the Sun-centred model. One of the reasons for this was that, for a long time, the Earth-centred model described the movement of planets more accurately than the Sun-centred model of Copernicus. Formulae of wrong models stay dominant when alternatives are not sufficiently developed. The gravity formulae of the theory of relativity and the law of universal gravitation by Newton don't explain how gravity works, but they can be used to calculate with. The pushing gravity model explains, in a very simple way, how gravity works, but when it comes to formulae the concept is, as was the model of Copernicus four centuries ago, still in its infancy. The same applies for aether theories, the extended Mach principle, the tired light model and the equilibrium temperature of the universe as an explanation for the cosmic background radiation. The power of the aforementioned alternatives is that they form, in a very simple way, a coherent whole within an infinite universe model.

Another reason for the late definitive capitulation of the Sun-centred model was that the new model endangered the position of authority held by the Catholic Church. Four centuries ago scientific knowledge was dictated by the Catholic Church. Those who wanted to make a career as a scientist, or just wanted to stay alive as a human, were forced to canonize the Earth-centred model.

Right now established science institutes dictate knowledge when it comes to the fields of physics, cosmology and astronomy. Physics professors Assis (Brazil) and Ghosh (India) independently developed the same alternative for the theory of relativity. Both have published their work, but within the established science institutes they don't find an audience. Professor of physics, the late Paul Marmet (Canada), attached questions to the fundamental laws of nature (like the theory of relativity) and had to leave the science institute where he did his research. Right now students learn to canonize the big bang and the theory of relativity.

At this moment career-fear is the big obstacle when it comes to progress in physics, cosmology and astronomy.

## 6 Are time and space properties of our reason?

Isaac Newton (1642–1726) thought that there was something like “absolute space” and “absolute time” and two centuries later Albert Einstein (1879–1955) melted these two together in the “space-time” concept. Newton and Einstein argued that space and time do exist physically, and ever since conventional scientists think that way too. However, it has been argued for centuries by scientists and philosophers (often scientists and philosophers at the same time) that space and time are not physically existing entities. Examples of such alternative thinkers are the Frenchman Rene Descartes (1596–1650), the Dutchman Christiaan Huygens (1629–1695), the German Gottfried Leibniz (1646–1716), the Irishman George Berkeley (1685–1753), the East-Prussian Immanuel Kant (1724–1804) and the already mentioned Austrian, Ernst Mach (1838–1916).

Our current natural sciences have their origin in Newton's laws and formulae. Many physicists, cosmologists and astronomers dismiss philosophy because they think it is misty. They feel safe with the basics and mathematics of the current conventional standard theories. Still, though mathematics is needed to do good predictions, sooner or later the whole bastion falls apart if mathematics is based upon wrong principles. Thinking about basic principles needs philosophy. Centuries ago it was the generalists, with philosophy and all the natural sciences in their package, who advocated that space and time were properties of our reason in the first place and not properties of the world. The theory of relativity has time as the fourth dimension. If time does not exist then the theory of relativity can be dismissed, and also the string theory, which has run wild with the mathematics of the theory of relativity and works with eleven dimensions.

Processes in an atomic clock slow down when the clock moves fast, and often this is seen as evidence for the existence of time. But in the case of an aether, processes in fast moving atomic clocks slow down because more aether slows down the processes in the clock. Our brains use time to compare the movement of mass with the movement of other mass. For instance the rotation of our Earth (24 hours or one day) and the orbit of our Earth around the Sun (365 days or one year). That is all; it does not mean that time really exists. If time does not exist physically then the whole scientific bastion as we have known it since Newton and, especially, as we have known it the last 100 years, falls apart.

## 7 Revolution by computer?

One can draw a parallel between what is happening now and what happened four centuries ago. Before Copernicus en-

tered the scene, the Catholic Church had passed on more or less definitely settled knowledge for more than thousand years. However, where knowledge did not change much with respect to its contents, a strong development took place with respect to the passing on and propagation of the knowledge. In the early Middle Ages convents arose, in the twelfth century came the cathedral-schools and around 1200 the first universities were founded. In the course of centuries these universities gained an ever more independent position with respect to the church, which finally made the church lose its position of authority with respect to science.

Next to that in the late Middle Ages the church lost its monopoly with respect to knowledge, faster, because of the invention of the art of printing. From that moment on more people could master knowledge themselves and could have their own thoughts about it and propagate those thoughts by printing and distributing their own books.

The third development, at the end of the Middle Ages, that would help the Copernican Revolution, was the invention of the telescope, which brought new possibilities for astronomy.

A few decennia ago the computer was developed. It brought the internet, which split itself from science and obtained its own independent position. The internet brings knowledge to a lot of people all over the world. Now people can publish their ideas with respect to physics, cosmology and astronomy, independently of the universities and established periodicals. The universities lose more and more their monopoly as guardians of science, and the same goes for the periodicals that serve as their extension piece. Before the internet alternative thinking scientists were unknown isolated islands who could not publish their ideas and did not know of each other's existence. Now there are web pages which form a vibrating net of interacting alternative models, a net that grows every day. Next to that it is thanks to the computer that very strong telescopes have been put into use these last decennia, and that ever stronger and better telescopes are on their way. Perhaps the science historians of the future will conclude that it was the computer that brought the Second Copernican Revolution.

## 8 Conclusions

Established conventional physicists and cosmologists behave as the church at the time of Galileo. Not by threatening with the death penalty, but simply by sniffing at alternative ideas. This will change as soon as the concerning noses smell funding money instead of career-fear. In our current society money and careers are the central issues where it comes to our necessities of life. Like four centuries ago the worries about the necessities of life are the driving forces behind the impasse. Still, just as at the time of Copernicus and Galileo: under the surface of the current standard theories the revolution may be going on at full speed. In June 2005

dissidents argued at the first ever crisis in cosmology conference in Monção, Portugal [13] that the big bang theory fails to explain certain observations. The biggest revolution in the history of science may be at hand.

## References

1. Harrison E.R. *Cosmology: the science of the universe*. Cambridge University Press, Cambridge, 2000.
2. Selleri F. *Lezioni di relativita' da Einstein all' etere di Lorentz*. Progedit, Bari, 2003.
3. Cahill R. T. The Michelson and Morley 1887 experiment and the discovery of absolute motion. *Progress in Physics*, 2005, v. 3, 25–29.
4. Assis A. K. T. *Relational Mechanics*. Apeiron, Montreal, 1999.
5. Ghosh A. *Origin of Inertia*. Apeiron, Montreal, 2000.
6. Van Lunteren F. *Pushing Gravity*, ed. by M. R. Edwards, 2002, 41.
7. Edwards M. R. *Pushing Gravity*, ed. by M. R. Edwards, 2002, 137.
8. Buonomano V. *Pushing Gravity*, ed. by M. R. Edwards, 2002, 303.
9. Crothers S.J. On the general solution to Einstein's vacuum field and its implications for relativistic degeneracy. *Progress in Physics*, 2005, v. 1, 68–73.
10. Crothers S. J. On the ramifications of the Schwarzschild space-time metric. *Progress in Physics*, 2005, v. 1, 74–80.
11. Assis A.K.T. and Neves M.C.D. History of the 2.7 K temperature prior to Penzias and Wilson. *Apeiron*, 1995, v.2, 79–84.
12. Crothers S.J. On the general solution of Einstein's vacuum field for the point-mass when  $\lambda \neq 0$  and its implications for relativistic cosmology. *Progress in Physics*, 2005, v. 3, 7–18.
13. Ratcliffe H. The first crisis in cosmology conference. *Progress in Physics*, 2005, v. 3, 19–24.

## Sources of Stellar Energy and the Theory of the Internal Constitution of Stars

Nikolai Kozyrev\*

This is a presentation of research into the inductive solution to the problem on the internal constitution of stars. The solution is given in terms of the analytic study of regularities in observational astrophysics. Conditions under which matter exists in stars are not the subject of a priori suppositions, they are the objects of research.

In the first part of this research we consider two main correlations derived from observations: “mass-luminosity” and “period – average density of Cepheids”. Results we have obtained from the analysis of the correlations are different to the standard theoretical reasoning about the internal constitution of stars. The main results are: (1) in any stars, including even super-giants, the radiant pressure plays no essential part – it is negligible in comparison to the gaseous pressure; (2) inner regions of stars are filled mainly by hydrogen (the average molecular weight is close to  $\frac{1}{2}$ ); (3) absorption of light is derived from Thomson dispersion in free electrons; (4) stars have an internal constitution close to polytropic structures of the class  $\frac{3}{2}$ .

The results obtained, taken altogether, permit calculation of the physical conditions in the internal constitution of stars, proceeding from their observational characteristics  $L$ ,  $M$ , and  $R$ . For instance, the temperature obtained for the centre of the Sun is about 6 million degrees. This is not enough for nuclear reactions.

In the second part, the Russell-Hertzsprung diagram, transformed according to physical conditions inside stars shows: the energy output inside stars is a simple function of the physical conditions. Instead of the transection line given by the heat output surface and the heat radiation surface, stars fill an area in the plane of density and temperature. The surfaces coincide, being proof of the fact that there is only one condition – the radiation condition. Hence stars generate their energy not in any reactions. Stars are machines, directly generating radiations. The observed diagram of the heat radiation, the relation “mass-luminosity-radius”, cannot be explained by standard physical laws. Stars exist in just those conditions where classical laws are broken, and a special mechanism for the generation of energy becomes possible. Those conditions are determined by the main direction on the diagram and the main point located in the direction. Physical coordinates of the main point have been found using observational data. The constants (physical coordinates) should be included in the theory of the internal constitution of stars which pretend to adequately account for observational data. There in detail manifests the inconsistency of the explanations of stellar energy as given by nuclear reactions, and also calculations as to the percentage of hydrogen and helium in stars.

Also considered are peculiarities of some sequences in the Russell-Hertzsprung diagram, which are interesting from the theoretical viewpoint.

\*Editor’s remark: This is the doctoral thesis of Nikolai Aleksandrovich Kozyrev (1908–1983), the famous astronomer and experimental physicist – one of the founders of astrophysics in the 1930’s, the discoverer of lunar volcanism (1958), and the atmosphere of Mercury (1963) (see the article *Kozyrev* in the *Encyclopaedia Britannica*). Besides his studies in astronomy, Kozyrev contributed many original experimental and theoretical works in physics, where he introduced the “causal or asymmetrical mechanics” which takes the physical properties of time into account. See his articles reporting on his many years of experimental research into the physical properties of time, *Time in Science and Philosophy* (Prague, 1971) and *On the Evolution of Double Stars, Comptes rendus* (Bruxelles, 1967). Throughout his scientific career Kozyrev worked at the Pulkovo Astronomical Observatory near St. Petersburg (except for the years 1946–1957 when he worked at the

Crimean branch of the Observatory). In 1936 he was imprisoned for 10 years without judicial interdiction, by the communist regime in the USSR. Set free in 1946, he completed the draft of this doctoral thesis and published it in Russian in the local bulletin of the Crimean branch of the Observatory (*Proc. Crimean Astron. Obs.*, 1948, v.2, and 1951, v.6). Throughout the subsequent years he continued to expand upon his thesis. Although this research was started in the 1940’s, it remains relevant today, because the basis here is observational data on stars of regular classes. This data has not changed substantially during the intervening decades. (Translated from the final Russian text by D. Rabounski and S. J. Crothers.)

The author dedicates this paper to the blessed memory of  
Prof. Aristarch A. Belopolski

## Contents

Introduction ..... 62

### PART I

#### Chapter 1 Deducing the Main Equations of Equilibrium in Stars

- 1.1 Equation of mechanical equilibrium ..... 63  
1.2 Equation of heat equilibrium ..... 64  
1.3 The main system of the equations. Transformation of the variables ..... 65

#### Chapter 2 Analysis of the Main Equations and the Relation “Mass-Luminosity”

- 2.1 Observed characteristics of stars ..... 66  
2.2 Stars of polytropic structure ..... 67  
2.3 Solution to the simplest system of the equations ..... 68  
2.4 Physical conditions at the centre of stars ..... 71  
2.5 The “mass-luminosity” relation ..... 72  
2.6 The radiant pressure inside stars ..... 74  
2.7 Comparing the obtained results to results obtained by other researchers ..... 75  
2.8 The rôle of convection inside stars ..... 76

#### Chapter 3 The Internal Constitution of Stars, Obtained from the Analysis of the Relation “Period – Average Density of Cepheids” and Other Observational Data

- 3.1 The main equation of pulsation ..... 78  
3.2 Calculation of the mean values in the pulsation equation by the perturbation method ..... 79  
3.3 Comparing the theoretical results to observational data ..... 80  
3.4 Additional data about the internal constitution of stars ..... 81  
3.5 Conclusions about the internal constitution of stars ..... 82

### PART II

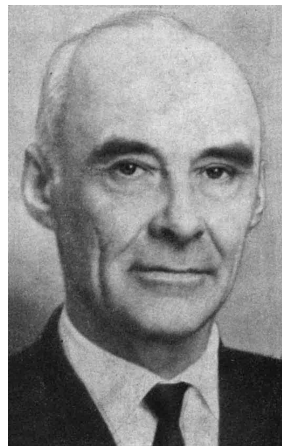
#### Chapter 1 The Russell-Hertzsprung Diagram and the Origin of Stellar Energy

- 1.1 An explanation of the Russell-Hertzsprung diagram by the theory of the internal constitution of stars ..... 83  
1.2 Transforming the Russell-Hertzsprung diagram to the physical characteristics, specific to the central regions of stars ..... 85  
1.3 The arc of nuclear reactions ..... 86  
1.4 Distribution of stars on the physical conditions diagram ..... 87  
1.5 Inconsistency of the explanation of stellar energy by Bethe’s thermonuclear reactions ..... 90  
1.6 The “mass-luminosity” relation in connection with the Russell-Hertzsprung diagram ..... 92  
1.7 Calculation of the main constants of the stellar energy state ..... 93

#### Chapter 2 Properties of Some Sequences in the Russell-Hertzsprung Diagram

- 2.1 The sequence of giants ..... 95  
2.2 The main sequence ..... 96  
2.3 White dwarfs ..... 97

## Introduction



Prof. Nikolai Kozyrev, 1970's

Energy, radiated by the Sun and stars into space, is maintained by special sources which should keep stars radiating light during at least a few billion years. The energy sources should be dependent upon the physical conditions of matter inside stars. It follows from this fact that stars are stable space bodies. During the last decade, nuclear physics discovered thermonuclear reactions that could be the energy source satisfying the above requirements.

The reactions between protons and numerous light nuclei, which result in transformations of hydrogen into helium, can be initiated under temperatures close to the possible temperature of the inner regions of stars — about 20 million degrees. Comparing different thermonuclear reactions, Bethe concluded that the energy of the Sun and other stars of the main sequence is generated in cyclic reactions where the main part is played by nitrogen and carbon nuclei, which capture protons and then produce helium nuclei [1]. This theory, developed by Bethe and widely regarded in recent years, has had no direct astrophysical verification until now. Stars produce various amounts of energy, e. g. stars of the giants sequence have temperatures much lower than that which is necessary for thermonuclear reactions, and the presence of bulk convection in upper shells of stars, supernova explosions, peculiar ultra-violet spectra lead to the conclusion that energy is generated even in the upper shells of stars and, sometimes, it is explosive. It is quite natural to inquire as to a general reason for all the phenomena. Therefore we should be more accurate in our attempts to apply the nuclear reaction theory to stars. It is possible to say (without exaggeration), that during the last century, beginning with Helmholtz’s contraction hypothesis, every substantial discovery in physics led to new attempts to explain stellar energy. Moreover, after every attempt it was claimed that this problem was finally solved, despite the fact that there was no verification in astrophysical data. It is probable that there is an energy generation mechanism of a particular kind, unknown in an Earthly laboratory. At the same time, this circumstance cannot be related to a hypothesis that some exclusive conditions occur inside stars. Conditions inside many stars (e. g. the infrared satellite of  $\epsilon$  Aurigae) are close to those that can be realized in the laboratory. The reason that such an energy generation mechanism remained elusive in experiments is due to peculiarities in the experiment statement and, possibly, in the necessity for large-scale considerations in the experiment. Considering physical theories, it is possible that their

inconsistency in the stellar energy problem arises for the reason that the main principles of interaction between matter and radiant energy need to be developed further.

Much of the phenomena and empirical correlations discovered by observational astrophysics are linked to the problem of the origin of stellar energy, hence the observational data have no satisfying theoretical interpretation. First, it is related to behaviour of a star as a whole, i. e. to problems associated with the theory of the internal constitution of stars. Today's theories of the internal constitution of stars are built upon a priori assumptions about the behaviour of matter and energy in stars. One tests the truth or falsity of the theories by comparing the results of the theoretical analysis to observational data. This is one way to build various models of stars, which is very popular nowadays. But such an approach cannot be very productive, because the laws of Nature are sometimes so unexpected that many such trials, in order to guess them, cannot establish the correct solution. Because empirical correlations, characterizing a star as a whole, are surely obtained from observations, we have therein a possibility of changing the whole statement of the problem, formulating it in another way — considering the world of stars as a giant laboratory, where matter and radiant energy can be in enormously different scales of states, and proceeding from our analysis of observed empirical correlations obtained in the stellar laboratory, having made no arbitrary assumptions, we can find conditions governing the behaviour of matter and energy in stars as some unknown terms in the correlations, formulated as mathematical equations. Such a problem can seem hopelessly intractable, owing to so many unknown terms. Naturally, we do not know: (1) the phase state of matter — Boltzmann gas, Fermi gas, or something else; (2) the manner of energy transfer — radiation or convection — possible under some mechanism of energy generation; (3) the rôle of the radiant pressure inside stars, and other factors linked to the radiant pressure, namely — (4) the value of the absorption coefficient; (5) chemical composition of stars, i. e. the average numerical value of the molecular weight inside stars, and finally, (6) the mechanism generating stellar energy. To our good fortune is the fact that the main correlation of observational astrophysics, that between mass and luminosity of stars, although giving no answer as to the origin of stellar energy, gives data about the other unknowns. Therefore, employing the relation “period — average density of Cepheids”, we make more precise our conclusions about the internal constitution of stars. As a result there is a possibility, even without knowledge of the origin of stellar energy, to calculate the physical conditions inside stars by proceeding from their observable characteristics: luminosity  $L$ , mass  $M$ , and radius  $R$ . On this basis we can interpret another correlation of observational astrophysics, the Russell-Hertzsprung diagram — the correlation between temperature and luminosity of stars, which depends almost exclusively on the last unknown (the me-

chanism generating stellar energy). The formulae obtained are completely unexpected from the viewpoint of theoretical physics. At the same time they are so typical that we have in them a possibility of studying the physical process which generates stellar energy.

This gives us an inductive method for determining a solution to the problem of the origin of stellar energy. Following this method we use some standard physical laws in subsequent steps of this research, laws which may be violated by phenomenology. However this circumstance cannot invalidate this purely astrophysical method. It only leads to the successive approximations so characteristic of the phenomenological method. Consequently, the results we have obtained in Part I can be considered as the first order of approximation.

The problem of the internal constitution of stars has been very much complicated by many previous theoretical studies. Therefore, it is necessary to consider this problem from the outset with the utmost clarity. Observations show that a star, in its regular duration, is in a balanced or quasi-balanced state. Hence matter inside stars should satisfy conditions of mechanical equilibrium and heat equilibrium. From this we obtain two main equations, by which we give a mathematical formulation of our problem. Considering the simplest case, we neglect the rotation of a star and suppose it spherically symmetric.

## PART I

### Chapter 1

#### Deducing the Main Equations of Equilibrium in Stars

##### 1.1 Equation of mechanical equilibrium

Let us denote by  $P$  the total pressure, i. e. the sum of the gaseous pressure  $p$  and the radiant energy pressure  $B$ , taken at a distance  $r$  from the centre of a star. The mechanical equilibrium condition requires that the change of  $P$  in a unit of distance along the star's radius must be kept in equilibrium by the weight of a unit of the gas volume

$$\frac{dP}{dr} = -g\rho, \quad (1.1)$$

where  $\rho$  is the gas density,  $g$  is the gravity force acceleration. If  $\varphi$  is the gravitational potential

$$g = -\text{grad } \varphi, \quad (1.2)$$

and the potential satisfies Poisson equation

$$\nabla^2 \varphi = -4\pi G\rho,$$

where  $G = 6.67 \times 10^{-8}$  is the gravitational constant. For spherical symmetry,

$$\nabla^2 \varphi = \text{div grad } \varphi = \frac{1}{r^2} \frac{dr^2 \text{ grad } \varphi}{dr}. \quad (1.4)$$



Comparing the equalities, we obtain the equation of mechanical equilibrium for a star

$$\frac{1}{\rho r^2} \frac{d}{dr} \left[ \frac{r^2 dP}{\rho dr} \right] = -4\pi G, \quad (1.5)$$

where

$$P = p + B. \quad (1.6)$$

Radiations are almost isotropic inside stars. For this reason  $B$  equals one third of the radiant energy density. As we show in the next paragraph, we can put the radiant energy density, determined by the Stephan-Boltzmann law, in a precise form. Therefore,

$$B = \frac{1}{3} \alpha T^4, \quad (1.7)$$

where  $\alpha = 7.59 \times 10^{-15}$  is Stephan's constant,  $T$  is the absolute temperature. The pressure  $P$  depends, generally speaking, upon the matter density and the temperature. This correlation is given by the matter phase state. If the gas is ideal, it is

$$p = nkT = \frac{\mathfrak{R}T}{\mu} \rho. \quad (1.8)$$

Here  $n$  is the number of particles in a unit volume of the gas,  $k = 1.372 \times 10^{-16}$  is Boltzmann's constant,  $\mathfrak{R} = 8.313 \times 10^7$  is Clapeyron's constant,  $\mu$  is the average molecular weight.

For example, in a regular Fermi gas the pressure depends only on the density

$$p = K \rho^{5/3}, \quad K = \mu_e^{5/3} K_H, \quad K_H = 9.89 \times 10^{12}, \quad (1.9)$$

where  $\mu_e$  is the number of the molecular weight units for each free electron.

We see that the pressure distribution inside a star can be obtained from (1.5) only if we know the temperature distribution. The latter is determined by the heat equilibrium condition.

## 1.2 Equation of heat equilibrium

Let us denote by  $\varepsilon$  the quantity of energy produced per second by a unit mass of stellar matter. The quantity  $\varepsilon$  is dependent upon the physical conditions of the matter in a star, so  $\varepsilon$  is a function of the radius  $r$  of a star. To study  $\varepsilon$  is the main task of this research. The heat equilibrium condition (known also as the energy balance condition) can be written as follows

$$\operatorname{div} F = \varepsilon \rho, \quad (1.10)$$

where  $F$  is the total flow of energy, being the sum of the radiant energy flow  $F_R$ , the energy flow  $F_c$  dragged by convection currents, and the heat conductivity flow  $F_T$

$$F = F_R + F_c + F_T. \quad (1.11)$$

First we determine  $F_R$ . Radiations, being transferred through a layer of thickness  $ds$ , change their intensity  $I$  through the layer of thickness  $ds$ , according to Kirchhoff's law

$$\frac{dI}{ds} = -\kappa \rho (I - E), \quad (1.12)$$

where  $\kappa$  is the absorption coefficient per unit mass,  $E$  is the radiant productivity of an absolute black body (calculated per unit of solid angle  $\omega$ ). In polar coordinates this equation is

$$\cos \theta \frac{\partial I}{\partial r} - \frac{\sin \theta}{r} \frac{\partial I}{\partial \theta} = -\kappa \rho (I - E), \quad (1.12a)$$

where  $\theta$  is the angle between the direction of the normal to the layer (the direction along the radius  $r$ ) and the radiation direction (the direction of the intensity  $I$ ). The flow  $F_R$  and the radiant pressure  $B$  are connected to the radiation intensity by the relations

$$F_R = \int I \cos \theta d\omega, \quad Bc = \int I \cos^2 \theta d\omega, \quad (1.13)$$

where  $c$  is the velocity of light, while the integration is taken over all solid angles. We denote

$$\int I d\omega = J. \quad (1.14)$$

Multiplying (1.12a) by  $\cos \theta$  and taking the integral over all solid angles  $d\omega$ , we have

$$c \frac{dB}{dr} - \frac{1}{r} (J - 3Bc) = -\kappa \rho F_R.$$

In order to obtain  $F_R$  we next apply Eddington's approximation

$$3Bc = J = 4\pi E, \quad (1.15)$$

thereby taking  $F_R$  to within high order terms. Then

$$F_R = -\frac{c}{\kappa \rho} \frac{dB}{dr}. \quad (1.16)$$

Let us consider the convective energy flow  $F_c$ . Everyday we see huge convection currents in the surface of the Sun (it is possible this convection is forced by sudden production of energy). To make the convective energy flow  $F_c$  substantial, convection currents of matter should be rapid and cause transfer of energy over long distances in a star. Such conditions can be in regions of unstable convection of matter, where free convection can be initiated. Schwarzschild's pioneering research [2], and subsequent works by other astrophysicists (Unsöld, Cowling, Bierman and others) showed that although a star is in the state of stable mechanical and heat equilibrium as a whole, free convection can start in regions where (1) stellar energy sources rapidly increase their power, or (2) the ionization energy is of the same order as the heat energy of the gas.

We assume convection currents flowing along the radius of star. We denote by  $Q$  the total energy per unit of convection current mass. Hence,  $Q$  is the sum of the inner energy of the gas, the heat function, the potential and kinetic energies. We regularly assume that a convection current retains its own energy along its path, i.e. it changes adiabatically, and dissipation of its energy occurs only when the current stops. Then the energy flow transferred by the convection, according to Schmidt [3], is

$$F_c = -A\rho \frac{dQ}{dr}, \quad A = \bar{v}\bar{\lambda}. \quad (1.17)$$

The quantity  $A$  is the convection coefficient,  $\bar{\lambda}$  is the average length travelled by the convection current,  $\bar{v}$  is the average velocity of the current. If the radiant pressure is negligible in comparison to the gaseous pressure, in an ideal gas (according to the 1st law of thermodynamics) we have

$$\frac{dQ}{dr} = c_v \frac{dT}{dr} + p \frac{d\frac{1}{\rho}}{dr}, \quad (1.18)$$

or, in another form,

$$\frac{dQ}{dr} = c_p \frac{dT}{dr} - \frac{1}{\rho} \frac{dp}{dr}, \quad (1.18)$$

where  $c_v$  is the heat capacity of the gas under constant volume,  $c_p$  is the heat capacity under constant pressure

$$c_p = c_v + \frac{\mathfrak{R}}{\mu}.$$

Denoting

$$\frac{c_p}{c_v} = \Gamma,$$

we have

$$c_p = \frac{\Gamma}{\Gamma - 1} \frac{\mathfrak{R}}{\mu}. \quad (1.20)$$

After an obvious transformation we arrive at the formulae

$$\frac{dQ}{dr} = -\frac{1}{\rho} \frac{dp}{dr} u, \quad u = 1 - \frac{\Gamma}{4(\Gamma - 1)} \frac{pdB}{Bdp}, \quad (1.21)$$

(for a monatomic gas  $\Gamma = 5/3$ ).

The heat conductivity flow has a formula analogous to (1.17). Because particles move in any direction in a gas, in the formula for  $A$  we have one third of the average velocity of particles instead of  $\bar{v}$ . In this case  $dQ/dr$  is equal to only the first term of equation (1.18), and so  $dQ/dr$  has the same-order numerical value that it has in the energy convective flow  $F_c$ . Therefore, taking  $A$  from  $F_c$  (1.17) into account, we see that  $F_c$  is much more than  $F_T$ . In only very rare exceptions, like a degenerate gas, can the heat conductivity flow  $F_T$  be essential for energy transfer.

Using formulae (1.10), (1.16), (1.17), (1.21), we obtain the heat equilibrium equation

$$\frac{1}{\rho r^2} \frac{1}{dr} \left[ \frac{r^2 db}{\kappa \rho dr} \right] - \frac{1}{c \rho r^2} \frac{1}{dr} \left[ r^2 A u \frac{dp}{dr} \right] = -\frac{\varepsilon}{c}. \quad (1.22)$$

We finally note that, because  $\varepsilon$  is tiny value in comparison to the radiation per mass unit, even tiny changes in the state of matter should break the equalities. Therefore even for large regions in stars the heat equilibrium condition (1.10) can be locally broken. The same can be said about the equation for the convective energy flow, because huge convections in stars can be statistically interpreted in only large surfaces like that of a whole star. Therefore the equations we have obtained can be supposed as the average along the whole radius of a star, and taken over a long time. Then the equations are true.

The aforementioned limitations do not matter in our analysis because we are interested in understanding the behaviour of a star as a whole.

### 1.3 The main system of the equations. Transformation of the variables

In order to focus our attention on the main task of this research, we begin by considering the equations obtained for equilibrium in the simplest case: (1) in the mechanical equilibrium equation we assume the radiant pressure  $B$  negligible in comparison to the gaseous pressure  $p$ , while (2) in the heat equilibrium equation we assume the convection term negligible. Then we obtain the main system of the equations in the form

$$\begin{aligned} \frac{1}{\rho r^2} \frac{d}{dr} \left[ \frac{r^2 dp}{\rho dr} \right] &= -4\pi G, \\ \frac{1}{\rho r^2} \frac{d}{dr} \left[ \frac{r^2 dB}{\kappa \rho dr} \right] &= -\frac{\varepsilon}{c}. \end{aligned} \quad (I)$$

The radiant pressure depends only on the gas temperature  $T$ , according to formula (1.7). The absorption coefficient  $\kappa$  (taken per unit mass) depends  $p$  and  $B$ . This correlation is unknown. Also unknown is the energy  $\varepsilon$  produced by a unit mass of gas. Let us suppose the functions known. Then in order to solve the system we need to have the state equation of matter, connecting  $\rho$ ,  $p$ , and  $B$ . In this case only two functions remain unknown: for instance  $p$  and  $B$ , whose dependence on the radius  $r$  is fully determined by equations (I). These functions should satisfy the following boundary conditions. In the surface of a star the total energy flow is  $F_0 = F_{R_0}$  ( $F_c = F_T = 0$ ). According formula (1.13),

$$F_{R_0} = \frac{1}{2} J_0 = \frac{3}{2} c B_0,$$

so, taking formula (1.16) into account, we obtain the condition in the surface of a star

$$\text{under } p = 0 \text{ we have } B = -\frac{2}{3} \frac{dB}{\kappa \rho dr}, \quad (1.23)$$

From equations (I) we see that the finite solution condition under  $r = 0$  is the same as

$$\text{under } r = 0 \text{ we have } \frac{dp}{dr} = 0, \quad \frac{dB}{dr} = 0. \quad (1.24)$$

The boundary conditions are absolutely necessary, they are true at the centre of any real star. The theory of the inner constitution of stars by Milne [4], built on solutions which do not satisfy these boundary conditions, does not mean that the boundary conditions are absolutely violated by the theory. In layers located far from the centre the boundary solutions can be realized, if derivatives of physical characteristics of matter are not continuous functions of the radius, but have breaks. Hence, Milne's theory permits a break a priori in the state equation of matter, so the theory permits stellar matter to exist in at least two different states. Following this hypothetical approach as to the properties of stellar matter, we can deduce conclusions about high temperatures and pressures in stars. Avoiding the view that "peculiar" conditions exist in stars, we obtain a natural way of starting our research into the problem by considering the phase state equations of matter.

Hence we carry out very important transformations of the variables in the system (I). Instead of  $r$  and other variables we introduce dimensionless quantities bearing the same physical conditions. We denote by index  $c$  the values of the functions in the centre of a star ( $r = 0$ ). Instead of  $r$  we introduce a dimensionless quantity  $x$  according to the formula

$$x = ar, \quad a = \rho_c \sqrt{\frac{4\pi G}{p_c}}, \quad (1.25)$$

and we introduce functions

$$\rho_1 = \frac{\rho}{\rho_c}, \quad p_1 = \frac{p}{p_c}, \quad B_1 = \frac{B}{B_c}, \quad \dots \quad (1.26)$$

Then, as it is easy to check, the system (I) transforms to the form

$$\begin{aligned} \frac{1}{\rho_1 x^2} \frac{d}{dx} \left[ \frac{x^2 dp_1}{\rho_1 dx} \right] &= -1, \\ \frac{1}{\rho_1 x^2} \frac{d}{dx} \left[ \frac{x^2 dB_1}{\kappa_1 \rho_1 dx} \right] &= -\lambda \varepsilon_1, \end{aligned} \quad (\text{Ia})$$

where

$$\lambda = \frac{\varepsilon_c \kappa_c}{4\pi G c \gamma_c}, \quad \gamma_c = \frac{B_c}{p_c}. \quad (1.27)$$

Numerical values of all functions in the system (Ia) are between 0 and 1. Then the conditions at in the centre of a star ( $x = 0$ ) take the form

$$p_1 = 1, \quad \frac{dp_1}{dx} = 0, \quad B_1 = 1, \quad \frac{dB_1}{dx} = 0. \quad (1.28)$$

In the surface of a star ( $x = x_0$ ), instead of (1.23), we can use the simple conditions

$$B_1 = 0, \quad p_1 = 0. \quad (1.29)$$

Here we can write the main system of the equations in terms of the new variables (Ia), taking convection into account. Because of (1.22), we obtain

$$\begin{aligned} \frac{1}{\rho_1 x^2} \frac{d}{dx} \left[ \frac{x^2 dp_1}{\rho_1 dx} \right] &= -1, \\ \frac{1}{\rho_1 x^2} \frac{d}{dx} \left[ \frac{x^2 dB_1}{\kappa_1 \rho_1 dx} \right] - \frac{\kappa_c \rho_c}{c \gamma_c} \frac{1}{\rho_1 x^2} \left[ x^2 Au \frac{dp_1}{dx} \right] &= -\lambda \varepsilon_1. \end{aligned} \quad (\text{II})$$

For an ideal gas, equation (1.21) leads to a very simple formula for  $u$

$$u = 1 - \frac{\Gamma}{4(\Gamma - 1)} \frac{p_1 dB_1}{B_1 dp_1}. \quad (1.30)$$

Owing to (1.5) and (1.6) it follows at last that the main system of the equations, taking the radiant pressure into account in the absence of convection, takes the form

$$\begin{aligned} \frac{1}{\rho_1 x^2} \frac{d}{dx} \left[ \frac{x^2 d(p_1 + \gamma_c B_1)}{\rho_1 dx} \right] &= -1, \\ \frac{1}{\rho_1 x^2} \frac{d}{dx} \left[ \frac{x^2 dB_1}{\kappa_1 \rho_1 dx} \right] &= -\lambda \varepsilon_1. \end{aligned} \quad (\text{III})$$

## Chapter 2

### Analysis of the Main Equations and the Relation "Mass-Luminosity"

#### 2.1 Observed characteristics of stars

Astronomical observations give the following quantities characterizing star: radius  $R$ , mass  $M$ , and luminosity  $L$  (the total energy radiated by a star per second). We are going to consider correlations between the quantities and parameters of the main system of the star equilibrium equations. As a result, the main system of the equations considered under any phase state of stellar matter includes only two parameters characterizing matter and radiation inside a star:  $B_c$  and  $p_c$ .

Because of formula (1.25), we obtain

$$R = \frac{1}{\rho_c} \sqrt{\frac{p_c}{4\pi G}} x_0, \quad (2.1)$$

where  $x_0$  is the value of  $x$  at the surface of a star, where  $p_1 = B_1 = 0$ . With this formula, and introducing a state equation of matter, we can easily obtain the correlation  $R = f(B_c, p_c)$ . It should be noted that in the general case the value of  $x_0$  in formula (2.1) is dependent on  $B_c$  and  $p_c$ . At the same time, because the equation system consists of functions variable between 0 and 1, the value of  $x_0$  should be of the same order (i. e. close to 1). Therefore the first multiplier in (2.1) plays the main rôle.

Because of

$$M = 4\pi \int_0^R \rho r^2 dr ,$$

we have

$$M = \frac{p_c^{3/2}}{G^{3/2} \sqrt{4\pi} \rho_c^2} M_{x_0} , \quad (2.2)$$

where

$$M_{x_0} = \int_0^{x_0} \rho_1 x^2 dx .$$

At last, the total luminosity of star is

$$L = 4\pi \int_0^R \varepsilon \rho r^2 dr ,$$

and we obtain

$$\frac{L}{M} = \varepsilon_c \frac{L_{x_0}}{M_{x_0}} , \quad L_{x_0} = \int_0^{x_0} \varepsilon_c \rho_1 x^2 dx . \quad (2.3)$$

Values of the quantities  $M_{x_0}$  and  $L_{x_0}$  should change a little under changes of  $p_c$  and  $B_c$ , remaining close to 1. If  $x_0$ ,  $M_{x_0}$ , and  $L_{x_0}$  are the same for numerous stars, such stars are homological, so the stars actually have the *same structure*.

As it is easy to see, the average density  $\bar{\rho}$  of star is connected to  $\rho_c$  by the formula

$$\bar{\rho} = \rho_c \frac{3M_{x_0}}{x_0^3} . \quad (2.4)$$

We find a formula for the total potential energy  $\Omega$  of star thus

$$\Omega = -G \int_0^R \frac{M_r}{r} dM_r .$$

Multiplying the term under the integral by  $R$ , and dividing by  $M^2$ , we obtain

$$\Omega = -\frac{GM^2}{R} \Omega_{x_0} \quad (2.5)$$

and also

$$\Omega_{x_0} = \frac{x_0}{M_{x_0}^2} \int_0^{x_0} x \rho_1 M_x dx .$$

Under low radiant pressure, taking the equation of mechanical equilibrium into account, the system (I) gives

$$\int_0^{x_0} x \rho_1 M_x dx = - \int_0^{x_0} x^3 dp_1 = 3 \int_0^{x_0} x^2 p_1 dx , \quad (2.5a)$$

from which we obtain

$$\Omega_{x_0} = \frac{3x_0 \int_0^{x_0} p_1 x^2 dx}{\left[ \int_0^{x_0} \rho_1 x^2 dx \right]^2} . \quad (2.6)$$

Because all the functions included in the main system of equations can be expressed through  $B_1$  and  $p_1$ , we can find the functions from the system of the differential equations with respect to two parameters  $B_c$  and  $p_c$ . Boundary conditions (1.28) are enough to find the solutions at the centre of a star. Hence, boundary conditions at the surface of a star (1.29) are true under only some relations between  $B_c$  and  $p_c$ . Therefore all quantities characterizing a star are functions of only one of two parameters, for instance  $B_c$ :  $R = f_1(B_c)$ ,  $M = f_2(B_c)$ ,  $L = f_3(B_c)$ . This circumstance, with the same chemical composition of stars, gives the relations: (1) ‘‘mass-luminosity’’  $L = \varphi_1(M)$  and (2) the Russell-Hertzsprung diagram  $L = \varphi_2(R)$ .

From the above we see that the equilibrium of stars has this necessary consequence: correlations between  $M$ ,  $L$ , and  $R$ . Thus the correlations discovered by observational astrophysics can be predicted by the theory of the inner constitution of stars.

## 2.2 Stars of polytropic structure

Solutions to the main system of the equations give functions  $p_1(x)$  and  $B_1(x)$ . Hence, solving the system we can as well obtain  $B_1(p_1)$ . If we set up a phase state, we can as well obtain the function  $p_1(\rho_1)$ .

Let us assume  $p_1(\rho_1)$  as  $p_1(\rho_1^\Gamma)$ , where  $\Gamma$  is a constant. Such a structure for a star is known as *polytropic*. Having stars of polytropic structure, we can easily find all the functions of  $x$ . Therefore, in order to obtain a representation of the solutions in the first instance, we are going to consider stars of polytropic structure. Emden’s pioneering research on the internal constitution of stars was done in this way.

The aforementioned polytropic correlation can be used instead of the heat equilibrium equation, so only the first equation remains in the system. We introduce a new variable  $T_1$  which, in an ideal gas, equals the reduced temperature

$$\frac{p_1}{\rho_1} = \rho_1^{\Gamma-1} = T_1 , \quad (2.7)$$

or, in another form,

$$\rho_1 = T_1^n , \quad n = \frac{1}{\Gamma-1} , \quad p_1 = T_1^{n+1} , \quad (2.7a)$$

so that we obtain

$$dp_1 = (n+1) T_1^n dT_1 .$$

Substituting the formulae into the first equation of the main system (I), we obtain

$$E [ T_1' ] = \frac{1}{x_1^2} \frac{1}{dx_1} \left[ x_1^2 \frac{dT_1}{dx_1} \right] = -T_1^n , \quad (2.8)$$

where a new variable  $x_1$  is introduced instead of  $x$

$$x = \sqrt{n+1} x_1 . \quad (2.9)$$

Emden's equation (2.8) can be integrated very easily if  $n=0$  or  $n=1$ . Naturally, under  $n=0$  (a star of constant density) we obtain

$$p_1 = T_1 = 1 - \frac{x_1^2}{6}, \quad (2.10)$$

so the remaining characteristics can be calculated just as easily. Under  $n=1$  the substitution  $n=T_1 x_1$  reduces the differential equation (2.8) to the simple form  $n''=-n$ . Hence, under  $n=1$ , we have

$$T_1 = \frac{\sin x_1}{x_1}, \quad p_1 = \frac{\sin^2 x_1}{x_1^2}. \quad (2.11)$$

With other polytropic indices  $n$ , we obtain solutions which are in series. All odd derivatives of the operator  $E$  should become zero under  $x_1=0$ . For even derivatives, we have

$$E_0^{(2i)} [T_1'] = \frac{2i+3}{2i+1} T_1^{(2i+2)}(0). \quad (2.12)$$

Now, differentiating equation (2.8), we obtain derivatives in different orders of the function  $T_1$  under  $x_1=0$ , so we obtain the coefficients of the series expansion. As a result we obtain the series

$$T_1 = 1 - \frac{x_1^2}{3!} + \frac{n}{5!} x_1^4 - \frac{n(8n-5)}{3 \times 7!} x_1^6 + \frac{n(122n^2 - 183n + 70)}{9 \times 9!} x_1^8 + \dots \quad (2.13)$$

Using (2.13), we move far away from the special point  $x_1=0$ . Subsequent solutions can be obtained by numerical integration. As a result we construct a table containing characteristics of stellar structures under different  $n$  (see Table 1).

The case of  $n=3/2$  corresponds to an adiabatic change of the state of monatomic ideal gas ( $\Gamma=5/3$ ) and also a regular Fermi gas (1.9). If  $n=3$ , we get a relativistic Fermi gas or an ideal gas under  $B_1=p_1$  (the latter is known as Eddington's solution).

In polytropic structures we can calculate exact values of  $\Omega_{x_0}$ . Naturally, the integral of the numerator of (2.6) can be transformed to

$$\int_0^{x_0} p_1 x^2 dx = \int_0^{x_0} T_1 dM_x = - \int_0^{x_0} M_x \frac{dT_1}{dx} dx.$$

Emden's equation leads to

$$M_x = -(n+1) x^2 \frac{dT_1}{dx}, \quad (2.14)$$

so we obtain

$$\begin{aligned} \int_0^{x_0} p_1 x^2 dx &= \frac{1}{n+1} \int_0^{x_0} \frac{M_x^2}{x^2} dx = \\ &= -\frac{M_{x_0}^2}{x_0(n+1)} + \frac{2}{n+1} \int_0^{M_{x_0}} \frac{M_x}{x} dM_x. \end{aligned}$$

Table 1

$n$	$x_0$	$M_{x_0}$	$\frac{x_0^2}{3M_{x_0}}$	$\Omega_{x_0}$
0	2.45	4.90	1.0	$3/5$
1	4.52	9.04	3.4	$3/4$
$3/2$	5.81	11.1	5.9	$6/7$
2	7.65	12.7	11.4	1
2.5	10.2	14.4	24.1	$6/5$
3	13.8	16.1	54.4	$3/2$
3.25	17.0	17.5	88.2	$12/7$

Formula (2.5a) leads to another relation between the integrals. As a result we obtain

$$\left[ 1 - \frac{6}{n+1} \right] \int_0^{x_0} p_1 x^2 dx = -\frac{M_{x_0}^2}{x_0(n+1)},$$

and, substituting this into (2.6), we obtain Ritter's formula

$$\Omega_{x_0} = \frac{3}{5-n}. \quad (2.15)$$

This formula, in addition to other conclusions, leads to the fact that a star can have a finite radius only if  $n < 5$ .

### 2.3 Solution to the simplest system of the equations

To begin, we consider the system (Ia), which is true in the absence of convection and if the radiant pressure is low. The absorption coefficient  $\kappa$ , the quantity of produced energy  $\varepsilon$ , and the phase state equation of matter, can be represented as products of different power functions  $p, B, \rho$ . Then the functions  $\kappa_1 = \kappa/\kappa_c, \varepsilon_1 = \varepsilon/\varepsilon_c$ , and the phase state equation, are dependent only on  $p_1, B_1, \rho_1$ ; they have no parameters  $p_c, B_c, \rho_c$ . In this case the coefficient  $\lambda$  remains the sole parameter of the system. In this simplest case we study the system (Ia) under further limitations: we assume an ideal gas and  $\kappa$  independent of physical conditions. Thus, we have the correlations

$$\kappa = \text{const: } \kappa_1 = 1, \quad p_1 = B_1^{1/4} \rho_1, \quad \varepsilon_1 = f(p_1, B_1), \quad (2.16)$$

$$\frac{1}{\rho_1 x^2} \frac{d}{dx} \left[ \frac{x^2 dp_1}{\rho_1 dx} \right] = -1, \quad (2.17)$$

$$\frac{1}{\rho_1 x^2} \frac{d}{dx} \left[ \frac{x^2 dB_1}{\rho_1 dx} \right] = -\lambda \varepsilon_1,$$

where

$$\lambda = \frac{\varepsilon_c \kappa_c}{4\pi G c \gamma_c} \quad \gamma_c = \frac{B_c}{p_c}. \quad (2.18)$$

Taking integrals on the both parts of (2.17), we obtain

$$\frac{x^2 dB_1}{\rho_1 dx} = -\lambda L_x, \quad \frac{x dp_1}{\rho_1 dx} = -M_x, \quad (2.19)$$

where we have introduced the notation

$$L_x = \int_0^x \varepsilon_1 \rho_1 x^2 dx, \quad M_x = \int_0^x \rho_1 x^2 dx. \quad (2.20)$$

Integrating (2.19) using boundary conditions, we obtain

$$\lambda = \frac{l}{\int_0^{x_0} L_x \frac{\rho_1}{x^2} dx}, \quad l = \int_0^{x_0} M_x \frac{\rho_1}{x^2} dx,$$

hence

$$\lambda = \frac{\int_0^{x_0} M_x \frac{\rho_1}{x^2} dx}{\int_0^{x_0} L_x \frac{\rho_1}{x^2} dx}. \quad (2.21)$$

From formulae (2.21) and (2.20) we conclude that the more concentrated are the sources of stellar energy, the greater is  $\lambda$ . If the source's productivity  $\varepsilon$  increases towards the centre of a star,  $\lambda > 1$ . If  $\varepsilon = \text{const}$  along the radius,  $\varepsilon_1 = 1$  and hence  $\lambda = 1$ . If stellar energy is generated mostly in the surface layers of a star,  $\lambda < 1$ . Equations (2.19) lead to

$$\frac{dB_1}{dp_1} = \frac{\lambda L_x}{M_x}. \quad (2.22)$$

Because of the boundary conditions  $p_1 = 0, B_1 = 0$  and  $p_1 = 1, B_1 = 1$ , the derivative  $dB_1/dp_1$  always takes the average value 1. Owing to

$$\left(\frac{dB_1}{dp_1}\right)_{x=0} = \lambda, \quad \left(\frac{dB_1}{dp_1}\right)_{x=x_0} = \frac{\lambda L_{x_0}}{M_{x_0}},$$

we come to the following conclusions: if energy sources are located at the centre of a star,  $\lambda L_{x_0}/M_{x_0} < 1$ ; if energy sources are located on the surface,  $\lambda L_{x_0}/M_{x_0} > 1$ . If energy sources are homogeneously distributed inside a star,  $\lambda L_{x_0}/M_{x_0} = 1$  and  $B_1 = p_1$ , so we have polytropic class 3, considered in the previous paragraph. This particular solution is the basis of Eddington's theory of the internal constitution of stars. If  $n > 3$ ,  $(dB_1/dp_1)_{x_0} \rightarrow \infty$  so we have  $L_{x_0} \rightarrow \infty$ . Therefore we conclude that polytropic classes  $n > 3$  characterize stars where energy sources concentrate near the surface. Polytropic classes  $n < 3$  correspond to stars where energy sources concentrate at the centre. Therefore the data of Table 1 characterize the most probable structures of stars. It should be noted that if  $n < 3$ , formulae (2.7) and (2.7a) lead to  $(dB_1/dp_1)_{x_0} = 0$ , and hence  $L_{x_0} = 0$ . So polytropic structures of stars where energy sources concentrate at the centre can exist only if there is an energy drainage in the upper layer of a star.

Differentiating formula (2.22) step-by-step and using the system (2.17) gives derivatives of  $B_1(p_1)$  under  $p_1 = 1$  and, hence, expansion of  $B_1(p_1)$  into a Taylor series. The first terms of the expansion take the form

$$B_1 = 1 + \lambda(p_1 - 1) + \frac{3}{10} \lambda \left[ \frac{\partial \varepsilon_1}{\partial p_1} + \lambda \frac{\partial \varepsilon_1}{\partial B_1} \right]_1 (p_1 - 1)^2 + \dots$$

The surface condition  $B_1 = 0$ , being applied to this formula under  $p_1 = 0$ , gives an equation determining  $\lambda$ . This method gives a numerical value of  $\lambda$  which can be refined by numerical integration of the system (2.17). This integration can be done step-by-step.

The centre of a star, i.e. the point where  $x = 0$ , is the singular point of the differential equations (2.17). We can move far away from the singular point using series and then (as soon as their convergence becomes poor) we apply numerical integration. We re-write the system (2.7) as follows

$$\begin{aligned} E \left[ \frac{B_1^{1/4} dp_1}{p_1 dx} \right] &= -p_1 B_1^{-1/4}, \\ E \left[ \frac{B_1^{1/4} dB_1}{p_1 dx} \right] &= -\lambda \varepsilon_1 p_1 B_1^{-1/4}. \end{aligned} \quad (2.23)$$

Formula (2.12) gives

$$E_0^{(2i)}[u] = \frac{2i + 3}{2i + 1} [u]_0^{(2i+1)}. \quad (2.24)$$

Then, differentiating formula (2.23) step-by-step using (2.24), we obtain different order derivatives of the functions  $p_1(x)$  and  $B_1(x)$  under  $x = 0$  that yields the possibility of expanding the functions into Laurent series. Here are the first few terms of the expansions

$$\begin{aligned} p_1 &= 1 - \frac{1}{3} \frac{x^2}{2!} + \frac{2}{15} [4 - \lambda] \frac{x^4}{4!} - \dots \\ B_1 &= 1 - \frac{\lambda}{3} \frac{x^2}{2!} + \\ &+ \frac{2\lambda}{15} \left[ (4 - \lambda) + \frac{3}{2} \left( \frac{\partial \varepsilon_1}{\partial p_1} + \lambda \frac{\partial \varepsilon_1}{\partial B_1} \right)_0 \right] \frac{x^4}{4!} - \dots \end{aligned} \quad (2.25)$$

In order to carry out numerical integration we use formulae which can be easily obtained from the system (2.23), namely

$$\begin{aligned} p_1'' &= -p_1^2 B_1^{-1/2} + p_1' \left[ \frac{p_1'}{p_1} - \frac{B_1'}{4B_1} - \frac{2}{x} \right], \\ B_1'' &= -\lambda \varepsilon_1 p_1^2 B_1^{-1/2} + B_1' \left[ \frac{p_1'}{p_1} - \frac{B_1'}{4B_1} - \frac{2}{x} \right]. \end{aligned} \quad (2.23a)$$

In this system, we introduce the reduced temperature  $T_1$  instead of  $B_1$ , and a new variable  $u_1 = p_1^{1/4}$  instead of  $p_1$

$$\begin{aligned} u_1'' &= -\frac{u_1^5}{4T_1^2} + u_1' \left[ \left( \frac{u_1'}{u_1} - \frac{T_1'}{T_1} \right) - \frac{2}{x} \right], \\ T_1'' &= -\frac{\lambda \varepsilon_1 u_1^8}{4T_1^5} + T_1' \left[ 4 \left( \frac{u_1'}{u_1} - \frac{T_1'}{T_1} \right) - \frac{2}{x} \right]. \end{aligned} \quad (2.23b)$$

This substitution gives a great advantage, because of small slow changes of the functions  $T_1$  and  $u_1$ .

A numerical solution can be obtained close to the surface layer, but not in the surface itself, because the equations (2.23) can be integrated in the upper layers without problems. Naturally, assuming  $M_x = M_{x_0} = \text{const}$  and  $L_x = L_{x_0} = \text{const}$  in formula (2.19), we obtain

$$\frac{dp_1}{\rho_1} = -\frac{M_{x_0}}{x^2} dx, \quad \frac{dB_1}{\rho_1} = -\frac{\lambda L_{x_0}}{x^2} dx, \quad (2.26)$$

$$B_1 = \frac{\lambda L_{x_0}}{M_{x_0}} p_1.$$

The ideal gas equation and the last relation of (2.26) permit us to write down

$$\frac{dp_1}{\rho_1} = B_1^{1/4} \frac{dp_1}{p_1} = B_1^{-3/4} dB_1.$$

Integrating the first equation of (2.26), we obtain

$$4T_1 = M_{x_0} \frac{x_0 - x}{x_0 x}, \quad (2.27)$$

which gives a linear law for the temperature increase within the uppermost layers of a star.

To obtain  $\lambda$  by step-by-step integration, we need to have a criterion by which the resulting value is true. It is easy to see from (2.26) that such a criterion can be a constant value for the quotient  $B_1/p_1$  starting from  $x$  located far away from the centre of a star. Solutions are dependent on changes of  $\lambda$ , therefore an exact numerical value of this parameter should be found. Performing the numerical integration, values of the functions near the surface of a star are not well determined. Therefore, in order to calculate  $L_{x_0}$  and  $M_{x_0}$  in would be better to use their integral formulae (2.20). If energy sources increase their productivity towards the centre of a star, we obtain an exact value for  $L_{x_0}$  even in a very rough solution for the system. The calculation of  $x_0$  is not as good, but it can be obtained for fixed  $M_{x_0}$  and  $x$  far away from the centre through formula (2.27)

$$x_0 = \frac{x}{1 - \frac{4T_1}{M_{x_0}} x}. \quad (2.27a)$$

Using the above method, exact solutions to the system are obtained. Table 2 contains the characteristics of the solutions in comparison to the characteristics of Eddington's model\*.

The last column contains a characteristic that is very important for the "mass-luminosity" relation (as we will see later).

Let us determine what changes are expected in the characteristics of the internal constitution of stars if the absorption coefficient  $\kappa$  is variable. If  $\kappa$  is dependent on the physical conditions, equation (2.22) takes the form

$$\frac{dB_1}{dp_1} = \frac{\kappa_1 \lambda L_x}{M_x}. \quad (2.22a)$$

\*In his model  $\varepsilon_1 = 1$ , so the energy sources productivity is  $\varepsilon = \text{const}$  along the radius (see the first row in the table). — Editor's remark.

Table 2

$\varepsilon_1$	$\lambda$	$x_0$	$M_{x_0}$	$L_{x_0}$	$\frac{\lambda L_{x_0}}{M_{x_0}^3}$
1	1	13.8	16.1	16.1	$3.8 \times 10^{-3}$
$B_1$	1.76	10	12.4	2.01	$1.8 \times 10^{-3}$
$B_1 p_1$	2.32	9	11.5	1.57	$2.2 \times 10^{-3}$

The variability of  $\kappa$  can be determined by a function of the general form

$$\kappa_1 = \frac{p_1^\alpha}{B_1^\beta}.$$

At first we consider the simplest case where energy sources are homogeneously distributed inside a star. In this case  $\varepsilon_1 = 1$ ,  $L_x = M_x$ , and equation (2.22a) can be integrated

$$B_1^{1+\beta} = \lambda \frac{1+\beta}{1+\alpha} p_1^{1+\alpha}.$$

Proceeding from the conditions at the centre of any star ( $B_1 = p_1 = 1$ ), we obtain

$$\lambda = \frac{1+\alpha}{1+\beta}, \quad B_1 = p_1^\lambda.$$

Hence the star has polytropic structure of class

$$n = \frac{4}{\lambda} - 1.$$

Looking from the physical viewpoint, the most probable effects are: decrease in the absorption coefficient of a star with depth, and also  $\alpha \geq -1$ . Because

$$\kappa_1 = p_1^{\frac{\alpha-\beta}{1+\beta}} = B_1^{\frac{\alpha-\beta}{1+\alpha}},$$

$\kappa_1$  decreases with increase of  $p_1$  and  $B_1$  only if  $\alpha < \beta$ . Then it is evident that  $\lambda < 1$  and  $n > 3$ . Hence, variability of  $\kappa$  results in an increase of polytropic class. According to the theory of photoelectric absorption,

$$\kappa_1 = \frac{\rho_1}{T_1^{3.5}}.$$

In this case  $\alpha = 1$ ,  $\beta = 1.125$  and hence  $n = 3.25$ . Table 1 gives respective numerical values of the characteristics  $x_0$  and  $M_{x_0}$ . Other calculated characteristics are  $\lambda = 0.94$  and  $\lambda L_{x_0}/M_{x_0}^3 = \lambda/M_{x_0}^2 = 3.06 \times 10^{-3}$ . All the numerical values are close to those calculated in Table 2. This is expected, if variability of  $\kappa$  leads to the same order effect for the other classes of energy source distribution inside stars.

Looking at Table 1 and Table 2 we see that the characteristics  $x_0 \simeq M_{x_0} \simeq 10$  and  $\lambda L_{x_0}/M_{x_0}^3 \simeq 2 \times 10^{-3}$  have tiny

changes under different suppositions about the internal constitution of stars (the internal distribution of energy sources)\*. There are three main cases: (1) sources of stellar energy, homogeneously distributed inside a star, (2) energy sources are so strongly concentrated at the centre of star that their productivity is proportional to the 8th order of the temperature, (3) polytropic structures where energy sources are concentrated at the surface — there is a drainage in the surface layer of a star. It should be noted that we did not consider other possible cases of distributed energy sources in a star, such as production of energy in only an “energetically active” layer at a middle distance from the centre. In such distributed energy sources, as it is easy to see from the second equation of the main system, there should be an isothermal core inside a star, and such a star is close to polytropic structures higher than class 3. In this case, instead of the former  $\varepsilon_1$ , we can build  $\varepsilon/\varepsilon_{\max} = \varepsilon_1$ ,  $0 \leq \varepsilon_1 \leq 1$ , which will be subsumed into  $\lambda$ . However in such a case  $\varepsilon_1$ , and hence all characteristics obtained as solutions to the system, is dependent on  $p_c$  and  $B_c$ , and the possibility to solve the system everywhere inside a star sets up as well correlations between the parameters. At last we reach the very natural conclusion that energy is generated inside a star only under specific relations between  $B$  and  $p$  in that quantity which is required by the compatibility of the equilibrium equations. In order to continue this research and draw conclusions, it is very important to note the fact that the characteristic  $\lambda L_{x_0}/M_{x_0}^3$  is actually the same for any stellar structure (see the last column in Table 2). This characteristic remains almost constant under even exotic distributions of energy sources in stars (exotic sources of stellar energy), because of a parallel increase/decrease of its numerator and denominator. Following a line of successive approximations, we have a right to accept the tables as the first order approximation which can be compared to observational data. All the above conclusions show that it is not necessary to solve the main system of the equilibrium equations (2.17) for more detailed cases of the aforementioned structures of stars. Therefore we did not prove the uniqueness of the parameter  $\lambda$ .

#### 2.4 Physical conditions at the centre of stars

The average density of the Sun is  $\bar{\rho}_\odot = 1.411$ . Using this numerical value in (2.4), we obtain a formula determining the central density of stars

$$\rho_c = 0.470 \frac{x_0^3}{M_{x_0}} \frac{\frac{M}{M_\odot}}{\left(\frac{R}{R_\odot}\right)^3}. \quad (2.28)$$

Taking this into account, formula (2.1) permits calculat-

\*It should be noted that the tables characterize the structure of stars only if the radiant pressure is low. In the opposite case all the characteristics  $x_0$ ,  $M_{x_0}$ , and others are dependent on  $\gamma_c$ .

ion of the gaseous pressure at the centre of a star

$$p_c = \frac{G}{4\pi} \left(\frac{M_\odot}{R_\odot}\right)^2 \frac{x_0^4}{M_{x_0}^2} \frac{\left(\frac{M}{M_\odot}\right)^2}{\left(\frac{R}{R_\odot}\right)^4}. \quad (2.29)$$

Because  $M_\odot = 1.985 \times 10^{33}$  and  $R_\odot = 6.95 \times 10^{10}$ , we obtain

$$p_c = 8.9 \times 10^{14} \frac{x_0^4}{M_{x_0}^2} \frac{\left(\frac{M}{M_\odot}\right)^2}{\left(\frac{R}{R_\odot}\right)^4}. \quad (2.30)$$

Thus the pressure at the centre of the Sun should be about  $10^{16}$  dynes/cm<sup>2</sup> (ten billion atmospheres). It should be noted, as we see from the deductive method, the formulae for  $\rho_c$  and  $p_c$  are applicable to any phase state of matter.

Let us assume stars consisting of an ideal gas. Then taking the ratio of (2.30) to (2.28) and using the ideal gas equation (1.8), we obtain the temperature at the centre of a star

$$T_c = 2.29 \times 10^7 \mu \frac{x_0}{M_{x_0}} \frac{\frac{M}{M_\odot}}{\frac{R}{R_\odot}}. \quad (2.31)$$

Hence, the temperature at the centre of the Sun should be about 10 million degrees. As another example, consider the infrared satellite of  $\varepsilon$  Aurigae. For this star we have  $M = 24.6 M_\odot$ ,  $\log(L/L_\odot) = 4.46$ ,  $R = 2,140 R_\odot$  [5]. Calculating the central density and temperature by formulae (2.30) and (2.31), we obtain  $T_c \simeq 2 \times 10^5$  and  $p_c \simeq 2 \times 10^5$ : thus the temperature is about two hundred thousand degrees and the pressure about one atmosphere. Because the star is finely located in the “mass-luminosity” diagram (Fig. 1) and the Russell-Hertzsprung diagram, we have reason to conclude: *the star has the internal constitution regular for all stars*. This conclusion can be the leading arrow pointing to the supposition that heat energy is generated in stars under physical conditions close to those which can be produced in an Earthly laboratory.

Let us prove that only inside white dwarfs (the stars of the very small radii — about one hundredth of  $R_\odot$ ), the degenerate Fermi gas equation (1.9) can be valid. Naturally, if gas at the centre of a star satisfies the Fermi equation, we obtain  $p_c = 1 \times 10^{13} \rho_c^{5/3} \mu_e^{-5/3}$ . Formulae (2.28) and (2.30) show that this condition is true only if

$$\frac{R}{R_\odot} = 3.16 \times 10^{-3} \frac{x_0 M_{x_0}^{1/3}}{\left(\frac{M}{M_\odot}\right)^{1/3}} \mu_e^{-5/3}. \quad (2.32)$$

This formula remains true independently of the state of matter in other parts of the star. The last circumstance can affect only the numerical value of the factor  $x_0 M_{x_0}^{1/3}$ . At the same time, table 1 shows that we can assume the numerical value approximately equal to 10.† Formula (2.32) shows that

†For stars of absolutely different structure, including such boundary instances as the naturally impossible case of equally dense stars, and the cases where energy sources are located at the surface. — Editor’s remark.



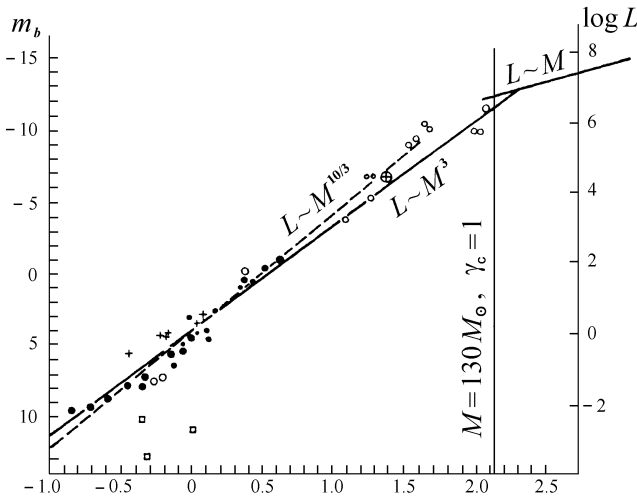


Fig. 1: The “mass-luminosity” relation. Here points are visual binaries, circles are spectral-binaries and eclipse variable stars, crosses are stars in Giades, squares are white dwarfs, the crossed circle is the satellite of  $\epsilon$  Aurigae.

for regular degeneration of gas, stars (under  $M = M_\odot$ ) should have approximately the same radius  $R \simeq 2 \times 10^9$ , i. e. about 20,000 km ( $R = 0.03 R_\odot$ ). Such dimensions are attributed to white dwarfs. For example, the satellite of Sirius has  $M = 0.94 M_\odot$  and  $R = 0.035 R_\odot$  [6]. If the density is more than the above mentioned (if the radius is less than  $R = 0.03 R_\odot$ ) and the mass of the star increases, formula (2.32) shows that regular degeneration can become relativistic degeneration

$$p = K \rho^{4/3}, \quad K = K_H \mu_e^{-4/3}, \quad K_H = 1.23 \times 10^{15}.$$

We apply these formulae to the centre of a star, and take equations (2.28) and (2.30) into account. As a result we see that the radius drops out of the formulae, so relativistic degeneration can be realized in a star solely in terms of the mass

$$\frac{M}{M_\odot} = 0.356 M_{x_0}, \quad (\mu_e = 1). \quad (2.32a)$$

Because of Table 1, we see:  $n = 0$  only if  $M_{x_0} = 16.1$ . Hence, the lower boundary of the mass of a non-degenerated gaseous star is  $5.7 M_\odot$ . In order to study degenerated gaseous stars in detail, we should use the phase state equation that includes the regular state, the boundary state between the regular and degenerated states, and the degenerated state. Applying formulae (2.28) and (2.30) to the above ratio, we obtain a correlation between the radius and the mass of a star, which is unbounded for small radii. It should be noted that introduction of a mass-radius correlation is the essence of Chandrasekhar’s theory of white dwarfs [7]. On the other hand, having observable sizes of white dwarfs, equation (2.32) taken under  $x_0 M_{x_0}^{1/3} = 10$  gives the same

numerical values for radii as Chandrasekhar’s table (his well-known relation between the radius and mass of star). The exact numerical value of the ultimate mass calculated by him coincides with our  $5.7 M_\odot$ . In Chandrasekhar’s formula, as well as in our formula (2.32), radius is correlated opposite to mass. Today we surely know masses and radii of only three white dwarfs: the white dwarfs do not confirm the opposite correlation mass-radius. So, save for the radius of Sirius’ satellite coinciding with our formula (2.32), we have no direct astrophysical confirmation about degeneration of gas inside white dwarfs.

Considering stars built on an ideal gas, we deduce a formula determining the mass of a star dependent on internal physical conditions. We can use formulae (2.30) and (2.31) or formula (2.2) directly. Applying the Boyle-Mariotte equation (1.8) to formula (2.2), and taking the Stephan-Boltzmann law (1.7) into account, we obtain

$$M = C \frac{\gamma_c^{1/2}}{\mu^2} M_{x_0}, \quad C = \frac{\mathfrak{R}^2}{G^{3/2} \sqrt{\frac{4}{3} \pi \alpha}} = 2.251 \times 10^{33}. \quad (2.33)$$

Introducing the mass of the Sun  $M_\odot = 1.985 \times 10^{33}$  into the equation, we obtain

$$M = 1.134 M_\odot \frac{\gamma_c^{1/2}}{\mu^2} M_{x_0}. \quad (2.34)$$

As we will see below, the “mass-luminosity” correlation shows  $\gamma_c$  is close to 1 for blue super-giants. Hence formula (2.34) gives the observed numerical values for masses of stars. The fact that we obtain true orders for numerical values of the masses of stars, proceeding only from numerical values of the fundamental constants  $G, \mathfrak{R}, \alpha$ , is excellent confirmation of the theory.

### 2.5 The “mass-luminosity” relation

In deducing the “mass-luminosity” correlation, we assume: (1) the radiant pressure is negligible in comparison to the gaseous pressure everywhere inside a star; (2) stars consist of an ideal gas; (3)  $\epsilon$  and  $\kappa$  can be approximated by functions like  $p^\alpha B^\beta$ . Then the main system of the equilibrium equations takes the form

$$\begin{aligned} \frac{1}{\rho_1 x^2} \frac{d}{dx} \left[ \frac{x^2 dp_1}{\rho_1 dx} \right] &= -1, \\ \frac{1}{\rho_1 x^2} \frac{d}{dx} \left[ \frac{x^2 dB_1}{\kappa_1 \rho_1 dx} \right] &= -\lambda \epsilon_1, \end{aligned} \quad (2.35)$$

where

$$\lambda = \frac{\epsilon_c \kappa_c}{4\pi G c \gamma_c}, \quad \gamma_c = \frac{B_c}{p_c}.$$

Solving the system, as we know, is possible under a numerical value of  $\lambda$  close to 1. Hence a star can be in equilibrium only if the energy generated inside it is determined

by the formula

$$\varepsilon_c = \frac{\lambda 4\pi Gc}{\kappa_c} \gamma_c. \quad (2.36)$$

If a star produces another quantity of energy, it will contract or expand until its new shape results in production of energy exactly by formula (2.36). Because  $\gamma_c$  determines the mass of a star (2.34) and  $\varepsilon_c$  determines the luminosity of a star, the “mass-luminosity” correlation should be contained in formula (2.36). In other words, the “mass-luminosity” correlation is the condition of equilibrium of stars.

Because of (2.3),

$$\varepsilon_c = \frac{L}{M} \frac{M_{x_0}}{L_{x_0}}.$$

Substituting this equation into (2.36), we obtain

$$L = \frac{4\pi Gc}{\kappa_c} \frac{\lambda L_{x_0}}{M_{x_0}} M \gamma_c.$$

The quantity  $\gamma_c$  can be removed with the mass of a star by (2.33)

$$L = \frac{4\pi G^4 4\pi \alpha}{3\kappa_c \mathfrak{R}^4} \mu^4 \left( \frac{\lambda L_{x_0}}{M_{x_0}^3} \right) M^3. \quad (2.37)$$

The luminosity of the Sun is  $L_\odot = 3.78 \times 10^{33}$ . Proceeding from formula (2.37), we obtain

$$\frac{L}{L_\odot} = 1.04 \times 10^4 \frac{\mu^4}{\kappa_c} \left( \frac{\lambda L_{x_0}}{M_{x_0}^3} \right) \left( \frac{M}{M_\odot} \right)^3. \quad (2.38)$$

The formula (2.38) gives a very simple correlation: the luminosity of a star is proportional to the third order of its mass. In deducing this formula, we accepted that  $\varepsilon$  is determined by a function  $\varepsilon \sim p^\alpha B^\alpha$ , so  $\varepsilon_1$  depends on  $p_1$  and  $B_1$ . It is evident that rejection of this assumption cannot substantially change the obtained correlation (2.38). Naturally, under arbitrary  $\varepsilon$ , the quantity  $\varepsilon_1$  depends on  $p_c$  and  $B_c$ . Thus the multiplier  $\lambda L_{x_0}/M_{x_0}^3$  in formula (2.38) will have different numerical values for different stellar structures. At the same time Table 2 shows that this multiplier is approximately the same for absolutely different structures, including boundary structures which are exotic. Therefore the “mass-luminosity” correlation gives no information about sources of stellar energy — the correlation is imperceptible to their properties. However, other assumptions are very important. As we see from the deductive path to formula (2.33), the correlation between mass and luminosity can be deduced only if the pressure depends on temperature, so our formula (2.38) can be obtained only if the gas is ideal. It is also important to make the absorption coefficient  $\kappa$  constant for all stars. The rôle of the radiant pressure will be considered in the next paragraph.

And so forth we are going to compare formula (2.38) to observational data. Fig. 1 shows masses and luminosities of

stars, according to today’s data. The diagram has been built on masses of stars taken from Kuiper’s data base [8], and the monograph by Russell and Moore [9]. We excluded Trumpler stars [10] from the Kuiper data, because their masses were measured uncertainly. Naturally, Trumpler calculated masses of such stars, located in stellar clusters, with the supposition that the  $K$ -term (the term for radiant velocities with respect to the whole cluster) is fully explained by Einstein’s red shift. For this reason the calculated masses of Trumpler stars can be much more than their real masses. Instead of Trumpler stars, in order to fill the spaces of extremely bulky stars in the diagram, we used extremely bulky eclipse variable stars (VV Cephei, V 381 Scorpii) and data for Plascett’s spectral-variable star BD +6° 1309.

As we see in Fig. 1, our obtained correlation  $L \sim M^3$  is in good accord with the observational data in all spectra of observed masses (having a small deviation inside  $1.5m$ ). The dashed line  $L \sim M^{10/3}$  is only a little different from our line. Parenago [11], Kuiper [8], Russell [9], and others accept this  $L \sim M^{10/3}$  line as the best representation of observational data. Some researchers found the exponent of mass more than our’s. For instance, Braize [12] obtained  $L \sim M^{3.58}$ . Even if such maximal deviation from our exponential index 3 is real, the theoretical result is excellent for most stars. The coefficient of proportionality in our formula (2.38) is very susceptible to  $\mu$ . For this reason, coincidence of our theoretical correlation and observational data is evidence that the chemical composition of stars is the same on the average. The same should be said about the absorption coefficient  $\kappa$ : because physical conditions inside stars can be very different even under the same luminosity (for example, red giants and blue stars located in the main direction), it is an unavoidable conclusion that the absorption coefficient of stellar matter is independent of pressure and temperature. The conclusions justify our assumption in §1.3, when we solved the main system of equilibrium equations.

The fact that white dwarfs lie off the main sequence can be considered as a confirmation of degenerate gas inside them. Because a large increase of the absorption coefficient in white dwarfs in comparison to regular stars is not very plausible, another explanation can be given only if the structural multiplier  $\lambda L_{x_0}/M_{x_0}$  in white dwarfs is  $\sim 100$  times more than in other stars. The location of white dwarfs in the Russell-Hertzsprung diagram can give a key to this problem.

At last, proceeding from observational data, we calculate the coefficient  $\mu^4/\kappa_c$  in our theoretical formula (2.38). The line  $L \sim M^3$ , which is the best representation of observational data, lies a little above the point where the Sun is located. For this reason, under  $M = M_\odot$ , we should have  $L = 1.8L_\odot$  in our formula (2.38). According to table 2, we assume  $\lambda L_{x_0}/M_{x_0}^3 = 2 \times 10^{-3}$ . Then we obtain

$$\frac{\mu^4}{\kappa_c} = 0.08. \quad (2.39)$$

## 2.6 The radiant pressure inside stars

In the above we neglected the radiant pressure in comparison to the gaseous one in the equation of mechanical equilibrium of a star. Now we consider the main system of the equation (III), which takes the radiant pressure into account. If the absorption coefficient  $\kappa$  is constant ( $\kappa_1 = 1$ ), this system takes the form

$$\begin{aligned} \frac{1}{\rho_1 x^2} \frac{d}{dx} \left[ \frac{x^2 dp_1}{\rho_1 dx} \right] &= -(1 - \lambda \gamma_c \varepsilon_1), \\ \frac{1}{\rho_1 x^2} \frac{d}{dx} \left[ \frac{x^2 dB_1}{\rho_1 dx} \right] &= -\lambda \varepsilon_1. \end{aligned} \quad (2.40)$$

After calculations analogous to those carried out in deducing formula (2.21), we obtain

$$\lambda(1 + \gamma_c) = \frac{\int_0^{x_0} M_x \frac{\rho_1}{x^2} dx}{\int_0^{x_0} L_x \frac{\rho_1}{x^2} dx}. \quad (2.41)$$

The ratio of integrals in this formula depends on the distribution of energy sources inside a star, i. e. on the structure of a star. This ratio maintains a numerical value close to 1 under any conditions. Thus  $\lambda(1 + \gamma_c) \sim 1$ . If energy sources are distributed homogeneously throughout the volume of a star, we have  $\varepsilon_1 = 1$ ,  $L_x = M_x$  and hence the exact equality  $\lambda(1 + \gamma_c) = 1$ . If energy sources are concentrated at the centre of a star,  $\lambda(1 + \gamma_c) > 1$ . In this case, if the radiant pressure takes high values ( $\gamma_c > 1$ ), the internal constitution of a star becomes very interesting, because in this case  $\lambda \gamma_c > 1$  and the right side term in the first equation of (2.40) is positive at the centre of a star, our formula (2.41) leads to  $p_1'' > 0$ , and hence at the centre of such a star the gaseous pressure and the density have a minimum, while their maximum is located at a distance from the centre\*.

From this we conclude that extremely bulky stars having high  $\gamma_c$  can be in equilibrium only if  $\lambda(1 + \gamma_c) \sim 1$ , or, in other words, if the next condition is true

$$\varepsilon_c \sim \frac{4\pi Gc}{\kappa}. \quad (2.42)$$

Thus, starting from an extremely bulky stellar mass wherein  $\gamma_c > 1$ , the quantity of energy generated by a unit of the mass should be constant for all such extremely bulky stars. The luminosity of such stars, following formulae (2.3) and (2.2), should be directly proportional to their mass:  $L \sim M$ . This correlation is given by the straight line drawn in the upper right corner of Fig. 1. Original data due to

\*This amazing conclusion about the internal constitution of a star is true under only high values of the radiant pressure. In regular stars the radiant pressure is so low that we neglect it in comparison to the gaseous pressure (see previous paragraphs). — Editor's remark.

Eddington [13] and others showed an inclination of the "mass-luminosity" line to this direction in the region of bulky stars (the upper right corner of the diagram). But further more exact data, as it was especially shown by Russell [9] and Baize [12], do not show the inclination for even extremely bulky stars (see our Fig. 2). Therefore we can conclude that there are no internal structures of stars for  $\gamma_c > 1$ ; the ultimate case of possible masses of stars is the case where  $\gamma_c = 1$ . Having no suppositions about the origin of energy sources in stars<sup>†</sup>, it is very difficult to give an explanation of this fact proceeding from only the equilibrium of stars. The very exotic internal constitution of stars under  $\gamma_c > 1$  suggests that if such stars really exist in nature, they are very rare exceptions.

In order to ascertain what influence  $\gamma_c$  has on the structure of a star, we consider the simplest (abstract) case where energy sources are distributed homogeneously throughout a star ( $\varepsilon_1 = 1$ ). In this case, as we know,

$$\lambda = \frac{1}{1 + \gamma_c}, \quad (2.43)$$

and the system (2.40) takes the form

$$\begin{aligned} \frac{1}{\rho_1 x^2} \frac{d}{dx} \left[ \frac{x^2 dp_1}{\rho_1 dx} \right] &= -\frac{1}{1 + \gamma_c}, \\ \frac{1}{\rho_1 x^2} \frac{d}{dx} \left[ \frac{x^2 dB_1}{\rho_1 dx} \right] &= -\frac{1}{1 + \gamma_c}. \end{aligned} \quad (2.44)$$

Introducing a new variable  $x_{\gamma_c=0}$  instead of  $x$

$$x = \sqrt{1 + \gamma_c} x_{\gamma_c=0}, \quad (2.45)$$

we obtain the main system in the same form as that in the absence of the radiant pressure. So, in this case the main characteristics of the internal constitution of star are

$$\begin{aligned} x_0 &= x_{0(\gamma_c=0)} (1 + \gamma_c)^{1/2}, \\ M_{x_0} &= M_{x_0(\gamma_c=0)} (1 + \gamma_c)^{3/2}, \\ L_{x_0} &= L_{x_0(\gamma_c=0)} (1 + \gamma_c)^{3/2}, \quad \lambda = \frac{\lambda_{\gamma_c=0}}{1 + \gamma_c}. \end{aligned} \quad (2.46)$$

Characteristics indexed by  $\gamma_c = 0$  are attributed to the structures of stars where  $\gamma_c \ll 1$ ; their numerical values can be taken from our Table 2. Because Table 2 shows very small changes in  $M_{x_0}$  for very different structures of stars, formulae (2.46) should as well give an approximate picture for other structures of stars. Under high  $\gamma_c$ , the mass of a star (2.34) becomes

$$M \simeq 1.134 M_{\odot} \frac{\gamma_c^{1/2}}{\mu^2} (1 + \gamma_c)^{3/2} M_{x_0(\gamma_c=0)}. \quad (2.47)$$

<sup>†</sup>That is the corner-stone of Kozyrev's research. — Editor's remark.

Astronomical observations show that maximum masses of stars reach  $\sim 120 M_\odot$  – see Fig. 1, showing an inclination of the “mass-luminosity” correlation near  $\log(M/M_\odot) = 2$ . Assuming this mass in (2.47), and assuming  $\gamma_c = 1$  and  $M_{x_0} = 10$  for it, we obtain the average molecular weight  $\mu = 0.51$ .

Then in such stars, by formula (2.39), we obtain  $\kappa = 0.8$ . On the other hand, because the “mass-luminosity” correlation has a tendency to the line  $L \sim M$  for extremely bulky masses (see Fig. 1), we obtain the ultimate value  $\bar{\epsilon} = 5 \times 10^4$ . For homogeneously distributed energy sources, formula (2.42) leads to  $\kappa = 0.5$ . If they are concentrated at the centre,  $\epsilon_c > \bar{\epsilon} = \epsilon_c(L_{x_0}/M_{x_0})$ . Even in this case formula (2.42) leads to  $\epsilon_c > \bar{\epsilon}$ . There is some compensation, so the calculated numerical value of the absorption coefficient  $\kappa$  is true. An exact formula for  $\bar{\epsilon}$  can be easily obtained as

$$\frac{L}{M} = \bar{\epsilon} = \frac{4\pi G c}{\kappa} \frac{L_{x_0}}{M_{x_0}} \frac{\int_0^{x_0} M_x \frac{\rho_1}{x^2} dx}{\int_0^{x_0} L_x \frac{\rho_1}{x^2} dx} \frac{\gamma_c}{1 + \gamma_c}. \quad (2.48)$$

So, having considered the “mass-luminosity” correlation, we draw the following important conclusions:

1. All stars (except possibly for white dwarfs) are built on an ideal gas;
2. In their inner regions, where stellar energy is generated, all stars have the same chemical composition,  $\mu = \text{const} = 1/2$ , so they are built on a mix of protons and electrons without substantial percentage of other nuclei;
3. The absorption coefficient per unit of mass  $\kappa$  is independent of the physical conditions inside stars, it is a little less than 1.

Thomson dispersion of light in free electrons has the same properties. Naturally, the Thomson dispersion coefficient per electron is

$$\sigma_0 = \frac{8\pi}{3} \left( \frac{e^2}{m_e c^2} \right)^2 = 6.66 \times 10^{-25}, \quad (2.49)$$

where  $e$  and  $m_e$  are the charge and the mass of the electron. In the mix of protons and electrons we obtain

$$\kappa_T = \frac{\sigma_0}{m_H} = \frac{6.66 \times 10^{-25}}{1.66 \times 10^{-24}} = 0.40. \quad (2.50)$$

The fact that our calculated approximate value of  $\kappa$  is close to  $\kappa_T = 0.40$  shows that the interaction between light and matter inside stars is determined mainly by the Thomson process – acceleration of free electrons by the electric field of light waves.

Because  $\mu$  stays in the “mass-luminosity” correlation (2.38) in fourth degree, the obtained theoretical value of  $\mu$  is

quite exact with respect to the real one. If  $\kappa = \kappa_T$ , as a result of (2.39) we have  $\mu = 0.43$ . Because  $\mu$  cannot be less than  $1/2$ , the obtained ultimate value of  $\kappa = 0.8$  is twice  $\kappa_T = 0.40$ . This fact can be explained by the circumstance that, in this case of extremely bulky masses, the structural coefficient in formula (2.38) should be twice as small. It is evident that we can accept  $\mu = 1/2$  to within 0.05. If all heavy nuclei are ionized, their average molecular weight is 2. If we assume the average molecular weight in a star to be 0.55 instead of  $1/2$ , the percentage of ionized atoms of hydrogen  $\chi_H$  becomes

$$2\chi_H + \frac{1}{2}(1 - \chi_H) = \frac{1}{0.55}, \quad \chi_H \simeq 90\%.$$

Thus the maximum admissible composition of heavy nuclei inside stars, permitted by the “mass-luminosity” correlation, is only a few percent. Under  $\mu = 1/2$  the mass of a star, where  $\gamma_c = 1$ , is obtained as  $130 M_\odot$ . This value is indicated by the vertical line in Fig. 1.

At last we calculate the radiant pressure at the centre of the Sun. Formula (2.34) leads to  $\gamma_{c\odot} \simeq 10^{-3}$ . In this case the radiant pressure term in the equation of mechanical equilibrium can be neglected.

## 2.7 Comparing the obtained results to results obtained by other researchers

To deduce the “mass-luminosity” correlation by the explanation according to the regular theory of the internal constitution of stars, becomes very complicated because the theoreticians take a priori the absorption coefficient as dependent on the physical conditions. They supposed the absorption of light inside stars due to free-connected transitions of electrons (absorption outside spectral series) or transitions of electrons from one hyperbolic orbit to another in the field of positive charged nuclei. The theory of such absorption was first developed by Kramers, and subsequently by Gaunt, and especially, by Chandrasekhar [14]. According to Chandrasekhar, the absorption coefficient depends on physical conditions as

$$\kappa_{Ch} = 3.9 \times 10^{25} \frac{\rho}{T^{3.5}} (1 - \chi_H^2), \quad (2.51)$$

where  $\chi_H^2$  is the percentage of hydrogen, the numerical factor is obtained for Russell’s composition of elements. In order to clarify the possible rôle of such absorption in the “mass-luminosity” correlation, we assume (for simplicity)

$$\kappa_{Ch} = \frac{\kappa_0}{\gamma}. \quad (2.52)$$

In this case, having small  $\gamma_c$ , formulae (2.38) and (2.33) show  $L \sim M^5$ . This exponent is large, so we cannot neglect  $\gamma_c$  in comparison to 1. If  $\gamma_c$  is large, the formulae show  $L \sim M^{3/2}$ . Thus, in order to coordinate theory and observations, we are forced to consider “middle” numerical values of

$\gamma_c$  and reject the linear correlation between  $\log L$  and  $\log M$ . Formulae (2.47) and (2.48) show

$$\begin{aligned} M^2 &\sim \frac{\gamma_c (1 + \gamma_c)^2}{\mu^4}, & M^2 &\sim \frac{1 - \beta}{\mu^4 \beta^4}, \\ L &\sim M \frac{\gamma_c^2}{1 + \gamma_c}, & L &\sim M^{3/2} (1 - \beta)^{3/2} \mu. \end{aligned} \quad (2.53)$$

Here are formulae where  $\gamma_c$  has been replaced with the constant  $\beta$ , one regularly uses in the theory of the internal constitution of stars

$$\beta = \frac{p_c}{p_0} = \frac{1}{1 + \gamma_c}. \quad (2.54)$$

Thus the “mass-luminosity” correlation, described by the two formulae (2.53), becomes very complicated. The formulae are in approximate agreement with Eddington’s formulae [15] and others. The exact formula for (2.51) introduces the central temperature  $T_c$  into them. Under large  $\gamma_c$ , as we see from formulae (2.46), the formula for  $T_c$  (2.31) includes the multiplier  $\beta$

$$T_c = 2.29 \times 10^7 \mu \beta \left( \frac{x_0}{M_{x_0}} \right)_{\gamma_c=0} \frac{\frac{M}{R}}{\frac{M_\odot}{R_\odot}}. \quad (2.55)$$

Then, through  $T_c$ , the radius and the reduced temperature of a star can be introduced into the “mass-luminosity” correlation. This is the way to obtain the well-known Eddington temperature correction.

In order to coordinate the considered case of “middle”  $\gamma_c$ , we should accept  $\gamma_c = 1$  starting from masses  $M \simeq 10 M_\odot$ . So, for the Sun we obtain  $\gamma_{c\odot} = 0.08$ . As we see from formula (2.47), it is possible if  $\mu \simeq 2$ . Then formula (2.39), using the numerical value  $\lambda L_{x_0} / M_{x_0}^3 = 3.8 \times 10^{-3}$  given by Eddington’s model, gives  $\kappa_{c\odot} = 170$  and  $\kappa_0 = 14$ . The theoretical value of  $\kappa_0$  can be obtained by comparing (2.52) and (2.51); it is

$$\kappa_0 = \frac{\alpha \mu}{3 \mathfrak{R} \sqrt{T_{c\odot}}} 3.9 \times 10^{25} (1 - \chi_H^2). \quad (2.56)$$

According to (2.55) we obtain  $T_{c\odot} = 4 \times 10^7$ . Then, by (2.56), we have  $\kappa_0 = 0.4$ . So, according to Eddington’s model, the theoretically obtained value of the absorption coefficient  $\kappa_0 = 14$  is 30 times less than the  $\kappa_0 = 0.4$  required, consistent with the observational data\*. This divergence is the well-known “difficulty” associated with Eddington’s theory, already noted by Eddington himself. According to Strömgen [16], this difficulty can be removed if we accept the hypothesis that stars change their chemical composition with luminosity. Supposing the maximum hydrogen content,  $\mu$  can vary within the boundaries  $1/2 \leq \mu \leq 2$ . Then, as we

\*As it was shown in the previous paragraph, Kozyrev’s theory gives  $\kappa_0 = 0.5-0.8$  for stars having different internal constitutions, which corresponds well to observations. — Editor’s remark.

see from (2.56), the theoretical value of  $\kappa_0$  decreases slightly. On the other hand, the previous paragraph showed that the value of  $\kappa_0$ , obtained from observations, decreases much more. As a result, the theoretical and observational values of  $\kappa$  can be matched (which is in accordance with Strömgen’s conclusion). All theoretical studies by Strömgen’s followers, who argued for evolutionary changes of relative amounts of hydrogen in stars, were born from the above hypothesis. The hypothesis became very popular, because it provided an explanation of stellar energy by means of thermonuclear reactions, as suggested by Bethe.

It is evident that the above theories are very strained. On the other hand, the simplicity of our theory and the general way it was obtained are evidence of its truth. It should be noted that our two main conclusions

$$(1) \mu = 1/2, \quad \chi_H^2 = 1; \quad (2) \kappa = \kappa_T,$$

obtained independently of each other, are physically connected. Naturally, if  $\chi_H^2 = 1$ , Chandrasekhar’s formula (2.51) becomes inapplicable. Kramers absorption (free-connected transitions) becomes a few orders less; it scarcely reaches the Thomson process. At the same time, our main result is that  $\gamma_c < 1$  for all stars, and this led to all the results of our theory. Therefore this result is so important that we mean to verify it by other astrophysical data. We will do it in the next chapter, analysing the correlation “period — average density of Cepheids”. In addition, according to our theory, the central regions of stars, where stellar energy is generated, consist almost entirely of hydrogen. This conclusion, despite its seemingly paradoxical nature, must be considered as an empirically established fact. We will see further that study of the problem of the origin of stellar energy will reconcile this result with spectroscopic data about the presence of heavy elements in the surface layers of stars.

## 2.8 The rôle of convection inside stars

In §1.3 we gave the equations of equilibrium of stars (II), which take convective transfer of energy into account. Assuming the convection coefficient  $A = \text{const}$ , the second equation of the system (the heat equilibrium equation) can be written as

$$\frac{1}{\rho_1 x^2} \frac{d}{dx} \left[ \frac{x^2 dB_1}{\rho_1 dx} \right] - \frac{\kappa_c \rho_c A}{c \gamma_c} \frac{1}{\rho_1 x^2} \left[ x^2 u \frac{dp_1}{dx} \right] = -\lambda \varepsilon_1, \quad (2.57)$$

where

$$u = 1 - \frac{\Gamma}{4(\Gamma - 1)} \frac{p_1}{B_1} \frac{dB_1}{dp_1}. \quad (2.58)$$

The convection term in (2.57) plays a substantial rôle only if

$$\frac{\kappa_c \rho_c A}{c \gamma_c} > 1, \quad A > \frac{c \gamma_c}{\kappa_c \rho_c}. \quad (2.59)$$

Table 3

$\kappa$	$x_1$	$M_{x_1}$	$\lambda L_{x_0}$	$x_0$	$M_{x_0}$	$\frac{x_0^3}{3M_{x_0}}$	$\frac{\lambda L_{x_0}}{M_{x_0}^3}$
const	2.4913	3.570	3.018	8.9	11.46	20.5	$1.97 \times 10^{-3}$
$\kappa_{Ch}$	1.88	1.25	1.25	11.2	12.4	37.0	$0.65 \times 10^{-3}$

Hence the convection coefficient for the Sun should satisfy  $A_\odot > 5 \times 10^7$ . In super-giants, convection would be substantial only under  $A > 10^{16}$ . The convection coefficient  $A$ , as we see from formula (1.17), equals the product of the convective current velocity  $\bar{v}$  and the average length  $\bar{\lambda}$  travelled by the current. Thus convection can influence energy transfer inside super-giants if convection currents are about the size of the star (which seems improbable). At the same time, if a convection instability occurs in a star, the average length of travel of the current becomes the size of the whole convection zone. Then the coefficient  $A$  increases so much that it can reach values satisfying (2.59). If  $A$  is much more than the right side of (2.59), taking into account the fact that all terms of the equilibrium equation (2.57) are about 1, the term in square brackets is close to 0. Then, if  $A$  is large,

$$u = 0, \quad \text{hence} \quad B_1 = p_1^{\frac{4(\Gamma-1)}{\Gamma}}, \quad (2.60)$$

which is the equation of adiabatic changes of state. For a monatomic gas,  $\Gamma = 5/3$  ( $n = 3/2$ ) and hence

$$B_1 = p_1^{8/5}. \quad (2.61)$$

Because, according our conclusions, stars are built up almost entirely of hydrogen,  $\Gamma$  can be different from  $5/3$  in only the upper layers of stars, which is insufficient in our consideration of a star as a whole. Therefore zones of free convection can appear because of an exotic distribution of energy sources.

Free convection can also start in another case, as soon as the temperature gradient of radiant equilibrium exceeds the temperature gradient of convective equilibrium. This is Schwarzschild's condition, and it can be written as

$$\left( \frac{d \log B_1}{d \log p_1} \right)_{\text{rad}} > \left( \frac{d \log B_1}{d \log p_1} \right)_{\text{con}},$$

which, taking (2.22) and (2.61) into account, leads to

$$\frac{\lambda L_x}{M_x} > 1.6 \frac{B_1}{p_1}. \quad (2.62)$$

From this formula we see that free convection is impossible in the surface layers of stars. In central regions we obtain the next condition for free convection

$$\lambda > 1.6.$$

Table 2 shows that even when  $\varepsilon_1 = B_1$ , any star should contain a convective core. If  $\varepsilon_1$  depends only on temperature and can be approximated by function  $\varepsilon_1 = T^m$ , the calculations show that  $\lambda$  reaches its critical value of 1.6 when  $m = 3.5$ . Thus a star has a convective core if  $m > 3.5$ . The radius  $x_1$  of the convective core is determined by equality between the temperature gradients (see above). Writing (2.62) as an equality, we obtain

$$\lambda L_{x_1} = 1.6 M_{x_1} \left( \frac{B_1}{p_1} \right)_{x_1} = 1.6 M_{x_1} \rho_{x_1}. \quad (2.63)$$

It is evident that the size of the convective core increases if the energy sources become more concentrated at the centre of a star. In the case of a strong concentration, all energy sources become concentrated inside the convective core. Then inside the region of radiant equilibrium we have  $\lambda L_x = \lambda L_{x_1} = \text{const}$ . Because the border of the convective core is determined by equality of the physical characteristics' gradients in regions of radiant equilibrium and convective equilibrium, not only are  $p_1$  and  $T_1$  continuous inside such stars but so are their derivatives. Therefore such a structure for a star can be finely calculated by solving the main system of the equilibrium equations under  $\varepsilon_1 = 0$  and boundary conditions: (1) under some values of  $x = x_1$ , quantities  $p_1, B_1$  and their derivatives should have numerical values satisfying the solution to Emden's equation under  $n = 3/2$ ; (2) under some value  $x = x_0$  we should have  $p_1 = B_1 = 0$ . The four boundary conditions fully determine the solution. We can find  $x_1$  by step-by-step calculations as done in §2.3 for  $\lambda$ .

The formulated problem, known as the problem of the internal constitution of a star having a point-source of energy and low radiant pressure, was first set up by Cowling [17]. In his calculations the absorption coefficient was taken as variable according to Chandrasekhar's formula (2.51):  $\kappa = \kappa_{Ch}$ . However in §2.6 we showed that  $\kappa = \kappa_T$  inside all stars. Only in the surface layers of a star should  $\kappa$  increase to  $\kappa_T$ . But, because of very slow changes of physical conditions along the radius of a star,  $\kappa$  remains  $\kappa_T$  in the greater part of the volume of a star. Therefore it is very interesting to calculate the internal structure of a star under given values of  $\kappa = \text{const}$ . We did this, differing thereby from Cowling's model, so that there are two alternatives: our model ( $\kappa = \text{const}$ ) and Cowling's model ( $\kappa_T$ ). All the calculations were carried out by numerical integration of (2.23b) assuming there that  $\varepsilon_1 = 0$ .

Table 4

$x$	$T_1$	$p_1$	$\rho_1$
0.00	1.000	1.000	1.000
0.50	0.983	0.958	0.975
1.00	0.935	0.845	0.904
1.50	0.856	0.677	0.791
2.00	0.762	0.507	0.665
2.50	0.652	0.346	0.530
3.00	0.544	0.211	0.388
3.50	0.451	0.117	0.259
4.00	0.370	$0.598 \times 10^{-1}$	0.161
4.50	0.328	$0.284 \times 10^{-1}$	$0.936 \times 10^{-1}$
5.00	0.245	$0.125 \times 10^{-1}$	$0.510 \times 10^{-1}$
5.50	0.195	$0.52 \times 10^{-2}$	$0.266 \times 10^{-1}$
6.00	0.154	$0.20 \times 10^{-2}$	$0.129 \times 10^{-1}$
6.50	0.118	$0.67 \times 10^{-3}$	$0.57 \times 10^{-2}$
7.00	0.087	$0.20 \times 10^{-3}$	$0.23 \times 10^{-2}$
7.50	0.060	$0.49 \times 10^{-4}$	$0.82 \times 10^{-3}$
8.00	0.036	$0.64 \times 10^{-5}$	$0.18 \times 10^{-3}$
8.50	0.015	$0.19 \times 10^{-6}$	$0.79 \times 10^{-4}$
8.90	0.000	0.000	0.000

Table 3 gives the main characteristics of the “convective” model of a star under  $\kappa = \text{const}$  and  $\kappa = \kappa_{\text{ch}}$ . The  $\kappa_{\text{ch}}$  are taken from Cowling’s calculations. Values of  $\lambda L_{x_0}$  were found by formula (2.62). In this model, distribution of energy sources inside the convective core does not matter. For this reason, the quantities  $\lambda$  and  $L_{x_0}$  are inseparable. If we would like to calculate them separately, we should set up the distribution function for them inside the convective core.

We see that the main characteristics of the structure of a star, the quantities  $x_0$ ,  $M_{x_0}$ , and  $\lambda L_{x_0}$ , are only a little different from those calculated in Table 2. The main difference between structures of stars under the two values  $\kappa = \text{const}$  and  $\kappa = \kappa_{\text{ch}}$  is that under our  $\kappa = \text{const}$  the convective core is larger, so such stars are close to polytropic structures of class  $3/2$ , and there we obtain a lower concentration of matter at the centre:  $\rho_c = 20.5 \bar{\rho}$ . Table 4 gives the full list of calculations for our convective model ( $\kappa = \text{const}$ ).

### Chapter 3

#### The Internal Constitution of Stars, Obtained from the Analysis of the Relation “Period – Average Density of Cepheids” and Other Observational Data

In the previous chapter we deduced numerous theoretical correlations, which give a possibility of calculating the phys-

ical characteristics of matter inside stars if their structural characteristics are known. In order to be sure of the calculations, besides our general theoretical considerations, it would be very important to obtain the structural characteristics proceeding from observational data, related at least to some classes of stars.

Properties of the internal structure of a star should manifest in its dynamical properties. Therefore we expect that the observed properties of variable stars would permit us to learn of their structures. For instance, the pulsation period of Cepheids should be dependent on both their physical characteristics and the distribution of the characteristics inside the stars. Theoretical deduction of this correlation can be done very strictly. Therefore we have a basis for this deduction in all its details.

Radiation of energy by an oscillating star must result in a dispersion of mechanical energy of its oscillations. It is most probable that the oscillation energy of variable stars is generated and supported by energy sources connected to the oscillation and radiation processes. In other words, such stars are self-inducing oscillating systems. Observable arcs of the oscillating luminosity and speed reveal a nonlinear nature for the oscillations, which is specific to self-inducing oscillating systems. The key point of a self-inducing oscillating system is a harmonic frequency equal to the natural frequency of the whole oscillating system. Therefore, making no attempt to understand the nature of the oscillations, we can deduce the oscillation period as the natural period of weak linear oscillations.

#### 3.1 The main equation of pulsation

Typical Cepheids have masses less than 10 solar masses. For instance,  $\delta$  Cephei has  $M \simeq 9 M_{\odot}$ . In this case equation (2.34) leads to  $\gamma_c < 0.1$ , so Cepheids should satisfy  $L \sim M^3$ , i. e. the “mass-luminosity” relation. Therefore the radiant pressure plays no rôle in such stars, so considering their internal constitutions we should take into account only the gaseous pressure. In solving this problem we will consider linear oscillations, neglecting higher order terms. This problem becomes much simpler because temperature changes in such a star satisfy adiabatic oscillations in almost its whole volume, except only for the surface layer. Naturally, in order to obtain the ratio between observed temperature variations and adiabatic temperature variations close to 1, the average change of energy inside 1 gram in one second should be about  $\bar{\epsilon}$ , i. e.  $\sim 10^2$ . This is  $10^8$  per half period. On the other hand, the heat energy of a unit of mass should be about  $\Omega/M$  (according to the virial theorem), that is  $\sim 10^{15}$  ergs by formula (2.5). Thus during the pulsation the relative change of the energy is only  $10^7$ , so pulsations of stars are adiabatic, with high precision. We assume that the pulsation of a star can be determined by a simple standing wave with

a frequency  $n/2\pi$

$$V(r, t) = V(r) \sin nt, \quad a = \frac{\partial^2 V}{\partial t^2} = -n^2 V(r) \sin nt, \quad (3.1)$$

where  $V(r)$  is the relative amplitude of the pulsation

$$V(r) = \frac{\delta r}{r}.$$

By making the above assumptions, Eddington had solved the problem of pulsation of a star.

Linking the coordinate  $r$  to the same particle inside a star, we have the continuity equation as follows

$$M_r = \text{const}, \quad r^2 \rho dr = \text{const}. \quad (3.2)$$

Using the condition of adiabatic changes  $\frac{\delta p}{p} = \Gamma \frac{\delta \rho}{\rho}$  and taking variation from the second equality, we obtain

$$\frac{\delta p}{p} = -\Gamma \left[ 3V + r \frac{dV}{dr} \right]. \quad (3.3)$$

It is evident that the equations of motion

$$\frac{dp}{\rho dr} = -(g + a), \quad g = \frac{GM_r}{r^2}$$

give, neglecting higher order terms,

$$\frac{d\delta p}{dr} = -a\rho + 4V \frac{dp}{dr}.$$

Substituting formula (3.3) into this equation, we obtain Eddington's equation of pulsation

$$\begin{aligned} \frac{d^2 V}{dr^2} + \frac{1}{r} \frac{dV}{dr} \left[ 4 + \frac{r}{p} \frac{dp}{dr} \right] + \\ + \frac{V}{r\Gamma} \frac{1}{p} \frac{dp}{dr} \left[ (3\Gamma - 4) - \frac{n^2 r}{g} \right] = 0. \end{aligned} \quad (3.4)$$

We introduce a dimensionless variable  $x$  instead of  $r$  (we used this variable in our studies of the internal constitution of stars). As it is easy to see

$$\frac{g}{r} = 4\pi G \frac{\bar{\rho}_r}{3} = 4\pi G \rho_c \frac{M_x}{x^3}. \quad (3.5)$$

Substituting (3.5) into formula (3.4), we transform the pulsation equation to the form

$$\begin{aligned} \frac{d^2 V}{dr^2} + \frac{1}{x} \frac{dV}{dr} \left[ 4 + \frac{x}{p_1} \frac{dp_1}{dr} \right] - \\ - \frac{V}{x\Gamma} \frac{1}{p_1} \frac{dp_1}{dr} \left[ (4 - 3\Gamma) + \frac{n^2}{4\pi G \rho_c} \frac{x^3}{3M_x} \right] = 0. \end{aligned} \quad (3.6)$$

We transform this equation to self-conjugated form. Multiplying it by  $x^4 p_1$ , we obtain

$$\frac{d}{dx} \left[ x^4 p_1 \frac{dV}{dx} \right] - V x^3 \frac{dp_1}{dx} \frac{(4 - 3\Gamma)}{\Gamma} \left[ 1 - \lambda \frac{x^3}{3M_x} \right] = 0, \quad (3.7)$$

where

$$\lambda = \frac{n^2}{4\pi G \rho_c \left( \Gamma - \frac{4}{3} \right)}. \quad (3.8)$$

So the problem of finding the pulsation period has been reduced to a search for those numerical values of  $\lambda$  by which the differential equation (3.7) has a solution satisfying the "natural" boundary conditions

$$x^4 p_1 \frac{dV}{dx} \Big|_0^{x_0} = 0. \quad (3.9)$$

Formula (3.8) gives the correlation "period – average density of Cepheids" and, hence, the general correlation "period – average density of a star". It is evident that  $\lambda$  depends on the internal structure of a star. Its expected numerical value should be about 1. For a homogeneously dense star,  $x^3/(3M_x) = 1$  everywhere inside it. In this case the differential equation (3.7) has the solution:  $V = \text{const}$ ,  $\lambda = 1$ . This solution determines the main oscillation of such a star. In order to find the main oscillations of differently structured stars, we proceed from the solution by applying the method of perturbations.

### 3.2 Calculation of the mean values in the pulsation equation by the perturbation method

We write the pulsation equation in general form

$$(py')' + qy(1 - \lambda\rho) = 0. \quad (3.10)$$

If we know a solution to this equation under another function  $\rho = \rho_0$

$$(py_0')' + qy_0(1 - \lambda_0\rho_0) = 0, \quad (3.11)$$

hence we know the function  $y_0$  and the parameter  $\lambda_0$ . After multiplying (3.10) by  $y_0$  and (3.11) by  $y$ , we subtract one from the other. Then we integrate the result, taking the limits 0 and  $x_0$ . So, we obtain

$$\int_0^{x_0} qyy_0 [\lambda_0\rho_0 - \lambda\rho] dx = 0,$$

hence

$$\lambda = \lambda_0 \frac{\int_0^{x_0} qyy_0\rho_0 dx}{\int_0^{x_0} qyy_0\rho dx}. \quad (3.12)$$

If the oscillations are small, equation (3.10) is the same as (3.11) with only an infinitely small correction

$$\rho = \rho_0 + \delta\rho, \quad y = y_0 + \delta y, \quad \lambda = \lambda_0 + \delta\lambda.$$



Then the exact formula for  $\delta\lambda$

$$\delta\lambda = -\lambda_0 \frac{\int_0^{x_0} qy y_0 \delta\rho dx}{\int_0^{x_0} qy y_0 \rho dx}$$

can be replaced by

$$\delta\lambda = -\lambda_0 \frac{\int_0^{x_0} qy_0^2 \delta\rho dx}{\int_0^{x_0} qy_0^2 \rho dx},$$

and thus we have

$$\lambda = \lambda_0 \frac{\int_0^{x_0} qy_0^2 \rho_0 dx}{\int_0^{x_0} qy_0^2 \rho dx}. \quad (3.13)$$

In our case  $y_0 = 1$  and  $\lambda_0 = 1$ . Comparing formulae (3.10) and (3.7), using (3.13), we obtain

$$\lambda = \lambda_0 \frac{3 \int_0^{x_0} x \rho_1 M_x dx}{\int_0^{x_0} x^4 \rho_1 dx}. \quad (3.14)$$

We re-write this equation, according to (2.5a), as follows

$$\lambda = \lambda_0 \frac{9 \int_0^{x_0} p_1 x^2 dx}{\int_0^{x_0} \rho_1 x^4 dx}. \quad (3.15)$$

If we introduce the average density  $\bar{\rho}$  into formula (3.8) instead of the central one  $\rho_c$ , then according to (2.4),

$$\bar{\lambda} = \frac{n^2}{4\pi G \bar{\rho} (\Gamma - \frac{4}{3})}, \quad (3.16)$$

$$\bar{\lambda} = \lambda \frac{\rho_c}{\bar{\rho}} = \frac{x_0^3}{3M_{x_0}} \lambda. \quad (3.17)$$

Using formulae (2.6) and (3.17) we re-write (3.15) as

$$\bar{\lambda} = \frac{x_0^2 \Omega_{x_0} M_{x_0}}{I_{x_0}}, \quad (3.18)$$

where  $I_{x_0}$  is the dimensionless moment of inertia

$$I_{x_0} = \int_0^{x_0} \rho_1 x^4 dx. \quad (3.19)$$

Formulae (3.16) and (3.18) determine the oscillation period of a star,  $P = 2\pi/n$ , independently of its average density

$\bar{\rho}$ . This result was obtained by Ledoux [18] by a completely different method. It is interesting that our equations (3.16) and (3.18) coincide with Ledoux's formulae.

We next calculate  $\lambda$  for stars of polytropic structures. In such cases  $I_{x_0}$  is

$$I_{x_0} = x_0^2 M_{x_0} - 6(n+1) \int_0^{x_0} T_1 x^2 dx, \quad (3.20)$$

where  $n$  is the polytropic exponent. Thus

$$\frac{1}{\bar{\lambda}} = \frac{5-n}{3} \left[ 1 - 6(n+1) \frac{\int_0^{x_0} T_1 x^2 dx}{M_{x_0} x_0^2} \right]. \quad (3.21)$$

Calculations of the numerical values of  $\bar{\lambda}$  for cases of different polytropic exponents are given in Table 5.

$n$	$\bar{\lambda}$
0	1.00
1	1.91
$3/2$	2.52
2	3.85
2.5	7.00
3	13.1

Under large  $\bar{\lambda}$ , much different from 1, the calculations for Table 5 are less precise. Therefore, in order to check the calculated results, it is interesting to compare the results for  $n = 3$  to those obtained by Eddington via his exact solution of his adiabatic oscillation equation for his stellar model. For the stars we consider, he obtained,  $\frac{n^2}{\pi G \rho_c \Gamma} = \frac{3}{10} (3 - 4/\Gamma)$ . Hence, comparing his result to our formula (3.8), we obtain  $\lambda = 9/40$  and  $\bar{\lambda} = \frac{9}{40} \frac{\rho_c}{\bar{\rho}} = 12.23$ . This is in good agreement with our result  $\bar{\lambda} = 13.1$  given in Table 5.

### 3.3 Comparing the theoretical results to observational data

We represent the "period – average density" correlation in the next form

$$P \sqrt{\bar{\rho}_0} = c_1, \quad (3.22)$$

where  $P$  is the period (days),  $\bar{\rho}_0$  is the average density expressed in the multiples of the average density of the Sun

$$n = \frac{2\pi}{86,400 P}, \quad \bar{\rho} = 1.411 \bar{\rho}_0.$$

Employing formula (3.16), it is easy to obtain a correlation between the coefficients  $\bar{\lambda}$  and  $c_1$

$$\bar{\lambda} \left( \Gamma - \frac{4}{3} \right) = 0.447 (10c_1)^{-2}. \quad (3.23)$$

By analysis of the "mass-luminosity" relation we have previously shown that the radiant pressure is much less than the gaseous pressure in a star. Therefore, because the inner

regions of a star are primarily composed of hydrogen, the heat energy there is much more than the energy of ionization. So we have all grounds to assume  $\Gamma = 5/3$ , the ratio of the heat capacities for a monatomic gas. Hence

$$\bar{\lambda} = 1.34(10c_1)^{-2}. \quad (3.24)$$

In order to express  $c_1$  in terms of the observed characteristics of a star, we replace  $\bar{\rho}_0$  in formula (3.22) with the reduced temperature and the luminosity, via the “mass-luminosity” formula. The “mass-luminosity” correlation has a general form  $L \sim M^\alpha$  for any star. We denote by  $\bar{T}$  the reduced temperature of a star (with respect to the temperature of the Sun), and by  $M_b$  its reduced stellar magnitude. Then, by formula (3.22), we obtain

$$\left(0.30 - \frac{1}{5\alpha}\right)(M_b - M_\odot) + \log P + 3 \log \bar{T} = \log c_1. \quad (3.25)$$

From this formula we see that, in order to find  $c_1$ , it is unnecessary to know the exact value of  $\alpha$  (if, of course,  $\alpha$  has a large numerical value). Eddington’s formula for the “mass-luminosity” relation, taken for huge masses, gives  $\alpha \sim 2$  (compare with 2.53). Therefore, Eddington’s value of  $c_1 = 0.100$  is overstated. Applying another correlation,  $L \sim M^{10/3}$ , Parenago [19] obtained  $c_1 = 0.071$ . Becker [20] carried out a precise analysis of observational data using Kuiper’s empirical “mass-luminosity” arc. He obtained the average value of  $c_1 = 0.076$  for Cepheids. Formula (2.4) gives  $\bar{\lambda} = 2.7$  or  $\bar{\lambda} = 2.3$ , so that Table 5 leads us to conclude that Cepheids have structures close to the polytropic class  $3/2$ , like all other stars. Hence Cepheids have a low concentration of matter at the centre:  $\rho_c = 6\bar{\rho}$ .

This result is in qualitative agreement with the “natural viewpoint” that sources of stellar energy increase their productivity towards the centre of a star. However (as we saw in §2.8) the model for a point-source of energy and for a constant absorption coefficient, giving stars of minimal average densities, leads to a strong concentration at the centre,  $\rho_c/\bar{\rho} = 20.5$ . Thus  $\bar{\lambda}$  for such a model should be more than an observable one. Really, having  $\int_0^{x_0} p_1 x^2 dx = 6.06$  and  $I_{x_0} = 140.0$  calculated by Table 4, formulae (3.15) and (3.17) give  $\bar{\lambda} = 8.0$  for models with the ultimate concentration of energy sources. So, such stars are of the polytropic class  $n = 2.5$ . If the absorption coefficient is variable (Cowling’s model), calculations give even more:  $\bar{\lambda} = 8.4$ .

Eddington and others, in their theoretical studies of the pulsation period within the framework of Eddington’s model, explain the deviation between the theoretical and observed values of  $\bar{\lambda}$  by an effect of the radiant pressure. Studies of pulsations under  $\gamma_c$  close to 1 show that the obtained formula for the period under low  $\gamma_c$  is true even if  $\Gamma$  is the reduced ratio of the heat capacities (which is, depending on the rôle of the radiant pressure,  $4/3 \leq \Gamma \leq 5/3$ ).

Equation (3.23) shows that when  $\bar{\lambda} = 12.23$  and the observable  $c_1 = 0.075$  we have  $\Gamma_{\text{eff}} = 1.40$ . At the same time  $\Gamma_{\text{eff}}$  should undergo changes independently of  $\gamma_c$ , i. e. depending upon the rôle of the radiant pressure. For a monatomic gas, Eddington [21] and others obtained this correlation as

$$\Gamma_{\text{eff}} - \frac{4}{3} = \frac{1}{3} \frac{1 + 4\gamma_c}{(1 + \gamma_c)(1 + 8\gamma_c)}. \quad (3.26)$$

Under  $\Gamma_{\text{eff}} = 1.40$  we obtain  $\gamma_c = 1.5$ . We accept this numerical value in accordance with the average period of Cepheids,  $P = 10^{\text{d}}$ . Then, by the “mass-luminosity” relation,  $M = 12 M_\odot$ . It is possible to think that this result is in good agreement with the conventional viewpoint on the rôle of the radiant pressure inside stars (see §2.7). However, because  $\lambda_c$  depends on the mass of a star, other periods give different  $\Gamma_{\text{eff}}$  (by formula 3.26) and hence other numerical values of  $c_1$ . Using formulae (3.26) and (3.23), we can calculate  $c_1$  for variable stars having longer pulsations, with periods  $20^{\text{d}} < P < 30^{\text{d}}$ . Instead of the average value  $\log c_1 = -1.12$  found by Becker for the stars, there should be  $\log c_1 = -1.00$ . Despite the small change, observations show no such increase of  $c_1$  [20]. Therefore, our conclusion about the negligible rôle of the radiant pressure in stars, even inside super-giants, finds a new verification. This result verifies as well our results  $\mu = 1/2$  and  $\kappa = \kappa_{\text{T}}$ , obtained in chapter 3.

### 3.4 Additional data about the internal constitution of stars

Some indications of the internal structure of stars can be obtained from analysis of the elliptic effect in the luminosity arcs of eclipse variable stars. Observations of such binaries gives the ratio of diameters at the equator of a star, which becomes elliptic because of the flow-deforming effect in such binary systems. For synchronous rotations of the whole system and each star in it, the compressed polar diameter of each star should be different (in the first order approximation) from the average equatorial one with a multiplier dependent on their masses. Thus, proceeding from the observed compression we can calculate the meridian compression  $\epsilon$ . According to Clairaut’s theory  $\epsilon$  is proportional to  $\varphi$ , the ratio of the centrifugal force at the equator to the force of gravity

$$\epsilon = \alpha \varphi, \quad \varphi = \frac{\omega^2}{3\pi G \bar{\rho}},$$

where  $\alpha$  is a constant dependent on the structure of the star. This constant was calculated for stars of polytropic structures by numerous researchers: Russell, Chandrasekhar and others. If  $n = 0$  (homogeneous star),  $\alpha = 1.25$ . If  $n = 1$ , we have  $\alpha = 15/(2\pi^2) = 0.755$ . If  $n = 5$  (the ultimate concentration, Roche’s model),  $\alpha = 0.50$ . We see that the constant  $\alpha$  is sensitive to changes in the structure of a star. Therefore determination of the numerical values of  $n$  in this way

requires extremely precise observations. The values of  $n$  so obtained are very uncertain, despite the simplicity of the theory. Shapley first concluded that stars are almost homogeneous. This was verified by Luiten [22] who found the average value  $\alpha = 0.57$  for a large number of stars like  $\beta$  Lyrae, and  $\alpha = 0.71$  for stars like Algol. His results correspond to the polytropic structures  $n = 3/2$  and  $n = 1$  respectively.

The observed motion of the line of apsides in numerous eclipse binaries can be explained, in numerous cases, by their elliptic form. Because matter is more strongly concentrated in a binary system than in regular stars, the binary components interact like two point-masses, so there should be no motion of the line of apsides. Therefore the velocity of the line of apsides should be proportional (in the first order approximation) to  $\alpha - 1/2$ , where  $\alpha$  is sensitive to changes in the structure of a star (as we showed above). Many theoretical studies on this theme give contradictory formulae for the velocity, depending on hypotheses about the properties of rotation in the pair. Russell, in his initial studies of this problem, supposed the rotating components solid bodies. This theory, being applied to the system Y Cygni by Russell and Dugan [23], gave  $\alpha - 1/2 = 0.034$ , which is the polytropic structure  $1/2 < n < 2$ . Other researchers, having made other suppositions, obtained larger  $n$ :  $n \simeq 3$ . It is probable that we can be most sure only that, because we observe motion of the line of apsides in binaries, the stars have no strong concentration of matter at the centre.

Blackett supposed a law according to which the ratio between the magnetic momentum  $P_H$  and angular momentum  $U$  is constant for all rotating space bodies. If this law is correct, we could have a possibility of determining the structures of stars in an independent way. We denote by  $k$  the ratio between the moments of the inertia of an arbitrary structured star rotating with the angular velocity  $\omega$  and of the same star if it would be homogeneous throughout. Then

$$U = \frac{2}{5} k \omega M R^2, \quad k = \frac{5}{3} \frac{I_{x_0}}{x^2 M_{x_0}},$$

where  $I_{x_0}$  is the dimensionless moment of inertia. Using Blanchett's formula [24]

$$\frac{P_H}{U} = \beta \frac{G^{1/2}}{2c} \tag{3.27}$$

( $\beta$  is a dimensionless multiplier, equal to about 1), and having the magnetic magnitude at the pole  $H = 2P_H/R^3$ , we can calculate  $k$ . For the Earth ( $k = 0.88$ ), we obtain  $\beta = 0.3$ . Supposing  $k = 0.16$  for stars, Blackett has found:  $\beta = 1.14$  for the Sun and  $\beta = 1.16$  for 78 Virginis (its magnetic field has been measured by Babcock).

If Blackett's law (3.27) is valid throughout the Universe and  $\beta = 0.3$  for all space bodies, not just for the Earth, then  $k = 0.60$  should be accepted for stars. Comparing  $k = 0.60$

Table 6

$n$	$k$
0	1.00
1	0.65
$3/2$	0.52
2	0.40
2.5	0.28
3	0.20

with Table 6, we come to the same conclusion that we have obtained by completely different methods: that stars have polytropic structures of class  $n = 3/2$ .

For the convective model of a star (calculated in §2.8) we obtain  $k = 0.26$ . This is much less than required. The same convective model with a variable absorption coefficient (Cowling's model) gives even less:  $k = 0.19$ .

The agreement of our value  $n = 3/2$  with other data, obtained by very different methods, verifies Blackett's law. It is possible his formula (3.27) should be written without  $\beta$ , but with the denominator  $2\pi c$ .

### 3.5 Conclusions about the internal constitution of stars

The most certain conclusions about the structure of stars are derived from the theory of pulsation of Cepheids. We have concluded that Cepheids have structures close to the polytropic one of class  $n = 3/2$ , for which  $\rho_c = 6\bar{\rho}$ . This conclusion is verified by other data, whereas each of them could be doubtful when being considered in isolation. At the same time all the data, characterizing stars of different classes, lead to the same result. It is probable that stars are really close to being homogeneous, having a low concentration of matter at the centre like the bulky planets, Jupiter and Saturn. Such a distribution of matter, as we saw in the ultimate case of the convective model, cannot be explained by a strong concentration of an energy source at the centre, or by a special kind of absorption coefficient. The real reason is that the radiant pressure  $B$  is included in the mechanical equilibrium equation through the gaseous pressure in the exponent  $1/4$ . Therefore the structural characteristics  $M_{x_0}$  and  $X_0$ , determined by the function  $\rho_1$ , have small changes even in very different models. Hence, in order to obtain the observable low concentration of matter at the centre of stars, we can search for the reason only in the heat equilibrium equation. The polytropic model  $n = 3/2$  differs from other polytropic models by a smaller value of  $x_0$ . In order to make  $x_0$  smaller, the gaseous pressure should decrease more strongly in the upper layers of a star. Such a rapid decrease in the pressure is possible only if the surface layers are heavy. In other words, in the case of the strong increase of the molecular weight in the surface layers of a star. Such an explanation is in complete agreement with our conclusion about the high concentration of hydrogen in the internal regions of stars. If the average molecular weight changes from  $\mu = 1/2$  at the centre to  $\mu = 2$  at the surface of a star, such a change of the molecular weight can be sufficient.

What is the goal of introducing the variable  $\mu$ ? Let us

assume that  $\mu$  depends on the temperature as

$$\mu_1 = \frac{1}{T_1^s}, \quad (3.28)$$

where  $s$  is a positive determined exponent. Increase of the molecular weight at the surface should result in an increase of the absorption coefficient  $\kappa$  (transition from  $\kappa = \kappa_T$  to  $\kappa = \kappa_{c_n}$ ). At the same time, under energy sources concentrated at the centre, the quantity  $\kappa_1 L_x / M_x$  can remain almost the same. If  $\kappa_1 L_x / M_x = \text{const} = 1$ , equation (2.22a) leads to

$$p_1 = B_1 = T_1^4, \quad \lambda = 1. \quad (3.29)$$

Instead of  $T_1$  we introduce the characteristics

$$u_1 = \frac{T_1}{\mu_1} = T_1^{1+s} = \mu_1^{-\frac{1+s}{s}}, \quad (3.30)$$

which keeps the ideal gas equation in the regular form  $p_1 = u_1 \rho_1$ . According to (3.29), we have

$$p_1 = u_1^{\frac{4}{1+s}}. \quad (3.31)$$

where we should equate the exponent  $4/(1+s)$  to  $n+1$  according to formula (2.7a).

Thus we have

$$\rho_1 = u_1^n, \quad n = \frac{3-s}{1+s}, \quad (3.32)$$

so the function  $u_1$  is determined by Emden's equation of class  $n$ . Hence, in order to obtain the structure  $n = 3/2$ , there should be  $s = 3/5$  — the very low increase of the molecular weight: for instance, under such  $s$  the molecular weight  $\mu$  increases 4 times at the distance  $x_1$  where

$$\mu_1 = \left(\frac{1}{4}\right)^{\frac{5}{3}} = 0.025, \quad T_1 = \left(\frac{1}{4}\right)^{\frac{5}{3}} = 0.10. \quad (3.33)$$

At  $x > x_1$  the molecular weight remains unchanged, the equilibrium of a star is determined by the regular system of the equilibrium equations. However at the numerical values (3.33) almost the whole mass of a star is accounted for (see Table 4, for instance), so we obtain small corrections to the polytropic structure  $n = 3/2$ . Naturally, tables of Emden's function taken under  $n = 3/2$  show that  $x_1 = 5.6$  and  $M_{x_1} = 11.0$ . Applying formula (2.27a), we obtain  $x_0 = 7.0$  instead of  $x_0 = 6$ , as expected for such a polytropic structure. These calculations show that the observed structures of stars\* verify our result about the high content of hydrogen in the internal regions of a star, obtained from the "mass-luminosity" relation. At the same time, it should be taken into account that the hydrogen content in the surface layers of stars is also

\*The fact that the molecular weight is variable does not change the formulas, determining the pulsation period of Cepheids. The variability of  $\mu$  can include a goal only if the whole structure of star has been changed.

substantial. Therefore on the average we have  $\mu < 2$  inside a star, so the problem about homogeneity of the molecular weight of stars is not completely solved with the above.

We saw that the dimensionless mass  $M_{x_0}$  is almost the same in completely different models of stars. For polytropic structures of the classes  $n = 3/2$  and  $n = 2$ , convective models, and models described in Table 2, we obtained approximately the same numerical values of  $M_{x_0}$ . Therefore we can surely accept  $M_{x_0} = 11$ . What about  $x_0$ ? According to observed structures of stars, we accept  $x_0 = 6$ . Hence  $\bar{\rho}_c = 6.5 \bar{\rho}$ . In order to obtain  $\kappa = \kappa_1$  from the observed "mass-luminosity" relation, we should have  $\lambda L_{x_0} / M_{x_0}^3 = 1.0 \times 10^{-3}$ . Thus we obtain  $\lambda L_{x_0} = 1.5$ . As a result, using these numerical values in formulae (2.28), (2.30), and (2.31), we have a way of calculating the physical conditions at the centre of any star. We now make this calculation for the Sun. Assuming  $\mu_{c_\odot} = 1/2$ , we obtain

$$\begin{aligned} \rho_{c_\odot} &= 9.2, & p_{c_\odot} &= 9.5 \times 10^{15} \text{ dynes/cm}^2, \\ \gamma_{c_\odot} &= 0.4 \times 10^{-3}, & B_{c_\odot} &= 3.8 \times 10^{12} \text{ dynes/cm}^2, \\ T_{c_\odot} &= 6.3 \times 10^6 \text{ degrees.} \end{aligned} \quad (3.34)$$

Of the data the most soundly calculated is  $\gamma_{c_\odot}$ , because it is dependent only on  $M_{x_0}$ . Thus a low temperature at the centre of the Sun, about 6 million degrees, is obtained because of low numerical values of  $\mu_{c_\odot}$  and  $x_0$ . Having such low temperatures, it is scarcely possible to explain the origin of stellar energy by thermonuclear reactions.

The results indicate possible ways to continue our research into the internal constitution of stars. They open a way for a physical interpretation of the Russell-Hertzsprung diagram, which is directly linked to the origin of stellar energy.

## PART II

### Chapter 1

#### The Russell-Hertzsprung Diagram and the Origin of Stellar Energy

##### 1.1 An explanation of the Russell-Hertzsprung diagram by the theory of the internal constitution of stars

The Russell-Hertzsprung diagram connects the luminosity  $L$  of a star to its spectral class or, in other words, the reduced temperature  $T_{\text{eff}}$ . The theory of the internal constitution of stars uses the radius  $R$  of a star instead of the effective temperature  $T_{\text{eff}}$ . It follows from the Stephan-Boltzmann law

$$L = 4\pi R^2 \sigma T_{\text{eff}}^4, \quad \sigma = \frac{1}{4} \alpha c,$$

where  $c$  is the velocity of light,  $\alpha$  is the radiant energy density constant. Thus, the Russell-Hertzsprung diagram is

the same for the correlation  $L(R)$  or  $M(R)$ , if we use the “mass-luminosity” relation. Due to the existence of numerous sequences in the Russell-Hertzsprung diagram (the main sequence, the sequences of giants, dwarfs, etc.) the correlations  $L(R)$  and  $M(R)$  are not sufficiently clear. In this paragraph we show that for most stars the correlations  $L(R)$  and  $M(R)$  are directly connected to the mechanism generating stellar energy. The essence of the correlation  $L(R)$  becomes clear, as soon as we replace the observable characteristics of stars (the masses  $M$ , the luminosities  $L$ , and the radii  $R$ ) with the parameters which determine the physical conditions inside stars. The method of such calculations and the precision of the obtained results were discussed in detail in Part I of this research.

First we calculate the average density of a star

$$\rho = \frac{3M}{4\pi R^3}. \quad (1.1)$$

Then, having the mechanical equilibrium of a star, we calculate the average pressure within. This internal pressure is in equilibrium with the weight of the column whose aperture is one square centimeter and whose length is the radius of the star. The pressure is  $p = g\rho R$ . Because of  $g = GM/R^2$ ,

$$p = \frac{3G}{4\pi} \frac{M^2}{R^4}. \quad (1.2)$$

What can be said about the temperature of a star? It should be naturally calculated by the energy flow of excess radiation  $F_R$

$$F_R = \frac{L}{4\pi R^2}, \quad (1.3)$$

because the flow is connected to the gradient of the temperatures. If we know what mechanism transfers energy inside a star, we can calculate the temperature  $T$  by formula (1.1) or (1.2)

$$T = f(L, M, R). \quad (1.4)$$

For instance, if energy is dragged by radiations, according to §1.2, we have

$$F_R = -\frac{c}{\kappa\rho} \frac{dB}{dr}, \quad (1.5)$$

where  $\kappa$  is the absorption coefficient per unit mass,  $B$  is the radiant pressure

$$B = \frac{1}{3} \alpha T^4. \quad (1.6)$$

We often use the radiant pressure  $B$  instead of the temperature. By formula (1.3) we can write

$$B \simeq \frac{\kappa F_R}{c} \rho R,$$

which, by using (1.1) and (1.3), gives

$$B \simeq \frac{3LM}{(4\pi)^2 c R^4} \kappa. \quad (1.4a)$$

If we know how  $\kappa$  depends on  $B$  and  $\rho$ , formula (1.4a) leads to equation (1.4). So formulae (1.1), (1.2), and (1.4a) permit calculation of the average numerical values of the density, the pressure, and the temperature for any star. Exact numerical values of the physical parameters at a given point inside a star (at the centre, for instance) can be obtained, if we multiply the formulae by dimensionless “structural” coefficients. We studied the structural coefficients in detail in Part I of this research. We studied them by both mathematical methods (solving the system of the dimensionless differential equations and mechanical equilibrium and heat equilibrium of a star) and empirical methods (the analysis of observable properties of stars).

Values of  $\rho$ ,  $p$ , and  $T$ , calculated by formulae (1.1), (1.2), and (1.4), should be connected by the equation of the phase state of matter. Hence, we obtain the first theoretical correlation

$$F_1(L, M, R) = 0, \quad (1.7)$$

which almost does not depend on the kind of energy generation in stars.

For instance, a star built on an ideal gas has

$$p = \frac{\mathfrak{R}T}{\mu} \rho.$$

Dividing (1.2) by (1.1), we obtain

$$T \simeq \frac{G}{\mathfrak{R}} \mu \frac{M}{R}, \quad B \simeq \frac{\alpha G^4}{3\mathfrak{R}^4} \mu \frac{M^4}{R^4}, \quad (1.8)$$

$$\gamma = \frac{B}{p} \simeq M^2 \mu^4. \quad (1.9)$$

Comparing (1.8) to formula (1.4a), obtained for the energy transfer by radiation, we obtain the correlation (1.7) in clear form

$$L \simeq M^3 \frac{\mu^4}{\kappa}. \quad (1.7a)$$

Another instance — a star built on a degenerate gas

$$p \simeq \rho^{5/3},$$

then formulae (1.1) and (1.2) lead to

$$RM^{1/3} = \text{const}, \quad (7.b)$$

so in this case we just obtain the correlation like (1.7), where there is no  $L$ .

Formula (1.7a), which is true for an ideal gas, can include  $R$  only through  $\kappa$ . Therefore this formula is actually the “mass-luminosity” relation, which is in good agreement with observational data  $L \sim M^3$ , if  $\mu^4/\kappa = \text{const} = 0.08$ . The calculations are valid under the low radiant pressure  $\gamma < 1$ . As we see from formula (1.9), inside extremely bulky stars the

value of  $\gamma$  can be more than 1. In such cases formula (1.2) will determine the radiant pressure

$$B \simeq \frac{M^2}{R^4},$$

not the gaseous one. Comparing to formula (1.4a), we have

$$L \simeq \frac{M}{\kappa}. \quad (1.7b)$$

Astronomical observations show that super-giants do not have the huge variations of  $M$  which are predicted by this formula. Therefore, in Part I, we came to the conclusion that  $\gamma \leq 1$  for stars of regular masses  $M \leq 100M_\odot$ , so formula (1.9) gives for them:  $\mu = 1/2$ . Hence,  $\kappa = 0.8$ , which is approximately equal to Thomson's absorption coefficient. This is very interesting, for we have obtained that the radiant pressure places a barrier to the existence of extremely large masses for stars, although there is no such barrier in the theory based on the equilibrium equations of stars.

Until now, we hardly used the heat equilibrium equation, which requires that the energy produced inside a star should be equal to its radiation into space. According to the heat equilibrium equation, the average productivity of energy by one gram of stellar matter can be calculated by the formula

$$\varepsilon = \frac{L}{M}. \quad (1.10)$$

On the other hand, if the productivity of energy is determined by some other reactions,  $\varepsilon$  would be a function of  $\rho$  and  $T$ . This function would also be dependent on the kinetics of the supposed reaction. Thus formulae (1.10), (1.1), (1.4), and the equation of the reaction demand the existence of the second correlation

$$F_2(L, M, R) = 0, \quad (1.11)$$

which is fully determined by the mechanism that generates energy in the reaction. For an ideal gas,  $R$  disappears from the first correlation  $F_1 = 0$  (1.7). For this reason formula (1.11) transforms into the relation  $L(R)$  or  $M(R)$ , which become directly dependent on the kind of energy sources in stars. For a degenerate gas we obtain another picture: as we saw above, in this case  $M(R)$  is independent of energy sources, and then  $M$  and  $L$  are connected by equation (1.11).

## 1.2 Transforming the Russell-Hertzsprung diagram to the physical characteristics specific to the central regions of stars

Our task is to find those processes which generate energy in stars. In order to solve this problem, we must know physical conditions inside stars. In other words, we should proceed from the observed characteristics  $L$ ,  $M$ ,  $R$  to physical parameters.

We denote by a bar all the quantities expressed in terms of their numerical values in the Sun. Assuming, according to our conclusion in Part I, that stars have the same structure, we can, by formulae (1.1), (1.2), and (1.10), strictly calculate the central characteristics of stars

$$\bar{p}_c = \frac{\bar{M}^2}{\bar{R}^4}, \quad \bar{\rho}_c = \frac{\bar{M}}{\bar{R}^3}, \quad \bar{\varepsilon}_c = \frac{\bar{L}}{\bar{M}}. \quad (1.12)$$

Even for very different structures of stars, it is impossible to obtain distorted results by the formulae. As we saw in the previous paragraph, we can calculate the temperature (or, which is equivalent, the radiant pressure) in two ways, either way being connected to suppositions. First, the radiant pressure can be obtained through the flow of energy, i. e. through  $\varepsilon$  by formula (1.4a). The exact formula of that relation, by equations (1.27) in §1.3 (Part I), is

$$B_c = \frac{\varepsilon_c \kappa_c}{4\pi G c \lambda} p_c, \quad (1.13)$$

where  $\lambda$  is the structural parameter of the main system of the dimensionless equations of equilibrium: its numerical value is about 1. Second, for an ideal gas, the radiant pressure can be calculated directly from formulae (1.12)

$$\frac{\bar{B}_c}{\bar{\mu}^4} = \left( \frac{\bar{p}_c}{\bar{\rho}_c} \right)^4 = \frac{\bar{M}^4}{\bar{R}^4}. \quad (1.14)$$

Formulae (1.13) and (1.14) must lead to the same result. This requirement leads to the "mass-luminosity" relation. Our conclusion that all stars (except for white dwarfs) are built on an ideal gas is so well grounded that it is fair to use formula (1.14) in order to calculate the temperature or the radiant pressure in stars. Naturally, Eddington [21] showed: under temperatures of about a few million degrees, because of the ionization of matter, the atoms of even heavy elements take up so little space (about one millionth of their normal sizes) that van der Waals' corrections are negligible if the density is even much more than 1. However, because of plasma, there could be substantial electrostatic interactions between particles, making the pressure negative, and the gas approaches properties of a super-ideal one. The approximate theory of such phenomena in strong electrolytes has been developed by Debye and Hückell. Eddington and Rosseland applied the theory to a gas inside stars. They came to the conclusion that the electric pressure cannot substantially change the internal constitution of stars. Giving no details of that theory, we can show directly that the electric pressure is negligible in stars built on hydrogen. We compare the kinetic energy of particles to the energy of Coulomb interaction

$$kT > \frac{z^2 e^2}{r}.$$

As soon as the formula becomes true in a gas, the gas becomes ideal. Cubing the equation we obtain

$$\frac{(kT)^3}{n} = \frac{(kT)^4}{p} > z^6 e^6,$$

where  $n$  is the number of particles in a unit volume. Because the radiant pressure is given by the formula

$$B = \frac{\pi^2 (kT)^4}{45 (\hbar c)^3}, \quad (1.6a)$$

a gas becomes ideal as soon as the ratio between the radiant pressure and the gaseous pressure becomes

$$\gamma > \frac{\pi^2 z^6}{45} \left( \frac{e^2}{\hbar c} \right)^3.$$

Because of formula (1.9), this ratio is determined by the mass of a star. Because  $\gamma = 1$  under  $\bar{M} = 100$ , we obtain  $\gamma^{\frac{1}{2}} \approx \bar{M}/100$ . So, for an ideal gas, we obtain the condition

$$100 M_{\odot} > M > \frac{100\pi}{\sqrt{45}} z^3 \left( \frac{e^2}{\hbar c} \right)^{3/2} M_{\odot}. \quad (1.15)$$

which is dependent only on the mass of a star.

For hydrogen or singly ionized elements, we have  $z = 1$ . Hence, for hydrogen contents of stars, the electric pressure can play a substantial rôle only in stars with masses less than 0.01–0.02 of the mass of the Sun.

It is amazing that of all possible states of matter in stars there are realized those states which are the most simple from the theoretical point of view.

Now, if we know  $\bar{M}$  and  $\bar{R}$  for a star, assuming the same molecular weight  $\bar{\mu} = 1$  for all stars (by our previous conclusions), we can calculate its central characteristics  $\bar{\rho}_c$  and  $\bar{T}_c$  by formulae (1.12) and (1.14). The range, within which the calculated physical parameters are located, is so large ( $10^{-8} < \bar{\rho}_c < 10^6$ ,  $10^{-2} < \bar{T}_c < 10^2$ ,  $10^{-3} < \bar{\varepsilon}_c < 10^4$ ), that we use logarithmic scales. We use the abscissa for  $\log \bar{\rho}_c$ , while the ordinate is used for  $\log \bar{B}_c$  (or equivalently,  $4 \log \bar{T}_c$ ). If an energy generation law like  $\varepsilon_c = f(\rho_c, T_c)$  exists in Nature, the points  $\log \bar{\varepsilon}_c$  plotted along the  $z$ -coordinate axis will build a surface. On the other hand, the equilibrium condition requires formula (1.13), so the equilibrium states of stars should be possible only at the transection of the above surfaces\*. Hence, stars should be located in the plane ( $\log \bar{\rho}_c$ ,  $\log \bar{B}_c$ ) along a line which is actually the relation  $M(R)$  transformed to the physical characteristics inside stars. There in the diagram, we draw the numerical values of  $\log \bar{\varepsilon}_c$  in order to picture the whole volume.

### 1.3 The arc of nuclear reactions

The equation for the generation of energy by thermonuclear reactions is

$$\varepsilon = A \rho \tau^2 \varepsilon^{-\tau}, \quad \tau = \frac{a}{T_m^{1/3}}, \quad (1.16)$$

\*The energy generation surface, drawn from the energy generation law  $\varepsilon_c = f(\rho_c, T_c)$ , and the energy drainage surface, drawn from formula (1.13).

where  $T_m$  is temperature expressed in millions of degrees. For instance, for the proton-proton reaction, the constants  $a$  and  $A$  take the values

$$a = 33.8, \quad A = 4 \times 10^3. \quad (1.17)$$

In order to find the arc of the relation between  $\rho_c$  and  $B_c$ , on which stars should be located if nuclear reactions are the sources of their energy, we eliminate  $\varepsilon_c$  from formula (1.16) by formula (1.13)

$$\lambda 4\pi G c B_c = A \kappa_c p_c \rho_c \tau_c^2 e^{-\tau_c}. \quad (1.18)$$

As the exponent indicates (see formula (1.16)),  $\varepsilon$  is very sensitive to temperature. Therefore, inside such stars, a core of free convection should exist, as was shown in detail in Part I, §2.8. We showed there that  $\lambda$  cannot be calculated separately for stars within which there is a convective core: the equilibrium equations determine only  $\lambda L_{x_0}$ , where  $L_{x_0}$  is the dimensionless luminosity

$$L_{x_0} = \int_0^{x_0} \varepsilon_1 \rho_1 x^2 dx. \quad (1.19)$$

In this formula  $x_0$  is the dimensionless radius (see Part I). The subscript 1 on  $\varepsilon$  and  $\rho$  means that the quantities are taken in terms of their numerical values at the centre of a star. In the case under consideration (stars inside which thermonuclear reactions occur).

$$L_{x_0} = \int_0^{x_0} \rho_1^2 \tau_1^2 e^{-(\tau_1 - \tau_c)} x^2 dx.$$

Because this integral includes the convective core (where  $\rho_1 = T_1^{3/2}$ ),

$$L_{x_0}(\tau_c) = \int_0^{x_0} T_1^{1/3} x^2 e^{-\tau_c (T_1^{-1/3} - 1)} dx. \quad (1.20)$$

The integral  $L_{x_0}(\tau_c)$  can be easily taken by numerical methods, if we use Emden's solution  $T_1(x)$  for stars of the polytropic structure  $3/2$ . The calculations show that numerical values of the integral taken under very different  $\tau_c$  are very little different from 1. For instance,

$$L_{x_0}(33.8) = 0.67, \quad L_{x_0}(7.3) = 1.15.$$

For the proton-proton reactions formula (1.17), the first value of  $L_{x_0}$  is 1 million degrees at the centre of a star, the second value is one hundred million degrees. Assuming  $L_{x_0} \approx 1$  (according to our conclusions in Part I), Table 3 gives  $\lambda \approx 3$  in stars where the absorption coefficient is constant.

In Part I of this research we found the average molecular weight  $1/2$  for all stars. We also found that all stars have structures very close to the polytropic structure of the class  $3/2$ . Under these conditions, the central temperature of the Sun should be  $6 \times 10^6$  degrees. Therefore Bethe's carbon-nitrogen

cycle is improbable as the source of stellar energy. As an example, we consider proton-proton reactions. Because of the numerical values obtained for the constants  $a$  and  $A$  (1.17), formula (1.18) gives

$$\log \rho_c = 0.217 \tau_c - 5.5 \log \tau_c + 5.26 - \frac{1}{2} \log \frac{\kappa_c}{\mu}. \quad (1.21)$$

Taking  $\kappa_c/\mu$  constant in this formula, we see that  $\rho_c$  has the very slanting minimum (independent of the temperature) at  $\tau_c = 11$  that is  $T_c = 30 \times 10^6$  degrees. In a hydrogen star where the absorption coefficient is Thomson, the last term of (1.21) is zero and the minimal value of  $\rho_c$  is 100. Hence, stars undergoing proton-proton reactions internally should be located along the line  $\rho_c \approx 100$  in the diagram for  $(\rho_c, B_c)$ . It appears that stars of the main sequence satisfy the requirement (in a rude approximation). Therefore, it also appears that the energy produced by thermonuclear reactions could explain the luminosity of most of stars. But this is only an illusion. This illusion disappears completely as soon as we construct the diagram for  $(\log \bar{\rho}_c, \log \bar{B}_c)$  using the data of observational astronomy.

#### 1.4 Distribution of stars on the physical conditions diagram

Currently we know all three parameters (the mass, the bolometric absolute stellar magnitude, and the spectral class) for approximately two hundred stars. In our research we should use only independent measurements of the quantities. For this reason, we cannot use the stellar magnitudes obtained by the spectroscopic parallax method, because the basis of this method is the “mass-luminosity” relation.

For stars of the main sequence we used the observational data collection published in 1948 by Lohmann [26], who generalized data by Parenago and Kuiper. For eclipse variable stars we used data collections mainly by Martynov [27], Gaposchkin [28], and others. Finally, we took particularly interesting data about super-giants from collections by Parenago [29], Kuiper [7], and Struve [30]. Some important data about the masses of sub-dwarfs were given to the writer by Prof. Parenago in person, and I'm very grateful to him for his help, and critical discussion of the whole research. Consequently, we used the complete data of about 150 stars.

The stellar magnitudes were obtained by the above mentioned astronomers by the trigonometric parallaxes method and the empirically obtained bolometric corrections (Petit, Nickolson, Kuiper). In order to go from the spectral class to the effective temperature, we used Kuiper's temperature scale. Then we calculated the radius of a star by the formula

$$5 \log \bar{R} = 4.62 - m_b - 10 \log \bar{T}_{\text{eff}}, \quad (1.22)$$

where  $m_b$  is the bolometric stellar magnitude of the star. Then, by formulae (1.12) and (1.14), we calculated  $\log \bar{\rho}_c$ ,

$\log \bar{B}_c, \log \bar{\epsilon}_c$ . We calculated the characteristics for every star on our list. The results are given in Fig. 2\*. There the abscissa takes the logarithm of the matter density,  $\log \bar{\rho}_c$ , while the ordinate takes the logarithm of the radiant energy density,  $\log \bar{B}_c$ , where both values are taken at the centre of a star<sup>†</sup>. Each star is plotted as a point in the numerical value of  $\log \bar{\epsilon}_c$  — the energy productivity per second from one gramme of matter at the centre of a star with respect to the energy productivity per second at the centre of the Sun. In order to make exploration of the diagram easier, we have drawn the net values of the fixed masses and radii. Bold lines at the left side and the right side are the boundaries of that area where the ideal gas law is true (stars land in exactly this area). The left bold line is the boundary of the ultimately large radiant pressure ( $\gamma = 1$ ). The bold line in the lower part of the diagram is the boundary of the ultimately large electric pressure, drawn for hydrogen by formula (1.15). This line leads to the right side bold lines, which are the boundaries of the degeneration of gas calculated for hydrogen (the first line) and heavy elements (the second line).

We built the right boundary lines in the following way. We denote by  $n_e$  the number of free electrons inside one cubic centimetre, and  $\mu_e$  the molecular weight per electron. Then

$$\rho = \mu_e m_H n_e,$$

so Sommerfeld's condition of degeneration

$$\frac{n_e \hbar^3}{2} \frac{1}{(2\pi m_e k T)^{3/2}} > 1 \quad (1.23)$$

can be re-written as

$$\rho > 10^{-8} \mu_e T^{3/2}. \quad (1.24)$$

For the variables  $p$  and  $\rho$ , we obtain the degeneration boundary equation<sup>‡</sup>

$$\begin{aligned} p &= k \mu_e^{5/3} \rho^{5/3}, \\ \bar{p} &= k \frac{\rho_{\odot}^{5/3}}{p_{\odot}} \bar{\rho}^{5/3} \mu_e^{5/3}, \end{aligned} \quad (1.25)$$

which coincides with the Fermi gas state equation  $p = K \rho^{5/3} = K_H \mu_e^{5/3} \rho^{5/3}$  (formula 1.9 in Part I), if

$$K \approx K_H = 9.89 \times 10^{12}.$$

\*Of course not all the stars are shown in the diagram, because that would produce a very dense concentration of points. At the same time, the plotted points show real concentrations of stars in its different parts. — Editor's remark.

<sup>†</sup>The bar means that both values are expressed in multiples of the corresponding values at the centre of the Sun. — Editor's remark.

<sup>‡</sup>The degeneration boundary equation is represented here in two forms: expressed in absolute values of  $p$  and in multiples of the pressure in the Sun. — Editor's remark.



At the centre of the Sun, as obtained in Part I of this research (see formula 3.34),

$$\begin{aligned} \rho_{c\odot} &= 9.2, & p_{c\odot} &= 9.5 \times 10^{15}, \\ \gamma_{c\odot} &= 0.4 \times 10^{-3}, & B_{c\odot} &= 3.8 \times 10^{12}, \\ T_{c\odot} &= 6.3 \times 10^6, \end{aligned} \quad (1.26)$$

then we obtain

$$\bar{p} = 4 \times 10^{-2} \bar{\rho}^{5/3} \mu_e^{5/3}.$$

The right side boundaries drawn in the diagram are constructed for  $\mu_e = 1$  and  $\mu_e = 2$ . At the same time these are lines along which stars built on a degenerate gas (the lines of Chandrasekhar's "mass-radius" relation) should be located. In this case the ordinate axis has the meaning  $\log(\bar{p}/\bar{\rho})^4$  that becomes the logarithm of the radiant energy density  $\log \bar{B}$  for ideal gases only. In this sense we have drawn white dwarfs and Jupiter on the diagram. Under low pressure, near the boundary of strong electric interactions, the degeneration lines bend. Then the lines become constant density lines, because of the lowering of the ionization level and the appearance of normal atoms. The lines were constructed according to Kothari's "pressure-ionization" theory [31]. Here we see a wonderful consequence of Kothari's theory: the maximum radius which can be attained by a cold body is about the radius of Jupiter.

Finally, this diagram contains the arc along which should be located stars whose energy is generated by proton-proton reactions. The arc is built by formula (1.21), where we used the central characteristics of the Sun (1.26) obtained in Part I.

The values  $\log \bar{\varepsilon}_c$  plotted for every star builds the system of isoergs — the lines of the same productivity of energy. The lines were drawn through the interval of ten changes of  $\bar{\varepsilon}_c$ . If a "mass-luminosity" relation for stars does not contain their radii,  $\bar{\varepsilon}_c$  should be a function of only the masses of stars. Hence, the isoergs should be parallel to the constant mass lines. In general, we can suppose the "mass-luminosity" relation as the function

$$L \sim M^\alpha, \quad (1.27)$$

then the interval between the neighbouring isoergs should decrease with increasing  $\alpha$  according to the picture drawn in the upper left part of the diagram. We see that the real picture does not correspond to formula (1.27) absolutely. Only for giants, and the central region of the main sequence (at the centre of the diagram) do the isoergs trace a path approximately parallel to the constant mass lines at the interval  $\alpha = 3.8$ . In all other regions of the diagram the isoergs  $\bar{\varepsilon}_c$  are wonderfully curved, especially in the regions of supergiants (the lower left part of the diagram) and hot sub-dwarfs (the upper right part). As we will soon see, the curvilinearity can be explained. In the central concentration

of stars we see two opposite tendencies of the isoergs to be curved. We have a large dataset here, so the isoergs were drawn very accurately. The twists are in exact agreement with the breaks, discovered by Lohmann [26], in the "mass-luminosity" relation for stars of the main sequence. It is wonderful that this tendency, intensifying at the bottom, gives the anomalously large luminosities for sub-giants (the satellites of Algol) — the circumstance, considered by Struve [30]. For instance, the luminosity of the satellite of XZ Sagittarii, according to Struve, is ten thousand times more than that calculated by the regular "mass-luminosity" relation. There we obtain also the anomalously large luminosity, discovered by Parenago [29], for sub-dwarfs of small masses. The increase of the opposite tendency at the top verifies the low luminosity of extremely hot stars, an increase which leads to Trumpler stars. It is very doubtful that masses of Trumpler stars measured through their Einstein red shift are valid. For this reason, the diagram contains only Trumpler stars of "intermediate" masses. Looking at the region of sub-giants and sub-dwarfs (of large masses and of small ones) we see that  $\varepsilon$  is almost constant there, and independent of the masses of the stars. Only by considering altogether the stars located in the diagram we can arrive at the result obtained in Part I of this research:  $L \sim M^3$ .

So, the first conclusion that can be drawn from our consideration of the diagram is: deviations from the "mass-luminosity" relation are real, they cannot be related to systematic errors in the observational data. The possibility of drawing the exact lines of constant  $\bar{\varepsilon}_c$  itself is wonderful: it shows that  $\varepsilon$  is a simple function of  $\rho$  and  $B$ . Hence, the luminosity  $L$  is a simple function of  $M$  and  $R$ . Some doubts can arise from the region located below and a little left of the central region of the diagram, where the isoergs do not coincide with  $L$  for sub-dwarfs of spectral class F–G and  $L$  of normal dwarfs of class M. It is most probable that the inconsistency is only a visual effect, derived from errors in experimental measurements of the masses and radii of the sub-dwarfs.

As a whole our diagram shows the plane image of the surface  $\varepsilon(\rho, B)$ . We obtained much more than expected: we should obtain only one section of the surface, but we obtained the whole surface, beautifully seen in the central region of the diagram. Actually, we see no tendency for stars to be distributed along a sequence  $\varepsilon = \text{const}$ . Thus, of the two equations determining  $\varepsilon$ , there remains only one: *the energy productivity in stars is determined by the energy drainage (radiation) only*. This conclusion is very important. Thus the mechanism that generates energy in stars is not of any kind of reactions, but is like the generation of energy in the process of its drainage. The crude example is the energy production when a star, radiating energy into space, is cooling down: the star compresses, so the energy of its gravitational field becomes free, cooling the star (the well-known Helmholtz-Kelvin mechanism). Naturally, in a cooling down (compress-

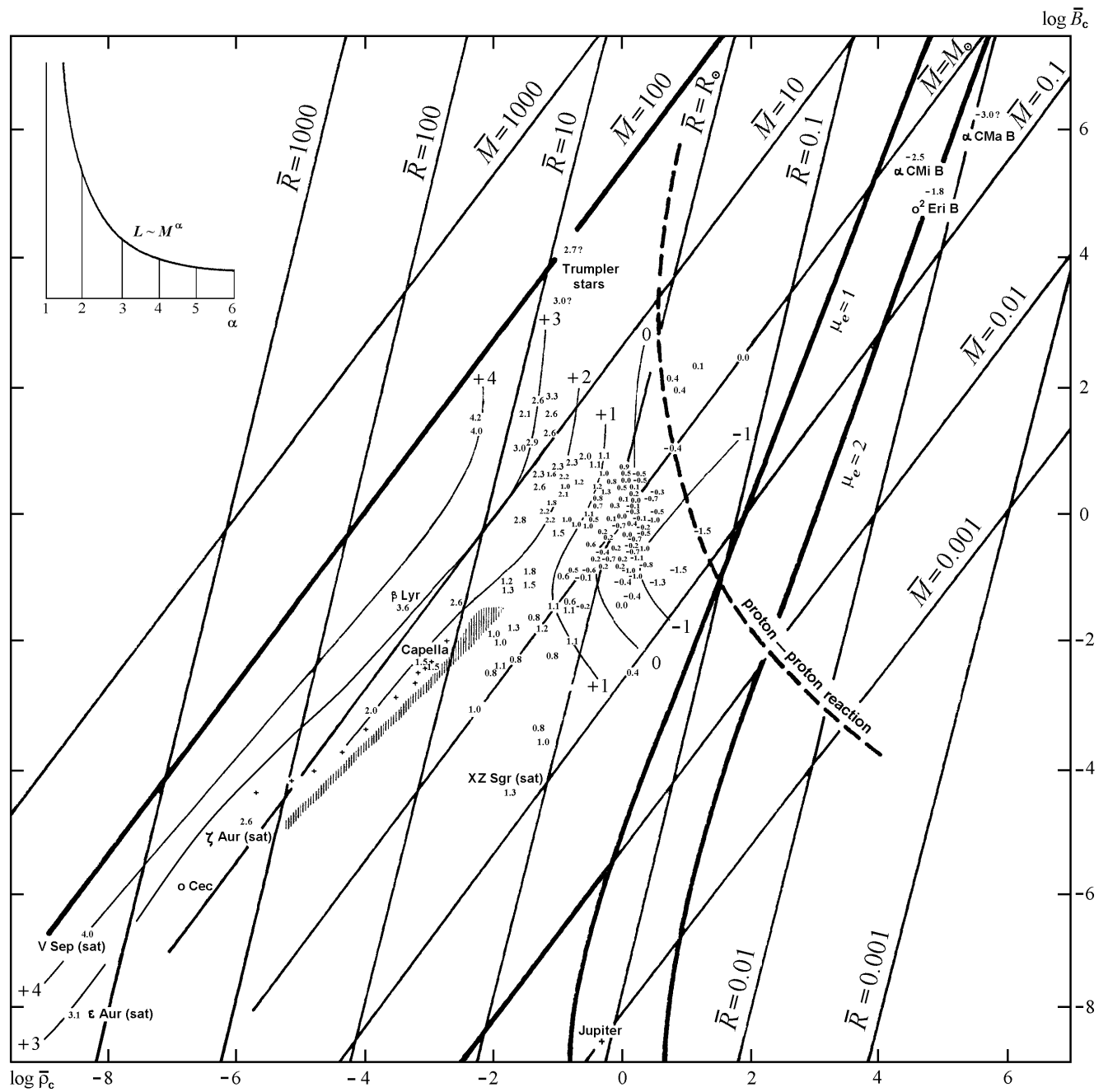


Fig. 2: The diagram of physical conditions inside stars (the stellar energy diagram); the productivity of stellar energy sources independence of the physical conditions in the central regions of stars. The abscissa is the logarithm of the density of matter, the ordinate is the logarithm of the radiant energy density (both are taken at the centre of stars in multiples of the corresponding values at the centre of the Sun). The small diagram at the upper left depicts the intervals between the neighbouring isoergs.

ing) star the quantity of energy generated is determined by the speed of this process. At the same time the speed is regulated by the heat drainage. Of course, the Helmholtz-Kelvin mechanism is only a crude example, because of the inapplicable short period of the cooling (a few million years). At the same time the mechanism that really generates energy in stars should also be self-regulating by the radiation. In contrast to reaction, such a mechanism should be called a *machine*.

It should be noted that despite many classes of stars in the diagram, the filling of the diagram has some limitations.

First there is the main direction along which stars are concentrated under a huge range of physical conditions — from the sequence of giants, then the central concentration in our diagram (the so-called main sequence of the Hertzsprung-Russel diagram), to sub-dwarfs of class A and white dwarfs. In order to amplify the importance of this direction, we indicated the main location of normal giants by a hatched strip. The main direction wonderfully traces an angle of exactly  $45^\circ$ . Hence, all stars are concentrated along the line, determined by the equation\*

$$B \sim \rho \mu^4. \quad (1.28)$$

Because stars built on a degenerate gas satisfy this direction, a more accurate formula is

$$p \sim \rho^{5/5} \quad (1.28a)$$

Second, there is in the main direction (1.28) a special point — the centre of the main sequence†, around which stars are distributed at greater distances, and in especially large numbers.

Thus, there must exist two fundamental constants which determine the generation of energy in stars:

1. The coefficient of proportionality of equation (1.28);
2. One of the coordinates of the “main point”, because its second coordinate is determined by the eq. (1.28).

The above mentioned symmetry of the surface  $\varepsilon(\rho, B)$  is connected to the same two constants.

Concluding the general description of the diagram, we note: this diagram can also give a practical profit in calculations of the mass of a star by its luminosity and the spectral class. Naturally, having the radius calculated, we follow the line  $R = \text{const}$  to that point where  $\log \bar{\varepsilon} + \log \bar{M}$  gives the observed value of  $\log \bar{L}$ .

### 1.5 Inconsistency of the explanation of stellar energy by Bethe's thermonuclear reactions

It is seemingly possible that the existence of the uncovered main direction along which stars are concentrated in our

diagram support a stellar energy mechanism like reactions. In the real situation the equation of the main direction (1.28) contradicts the kinetics of any reaction. Naturally, equation (1.28) can be derived from the condition of energy drainage (1.13) only if

$$\varepsilon \sim \frac{1}{T}, \quad \text{under } \rho \sim T^4, \quad (1.29)$$

i. e. only if the energy productivity increases with decrease in temperature and hence the density. The directions of all the isoergs in the diagram, and also the numerical values  $\varepsilon = 10^3 - 10^4$  in giants and super-giants under the low temperatures inside them (about a hundred thousands degrees) cannot be explained by nuclear reactions. It is evident therefore, that the possibility for nuclear reactions is just limited by the main sequence of the Russell-Hertzsprung diagram (the central concentration of stars in our diagram).

The proton-proton reaction arc is outside the main sequence of stars. If we move the arc to the left, into the region of the main sequence stars, we should change the constant  $A$  in the reaction equation (1.16) or change the physical characteristics at the centre of the Sun (1.26) as we found in Part I. Equation (1.18) shows that the shift of the proton-proton reaction arc along the density axis is proportional to the square of the change of the reaction constant  $A$ . Hence, in order to build the proton-proton reaction arc through the main concentration of stars we should take at least  $A = 10^5 - 10^6$  instead of the well-known value  $A = 4 \times 10^3$ . This seems very improbable, for then we should ignore the central characteristics of the Sun that we have obtained, and hence all conclusions in Part I of this research which are in fine agreement with observational data. Only in a such case could we arrive at a temperature of about 20 million degrees at the centre of the Sun; enough for proton-proton reactions and also Bethe's carbon-nitrogen cycle.

All theoretical studies to date on the internal constitution of stars follow this approach. The sole reason adduced as proof of the high concentration of matter in stars, is the slow motion of the lines of apsides in compact binaries. However the collection published by Luyten, Struve, and Morgan [32] shows no relation between the velocity of such motion and the ratio of the star radius to the orbit semi-axis. At the same time, such a relation would be necessary if the motion of the lines of apsides in a binary system is connected to the deformations of the stars. Therefore we completely agree with the conclusion of those astronomers, that no theory correctly explains the observed motions of apsides. Even if we accept that the arc of nuclear reactions could intersect the central concentration of stars in our diagram (the stars of the main sequence in the Russell-Hertzsprung diagram), we should explain why the stars are distributed not along this arc, but fill some region around it. One could explain this circumstance by a “dispersion” of the parameters included in the main equations. For instance, one relates this dispersion

\*See formula (1.14). — Editor's remark.

†The main sequence in the sense of the Russell-Hertzsprung diagram, is here the central concentration of stars. — Editor's remark.

to possible differences in the chemical composition of stars, their structure etc. Here we consider the probability of such explanations.

The idea that stars can have different chemical compositions had been introduced into the theory in 1932 by Strömngren [16], before Bethe's hypothesis about nuclear sources for stellar energy. He used only the heat drainage condition (1.13), which leads to the "mass-luminosity" relation (1.7a) for ideal gases. In chapter 2 of Part I we showed in detail that the theoretical relation (1.7a) is in good agreement (to within the accuracy of Strömngren's data) with the observed correlation for hydrogen stars (where we have Thomson's absorption coefficient, which is independent of physical conditions). Introducing some a priori suppositions (see §2.7, Part I), Eddington, Strömngren and other researchers followed another path; they attempted to explain non-transparency of stellar matter by high content of heavy elements, which build the so-called Russell mix. At the same time the absorption theory gives such a correlation  $\kappa(\rho, B)$  for this mix which, being substituted into formula (1.7a), leads to incompatibility with observational data. Strömngren showed that such a "difficulty" can be removed if we suppose different percentages of heavy elements in stars, which substantially changes the resulting absorption coefficient  $\kappa$ . Light element percentages  $X$  can be considered as the hydrogen percentage. Comparing the theoretical formula to the observable "mass-luminosity" relation gives the function  $X(\rho, B)$  or  $X(M, R)$ . Looking at the Strömngren surface from the physical viewpoint we can interpret it as follows. As we know, the heat drainage equation imposes a condition on the energy generation in stars. This is condition (1.13), according to which  $\kappa$  and  $\mu$  depend on the chemical composition of a star. Let us suppose that the chemical composition is determined by one parameter  $X$ . Then

$$\varepsilon = f_1(\rho, B, X). \quad (\text{I})$$

For processes like a reaction, the energy productivity  $\varepsilon$  is dependent on the same variables by the equation of this reaction

$$\varepsilon = f_2(\rho, B, X). \quad (\text{II})$$

So we obtain the condition  $f_1 = f_2$ , which will be true only if a specific relation  $X(\rho, B)$  is true in the star. The parameter  $X$  undergoes changes within the narrow range  $0 \leq X \leq 1$ , so stars should fill a region in the plane  $(\rho, B)$ . Some details of the Russell-Hertzsprung diagram can be obtained as a result of an additional condition, imposed on  $X(\rho, B)$ : Strömngren showed that arcs of  $X = \text{const}$  can be aligned with the distribution of stars in the Russell-Hertzsprung diagram. Kuiper's research [33] is especially interesting in this relation. He discovered that stars collected in open clusters are located along one of Strömngren's arcs  $X = \text{const}$  and that the numerical values of  $X$  are different for different clusters. Looking at this result, showing that stellar

clusters are different according to their hydrogen percentage, one can perceive an evolutionary meaning — the proof of the nuclear transformations of elements in stars.

Strömngren's research prepared the ground for checking the whole nuclear hypothesis of stellar energy: substituting the obtained correlation  $X(\rho, B)$  into the reaction equation (II), we must come to the well-known relation (I). The nuclear reaction equation (1.16), where  $X$  is included through  $A$ , had not passed that examination. Therefore they introduced the second parameter  $Y$  into the theory — the percentage of helium. As a result, every function  $f_1$  and  $f_2$  can be separately equated to the function  $\varepsilon(\rho, B)$  known from observations. Making the calculations for many stars, it is possible to obtain two surfaces:  $X(\rho, B)$  and  $Y(\rho, B)$ . However, both surfaces are not a consequence of the equilibrium conditions of stars. It remains unknown as to why such surfaces exist, i.e. why the observed  $\varepsilon$  is a simple function of  $\rho$  and  $B$ ? It is very difficult to explain this result by evolutionary transformations of  $X$  and  $Y$ , if the transformation of elements proceeds in only one direction. Of course, taking a very small part of the plane  $(\rho, B)$ , the evolution of elements can explain changes of  $X$  and  $Y$ . For instance, calculations made by Masevich [34] gave a monotone decrease of hydrogen for numerous stars located between the spectral classes B and G. To the contrary, from the class G to the class M, the hydrogen percentage increases again (see the work of Lohmann work [26] cited above). As a result we should be forced to think that stars evolve in two different ways. In such a case the result that the chemical composition of stars is completely determined by the physical conditions inside them can only be real if there is a balanced transformation of elements. Then the mechanism that generates energy in stars becomes the Helmholtz-Kelvin mechanism, not reactions. Nuclear transformations of elements only become an auxiliary circumstance which changes the thermal capacity of the gas. At the same time, the balanced transformation of elements is excluded from consideration, because it is possible only if the temperature becomes tens of billions of degrees, which is absolutely absent in stars.

All the above considerations show that the surfaces  $X(\rho, B)$  and  $Y(\rho, B)$  obtained by the aforementioned researchers are only a result of the trimming of formulae (I) and (II) to the observed relation  $\varepsilon(\rho, B)$ . Following this approach, we cannot arrive at a solution to the stellar energy problem and the problem of the evolution of stars. This conclusion is related not only to nuclear reactions; it also shows the impossibility of any sources of energy whose productivity is not regulated by the heat drainage condition. Naturally, the coincidence of the surfaces (I) and (II) manifests their identity. In a real situation the second condition is not present\*.

\*For reactions, the energy productivity increases with the increase of the density. In the heat drainage condition we see the opposite: equation (1.13). Therefore the surfaces (I) and (II), located over the plane  $(\rho, B)$ , should be oppositely inclined — their transection should be very sharp.

So we get back to our conclusion of the previous paragraph: there are special physical conditions, the main direction (1.28) and the main point in the plane  $(\rho, B)$ , about which stars generate exactly as much energy as they radiate into space. In other words, stars are *machines* which generate radiant energy. The heat drainage is the power regulation mechanism in the machines.

### 1.6 The “mass-luminosity” relation in connection with the Russell-Hertzsprung diagram

The luminosity of stars built on an ideal gas, radiant transfer of energy and low radiant pressure, is determined by formula (1.7a). This formula is given in its exact form by (2.38) in Part I. We re-write formula (2.38) as

$$\bar{\varepsilon} = \frac{\bar{L}}{\bar{M}} = 1.04 \times 10^4 \frac{\mu^4}{\kappa_c} \left( \frac{\lambda L_{x_0}}{M_{x_0}^3} \right) \bar{M}^2, \quad (1.30)$$

where  $M_{x_0}$  is the dimensionless mass of a star,  $\kappa_c$  is the absorption coefficient at its centre. It has already been shown that the structural multiplier of this formula has approximately the same numerical value

$$\frac{\lambda L_{x_0}}{M_{x_0}^3} \simeq 2 \times 10^{-3} \quad (1.31)$$

for all physically reasonable models of stars. The true “mass-luminosity” relation is shown in Fig. 2 by the system of isoergs  $\bar{\varepsilon} = \bar{L}/\bar{M} = \text{const}$ . If we do not take the radius of a star into account, we obtain the correlation shown in Fig. 1, Part I. There  $L$  is approximately proportional to the cube of  $M$ , although we saw a dispersion of points near this direction  $L \sim M^3$ . As we mentioned before, in Part I, the comparison of this result to formula (1.30) indicates that: (1) the radiant pressure plays no substantial rôle in stars, (2) stars are built on hydrogen.

Now we know that the dispersion of points near the average direction  $L \sim M^3$  is not stochastic. So we could compare the exact correlation to the formula (1.30), and also check our previous conclusions.

Our first conclusion about the negligible rôle of the radiant pressure is confirmed absolutely, because of the mechanical equilibrium of giants. Naturally, comparing formula (1.7b) to (1.7a), we see that the greater the rôle of the radiant pressure, the less  $\varepsilon$  is dependent on  $M$ , so the interval between the neighbouring isotherms should increase for large masses. Such a tendency is completely absent for bulky stars (see the stellar energy diagram, Fig. 2). This result, in combination with formula (1.9) (its exact form is formula 2.47, Part I), leads to the conclusion that giants are built mainly on hydrogen (the molecular weight  $1/2$ ). Thus we calculate the absorption coefficient for giants. We see in the diagram that red giants of masses  $\approx 20M_\odot$  have  $\log \bar{\varepsilon} = 3$ .

By formulae (1.30) and (1.31), we obtain

$$\frac{\kappa_c}{\mu^4} = 8. \quad (1.32)$$

If  $\mu = 1/2$ , we obtain  $\kappa_c = 0.5$ . This result implies that the non-transparency of giants is derived from Thomson’s dispersion of light in free electrons ( $\kappa_T = 0.40$ ), as it should be in a pure hydrogen star.

The main peculiarity of the “mass-luminosity” relation is the systematic curvilinearity of the isoergs in the plane  $(\rho, B)$ . Let us show that this curvilinearity cannot be explained by the changes of the coefficient in formula (1.30). First we consider the multiplier containing the molecular weight and the absorption coefficient.

The curvilinearity of the isoergs shows that for the same mass the diagram contains anomalous low luminosity stars at the top and anomalous bright stars at the bottom. Hence, the left part of (1.32) should increase under higher temperatures, and should decrease with lower temperatures. Looking from the viewpoint of today’s physics, such changes of the absorption coefficient are impossible. Moreover, for the ultimate inclinations of the isoergs, we obtain absolutely impossible numerical values of the coefficient (1.32). For instance, in the case of super-giants, the lower temperature stars, this coefficient is 100 times less than that in giants. Even if we imagine a star built on heavy elements, we obtain that  $\kappa$  is about 1. In hot super-giants (the direction of Trumpler stars) the coefficient (1.32) becomes 200. Because of high temperatures in such stars, the absorption coefficient cannot be so large.

In order to explain the curvilinearity by the structural multiplier (1.31), we should propose that it be anomalously large in stars of high luminosity (sub-giants) and anomalously small in stars like Trumpler stars. We note that the dimensionless mass  $M_{x_0}$  included in (1.31) cannot be substantially changed, as shown in Part I. So the structural multiplier (1.31) can be changed by only  $\lambda L_{x_0}$ . Employing the main system of the dimensionless equations of equilibrium of stars, we easily obtain the equation

$$\frac{dB_1}{dp_1} = \frac{\lambda L_x}{M_x}, \quad (1.33)$$

which is equation (2.22) of Part I, where  $B_1$  and  $p_1$  are the radiant pressure and the gaseous pressure expressed in multiples of their values at the centre of a star. Here the absorption coefficient  $\kappa$  is assumed constant from the centre to the surface, i. e.  $\kappa_1 = 1$ . Applying this equation to the surface layers of a star, we deduce that the structural coefficient is

$$\frac{\lambda L_{x_0}}{M_{x_0}} = \frac{B_1}{p_1}. \quad (1.34)$$

We denote the numerical values of the functions at the boundary between the surface layer and the “internal” layers

of a star by the subscript 0. We consider two ultimate cases of the temperature gradients within the “internal” layers:

1. The “internal” zone of a star is isothermal:

$$\frac{\lambda L_{x_0}}{M_{x_0}} = \frac{1}{p_{1_0}}, \quad (1.34a)$$

2. The “internal” zone of a star is convective ( $B_1 = p_1^{8/5}$ ):

$$\frac{\lambda L_{x_0}}{M_{x_0}} = p_{1_0}. \quad (1.34b)$$

In the first theoretical case, spreading the isothermal zone to almost the surface of a star, we can make the structural coefficient as large as we please. This case is attributed to sub-giants and anomalous bright stars in general. The second theoretical case can explain stars of anomalously low luminosity. Following this way, i. e. spreading the convective zone inside stars, Tuominen [35] attempted to explain the low luminosity of Trumpler stars.

The isothermy can appear if energy is generated mainly in the upper layers of a star. The spreading of the convective zone outside the Schwarzschild boundary can occur if energy is generated in moved masses of stellar gas, i. e. under forced convection. A real explanation by physics should connect the above peculiarities of the energy generation to the physical conditions inside stars or their general characteristics  $L$ ,  $M$ ,  $R$ . Before attempting to study the theoretical possibility of such relations, it is necessary to determine them first from observational data. Dividing  $\bar{\epsilon}$  by  $\bar{M}^2$  for every star, we obtain the relation of the structural coefficient of formula (1.30) for  $\rho$  and  $B$ . But, at the same time, the determination of this relation in this way is somewhat unclear. There are no clear sequences or laws, so we do not show it here. Generally speaking, a reason should be simpler than its consequences. Therefore, it is most probable that the structural coefficient is not the reason. It is most probable that the reason for the incompatibility of the observed “mass-luminosity” relation with formula (1.30) is that equation (1.30) itself is built incorrectly. This implies that the main equations of equilibrium of stars are also built incorrectly. This conclusion is in accordance with our conclusion in the previous paragraph: energy is generated in stars like in machines — their workings are incompatible with the standard principles of today’s mechanics and thermodynamics.

### 1.7 Calculation of the main constants of the stellar energy state

The theoretical “mass-luminosity” relation (1.30) is obtained as a result of comparing the radiant energy  $B$  calculated by the excess energy flow (formula 1.4a or 1.13) to the same  $B$  calculated by the phase state equation of matter (through  $p$  and  $\rho$  by formula 1.14). Therefore the incompatibility of the theoretical correlation (1.30) to observational data can be

considered as the incompatibility of both the values of  $B$ . So we denote by  $B^*$  the radiant pressure calculated by the ideal gas equation. For the radiant transport of energy in a star, formulae (1.4a) and (1.13) lead to

$$\frac{\bar{B}^*}{\bar{\kappa}} = \bar{\epsilon} \bar{p}. \quad (1.35)$$

By this formula we can calculate  $\bar{B}^*/\bar{\kappa}$  for every star of the stellar energy diagram (Fig. 2). As a result we can find the correlation of the quantity  $\bar{B}^*/\bar{\kappa}$  to  $\bar{p}$  and  $\bar{\rho}$ . Fig. 3 shows the stellar energy diagram transformed in this fashion. Here the abscissa is  $\log \bar{\rho}$ , while the ordinate is  $\log \bar{p}$ . In order to make the diagram readable, we have not plotted all stars. We have plotted only the Sun and a few giants. At the same time we draw the lines of constant  $\bar{B}^*/\bar{\kappa}$  through ten intervals. The lines show the surface  $\log \bar{B}^*/\bar{\kappa}(\log \bar{\rho}, \log \bar{p})$ . For the constant absorption coefficient  $\kappa$ , the lines show the system of isotherms. If  $B^* = B$ , there should be a system of parallel straight lines, inclined at  $45^\circ$  to the  $\log \bar{p}$  axis and following through the interval 0.25. As we see, the real picture is different in principle. There is in it a wonderful symmetry of the surface  $\log \bar{B}^*/\bar{\kappa}$ . Here the origin of the coordinates coincides with the central point of symmetry of the isoergs. At the same time it is the main point mentioned in relation in the stellar energy diagram. The coordinates of the point with respect to the Sun are

$$\begin{aligned} \log \bar{\rho}_0 &= -0.58, & \log \bar{p}_0 &= -0.53, \\ \log \bar{B}_0 &= +0.22, & \log \bar{B}_0^* &= +0.50. \end{aligned} \quad (1.36)$$

Using the data, we deduce that the main point is attributed to a star of the Russell-Hertzsprung main sequence, which has spectral class A4. Rotating the whole diagram around the main point by  $180^\circ$ , we obtain almost the same diagram, only the logarithms of the isotherms change their signs. Hence, if

$$\frac{\frac{B^*}{\kappa}}{\frac{\bar{B}_0^*}{\bar{\kappa}}} = f\left(\frac{p}{p_0}, \frac{\rho}{\rho_0}\right),$$

we have

$$f\left(\frac{p}{p_0}, \frac{\rho}{\rho_0}\right) f\left(\frac{p_0}{p}, \frac{\rho_0}{\rho}\right) = 1. \quad (1.37)$$

The relation (1.37) is valid in the central region of the diagram. An exception is white dwarfs, in which  $B^*/\kappa$  is 100 times less than that required by formula (1.37), i. e. 100 times less than that required for the correspondence to giants after the  $180^\circ$  rotation of the diagram. It is probable that this circumstance is connected to the fact that white dwarfs are located close to the boundary of degenerate gas.

Besides the isotherms, we have drawn the main direction along which stars are distributed. Now the equation of the direction (1.28) can be written in the more precise form

$$\log \frac{\bar{B}}{\bar{\rho}} = +0.80. \quad (1.38)$$

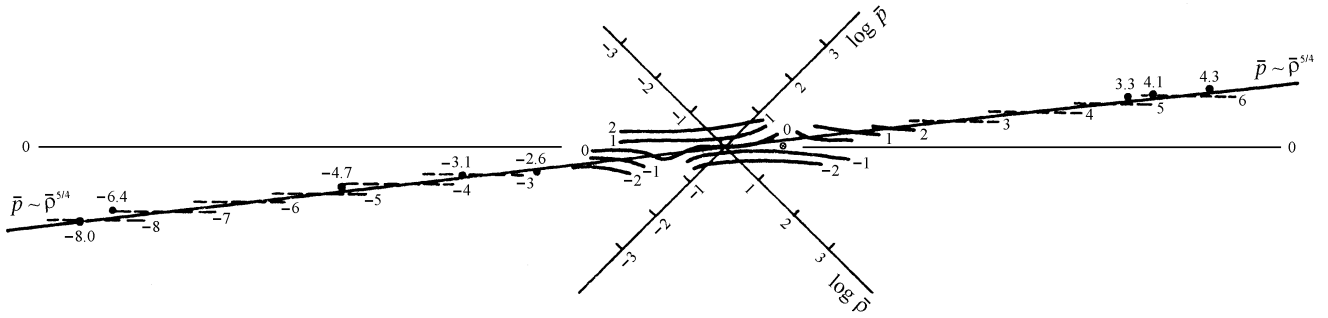


Fig. 3: Isotherms of stellar matter. The coordinate axes are the logarithms of the matter density and the gaseous pressure. Dashed lines show isotherms of an ideal gas.

Because of the very large range of the physical states in the diagram, the main direction is drawn very precisely (to within 5%). It should be noted that, despite their peculiarities, white dwarfs satisfy the main direction like all regular stars.

A theory of the internal constitution of stars, which could explain observational data (the relation 1.37, for instance), should be built on equations containing the coordinates of the main point. This circumstance is very interesting: it shows that there is an absolute system of “physical coordinates”, where physical quantities of absolutely different dimensions can be combined. Such combinations can lead to a completely unexpected source of stellar energy. Therefore it is very important to calculate the absolute numerical values of the constants (1.36). Assuming in (1.36) a mostly hydrogen content for stars  $\mu = 1/2$ , and using the above calculated physical characteristics at the centre of the Sun (1.26), we obtain

$$\rho_0 = 2.4, \quad p_0 = 2.8 \times 10^{15}, \quad B_0 = 6.3 \times 10^{12}. \quad (1.39)$$

We calculate  $B_0^*$  by formula (1.13). Introducing the average productivity of energy  $\varepsilon$

$$B_c^* = \frac{\varepsilon \kappa_c p_c M_{x_0}}{4\pi G c \lambda L_{x_0}}, \quad (1.40)$$

assuming  $\kappa_c$  equal to Thomson’s absorption coefficient,  $\varepsilon_0 = 1.9$ ,  $M_{x_0} = 11$ , and the structural multiplier according to (1.31). We then obtain for the Sun,  $B_{c\odot}^* = 1.1 \times 10^{12}$  instead of  $B_{c\odot} = 3.8 \times 10^{12}$ . Hence,

$$B_0^* = 4.1 \times 10^{12} \approx B_0. \quad (1.41)$$

We introduce the average number of electrons in one cubic centimetre  $n_e$  instead of the density of matter:  $\rho = 1.66 \times 10^{-24} n_e$ . Then the equation of the main direction becomes

$$\frac{3B}{n_e} = 1.4 \times 10^{-11} = 8.7 \text{ eV}, \quad (1.42)$$

which is close to the hydrogen ionization potential, i. e.  $\chi_0 = 13.5 \text{ eV}$ . Thus the average radiant energy per particle in stars (calculated by the ideal gas formula) is constant and

is about the ionization energy of the hydrogen atom. Fig. 3 shows that, besides the main direction, the axis  $\rho = \rho_0$  is also important. Its equation can be formulated through the average distance between particles in a star

$$r = 0.55 (n_e)^{-1/3}$$

as follows

$$r = 0.51 \times 10^{-8} = r_H = \frac{e^2}{2\chi_0}, \quad (1.43)$$

where  $r_H$  is the radius of the hydrogen atom,  $e$  is the charge of the electron. As a result we obtain the very simple correlation between the constants of the lines (1.42) and (1.43), which bears a substantial physical meaning.

In the previous paragraph we showed that the peculiarities of the “mass-luminosity” relation\* cannot be explained by changes of the absorption coefficient  $\kappa$ . Therefore the lines  $B^*/\kappa = \text{const}$  should bear the properties of the isotherms. The isotherms drawn in Fig. 3 are like the isotherms of the van der Waals gas. The meaning of this analogy is that there is a boundary near which the isotherms become distorted, at which the regular laws of thermodynamics are violated. The asymptotes of the boundary line (the boundary between two different phases in the theory of van der Waals) are axes (1.42) and (1.43). The distortion of the isotherms increases with approach to the axis  $\rho = \rho_0$  or  $r = r_H$ . That region is filled by stars of the Russell-Hertzsprung main sequence. The wonderful difference from van der Waals’ formula is the fact that there are two systems of the distortions, equation (1.37), which become smoothed with the distance from the axis  $\rho = \rho_0$  (for both small densities and large densities).

Stars can radiate energy for a long time only under conditions close to the boundaries (1.42) and (1.43). This most probably happens because the mechanism generating energy in stars works only if the standard laws of classical physics are broken.

The results are completely unexpected from the viewpoint of contemporary theoretical physics. The results show

\*The dispersion of showing-stars points around the theoretically calculated direction “mass-luminosity”. — Editor’s remark.

that in stars the classical laws of mechanics and thermodynamics are broken much earlier than predicted by Einstein's theory of relativity, and it occurs under entirely different circumstances. The main direction constants (1.42) and (1.43) show that the source of stellar energy is not Einstein's conversion of mass and energy (his mass-energy equivalence principle), but by a completely different combination of physical quantities.

Here we limit ourselves only to conclusions which follow from the observational data. A generalization of the results and subsequent theoretical consequences will be dealt with in the third part of this research. In the next chapter we only consider some specific details of the Russell-Hertzsprung diagram, not previously discussed.

### Chapter 2

#### Properties of Some Sequences in the Russell-Hertzsprung Diagram

##### 2.1 The sequence of giants

The stellar energy diagram (see Fig. 2) shows that the "mass-luminosity" relation has the most simple form for stars of the Russell-Hertzsprung main sequence

$$L \sim M^\alpha, \quad \alpha = 3.8. \quad (2.1)$$

Cepheids, denoted by crosses in the diagram, also satisfy the relation (2.1). Using the pulsation equation  $P\sqrt{\rho} = c_1$  we obtained (see formula 3.25 of Part I)

$$\left(0.30 - \frac{1}{5\alpha}\right)(m_b - 4.62) + \log P + 3 \log \bar{T}_{\text{eff}} = \log c_1, \quad (2.2)$$

where  $\bar{T}_{\text{eff}}$  is the reduced temperature of a star, expressed in multiples of the reduced temperature of the Sun,  $m_b$  is the absolute stellar magnitude,  $P$  is the pulsation period (days). We plot stars in a diagram where the abscissa is  $m_b - 4.62$ , while the ordinate is  $\log P + \log \bar{T}_{\text{eff}}$ . As a result we should obtain a straight line, which gives both the constant  $c_1$  (see §3.3 of Part I) and the angular coefficient  $0.30 - 1/5\alpha$ . Fig. 4 shows this diagram, built using the collected data of Becker [36], who directly calculated  $\bar{T}_{\text{eff}}$  and  $m_b$  by the radiant velocities arc (independently of the distances). As a result the average straight line satisfying all the stars has the angular coefficient 0.25 and  $c_1 = 0.075$ . Hence,  $\alpha = 4$ , which is in fine accordance with the expected result ( $\alpha = 3.8$ ). Such a coincidence makes Melnikov's conclusion unreasonable: that Cepheids have the same masses ( $\alpha = \infty$ ), as shown by the dashed line in Fig. 4.

In §1.5 of Part I we showed that the "mass-luminosity" relation for giants is explained by the fact that the structural coefficient  $\lambda L_{x_0}/M_{x_0}^3$  has the same value  $\simeq 2 \times 10^{-3}$  (1.31) for all stars. In order to obviate difficulties which appear if

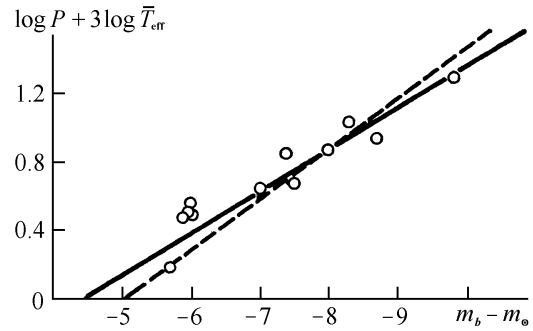


Fig. 4: Finding the exponent index  $\alpha$  in the  $L \sim M^\alpha$  relation for Cepheids.

one attempts to explain the luminosity of giants by nuclear reactions, one attributes to them an exotic internal constitution (the large shell which covers a normal star). Therefore, the simple structure of giants we have obtained gives an additional argument for the inconsistency of the nuclear sources of stellar energy. At the same time, because of their simple structure, giants and super-giants are quite wonderful. For instance, for a giant like the satellite of  $\epsilon$  Aurigae we obtain its central density at  $10^{-4}$  of the density of air, and the pressure at about 1 atmosphere. Therefore, it is quite possible that in moving forward along the main direction we can encounter nebulae satisfying the condition (1.42). Such nebulae can generate their own energy, just like stars.

Because of the physical conditions in giants, obtained above, the huge amounts of energy radiating from them cannot be explained by nuclear reactions. Even if this were true, their life-span would be very short. For reactions, the upper limit of the life-span of a star (the full transformation of its mass into radiant energy) can be obtained as the ratio of  $\bar{\epsilon}$  to  $c^2$ . So, by formula (1.40), we obtain

$$t = \frac{t_0}{4\gamma_c} \left( \frac{M_{x_0}}{\lambda L_{x_0}} \right), \quad (2.3)$$

where

$$t_0 = \frac{\kappa_T C}{\pi G} = 6 \times 10^{16} \text{ sec} = 2 \times 10^9 \text{ years} \quad (2.4)$$

and  $\gamma_c = B_c/p_c$  is the ratio of the radiant pressure to the gaseous one. As obtained, the structural multiplier here is about 4. Therefore

$$t = \frac{t_0}{\gamma_c}. \quad (2.5)$$

In giants  $\gamma_c \approx 1$ , so we obtain that  $t$  is almost the same as  $t_0$ . At the same time, as we know, the percentage of energy which could be set free in nuclear reactions is no more than 0.008. Hence, the maximum life-span of a giant is about  $1.6 \times 10^7$  years, which is absolutely inapplicable. This gives additional support for our conclusion that the mechanism of stellar energy is not like reactions.



It is very interesting that the constant (2.4) has a numerical value similar to the time constant in Hubble's relation (the red shift of nebulae). It is probable that the exact form of the Hubble equation should be

$$\nu = \nu_0 e^{-t/t_0}, \quad (2.6)$$

where  $\nu$  is the observed frequency of a line in a nebula spectrum when it is located at  $t$  light years from us,  $\nu_0$  is its normal frequency. According to the General Theory of Relativity the theoretical correlation between the constant  $t_0$  and the average density  $\bar{\rho}$  of matter in the visible part of the Universe

$$t_0 \simeq \frac{1}{\sqrt{\pi G \bar{\rho}}}, \quad (2.7)$$

which, independently of its theoretical origin, is also the very interesting empirical correlation. Because of (2.4) and (2.7), we re-write equation (2.6) as follows

$$\nu = \nu_0 e^{-\kappa_{\tau} \bar{\rho} x}, \quad (2.8)$$

where  $x = ct$  is the path of a photon. Formula (2.8) is like the formula of absorption, and so may give additional support to the explanation of the nebula red shift by unusual processes which occur in photons during their journey towards us. It is possible that in this formula  $\bar{\rho}$  is the average density of the intergalactic gas.

## 2.2 The main sequence

The contemporary data of observational astronomy has sufficiently filled the Russell-Hertzsprung diagram, i. e. the "luminosity – spectral class" plane. As a result we see that there are no strong arcs  $L(\bar{T}_{\text{eff}})$  and  $L(R)$ , but regions filled by stars. In the previous chapter we showed that such a dispersion of points implies that the energy productivity in stars is regulated exclusively by the energy drainage (the radiation). So the mechanism generating stellar energy is not like any reactions. It is possible that only the main sequence of the Russell-Hertzsprung diagram can be considered a line along which stars are located. According to Parenago [38], this direction is

$$m_b = m_{\odot} - 1.62x, \quad x = 10 \log \bar{T}_{\text{eff}}. \quad (2.9)$$

An analogous relation had been found by Kuiper [8] as the  $M(R)$  relation

$$\log \bar{R} = 0.7 \log \bar{M}. \quad (2.10)$$

Using formulae (1.12) and (1.14), we could transform formula (2.10) to a correlation  $B(\rho)$ . At the same time, looking at the stellar energy diagram (Fig. 2), we see that the stars of the Russell-Hertzsprung "main sequence" have no  $B(\rho)$  correlation, but fill instead a ring at the centre of the diagram. This incompatibility should be considered in detail.

In the stellar energy diagram, the Russell-Hertzsprung main sequence is the ring of radius  $c$  filled by stars. The boundary equation of this region is

$$\log^2 \bar{B} + \log^2 \bar{\rho} = c^2. \quad (2.11)$$

We transform this equation to the variables  $\bar{M}$  and  $\bar{R}$  by formulae (1.12) and (1.14). We obtain

$$17 \log^2 \bar{M} - 38 \log \bar{M} \log \bar{R} + 25 \log^2 \bar{R} = c^2. \quad (2.12)$$

As we have found, for stars located in this central region (the Russell-Hertzsprung main sequence), the exponent of the "mass-luminosity" relation is about 4. Therefore, using formulae

$$\log \bar{M} = -0.1 m_b, \quad 5 \log \bar{R} = -m_b - x,$$

we transform (2.12) to the form

$$m_b^2 + 2 \times 1.51 m_b x + 2.44 x^2 = c_1^2. \quad (2.13)$$

The left side of this equation is almost a perfect square, hence we have the equation of a very eccentric ellipse, with an angular coefficient close to 1.51. The exact solution can be found by transforming (2.13) to the main axes using the secular equation. As a result we obtain

$$\frac{a}{b} = 8.9, \quad \alpha = -1.58, \quad (2.14)$$

where  $a$  and  $b$  are the main axis and the secondary axis of the ellipse respectively,  $\alpha$  is the angle of inclination of its main axis to the abscissa's axis. Because of the large eccentricity, there is in the Russell-Hertzsprung diagram the illusion that stars are concentrated along the line  $a$ , the main axis of the ellipse. The calculated angular coefficient  $\alpha = -1.58$  (2.14) is in close agreement with the empirically determined  $\alpha = -1.62$  (2.9).

Thus the Russell-Hertzsprung main sequence has no physical meaning: it is the result of the scale stretching used in observational astrophysics. In contrast, the reality of the scale used in our stellar energy diagram (Fig. 2) is confirmed by the homogeneous distribution of the isoergs.

As obtained in Part I of this research, from the viewpoint of the internal constitution of stars, stars located at the opposite ends of the main sequence (the spectral classes O and M) differ from each other no more than stars of the same spectral class, but of different luminosity. Therefore the "evolution of a star along the main sequence" is a senseless term.

The results show that the term "sequence" was applied very unfortunately to groups of stars in the Russell-Hertzsprung diagram. It is quite reasonable to change this terminology, using the term "region" instead of "sequence": the region of giants, the main region, etc.

### 2.3 White dwarfs

There is very little observational data related to white dwarfs. Only for the satellite of Sirius and for  $\sigma^2$  Eridani do we know values of all three quantities  $L$ ,  $M$ , and  $R$ . For Sirius' satellite we obtain

$$\begin{aligned} \bar{M} &= 0.95, & \bar{R} &= 0.030, & \varepsilon &= 1.1 \times 10^{-2}, \\ \rho &= 10^4, & \rho_c &= 3 \times 10^5, & p_c &= 1 \times 10^{22}. \end{aligned} \quad (2.15)$$

For an ideal gas and an average molecular weight  $\mu = 1/2$ , we obtain  $T_c = 2 \times 10^8$  degrees. The calculations show that white dwarfs generate energy hundreds of times smaller than regular stars. Looking at the isoergs in Fig. 2 and the isotherms in Fig. 3, we see that the deviation of white dwarfs from the "mass-luminosity" relation is of a special kind; not the same as that for regular stars. At the same time white dwarfs satisfy the main direction in the stellar energy diagram: they lie in the line following giants. Therefore it would be natural to start our brief research into the internal constitution of white dwarfs by proceeding from the general supposition that they are hot stars whose gas is at the boundary of degeneration

$$\rho = A T^{3/2}, \quad A = 10^{-8} \mu_e. \quad (2.16)$$

We now show that, because of high density of matter in white dwarfs, the radiant transport of energy  $F_R$  is less than the transport of energy by the electron conductivity  $F_T$

$$F_R = -\frac{1}{3} \bar{v}_e \bar{\lambda} \bar{c}_v n_e \frac{dT}{dr},$$

where  $\bar{\lambda}$  is the mean free path of electrons moved at the average velocity  $\bar{v}_e$ ,  $\bar{c}_v$  is the average heat capacity per particle. Also

$$\lambda = \frac{1}{n_i \sigma}, \quad n_i = \frac{n_e}{z}, \quad \sigma = \pi r^2, \quad c_v = \frac{3}{2} k, \quad (2.18)$$

where  $n_i$  is the number of ions deviating the electrons,  $\sigma$  is the ion section determined by the  $90^\circ$  deviation condition

$$m_e v_e^2 = \frac{z e^2}{r}, \quad (2.19)$$

i. e. the condition to move along a hyperbola.

Substituting (2.19) and (2.18) into formula (2.17) and eliminating  $\bar{v}$  by the formula

$$\bar{v}^5 = \frac{12}{\sqrt{\pi}} \left( \frac{2kT}{m_e} \right)^{5/2},$$

we obtain

$$F_T = -\frac{24}{z e^4} \left( \frac{2k^7 T^5}{\pi^3 m_e} \right)^{1/2} \frac{dT}{dr}. \quad (2.20)$$

The radiant flow can be written as

$$F_R = -\frac{4}{3} \frac{c \alpha T^3}{\kappa \rho} \frac{dT}{dr}, \quad (2.21)$$

hence

$$\frac{F_R}{F_T} = \frac{z T^{1/2}}{\kappa \rho} \left( \frac{\alpha c e^4 \pi^{3/2} m_e^{1/2}}{k^{7/2} 18 \sqrt{2}} \right) = \frac{2.6 z T^{1/2}}{\kappa \rho}. \quad (2.22)$$

Using (2.15) it is easily seen that even if  $\kappa \simeq 1$ ,  $F_R < F_T$  in the internal regions of white dwarfs. We can apply the formulae obtained to the case of the conductive transport of energy, if we eliminate  $\kappa$  with the effective absorption coefficient  $\kappa^*$

$$\kappa^* = \frac{2.6 z T^{1/2}}{\rho}. \quad (2.23)$$

Thus, if white dwarfs are built on an ideal gas whose state is about the degeneration boundary, their luminosity should be more than that calculated by the "mass-luminosity" formula (the heat equilibrium condition).

We consider the regular explanation for white dwarfs, according to which they are stars built on a fully degenerate gas. For the full degeneration, we use Chandrasekhar's "mass-radius" formula (see formula 2.32, Part I). With  $\bar{M} = 1$  we obtain

$$\bar{R} = 0.042 \quad (\mu_e = 1), \quad \bar{R} = 0.013 \quad (\mu_e = 2).$$

The observable radius (2.15) cannot be twice as small, so we should take Sirius' satellite as being composed of at least 50% hydrogen. From here we come to a serious difficulty: because of the high density of white dwarfs, even for a few million degrees internally, they should produce much more energy than they can radiate. We now show that such temperatures are necessary for white dwarfs.

Applying the main equations of equilibrium to the surface layer of a star, we obtain

$$\frac{B}{p} = \frac{L \kappa}{4\pi G c M} = \frac{\varepsilon \kappa}{4\pi G c}, \quad (2.24)$$

where  $\kappa$  is the absorption coefficient in the surface layer. At the boundary of degeneration we can transform the left side by (2.16)

$$\rho_0 = \frac{3 \varepsilon \kappa}{4\pi G c} \frac{A^2 \mathfrak{R}}{\mu \alpha}$$

so that

$$\rho_0 = 125 \varepsilon \kappa \left( \frac{\mu_e^2}{\mu} \right), \quad (2.25)$$

$$T_0^{3/2} = 1.25 \times 10^{10} \varepsilon \kappa \left( \frac{\mu_e}{\mu} \right).$$

We see from formula (2.22) that even in the surface layer the quantity  $F_T$  can be greater than  $F_R$ . Substituting  $\kappa^*$  (2.23) into (2.25), we obtain

$$T_0 = 2.5 \times 10^7 e^{2/5} \left( \frac{z}{\mu} \right)^{2/5}. \quad (2.26)$$

For  $\varepsilon = 10^{-2}$ ,  $\mu = 1$ , and  $z = 1$ , we obtain

$$T_0 = 4 \times 10^6, \quad \rho_0 = 80, \quad \kappa_0^* = 65,$$

thus for such conditions,  $\kappa > \kappa^*$ .

We know that in the surface layer the temperature is linked to the depth  $h$  as follows

$$T = \frac{g\mu}{4\mathfrak{R}} h. \quad (2.27)$$

In the surface of Sirius' satellite we have  $g = 3 \times 10^7$ . Hence  $h_0 = 3 \times 10^7$ . Therefore the surface layer is about 2% of the radius of the white dwarf, so we can take the radius at the observed radius of the white dwarf.

It should be isothermal in the degenerated core, because the absorption coefficient rapidly decreases with increasing density. For a degenerate gas we can transform formula (2.23) in a simple way, if we suppose the heat capacity proportional to the temperature. Then, in the formula for  $F_R$  (2.20), the temperature remains in the first power, while  $T_0^{3/2}$  should be eliminated with the density by (2.16). As a result we obtain  $F_R \sim \rho T$  and also

$$\kappa_1^* \simeq 2.6 \times 10^{-8} \left( \frac{T}{\rho} \right)^2 z \mu_e. \quad (2.28)$$

Even for  $4 \times 10^6$  degrees throughout a white dwarf, the average productivity of energy calculated by the proton-proton reaction formula (1.16) is  $\varepsilon = 10^2$  erg/sec, which is much more than that observed. In order to remove the contradiction, we must propose a very low percentage of hydrogen, which contradicts the calculation above,\* which gives hydrogen as at least 50% of its contents. So the large observed value of the radius of Sirius' satellite remains unexplained.

So we should return to our initial point of view, according to which white dwarfs are hot stars at the boundary of degeneration, but built on heavy elements. The low luminosity of such stars is probably derived from the presence of endothermic phenomena inside them. That is, besides energy generating processes, there are also processes where  $\varepsilon$  is negative. This consideration shows again that the luminosity of stars is unexplained within the framework of today's thermodynamics.

## References

1. Bethe H. A. Energy production in stars. *Physical Review*, 1939, v. 55, No. 5, 434–456.
2. Schwarzschild K. Über das Gleichgewicht der Sonnenatmosphäre. *Nachrichten von der Königlichen Gesellschaft der Wissenschaften zu Göttingen. Mathematisch — physicalische Klasse*. 1906, H. 6, 41–53.
3. Schmidt W. Der Massenaustausch in freier Luft und verwandte Erscheinungen. Hamburg, 1925 (*Probleme der Kosmischen Physik*, Bd. 7).
4. Milne E. A. The analysis of stellar structure. *Monthly Notices of the Royal Astronomical Society*, 1930, v. 91, No. 1, 4–55.
5. Kuiper G. P. Note on Hall's measures of  $\varepsilon$  Aurigae. *Astrophys. Journal*, 1938, v. 87, No. 2, 213–215.
6. Parenago P. P. Physical characteristics of sub-dwarfs. *Astron. Journal — USSR*, 1946, v. 23, No. 1, 37.
7. Chandrasekhar S. The highly collapsed configurations of a stellar mass. Second paper. *Monthly Notices of the Royal Astronomical Society*, 1935, v. 88, No. 4, 472–507.
8. Kuiper G. P. The empirical mass-luminosity relation. *Astrophys. Journal*, 1938, v. 88, No. 4, 472–507.
9. Russell H. N., Moore Ch. E. The masses of the stars with a general catalogue of dynamical parallaxes. *Astrophys. Monographs*, Chicago, 1946.
10. Trumpler R. J. Observational evidence of a relativity red shift in class O stars. *Publications of the Astron. Society of the Pacific*, 1935, v. 47, No. 279, 254.
11. Parenago P. P. The mass-luminosity relation. *Astron. Journal — USSR*, 1937, v. 14, No. 1, 46.
12. Baize P. Les masses des étoiles doubles visuelles et la relation empirique masse-luminosité. *Astronomie — Paris*, 1947, t. 13, fasc. 2, 123–152.
13. Eddington A. S. The internal constitution of the stars. Cambridge, 1926, 153.
14. Chandrasekhar S. An introduction to the study of stellar structure. *Astrophys. Monographs*, Chicago, 1939, 412.
15. Eddington A. S. The internal constitution of the stars. Cambridge, 1926, 135.
16. Strömgen B. The opacity of stellar matter and the hydrogen content of the stars. *Zeitschrift für Astrophysik*, 1932, Bd. 4, H. 2, 118–152; On the interpretation of the Hertzsprung-Russell-Diagram. *Zeitschrift für Astrophysik*, 1933, Bd. 7, H. 3, 222–248.
17. Cowling T. G. The stability of gaseous stars. Second paper. *Monthly Notices of the Royal Astronomical Society*, 1935, v. 96, No. 1, 57.
18. Ledoux P. On the radial pulsation of gaseous stars. *Astrophys. Journal*, 1945, v. 102, No. 2, 143–153.
19. Parenago P. P. Stellar astronomy. Moscow, 1938, 200.
20. Becker W. Spektralphotometrische Untersuchungen an  $\delta$  Cephei-Sternen X. *Zeitschrift für Astrophysik*, 1940, Bd. 19, H. 4/5, 297.
21. Eddington A. S. The internal constitution of the stars. Cambridge, 1926, 191.
22. Luyten W. J. On the ellipticity of close binaries. *Monthly Notices of the Royal Astronomical Society*, 1938, v. 98, No. 6, 459–466.
23. Russell H. N., Dugan R. S. Apsidal motion in Y Cygni and other stars. *Monthly Notices of the Royal Astronomical Society*, 1930, v. 91, No. 2, 212–215.

\*By Chandrasekhar's formula for a fully degenerate gas. — Editor's remark.

24. Blackett P. M. S. The magnetic field of massive rotating bodies. *Nature*, 1947, v. 159, No. 4046, 658–666.
  25. Eddington A. S. The internal constitution of the stars. Cambridge, 1926, 163.
  26. Lohmann W. Die innere Struktur der Masse-Leuchtkraftfunktion und die chemische Zusammensetzung der Sterne der Hauptreihe. *Zeitschrift für Astrophysik*, 1948, Bd. 25, H. 1/2, 104.
  27. Martynov D. Ya. Eclipse variable stars. Moscow, 1939.
  28. Gaposchkin S. Die Bedeckungsveränderlichen. *Veröffentlichungen der Universitätssternwarte zu Berlin-Babelsberg*, 1932, Bd. 9, H. 5, 1–141.
  29. Parenago P. P. Physical characteristics of sub-dwarfs. *Astron. Journal — USSR*, 1946, v. 23, No. 1, 31–39.
  30. Struve O. The masses and mass-ratios of close binary systems. *Annales d’Astrophys.*, 1948, t. 11, Nom. 2, 117–123.
  31. Kothari D. S. The theory of pressure-ionization and its applications. *Proceedings of the Royal Society of London*, Ser. A, 1938, v. 165, No. A923, 486–500.
  32. Luyten W. J., Struve O., Morgan W. W. Reobservation of the orbits of ten spectroscopic binaries with a discussion of apsidal motions. *Publications of Yerkes Observatory*, Univ. of Chicago, 1939, v. 7, part. 4, 251–300.
  33. Kuiper G. P. On the hydrogen contents of clusters. *Astrophys. Journal*, 1937, v. 86, No. 2, 176–197.
  34. Masevich A. G. Stellar evolution where is corpuscular radiations, considered from the viewpoint of the internal constitution of stars. *Astron. Journal — USSR*, 1949, v. 26, No. 4, 207–218.
  35. Tuominen J. Über die inneren Aufbau der TRÜMPLERSchen Sterne. *Zeitschrift für Astrophysik*, 1943, Bd. 22, H. 2, 90–110.
  36. Becker W. Spektralphotometrische Untersuchungen an  $\delta$  Cephei-Sternen X. *Zeitschrift für Astrophysik*, 1940, Bd. 19, H. 4/5, 297; Spektralphotometrische Untersuchungen an  $\delta$  Cephei-Sternen. *Zeitschrift für Astrophysik*, 1941, Bd. 20, H. 3, 229.
  37. Melnikov O. A. On the stability of masses of long-periodical Cepheids. *Proceedings of Pulkovo Astron. Observatory*, 1948, v. 17, No. 2 (137), 47–62.
  38. Parenago P. P. The generalized relation mass-luminosity. *Astron. Journal — USSR*, 1939, v. 16, No. 6, 13.
-

*Progress in Physics* is a quarterly issue scientific journal, registered with the Library of Congress (DC).

This is a journal for scientific publications on advanced studies in theoretical and experimental physics, including related themes from mathematics.

Electronic version of this journal:  
[http://www.geocities.com/ptep\\_online](http://www.geocities.com/ptep_online)

Editor in Chief

Dmitri Rabounski      ✉ [rabounski@yahoo.com](mailto:rabounski@yahoo.com)

Associate Editors

Prof. Florentin Smarandache      ✉ [smarand@unm.edu](mailto:smarand@unm.edu)

Dr. Larissa Borissova      ✉ [lborissova@yahoo.com](mailto:lborissova@yahoo.com)

Stephen J. Crothers      ✉ [thenarmis@yahoo.com](mailto:thenarmis@yahoo.com)

*Progress in Physics* is peer reviewed and included in the abstracting and indexing coverage of: Mathematical Reviews and MathSciNet of AMS (USA), DOAJ of Lund University (Sweden), Referativnyi Zhurnal VINITI (Russia), etc.

Department of Mathematics, University of New Mexico,  
200 College Road, Gallup, NM 87301, USA

Printed in the United States of America

**Issue 2005, Volume 3**  
**US \$ 20.00**

ISSN 1555-5534

